Title

NMR IMAGING AND SPECTROSCOPY OF THE MAMMALIAN CENTRAL NERVOUS SYSTEM AFTER IIEAW ION RADIATION.

Author

Richards, T.

Publication Date

1984-09-01

Lawrence Berkeley Laboratory
UNIVERSITY OF CALIFORNIA

NMR IMAGING AND SPECTROSCOPY OF THE MAMMALIAN CENTRAL NERVOUS SYSTEM AFTER HEAVY ION RADIATION

T. Richards
(Ph.D. Thesis)

September 1984

Donner Laboratory

Biology & Medicine Division

Prepared for the U.S. Department of Energy under Contract DE-AC03-76SF00098

DISCLAIMER

LBL-18148

NMR IMAGING AND SPECTROSCOPY OF THE MAMMALIAN CENTRAL NERVOUS SYSTEM AFTER HEAVY ION RADIATION

Todd Richards

Ph.D Disseration - September 1984

Lawrence Berkeley Laboratory
University of California
Berkeley, California 94720

This work was supported by the Office of Health and Environmental Research of the United States Department of Energy under Contract DE-AC03-76SF00098.

TABLE OF CONTENTS

NMR IMAGING AND SPECTROSCOPY OF THE MAMMALIAN CENTRAL NERVOUS SYSTEM AFTER HEAVY ION RADIATION

Todd Richards

ABSTRACT-

NMR imaging, NMR spectroscopic, and histopathologic techniques were used to study the proton relaxation time and related biochemical changes in the central nervous system after helium beam in vivo irradiation of the rodent brain. In order to measure the NMR relaxation times, the following imaging techniques were used: spin-echo imaging with projection-reconstruction; 2D Fourier transform spin-echo imaging; and saturation recovery with projection reconstruction. The spectroscopic observations reported in this dissertation were made possible by developement of methods for measuring the NMR parameters of the rodent brain in vivo and in vitro. These technological developements were a major part of this work. The methods include (1) depth selective spectroscopy using an optimization of rf pulse energy based on a priori knowledge of N-acetyl aspartate and lipid spectra of the normal brain, (2) phase-encoded proton spectroscopy of the living rodent using a surface coil, and (3) dual aqueous and organic tissue extraction technique for spectroscopy. Radiation-induced increases were observed in lipid and p-choline peaks of the proton spectrum, in vivo. Proton NMR spectroscopy measurements on brain extracts (aqueous and organic solvents) were made to observe chemical changes that could not be seen

in vivo. Radiation-induced changes were observed in lactate, GABA, glutamate, and p-choline peak areas of the aqueous fraction spectra. In the organic fraction, decreases were observed in peak area ratios (normalized to the methylene peak area) of the terminal-methyl peaks, the N-methyl groups of choline, and at a peak at 2.84 ppm (phosphatidyl ethanolamine and phosphatidyl serine resonances) relative to TMS. With histology and Evans blue injections, blood-brain barrier alterations were seen as early as 4 days after irradiation.

The major findings from 3 independent non-invasive measurement techniques on relaxation and spin density are: 1)a decrease in spin density and T1 relaxation on the irradiated side; 2) an increase in T2 on the irradiated side; and 3) an increase in T1 and spin density on the control side of irradiated brain relative to controls (4 - 14 days post-irradiation). Using the saturation recovery experiment with the surface coil, an increase in T1 was measured on the irradiated side 81 days post-irradiation. The most likely explanation for the early decrease in T1 of irradiated brain is that radiation causes chemical-bond breakage and protein conformational changes that would expose a greater amount of water to relaxation centers of both proteins and lipids. The time related changes in T1 correlated with lipid changes measured in the organic fraction spectra at 4 and 81 days after irradiation. The increase in T1 on the control side of irradiated brains may be related to ventricular enlargement known to occur from examination of the histological sections.

SYMBOLS AND DEFINITIONS

2DFT - two dimensional Fourier transform

A image - a parametric image calculated from several spin-echo intensity images by fitting the intensity values to the following equation pixel by pixel:

$I(t) = A * \exp(-t/T2)$

where $I(t)$ = spin-echo intensity for a given image pixel

A = related to spin density if pulse interval is much greater than T1

t = echo time after 90 degree rf pulse.

The A fitted values are displayed in the gray level image.

A1 image - a parametric image calculated from two or more intensity images by varying the T1 dependent variable t and by fitting the intensity values to the equation pixel by pixel:

$I(t) = A1 * (1-\exp(-t/T1))$

where $I(t)$ = intensity from T1 pulse experiment

$A1$ = related to spin density if pulse interval is much greater than T1

t = time delay between the two pulses during which the relaxation process occurs.

The A1 fitted values are displayed in the gray level image.

B1 field - the x-y magnetic field component of the radio-frequency wave which causes the net magnetization vector to tip in the x-y plane.

CNS - central nervous system

Delay time - in the NMR pulse sequence, usually refers to the time between two pulses during which the relaxation process process can occur.

DNA - deoxyribonucleic acid

Intensity image - an image constructed from the NMR free induction decay signal.

MHz - mega hertz; 1,000,000 hertz

NMR - nuclear magnetic resonance

P-choline - choline containing molecules such as phosphorylcholine, phosphocholine, phosphatidylcholine, etc.

PCR+CR - phosphocreatine + creatine

ppm - parts per million; in spectroscopy, the chemical shift axis is expressed in ppm using the following equation:

$$ppm = 10E\text{-}6 * \frac{w - w(ref.)}{w(ref.)}$$

RF - radio-frequency; used to describe the range of electromagnetic radiation between 15,000 Hz to 100,000 MHz.

Saturation recovery - NMR pulse sequence used to measure T1 relaxation time.

T1 - spin-lattice relaxation time.

T1 image - a parametric image similar to the A1 image except the T1 fitted values are displayed in the gray-level image.

T2 - spin-spin relaxation time.

T2 image - a parametric image similar to the A image, except the T2 fitted values are displayed in the gray-level image.

TMS - tetramethylsilane; a chemical used for chemical shift reference.

VAX - Digital Equipment Corporation computer.

Chapter 1. - INTRODUCTION

1.1 Purpose and scope

Proton NMR offers a promising new non-invasive method for evaluating the anatomical and chemical changes in radiation brain injury. Ionizing radiation disrupts chemical bonds and creates free radicals which eventually lead to changes in tissue chemistry and structure. The purpose of this research was to measure the proton relaxation time and related biochemical changes in CNS tissue after helium beam irradiation using nuclear magnetic resonance. The motivation for this research comes from cancer radiotherapy where the therapist needs to find a non-invasive way to quantitate the CNS tissue response to the radiation. Heavy ions are of special interest in the treatment of tumors because they have two important features: 1) the "Bragg peak effect" which allows a high killing dose to be localized to the tumor while sparing normal tissues lying in the treatment volume, and 2) a low OER (oxygen enhancement ratio) relative to X-rays which reduces the radioresistance of hypoxic cells (Blakely et al., 1984). The following scientific questions are posed:

1) What are the effects of heavy ion radiation on proton relaxation parameters (T1, T2, and spin density) of the CNS?

2) What are the molecular mechanisms that cause these parameters to change in irradiated tissue?

In order to answer these questions, techniques were studied and developed to make NMR measurements on CNS tissue (in vitro and in vivo). Once these techniques were understood, the NMR parameters were used in the assessment of heavy ion radiation damage to the CNS. The NMR parameters of interests are T1 (spin-lattice relaxation time), T2 (spin-spin relaxation time), spin density, and the high resolution chemical shift spectrum. Proton spectroscopy was done in order to understand some of the radiation-induced chemical changes (proton resonances) that may be related to the proton T1 relaxation time of the CNS.

This dissertation is divided into 9 chapters. Chaptes 2 through 4 describe three different NMR imaging techniques used to measure the relaxation parameters in vivo:

SPIN-ECHO IMAGING WITH PROJECTION RECONSTRUCTION (Ch 2)

2D FOURIER TRANSFORM SPIN-ECHO IMAGING (Ch 3)

SATURATION RECOVERY IMAGING WITH PROJECTION RECONSTRUCTION (Ch 4).

Chapters 5 through 7 describe different NMR spectroscopic techniques to measure the high resolution proton spectrum:

SPIN-ECHO SPECTROSCOPY WITH RF ENERGY OPTIMIZATION (Ch 5)

2D FOURIER TRANSFORM PROTON SPECTROSCOPY (Ch 6)

PROTON CHEMICAL SHIFTS OF AQUEOUS AND ORGANIC FRACTIONS OF BRAIN EXTRACTS (Ch 7).

In each of these chapters, the method and results are discussed, however a discussion of the implications of the results for radiation injury is reserved until chapter 9 (Summary and Discussion). Chapter 8 describes the correlation of the NMR results with conventional histological techniques.

1.2 Acknowledgements

First of all, I wish to thank my research advisor, Professor Thomas F. Budinger, who made it possible for me to do the research. The other thesis committee members have also been very helpful: Professors Paola S. Timiras and Cornelius A. Tobias. I thank Dr. Joseph Castro who encouraged and financially supported me during this work. The moral support of Dr. W. Lynn Richards, Alicia Richards, Joy Richards, and Julie Wilson was critical for the completion of this work. There were many different phases of this research and each phase was done with much appreciated personal assistance. I thank the following people:

NMR spectroscopy and imaging (UCB chemistry department, Latimer hall)-
Rudi Nunlist and Rich Mazzarisi
Helium beam irradiation (184 inch cyclotron)-
Dr. Katie Brennan, Dr. John Lyman, Julie Twitchel, Brian Moyer, Jay Joseph, Leal Kanstein, Fred Yeater, George Hampton, and James MacMullen
NMR imaging at the Baylor College of Medicine, Houston, Texas-
Drs. M. Robert Willcott, R. Nick Bryan, Joseph Ford, Bub Wendt, Joseph Foster, and Nicholas Schneiders.
NMR imaging at the Radiologic Imaging Laboratory, UCSF-
Drs. George Wesbey, and Barry Englestad
Brain extract preparation- Reese Jones, Jay Joseph, and Jeff Teckman
Instruction and assistance in histological techniques- Virginia Havens
Histopathological instruction (Brookside Hospital)- Dr. Kay Woodruff
Machine shop (NMR rat probe fabrication)- E. (Pete) Dowling, Ed Chubak,

Chip Hollister, and Bud Deuberry

Electronic shop (gradient power supply fabrication)- Frank Upham, Blair Jarrett, and John Gurule

Graphics and Figures- Robert Stevens and Flavio Robles Jr.

Computer software consultants- Drs. Samuel Pitluck and William Holley.

This work was supported by the office of Health and Environmental Research of the United States Department of Energy under Contract DE-AC03-76SF00098.

1.3 BACKGROUND

1.3.1 Radiation biophysics of the CNS

The sequence of events in ionizing radiation damage can be divided into five categories 1) initial energy deposition; 2) primary chemical events; 3) secondary chemical events; 4) early biological damage; and 5) delayed biological damage. The first three categories are applicable to any biological tissue, but the last two sections are centered on the effects on the brain. NMR relaxation and spectroscopic parameters would be influenced by the biophysical effects of ionizing radiation which cause a change in the number of relaxation centers or a change in the chemical concentration of visible NMR resonances. The relationship between NMR relaxation parameters and the molecular environment is described in section 1.3.2.

1.3.2.1 Initial energy deposition

As ionizing radiation passes through biological tissue, it causes molecular ionization and excitation (Andrews, 1974). The pattern of energy deposition is different for heavy ion radiation than it is for X-rays. As a beam of X-rays passes through the tissue, it is exponentially attenuated because the photons are absorbed and deflected by electrons (compton scattering, photoelectric effect, etc.) and more energy is deposited at the beginning of the beam path than at the end (Andrews, 1974). On the other hand, as a beam of heavy ion particles passes through the tissue, most of the particles in the beam are not deflected or absorbed by the tissue until the beam reaches the end of its path and the amount of ionization caused by each particles increases

as it slows down (linear energy transfer is inversely proportional to the particle velocity squared).

1.3.2.2 Primary chemical events

The absorbed energy from the radiation is initially distributed among the tissue molecules approximately in proportion to the electron density of its constituents or with heavier atoms present, on the photoelectric absorption coefficient. The mammalian brain is composed of about 80% water and 20% organic molecules (Logan, 1961; Crowell, 1934). Therefore, most of the energy is deposited in the tissue water and the reactive chemical species from the radiolysis of water would be the most important. These species include ions, ion radicals, and free radicals. The most important reactive species are the hydrated electron, the hydroxyl radical, the hydrogen atom, and hydrogen peroxide. These species are very short lived (10E-3 seconds) and are either deactivated or react with other water products or macromolecules depending on proximity and oxygen content (Singh and Singh, 1982). The direct interaction of the radiation with the organic molecule results in organic free radicals, organic molecules in an exited state, free electrons, hydrogen atoms and organic ions (Singh and Singh, 1982).

1.3.2.3 Secondary chemical events

The reactive species mentioned in the previous section can react with oxygen, water, radicals, or macromolecules to form longer lived damaged molecules. Since most of the tissue is comprised of water, most of the damage is caused by the water derived reactive species which

diffuse through the tissue and react with the biologically important macromolecules. This secondary phenomenon is known as the indirect effect of radiation and occurs between 10E-10 and 10E-3 seconds. The products formed from these interactions would be organic peroxides, organic free radicals, organic hydroperoxides, and hydrogen peroxide (Singh and Singh 1982). The consequences of interaction with these products include: 1) DNA and RNA damage (Okada, 1979); 2) enzyme inactivation and activation (Altman, 1970), 3) oxidation of sulfides; 4) lipid peroxidation (Pritchard and Singh, 1968); and conformational changes in protein structure (Todo, 1982).

1.3.2.4 Early biological damage

The immediate biological effect of radiation at the cellular level is an alteration in the biochemical processes directing and controlling RNA synthesis, and the synthesis of proteins and lipids necessary for structure and metabolism of the cell. These effects occur between 10 seconds and 10 hours (Singh and Singh 1982). Damage done to DNA is particularly important because the same base-pair coded section is used many times in directing the cell's metabolism. For example, if damage was done to the section of DNA required to encode succinate dehydrogenase, then every time this enzyme is made from this section, it would be misfabricated and the effect would be amplified. The maintenance of DNA is so important that the cell responds to damage by inducing DNA repair mechanisms (Elkind,1971; Roberts,1975). Other early biological effects would be caused by membrane disruption (Singh and Singh, 1982).

1.3.2.5 Radiation brain injury - techniques and results

Techniques used for the study of radiation injury to the central nervous system can be divided into three categories: 1) histological - chemical (invasive); 2) non-invasive; and 3) clinical methods.

Invasive methods include histochemistry (Haymaker, 1969), electron microscopy (Maxwell and Kruger, 1964), injection of radioactive tracers (Zeman and Samorarjski, 1971) and florescent dies (Van Dyke et al., 1962), and chemical isolation analysis (Egana, 1971). These techniques can only be used once per animal and cannot give dynamic information about the biological processes involved. However, experiments by invasive means have provided a wealth of information concerning the morphological and biochemical nature of the damage in the static condition.

Non-invasive techniques (in this case, non-invasive is defined as a method that does not require animal sacrifice) of measuring radiation damage include: 1) the penicillin-EEG method (Remler and Marcussen, 1981), 2) electroshock seizure induction (Rosenthal and Timiras, 1961), 3) positron emission tomography (Saunders and Budinger, 1984), 4) X-ray CT (Fike et al., 1984), and 5) nuclear magnetic resonance (Richards et al., 1983).

In addition to the invasive and non-invasive methods, observational procedures of clinical signs and symptoms have been used to divide radiations effects into three categories: 1)acute reactions which occur during the course of irradiation treatment; 2)early delayed reactions which occur from a few weeks to a few months after irradiation; and

3)late delayed reactions which occur several months to years after irradiation (Sheline, 1982). Edema is believed to be the major mechanism for the early acute reaction; demyelination is associated with transient and nonlethal neurological symptoms in the early delayed reaction; and radionecrosis and vascular abnormalities have been associated with the late delayed reaction (Sheline, 1982).

The effects of radiation on the CNS vary greatly from one animal species to the next and also are sensitive to irradiation parameters such as dose, dose rate, volume of tissue irradiated, time after irradiation, and the part of the brain irradiated. In the dose range from 1000 to 6000 rads, there are several histological changes that have been observed: edema (Miquel and Haymaker, 1967; Caveness, 1980), endothelial cell reactions (Lierse and Frank, 1967), altered blood brain barrier (Van Dyke et al, 1962; Remler and Marcussen, 1981), decreased regional blood flow (Tanaka et al., 1979), and glycogen accumulation (Miquel et al.,1966). Ordy and associates have recorded a reduction in alkaline phosphatase of endothelial cells of the mouse brain irradiated at 5000 rads. Functional effects of radiation include an increase in brain exitability (measured by the electroconvulsive threshold) after 500 rads and a decrease after 5000 or 10,000 rads proton radiation (Sherwood, Welch, and Timiras, 1967). Metabolic effects of radiation have been reported by Timiras et al., (1964) as measured by an increase in oxygen uptake and a decrease in carbon dioxide of the cortex after early postnatal whole-body x-radiation. Other biochemical effects

include changes in protein composition, a decrease in oxidative phosphorylation, and a decrease in glucose oxidation (Gerber and Altman, 1970)

The delayed reactions of the brain to radiation have puzzled scientists and clinicians for at least 30 years. Delayed radionecrosis is characterized by 1) an initial development of partial tissue necrosis; 2) a preceeding pathological silent interval ranging from months to years; 3) selective damage to certain central nervous system structures; and 4) a lesion that grows in volume as initially scattered foci enlarge and coalesce (Zeman and Samorajski, 1971). There are many reports of delayed radionecrosis in man as well as in experimental animals. The reaction is accompanied by: demyelination (Lampert et al., 1959, Caveness, 1980), degenerative changes in blood vessels (Zeman and Samorajski, 1971), functional changes in the vasculature (Moustafa and Hopewell, 1980), and complete cavitation and necrosis (Caveness, 1980). There are two theories that attempt to explain the phenomenon. Zeman and associates believe that the radiation directly effects the glial cells which then cause the progressive necrosis of the rest of the tissue (Zeman and Samorajski, 1971). These changes may come about by alteration in the proliferation of lysosomes and the release of proteolytic enzymes. On the other hand, Haymaker and his associates (1969) believe that the damage is caused indirectly by the effects on the CNS vasculature, which is important in providing vital nutrients to the cells and in inhibiting toxic chemicals from reaching the sensitive neurons. Other mechanisms proposed for the delayed manifestation of radiation damage are: 1) long lived peroxides; and 2) slow virus

induction; and 3) immune response to altered macromolecular structure (proteins and membranes).

1.3.2 Relationship between NMR relaxation parameters and CNS pathology

NMR relaxation parameters are sensitive to tissue pathology which result in a change in the structural state of tissue water. In this section, the molecular mechanisms and CNS pathology related to NMR relaxation times will be discussed.

The state of water in biological tissue is very different from the state of the molecules in pure water (Hazlewood, 1979; Mather-De Vre, 1979). Spin-lattice relaxation time (T1) is related to the structural state of the water in the tissue and it is characterized by the rate at which energy is exchanged between the magnetic nuclei (hydrogen) and the lattice. NMR relaxation is not spontaneous, but is induced by interactions of protons with the time-varying magnetic fields of neighboring nuclei. The correlation time is related to the frequency of these local fields, and is defined as the time between molecular collisions. The collection of protons is exposed to a spectrum of changing (vibrating) magnetic fields (Fullerton et al., 1982). In order for effective energy exchange to take place, the frequency of the vibrations must be near the Larmor frequency. In this condition, the relaxation process occurs and the magnetic moment of the spin can align in the main magnetic field. As magnetic equilibrium is reached, the net magnetic vector grows along the main magnetic field, and the rate at which it grows is characterized by T1. In order to determine T1, the sample is placed in a magnetic field, a radio-frequency pulse is applied

to tip the net magnetization vector away from alignment of the field, and then the amount of sample magnetization that has re-aligned in the main field is measured at several different delay times. T1 is calculated by fitting the data points to an exponential equation.

Spin-spin relaxation time (T2) is influenced by the rate at which spins exchange energy with each other and is characterized by the rate at which the nuclei dephase after an rf pulse is applied. In order to determine T2, a radio-frequency pulse is applied to tip the net magnetization vector 90 degrees away from alignment of the field (called a 90 degree pulse), and then a 180 degree pulse is applied after a variable delay time. This 180 degree pulse causes the dephasing spins to refocus and form an echo (spin-echo) with an amplitude dependent on the inherent T2 relaxation time. T2 is calculated by fitting the echo amplitudes from several different delay times to a decaying exponential equation.

Molecular Environment

The relaxation times, T1 and T2, are sensitive to dynamic processes occurring at different frequencies (Ferrar and Becker, 1971). T1 is sensitive to motions which occur near the Larmor frequency (the characteristic NMR frequency of the main magnetic field) and T2 is sensitive to those frequencies which affect T1 and also the local magnetic fluctuations at the lower frequencies (Ferrar and Becker, 1971). In pure liquid samples, the relaxation times are very long because the water molecules tumble around fast enough to average out the magnetic interactions. However, water in macromolecular solutions

divides into two compartments; free water and hydration (bound) water (Berendsen, 1975). The free water has the same characteristics of water in pure solutions (i.e., mobile and unrestricted). However, the water in the hydration layer of the macromolecules is more restricted, and in this state the magnetic interactions are not averaged out and energy exchange processes can occur more readily (Mathur-De Vre, 1979). Therefore, the T1 relaxation rate is faster in the hydration layer than it is in the free water. Energy is readily exchanged between spins of the two compartments (bound and free) and this is described as rapid exchange. This condition has been shown to exist in protein solutions (Berendsen, 1975). The equation used to describe the relaxation time under conditions of rapid exchange is

$$1/T1 = f\ (1/T1f) + h\ (1/T1h)$$

where T1 = observed T1 relaxation time

f = fraction of free water

T1f = T1 relaxation time of free water

h = fraction of hydrated water

T1h = T1 relaxation time of hydrated water

(Fullerton et al., 1982)

This equation describes a two component system; one component in which the water is freely rotating and one component in which the water is rigidly bound in the hydration layer. The fraction of water in the hydration layer affects the relaxation rates and is dependent on: 1) total water concentration, 2) type of protein in solution and its concentration (Kuntz, 1974), 3) the conformation of the protein (Dodson, 1984), and 4) the concentration of lipids (Gaggelli, 1982). The

presence of paramagnetic substances also affects relaxation parameters. Paramagnetic substances include iron complexes (Ashley et al., 1980), oxygen, and free radicals (Brasch, 1983).

At the cellular level, T1 and T2 are affected by malignant transformation, movement through the cell cycle, growth, differentiation, and exposure to chemicals which damage DNA (Kennedy, 1984; Beall, 1979).

CNS Pathology

NMR imaging is proving to be very valuable in studying diseases of the CNS (Bydder et al., 1982). However, little is known about the effects of ionizing radiation on the NMR relaxation parameters in the CNS. Several of the CNS reactions described in section 1.3.1 have been observed on NMR images although the reactions were not induced by radiation. Edema causes an increased T1 relaxation time because the percentage of free water is increased (Asato et al., 1983; Go and Edzes, 1975, Naruse et al., 1982; Bakay et al., 1975; Bartkowski, 1983; Bradley, 1983). Demyelination, which results in a decrease of lipids and an increase in water content, causes T1 to increase (Bydder, 1982; Mills, 1982). The relationship between lipid content and T1 relaxation is not clear because the proton lipid resonance is very small in CNS tissue and does not contribute to the imaging signal. The origin of the normal low T1 in white matter relative to gray matter is probably due to the structural relation of water protons to membrane relaxation centers (lipids and membrane proteins). Hemorrhaging results in a greater amount of water exposed to paramagnetic iron (hemoglobin), and

the hemorrhagic lesion is usually characterized by a short T1 at the edge of the region and a long T1 in the center (Pennock et al., 1983; Sipponen, 1983). Infarction results in prolongation of T2 (Crooks, 1983; Bryan, 1983).

CHAPTER 2. SPIN-ECHO IMAGING WITH PROJECTION RECONSTRUCTION

An experiment was performed in collaboration with Drs. Robert Willcott and Nick Bryan in order to measure radiation induced changes in spin echo intensity and T2 relaxation time. The rats were irradiated in Berkeley and taken to the Baylor College of Medicine in Houston for the NMR imaging experiment.

2.1 Methods

The right hemisphere of the brain of 6 Sprague-Dawley rats (age - 40 days) was irradiated using the helium beam at the 184 inch cyclotron (See Figure 2.1). The rats received 3000 rads in the plateau region of the beam with a dose rate of approximately 500 rads/min. The beam passed through the head in the posterior-anterior (PA) direction and a D-shaped collimator (11.5 X 16 mm) was used to limit the radiation to one side of the brain. A diagnostic X-ray (AP) was taken of rat's head with a beam spot in order to accurately position the beam (See Figure 2.2). The beam range was 14.7 cm and therefore, the beam passed completely through the rat's head, depositing energy fairly uniformly along its path.

Two of the irradiated rats were imaged one week post-irradiation on a 4.7 Tesla Bruker spectrometer modified for imaging. One of the rats was anesthetized with nembutal and the brain was fixed in situ by perfusing 10% formalin into the left ventricle of the heart. After the

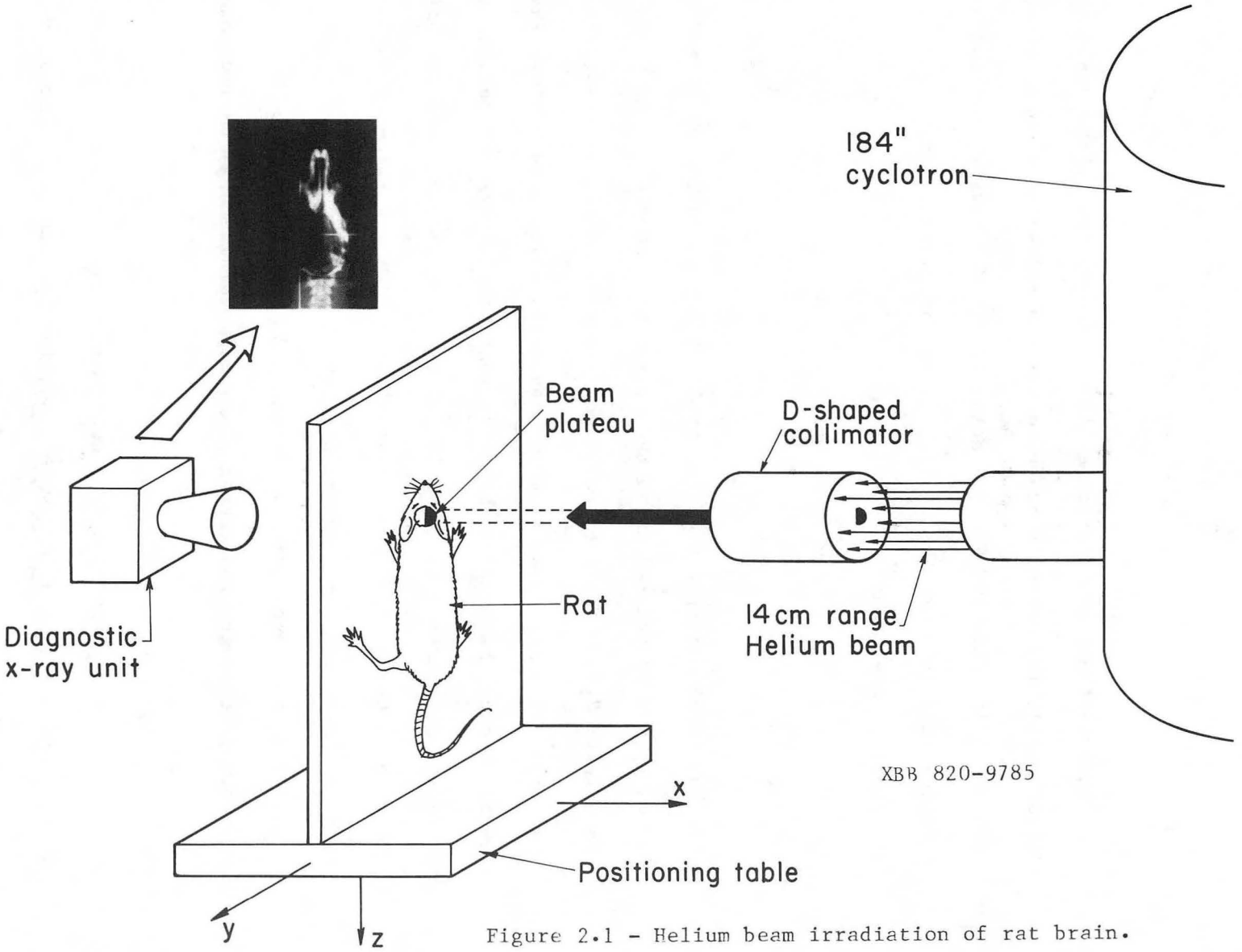

Figure 2.1 - Helium beam irradiation of rat brain.

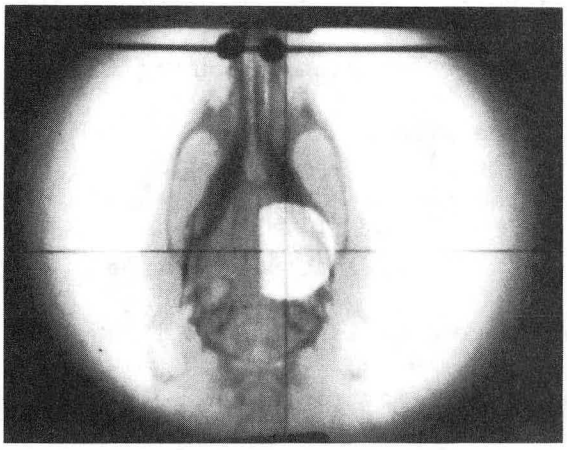

XBB 849-6803

Figure 2.2 - X-ray of rat head with beam spot. The beam was positioned to pass through the right side cerebrum with sparing of the cerebellum.

brain was thoroughly fixed, it was excised and kept in formalin solution until the imaging was performed. The other rat was anesthetized and the brain was excised without formalin fixation. The brain was then imaged within one hour after excision. Imaging was done using the projection reconstruction method with a modified Carr-Purcell-Meiboom-Gill pulse sequence which produced 16 echos (Schneiders et al, 1983). Slice selection was done with a carefully shaped rf pulse and selective saturation. The slice thickness was 1.5mm (Schneiders et al., 1983). Groups of four echos were averaged before back projection in order to improve signal to noise, and thus four images were produced for each experiment (Figure 2.3). The four spin-echo images were used to calculate T2 images according to the following equation:

$$I(t) = A * \exp(-t/T2) \quad (2.1)$$

where I = NMR intensity of spin echo

t = time of spin echo after 90 degree pulse

T2 = spin-spin relaxation time

A is proportional to spin density and is influenced by rf strength and short T2 components.

2.2 Results - Non-fixed brain

The four spin-echo intensity images from the non-fixed irradiated brain are shown at the top of Figure 2.4. From the intensity values of these images, T2 and A images were calculated (bottom of Figure 2.4). The first spin-echo image shows a decrease in intensity on the irradiated side (Figure 2.5). However, this contrast between right and

IMAGE RECONSTRUCTION FROM A GROUP OF ECHOES

(CARR-PURCELL-SEQUENCE , MEIBOOM-GILL-MODIFICATION)

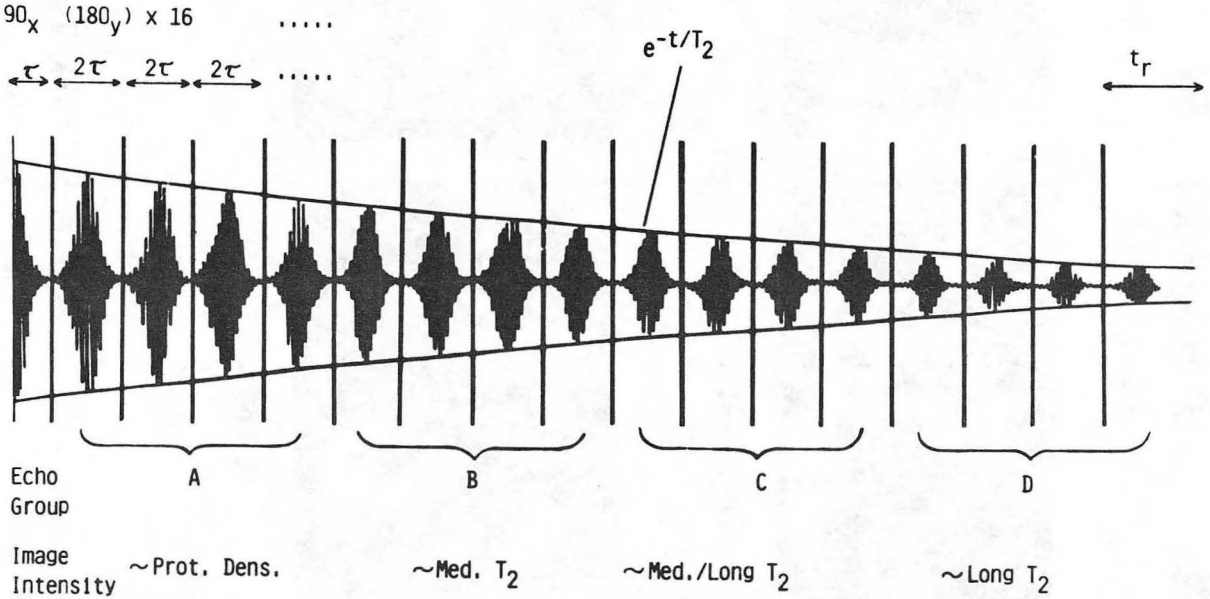

Figure 2.3 - NMR signal during the Carr-Purcell-Meiboom-Gill spin-echo train. The echos from group A are averaged to give an image strongly influenced by proton density and the echos from group D are averaged to give an image strongly influenced by long T2 relaxation times. (Courtesy of Dr. B. Knuttel, Bruker Instruments)

XBL 8210-3118

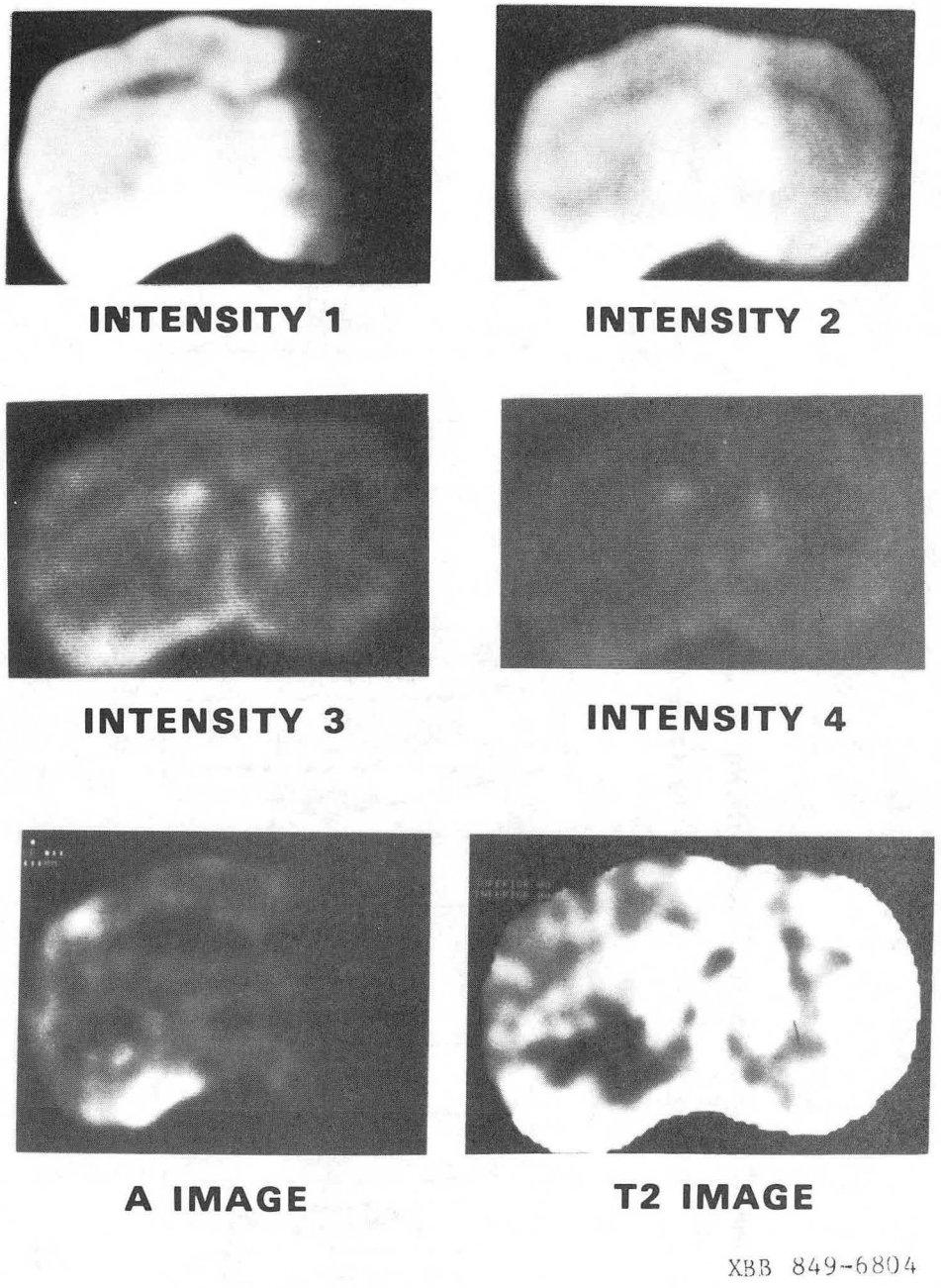

XBB 849-6804

$$I = A \cdot EXP(-t/T2)$$

Figure 2.4 - Intensity and parametric images from non-fixed irradiated rat brain (3000 rads). Irradiated side is on viewer's right.

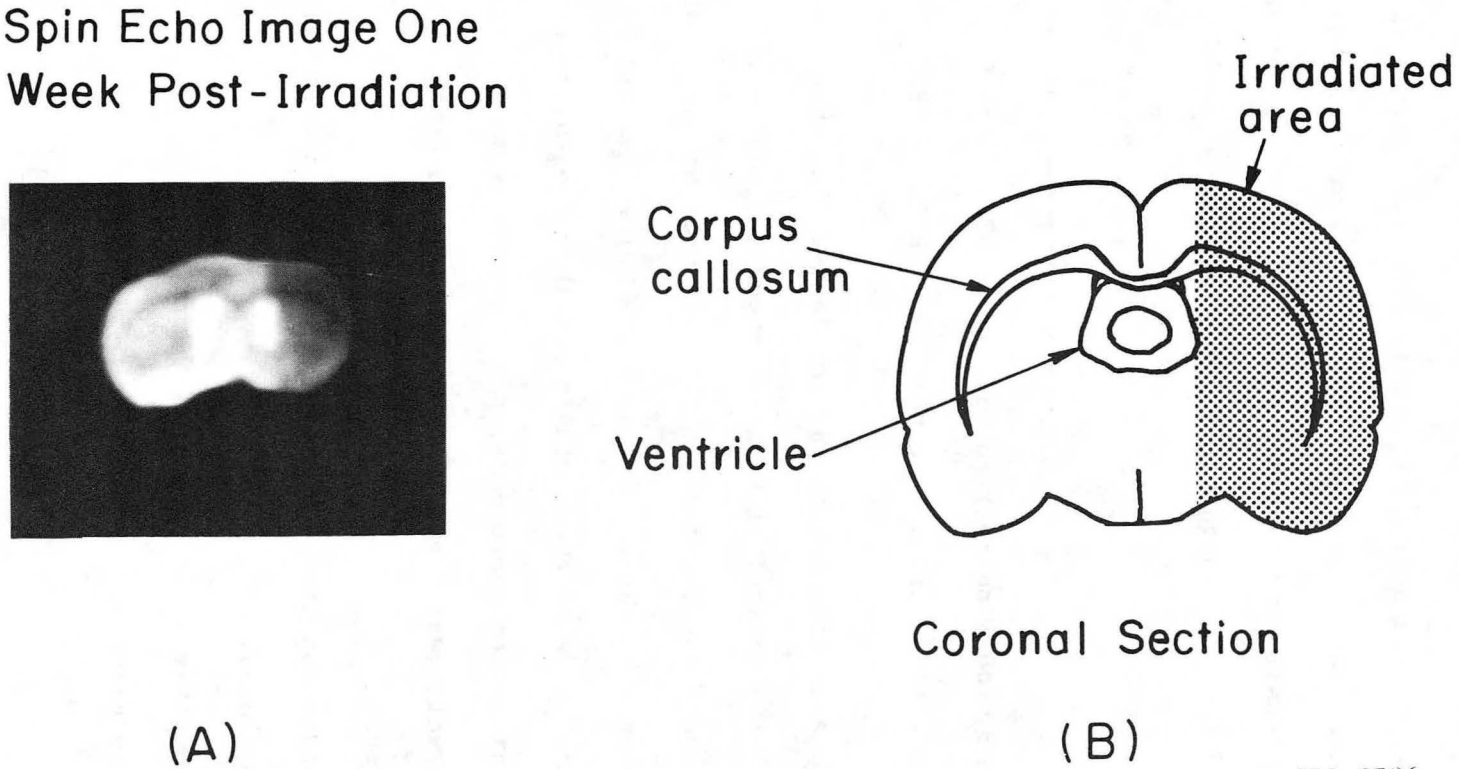

Figure 2.5 - Spin-echo image from group A echos (Fig. 2.3) with anatomical diagram.

left sides of the brain is not seen in the other spin-echo images in Figure 2.4. In order to understand the spin-echo intensity contrast in these images, the average intensity from two regions of interests which represented the right and left cortex were defined and this average signal intensity was plotted as a function of spin-echo delay time (Figure 2.6). The calculated T2 and A values are shown below.

	A	T2 (msec)
left side (control) cortex	437.	59.0
right side (irrad.) cortex	276.	69.7

The irradiated side region had a longer T2 than the control side; however, the control side had a larger computed A value. This explains why the radiation induced contrast was seen on the first spin-echo image and not on the others. The larger A value (related to spin density) on the control side of the brain is possibly due to an increase in total free water. From these data, there are three main facts:

1) The A value was greater on the control side than on the irradiated side cortex.

2) T2 relaxation time was greater on the irradiated side cortex (more mobile protons).

3) The decrease in intensity on the irradiated side image is due to lower spin density.

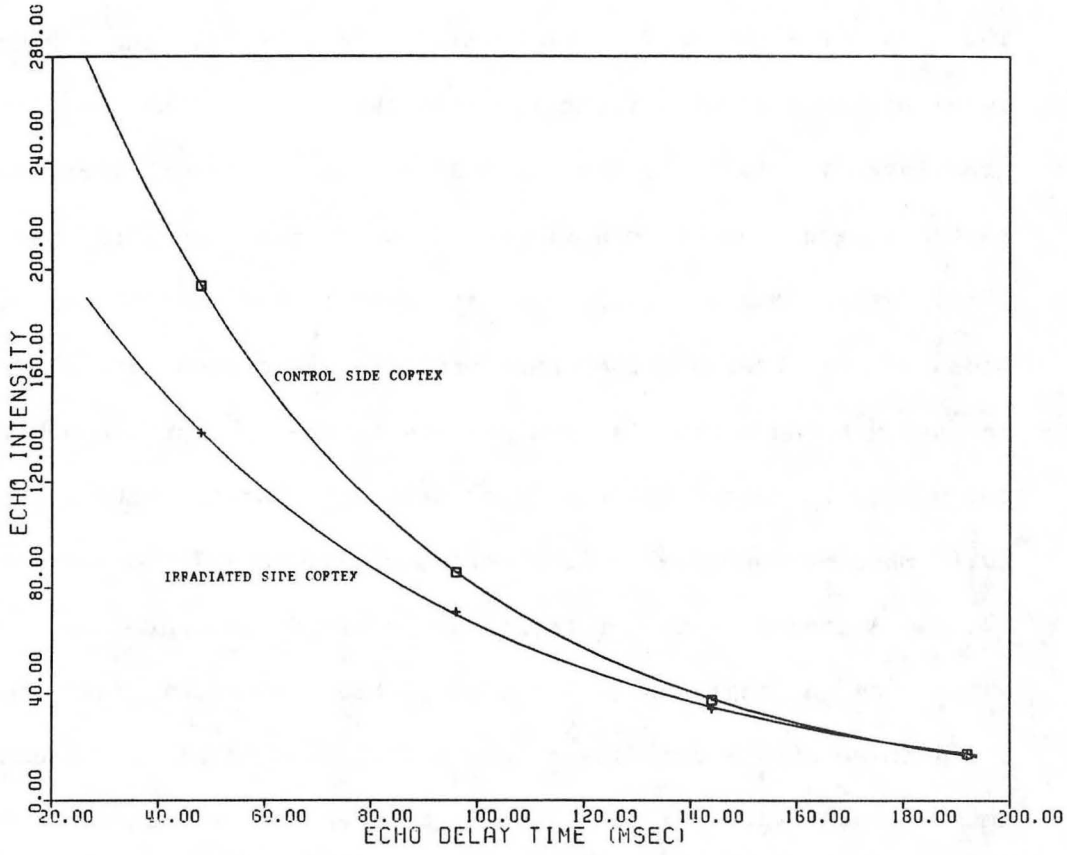

XBL 849-3687

Figure 2.6 - Plot of echo intensity vs. echo delay time from regions of interest of the control (boxes) and irradiated side (pluses) cortex. The solid line shows the computer fit through the data points using equation 2.1.

2.3 Results - Fixed brain

Two coronal sections from the formalin fixed brain were imaged. The top of Figure 2.7 shows coronal spin-echo, T2, and A images at the level of the reticular formation, and the images show an increase in gray level intensity on the irradiated side. Although formalin fixation causes a reduction in both T1 and T2 relaxation time (Richards et al., 1982), the images still show contrast between irradiated and control sides of the brain. The sub-cortical structures are very low in intensity because the fixation process reduces the proton mobility. The calculated T2 values for the irradiated and control cortex are 49.2 and 40.1 msec, respectively. The bottom of Figure 2.7 shows the spin-echo, T2, and A images of the brain at the level of the anterior commissure, which was a region near the edge of the beam path. The intensity and the A image show a decrease on the irradiated side; however, the T2 image shows very little contrast between the two sides. The two main results from these data are:

1) Image contrast between irradiated and control side was still seen on the images of formalin-fixed brain.

2) T2 relaxation time was greater on the irradiated side (more mobile protons).

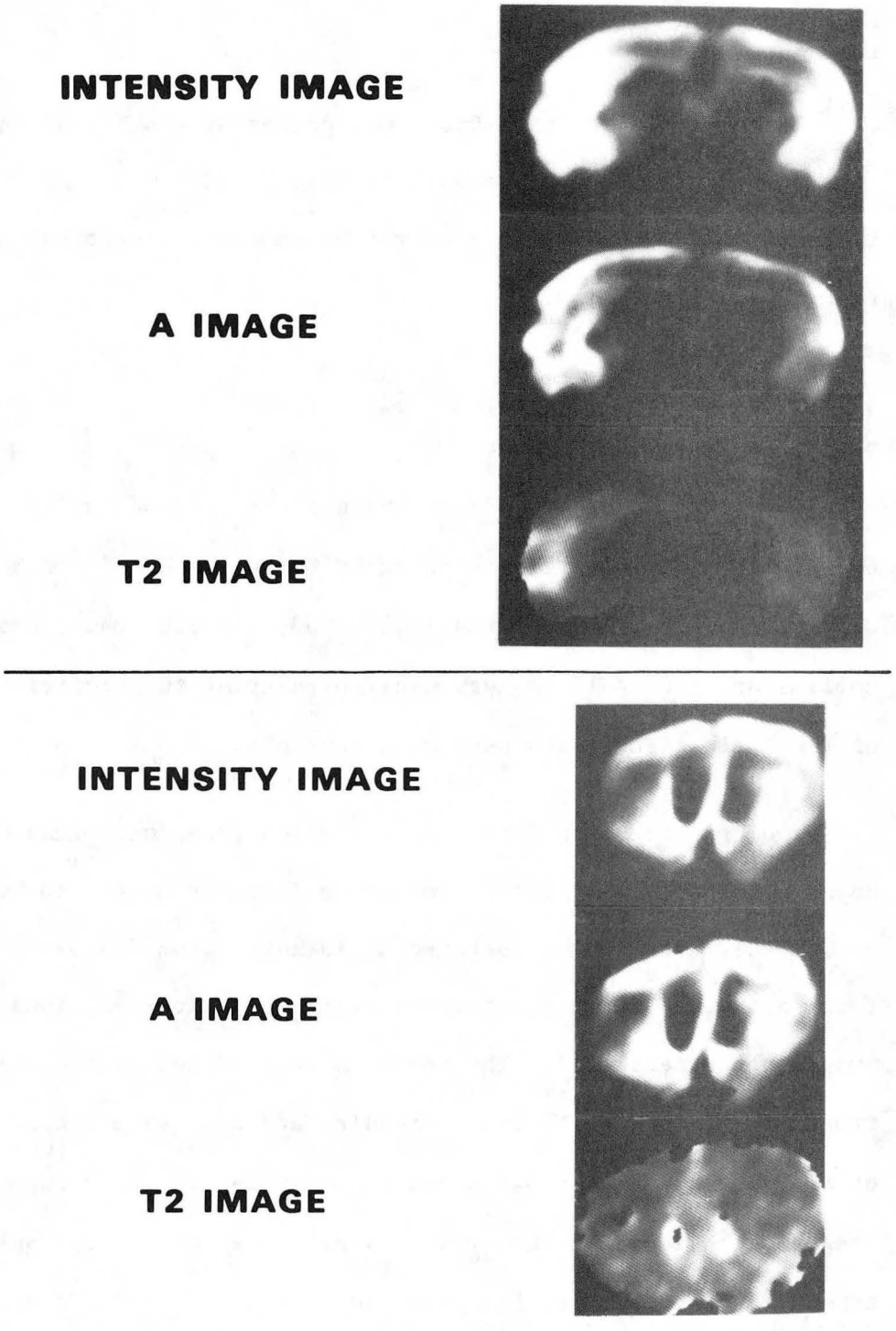

Figure 2.7 - Images of formalin-fixed irradiated brain (3000 rads) at two different levels of the brain. Irradiated side is on viewer's left.

XBB 849-6805

CHAPTER 3. 2D FOURIER TRANSFORM SPIN-ECHO IMAGING

In collaboration with Drs. George Wesbey and Barry Englestad, an experiment was done to measure in vivo T1 and T2 proton NMR relaxation times of helium beam irradiated rat brains as a function of dose and time after irradiation.

3.1 Methods

The left hemisphere of the brain of 16 Sprague-Dawley rats (age - 60 days) was irradiated according to the procedure described in section 2.1. Groups of rats received 1000, 2000, and 3000 rads, and a D-shaped collimator (10 X 13 mm) was used to restrict the radiation to one side of the brain. Four rats served as controls.

Two or three rats from each radiation group were imaged 14 and 52 days at the small animal imager designed by Larry Crooks (Kaufman et al., 1982). The imager operated at 15 Mhz proton frequency and produced four spin-echo images for 5 different anatomical sections (total of 20 images per experiment). The images were produced using the 2D-Fourier transform method with phase-encoding and selective excitation (Kaufman et al., 1982). Figure 3.1 shows an example of 5 sequential coronal images which included the eyes, brain, and spinal cord. Spin-echos were taken at 28 and 56 msec for both the .5 and 2. second repetition rates (Figure 3.2). Figure 3.3 shows the four spin-echo intensity images for one coronal section which included the brain.

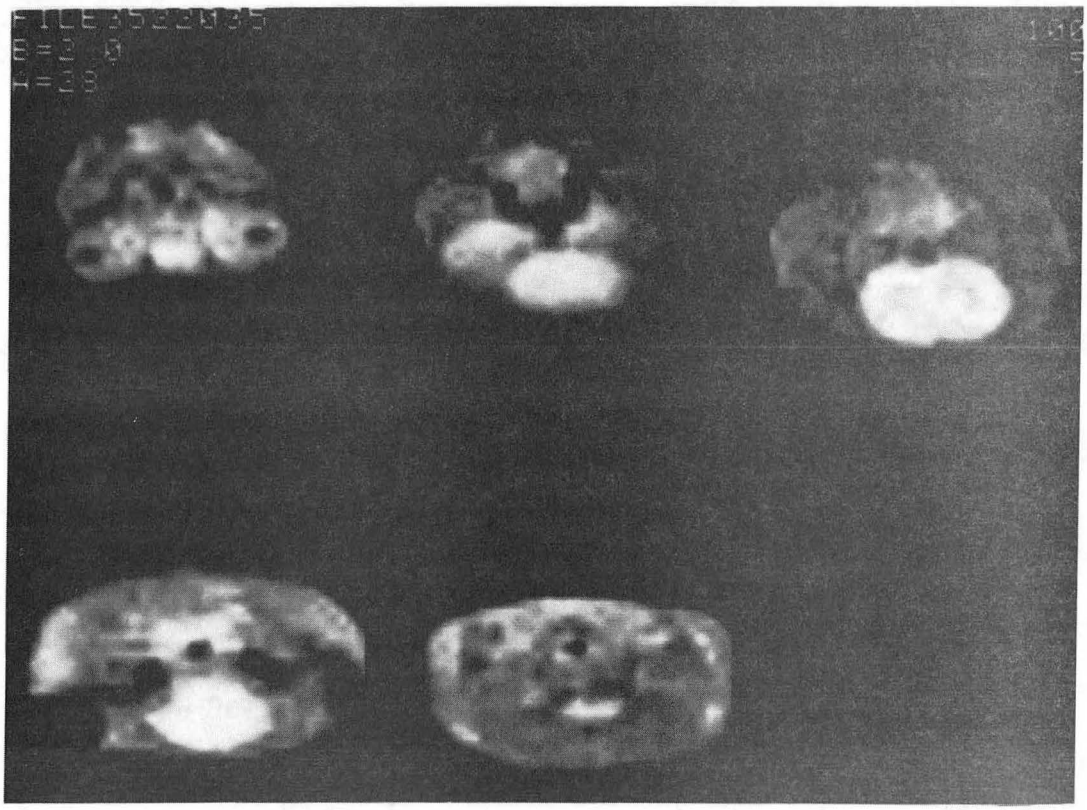

XBB 845-3978

Figure 3.1 - Five sequential spin-echo images using a 2 second repetition rate and 28 msec echo time.

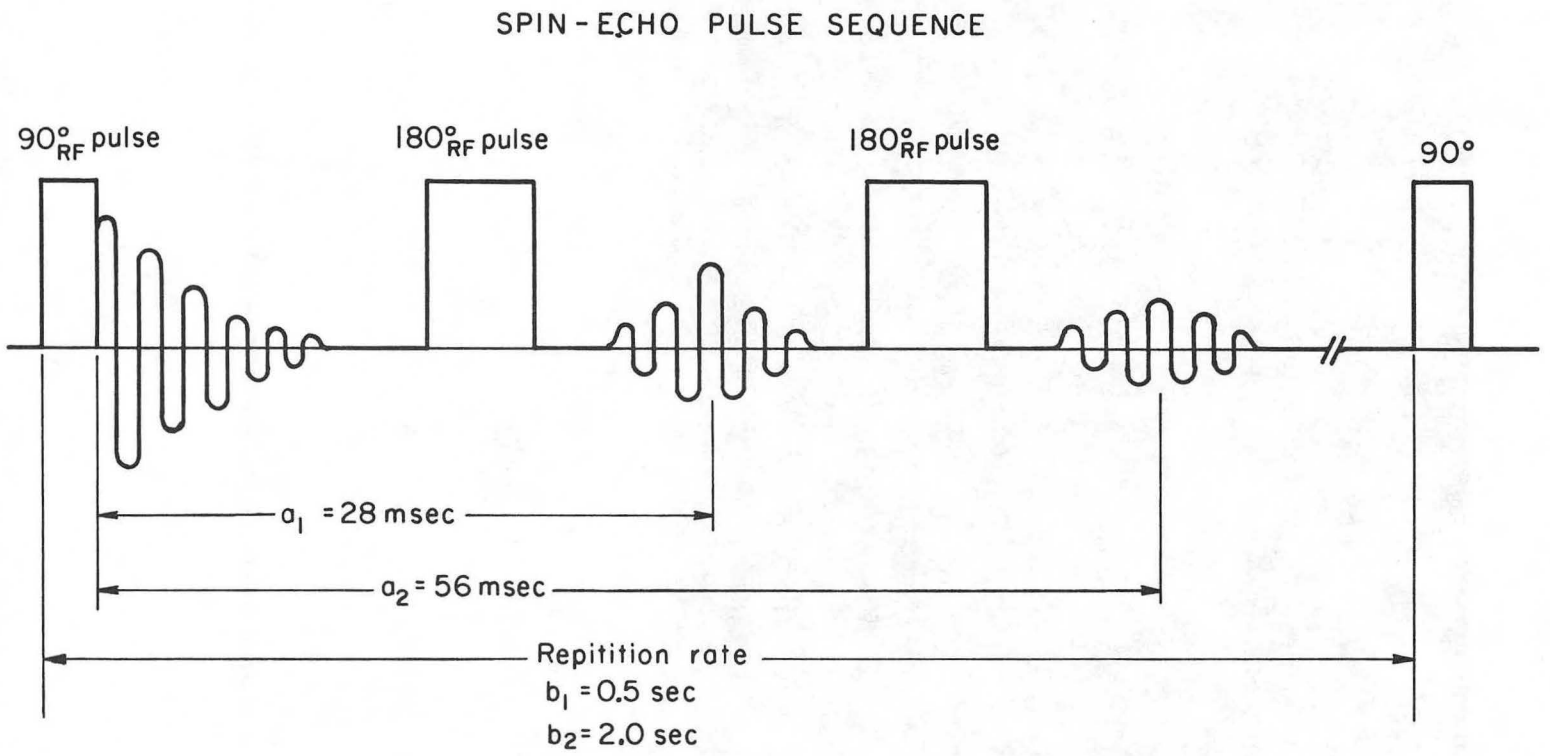

Equation used to calculate T1 & T2 :

$$I = H\, f(u) \left[\exp(-a/T_2)\right] \left[1 - \exp(-b/T_1)\right]$$

H = hydrogen density
f(u) = flow factor
T_2 = Spin - spin relaxation
T_1 = Spin - lattice relaxation

XBL838-3906

Figure 3.2 - Spin-echo pulse sequence used for imaging. (Equation taken from Kaufman et al., 1982).

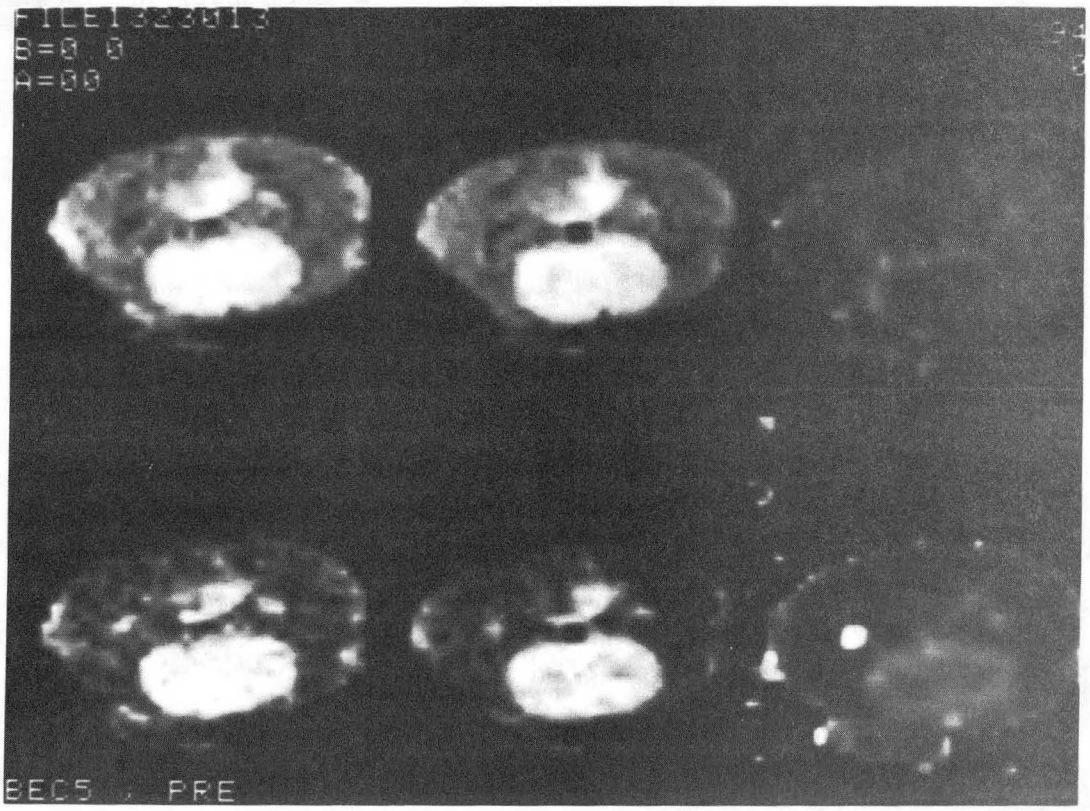

Figure 3.3 - Four intensity images (left) used to calculate the T1 image (upper right) and the T2 image (lower right).

XBB 845-3977

T1 images were calculated by using the intensity values from the 28 msec echo from both the .5 second and 2 second repetition rate and then fitting the intensity values to the following equation:

$$I(tr) = A1 * (1 - \exp(-tr/T1) \qquad (3.1)$$

where I = intensity

tr = repetition time

T1 = spin-lattice relaxation time

A1 = amplitude factor related to spin-density and flow.

The T2 images were calculated by using the intensity values from the 28 and 56 msec echo from the 2 second repetition rate and the intensity values were fit to equation 2.1.

Regions of interests which represented right and left sides of the cerebral cortex were chosen by 1)automatically contouring the brain with a threshold detection routine (courtesy of Dr. Sam Pitluck) and 2) extracting pixels which lie immediately inside the contour on both sides of the brain. Figure 3.4 shows an image with the brain contour and regions of interests. The intensity values from the regions of interests were averaged and fit to the equation 2.1 and 3.1 to calculate T1 and T2.

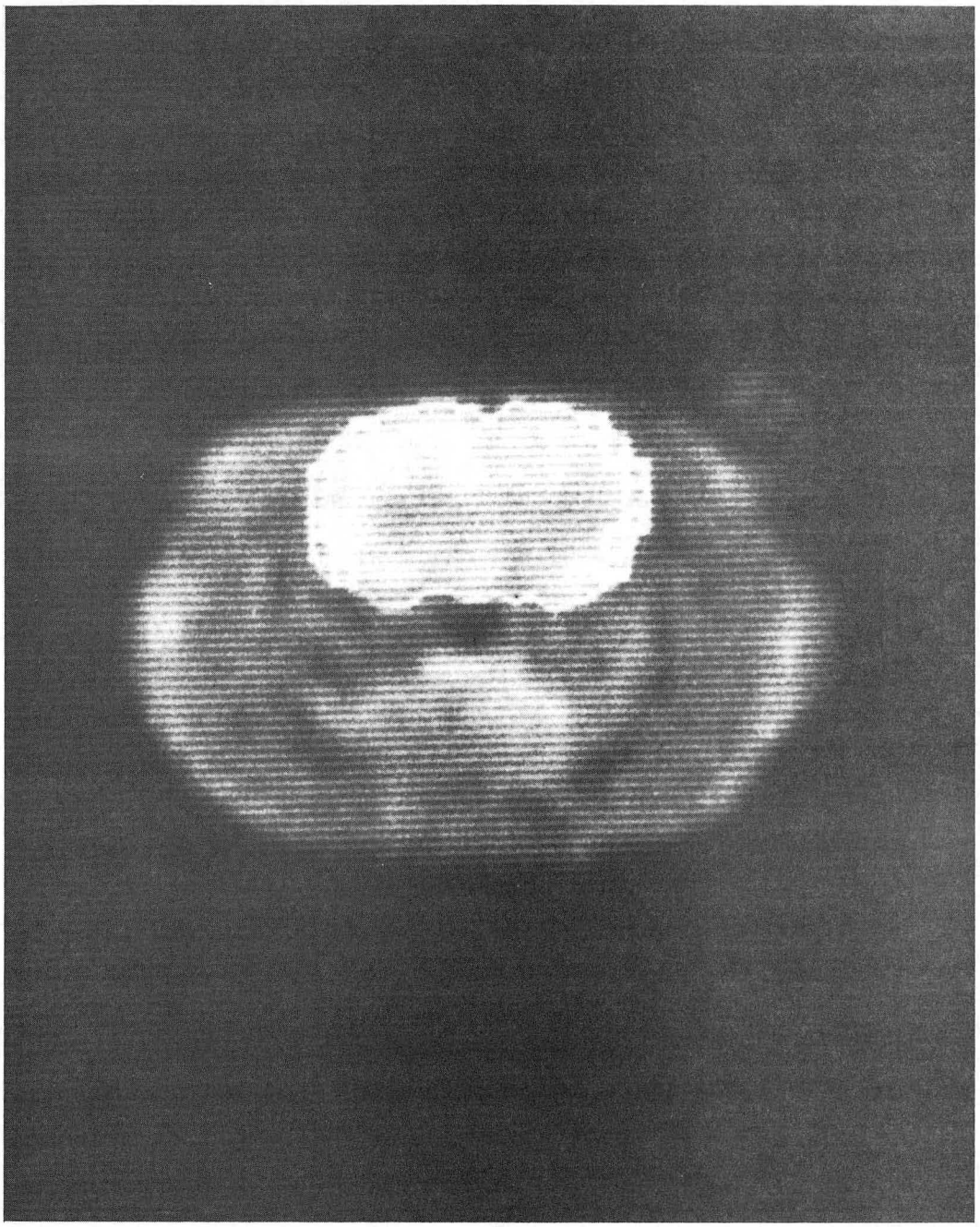

Figure 3.4 - Spin-echo image of irradiated brain with brain contour and cortical regions of interest (boxes) chosen by automatic contouring (See text).

XBB 837-6635

3.2 Results

Imaging-

As shown in Figure 3.5, an increase in T1 of the control side of the 3000 rad rats can be seen in the T1 image; however, this effect was not seen on the T1 images of control rats. This increase was also seen using the projection imaging technique of chapter 4. Little contrast between the two sides was seen on the T2 images of irradiated and control rats. However, the T2 values calculated from this technique were probably not accurate because of spin diffusion (Wesbey, 1984). The A1 and spin-echo images of 3000 rad irradiated rats displayed a similar pattern: there was a decrease in intensity on the irradiated side with respect to the control side. This effect was also seen using the projection imaging technique (see section 4.3.3). In order to understand the contrast seen in the spin-echo images, a plot was made of repetition time versus intensity for regions of interest from both the irradiated side and the control side of the brain. The bottom of Figure 3.6 shows an example of the relaxation curve for one of the 3000 rad brains at 14 days after irradiation. The decrease in intensity on the irradiated side is not due to a difference in T1, but rather a decrease in the A1 value as shown in the relaxation curve. The relaxation curves are similar for the left and right sides of the control spin-echo image (top of Figure 3.6).

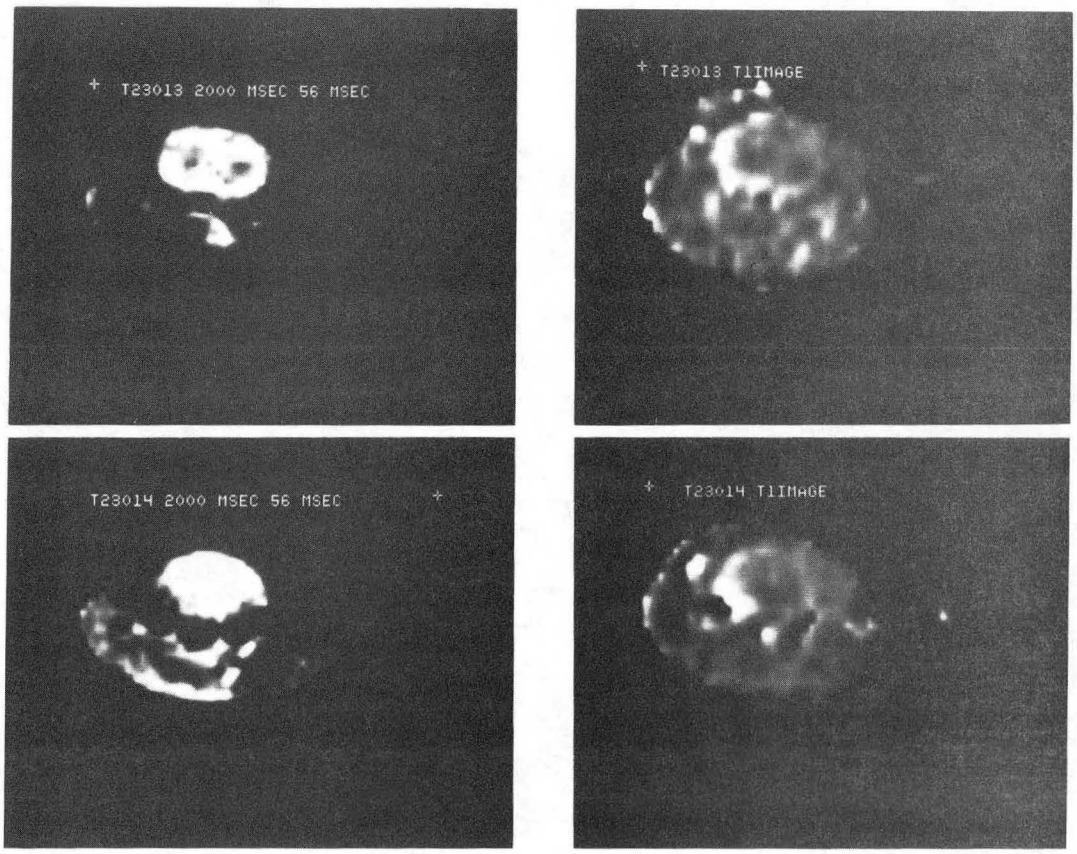

Figure 3.5 - Spin-echo images (left) and T1 images (right) at two different levels of the same rat brain.

XBB 837-6637

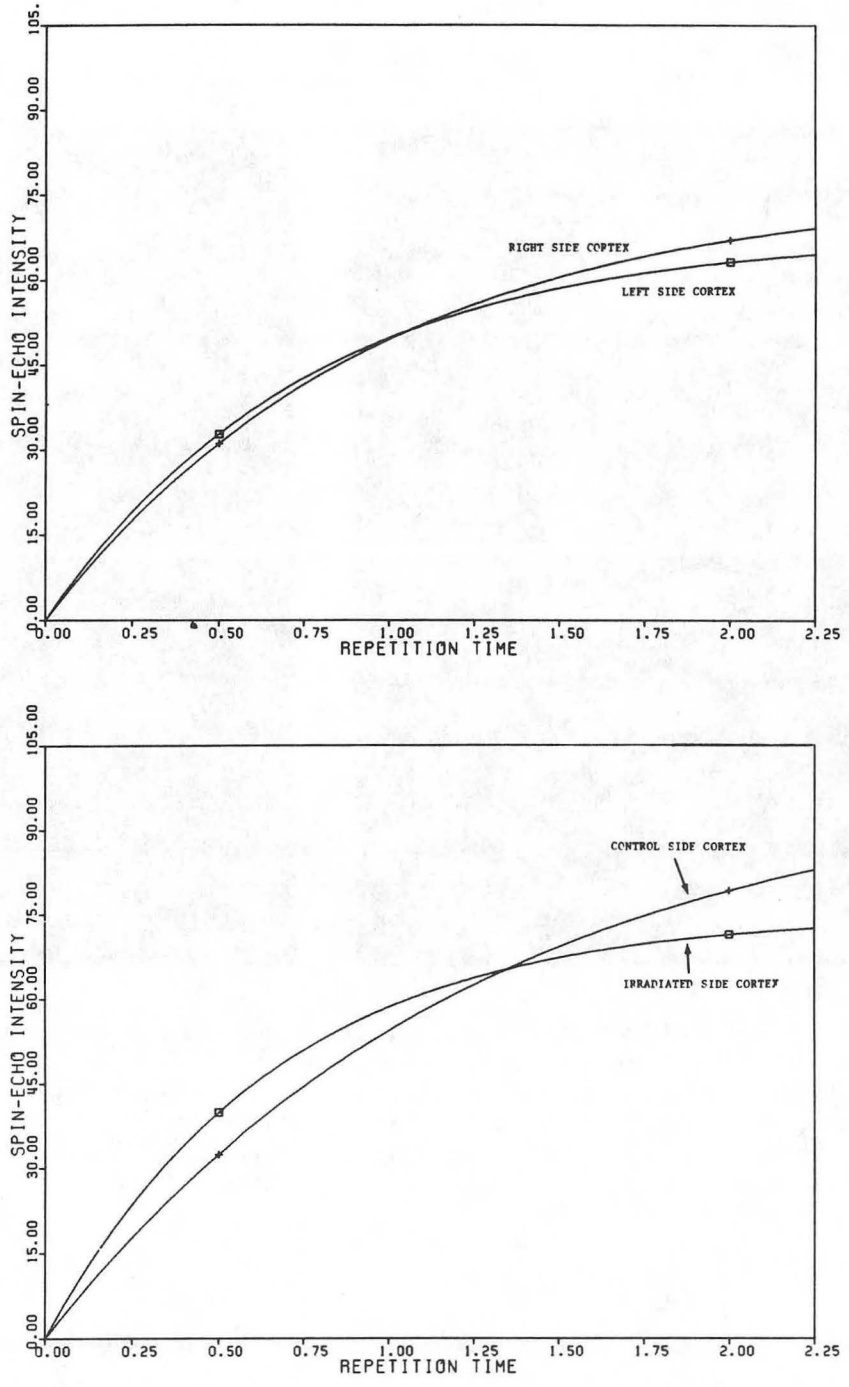

XBL 849-3686

Figure 3.6 - Plots of spin-echo intensity vs. repetition time for control brain (top) and irradiated brain (bottom). The solid line shows the calculated fit through the two data points using equation 3.1.

Regions of interest-

Using the regions of interest shown in Figure 3.4, T1 and T2 values were calculated as a function of dose. At 14 days, T1 increased with dose on the control side and decreased slightly with dose on the irradiated side (Figure 3.7). At 52 days, an increase in T1 on the control side was seen in 3 (T1 value greater than 1200 msec) of the irradiated brain images. A decrease in T1 was seen on the irradiated side in 7 of the irradiated animals (T1 value less than 700 msec, as shown in Table 3.1). However, the spread of the T1 values was very large compared with the data at 14 days.

Table 3.1 - T1 values at 52 days post irradiation.

	IRRADIATED SIDE		CONTROL SIDE	
RAT NO.	DOSE	T1 (MSEC)	DOSE (rads)	T1 (MSEC)
1	3000.	584.	3000.	1035.
2	3000.	577.	3000.	1034.
3	3000.	691.	3000.	1054.
4	3000.	928.	3000.	834.
5	2000.	972.	2000.	742.
6	2000.	679.	2000.	876.
7	2000.	622.	2000.	1153.
8	1000.	630.	1000.	928.
9	1000.	705.	1000.	1453.
10	1000.	680.	1000.	1260.
11	0.	817.	0.	1044.
12	0.	930.	0.	1145.
13	0.	796.	0.	733.

NOTE: The control side region of interest possibly included CSF fluid which would explain why the T1 values of the left and right sides of control animal brains are not the same.

Figure 3.8 shows the dose-response curve for the T1 right/left ratio for both 14 and 52 days. The data at 14 days have much smaller error bars than the data at 52 days. The ratio of right cortex T2 to left cortex

T2 was slightly shorter for the irradiated brains than for the controls (Figure 3.9).

In summary, the main results from these experiments are: 1) T1 and A1 values decreased on the irradiated side; and 2) T1 and A1 values increased on the control side of irradiated animals relative to control animals early after irradiation (14 days).

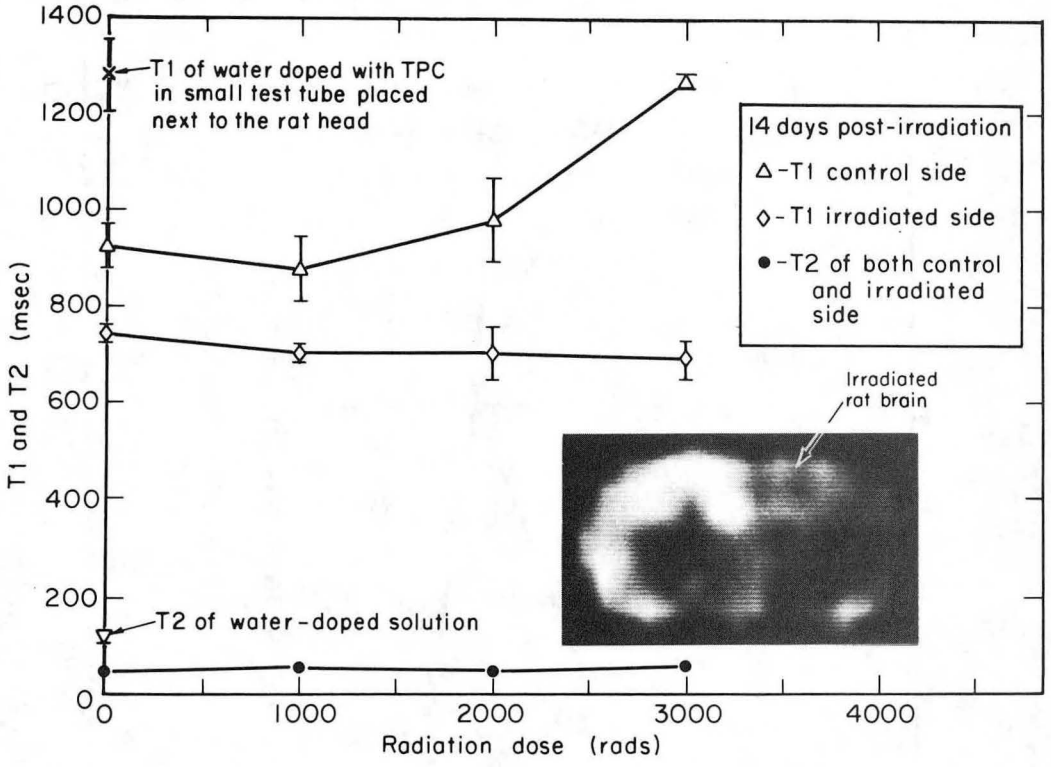

Figure 3.7 - Plot of helium beam radiation dose vs. T1 and T2 of both right (control side) and left (irradiated side) cerebral cortex 14 days post- irradiation. Insert: spin-echo image 14 days post-irradiation of a rat that received 3000 rads to the left side of the brain (see arrow). Contrast between cortical and sub-cortical areas is greater on the control side of the brain.

XBB 841-164

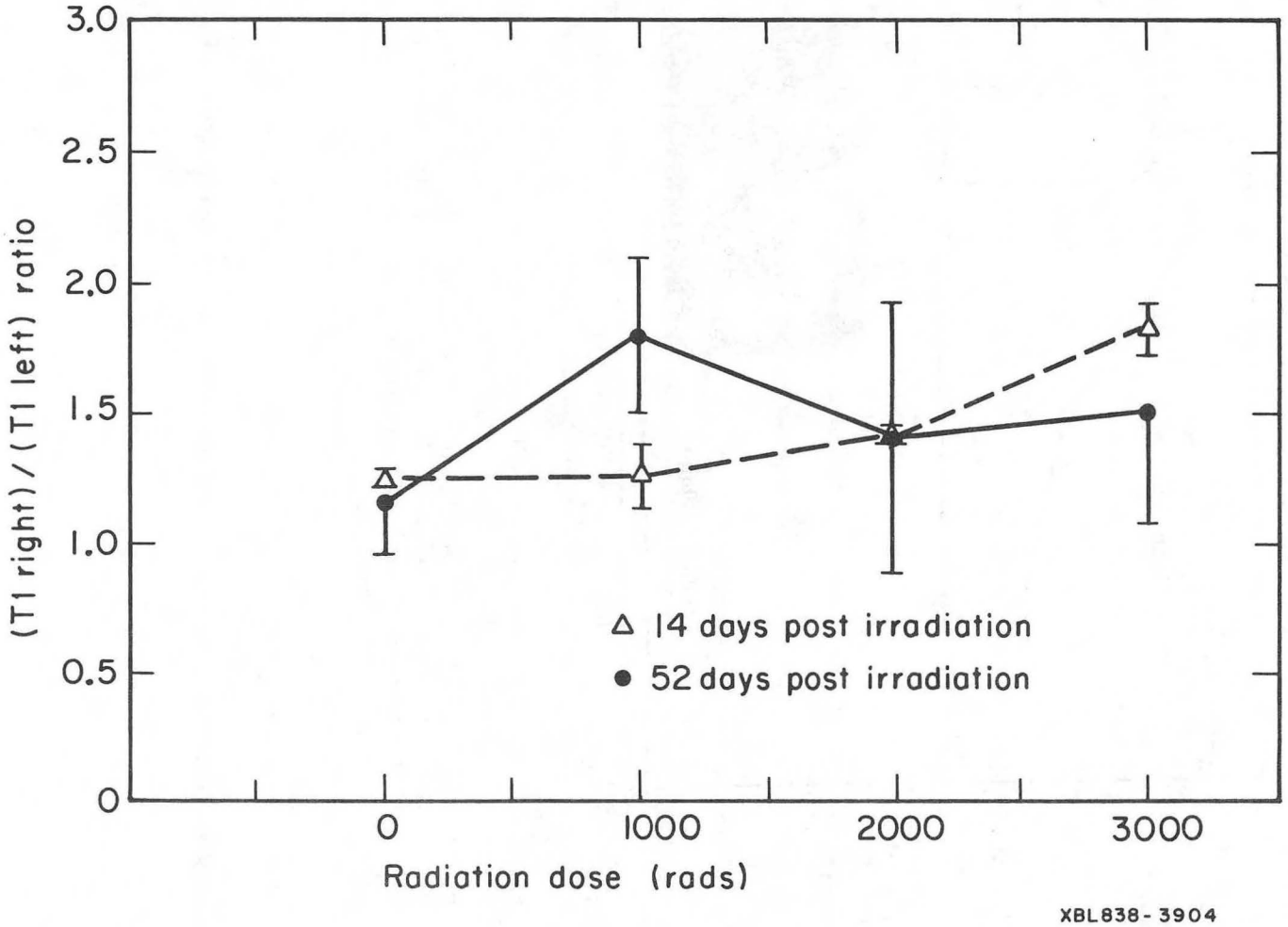

Figure 3.8 - Plot of dose vs. T1 right/T1 left ratio for both 14 days (dashed line) and 52 days (solid line) post-irradiation.

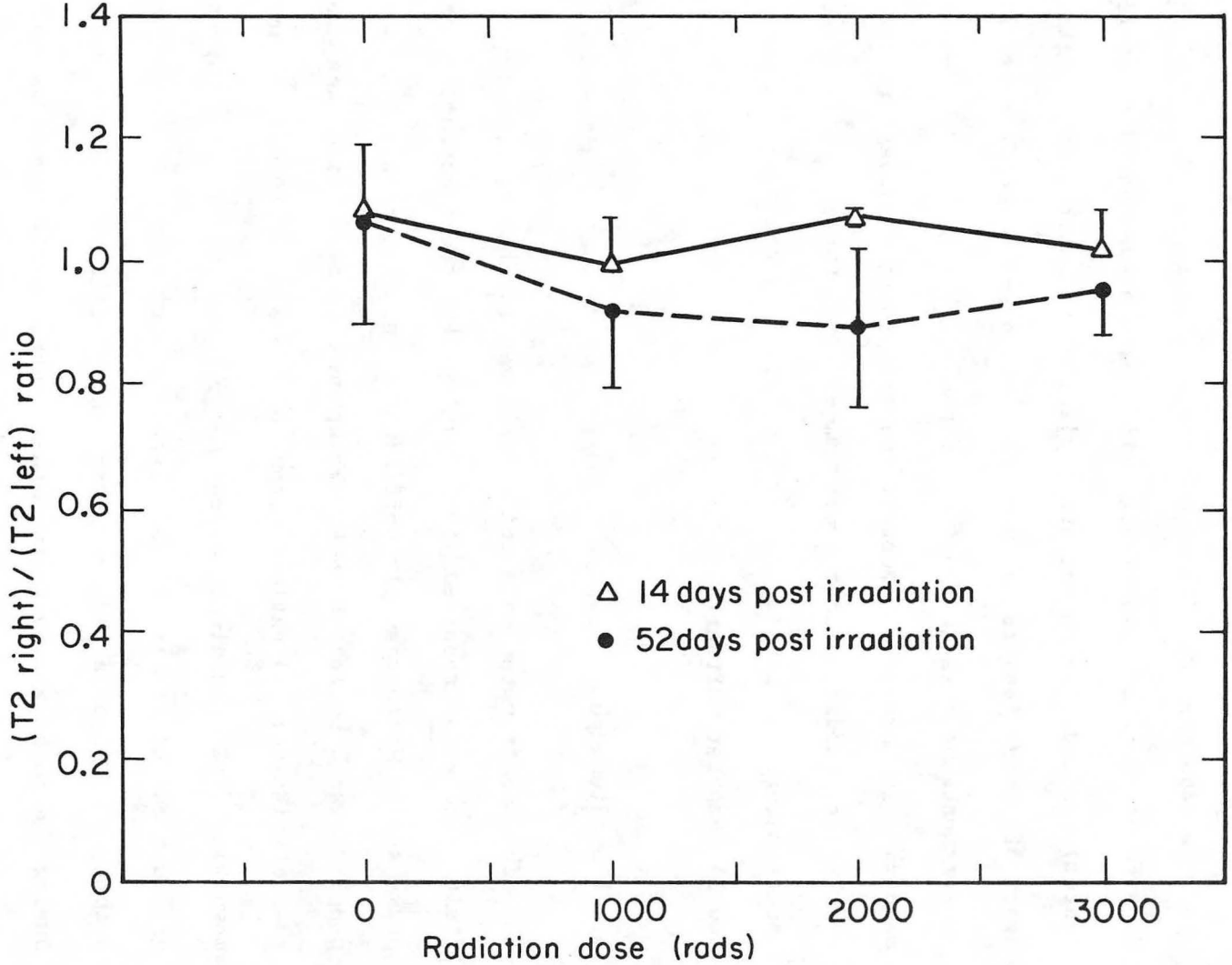

Figure 3.9 - Plot of dose vs. T2 right/T2 left ratio for both 14 days (solid line) and 52 days (dashed line) post-irradiation. XBL838-3905

CHAPTER 4. SATURATION RECOVERY WITH PROJECTION RECONSTRUCTION

4.1 Modifications of the UCB-180 spectrometer for imaging.

The 180 MHz FT NMR spectrometer built by the UCB chemistry department (Bruker 4.3 Tesla wide bore magnet and Nicolet 1180 data system) was modified to perform projection-reconstruction imaging. The goal of this conversion was to obtain accurate T1 relaxation time measurements of selected regions of the rat brain in a non-invasive manner. In order to convert the spectrometer to perform the imaging experiment, modifications were made in three aspects of the spectrometer: 1) gradient power supply; 2) probe body and electronics; and 3) computer software.

4.1.1 Gradient power supply.

The spectrometer shim coils were used for the X, Y, and Z magnetic field gradients required for imaging, but the spectrometer shim coil power supply did not supply sufficient bipolar current. A new power supply was built by Frank Upham et al. with the following characteristics: 1) current output of +/- 3 amps (used to achieve a magnetic field gradient strength of 3000 Hz/cm, see appendix for gradient calculation); 2) bipolar current source; and 3) current output controllable by computer DAC (digital to analog converter). During the imaging experiment, the power supply receives an analog signal from the computer and then supplies current to the gradient coils. The current magnitude is controlled by input analog signal level (see Figure 4.1).

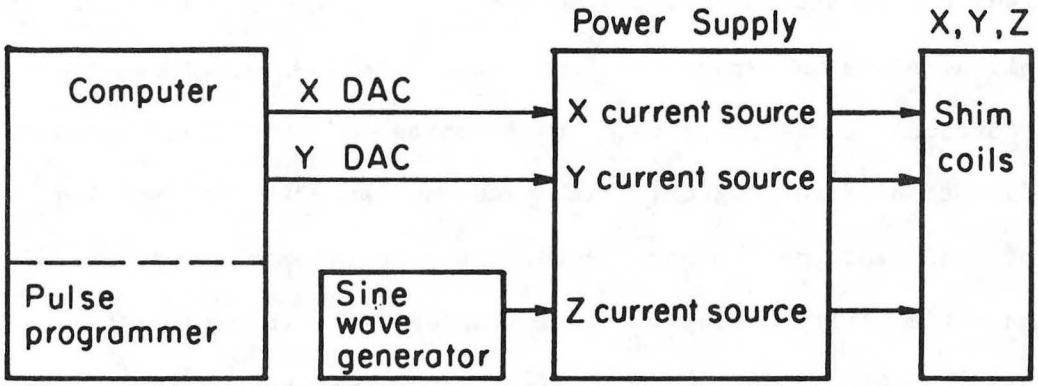

XBL 849-3685

Figure 4.1 - Hardware for 2D-projection reconstruction.

4.1.2 Rat body holder and manual adjustments

A cylindrical lucite holder was fabricated to house the rat while inside the magnet (Figure 4.2). The lucite holder sits on top of 3 aluminum poles which are free to slide along the base aluminum plate (which is attached to the bottom of the magnet). One of the poles had alignment marks (spaced at 1 mm intervals) engraved on it to allow reproducible and flexible positioning of the rat brain in the Z direction of the magnet. With these adjustments, the section of brain of interest can be positioned in the most homogeneous part of the main magnetic field. A rotational adjustment is also possible by releasing the three screws on the bottom of the base plate. This makes it possible to position the sagittal axis of the rat brain along the X or Y magnetic field gradient. The entire assembly down to the base aluminum plate fits inside a cylindrical aluminum shell in order to shield from outside rf leakage.

4.1.3 Head Holder

A small lucite holder was designed for the rat head in order to immobilize the rat and reproducibly position the left and right hemispheres of the rat brain in the center of the magnetic field. The inside of the holder was cone shaped so that the head fits tightly against the holder. Figure 4.3 is an X-ray picture of the rat in the holder. A wire was placed around the front two incisors of the rat and attached to screws on the top of the holder which held the head firmly against the cone. The head holder was attached to the top plate by two adustable screws.

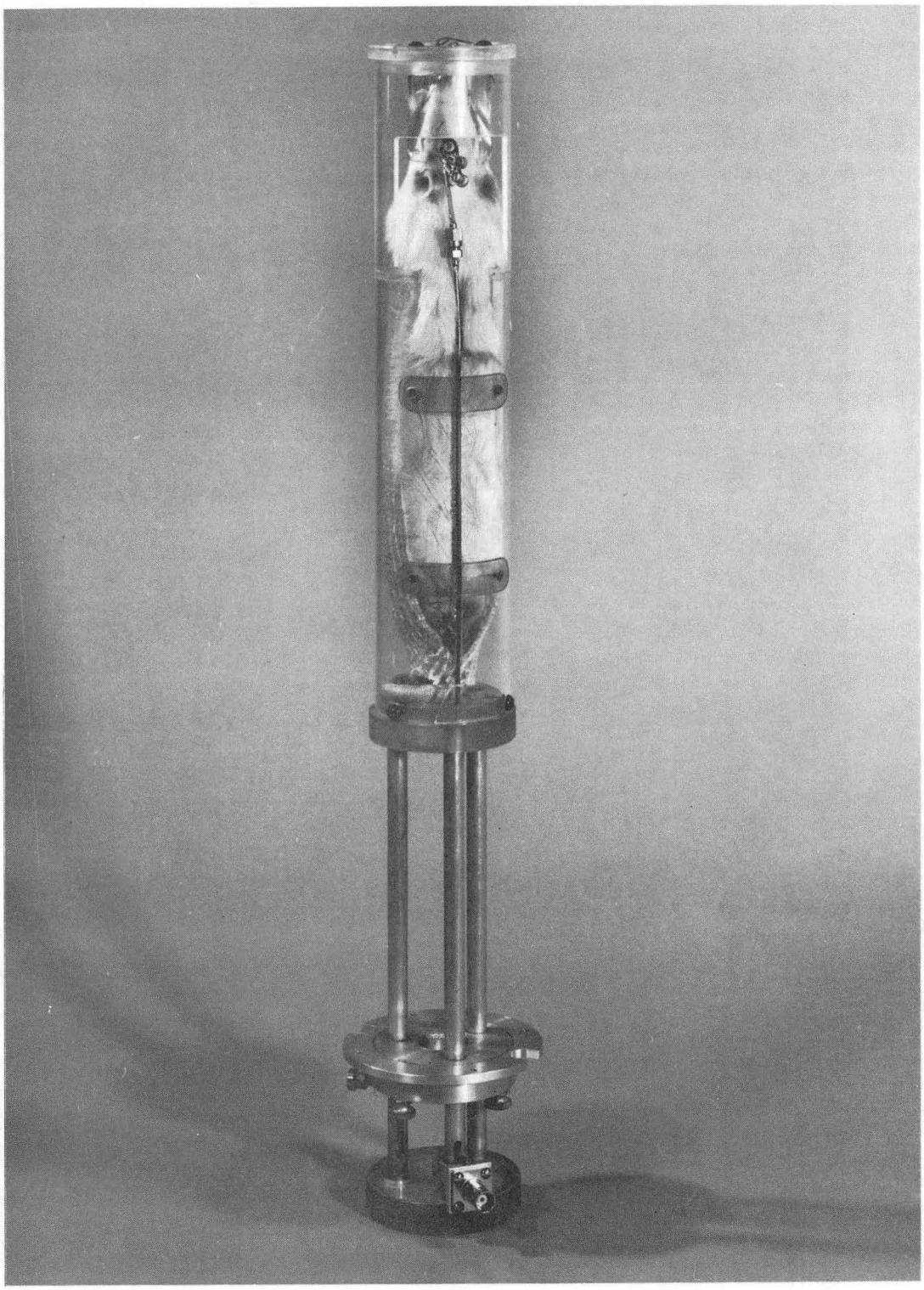

Figure 4.2 - NMR probe used for imaging and spectroscopy of the rat head in vivo.

CBB 833-2659

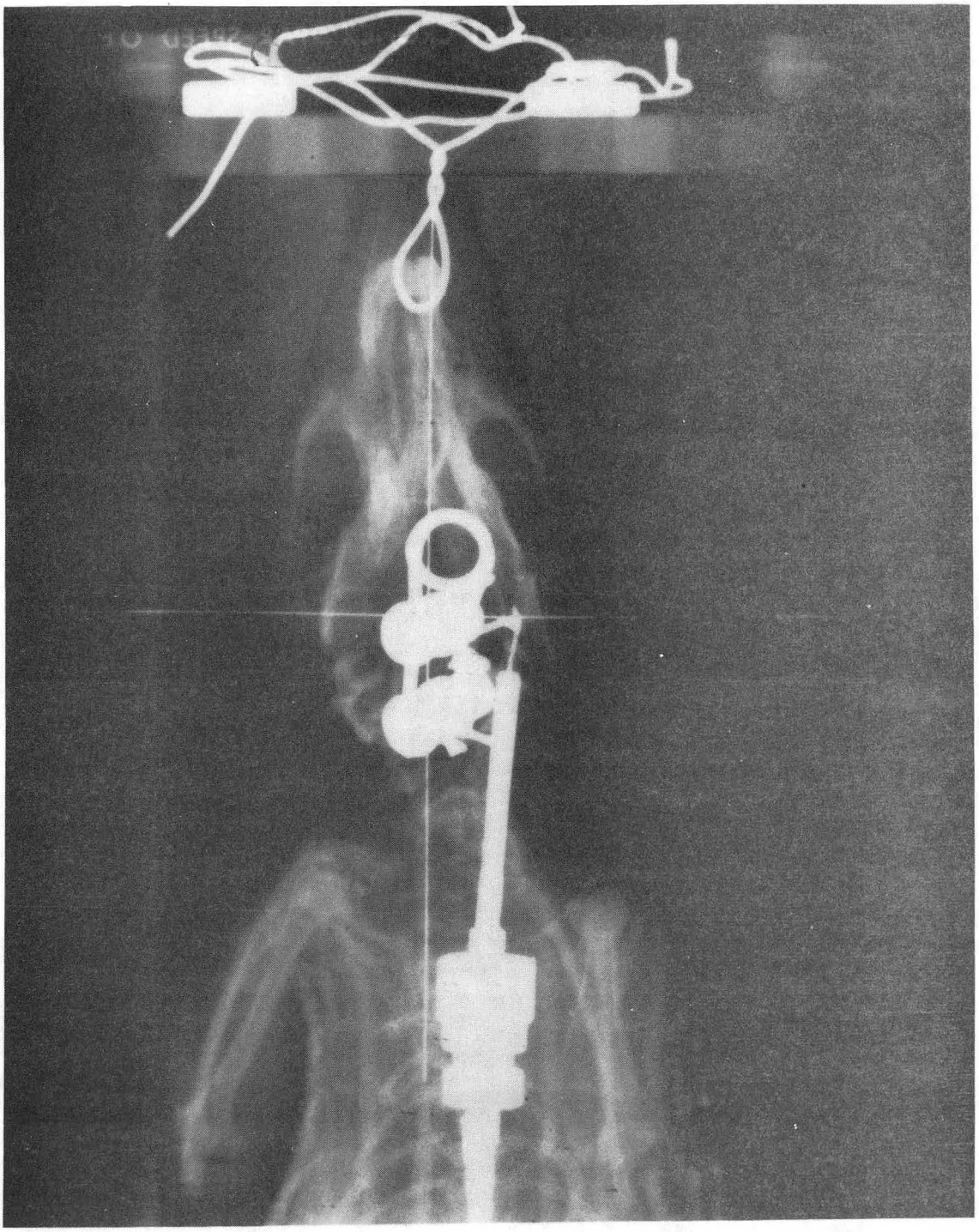

Figure 4.3 - X-ray of rat in NMR probe.

XBB 834-3487

4.1.4 RF electronic circuitry

The electronic circuitry consists of 1) the RF coil, 2) the tuning and matching capacitors, and 3) high frequency SMA connector for rigid coax cable (Figure 4.4). The surface coil (Ackerman et al.,1980) was chosen because of its high sensitivity and ease of implementation. A two-turn elliptical shaped surface coil (2.5 cm X 1.5 cm) was tuned to the proton frequency (180 MHz) using a sweep wave generator, oscilloscope, and RF detector connected to the probe. The tuning and matching capacitors (Johansen variable capacitors) were adjusted while observing the resonant frequency on the oscilloscope. The SMA connection made it possible to easily change from the measurement of one nucleus to another by simply replacing the tuned coil.

4.1.5 Computer software

4.1.5.1 Data acquisition

In order to perform imaging by the projection reconstruction technique, the magnetic field gradients were controlled outside of the pulse programmer (Figure 4.1). The value of the X and Y DACs were controlled by software which changed the values after each projection. Subroutines written by Jean Delayre for the Nicolet 1280 computer were adapted for the 1180 computer. The subroutine basically sweeps the gradient angle through 180 degrees by incrementing the angle in the

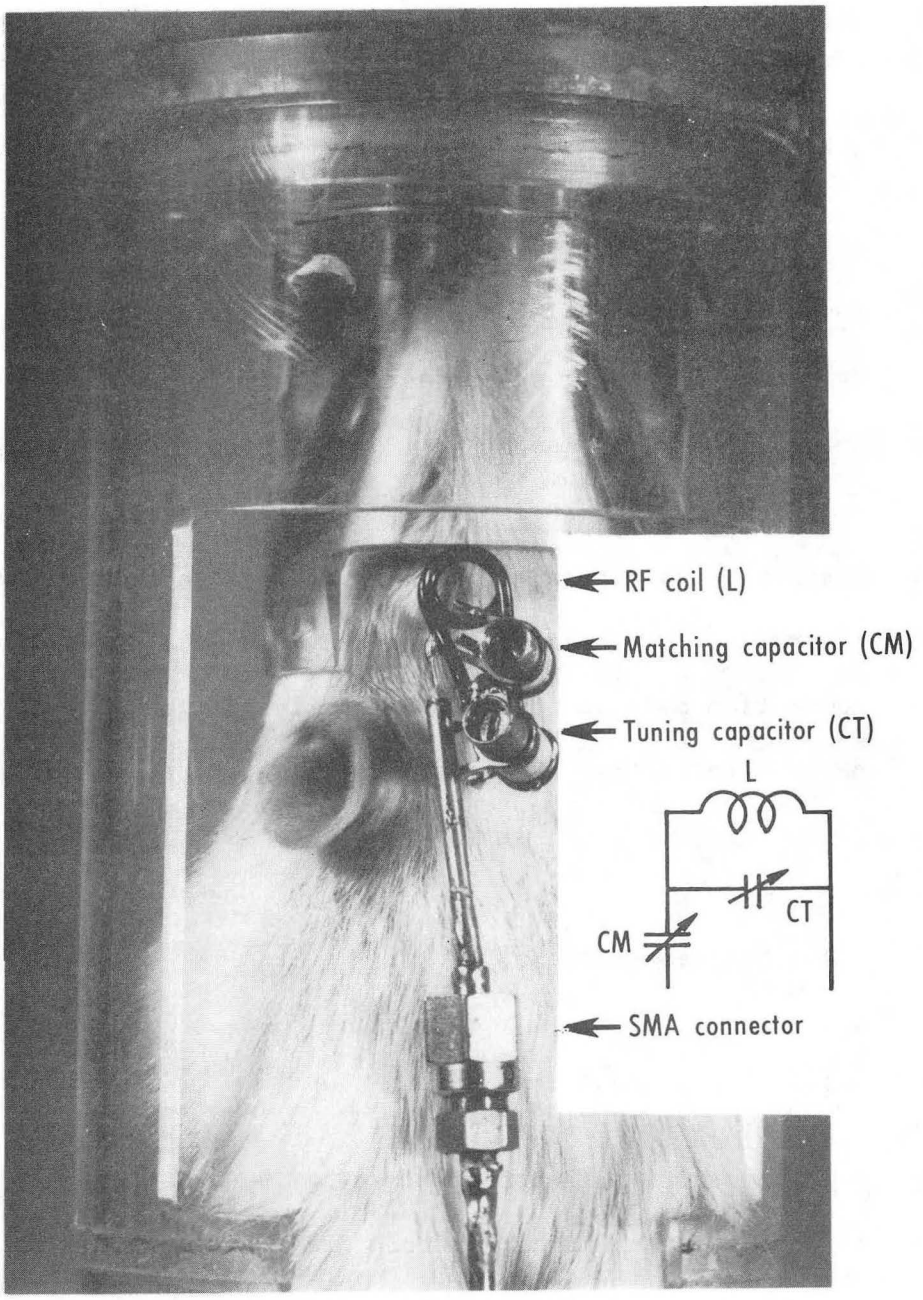

Figure 4.4 - Radio-frequency electronics of the surface coil.

XBB 842-802

following equations:

XDAC = Cosine(angle)

YDAC = Sine(angle)

The Nicolet program NTCFTB.180 was used to do the saturation recovery experiment. In this pulse sequence, the spins are saturated (i.e., no net magnetization left along the Z axis) first by giving several closely spaced "180" degree pulses at different phases and then a "90" degree rf pulse is applied after a variable delay time. The FID is acquired immediately after the 90 degree pulse and the amplitude of the signal is a measure of the magnetization that has re-aligned along the Z direction. The imaging gradient is left on during the pulse sequence. The steps in the computer program to perform the imaging experiment are listed below:

1. The magnetic field gradient is reset and the angle increment is chosen (the number of projections is calculated from the angle increment).
2. The magnetic field gradient is turned on and incremented by an amount chosen in step 1.
3. The saturation recovery experiment is performed while the gradient is left on.
4. The free induction decay is digitized and stored in memory.
5. Steps 2 through 4 are re-executed until the gradient angle has swept through 180 degrees.

No Z gradient was used in these experiments. Slice selection and thickness were defined by the surface coil sensitive region as described in the phantom studies of section 4.2.

4.1.5.2 Data transmission and image reconstruction.

The raw image data was transmitted over a phone line to the VAX computer where the image reconstruction was performed and displayed. New software was written on the VAX (program READNTC listed in the appendix) to interact with program IOTRAN (already existing) on the Nicolet computer. The data transfer occurs like this: program IOTRAN sends an SOS character to the VAX and then program READNTC returns an acknowledgement character. IOTRAN, then, proceeds to transmit the data, block by block, to the VAX. Software was also written to convert Nicolet 20-bit words to VAX words and put the data in the correct format for the reconstruction program (routine READ, see appendix). Image reconstruction was done by Fourier transforming the FIDs to get the gradient projections and then by performing the standard filtered back projection algorithm. The flow of NMR information from the rat brain to the image display hardware is shown in Figure 4.5.

4.2 Phantom studies

Two different phantoms were imaged to test the imaging process for accuracy in gradient projections, image reconstruction, and T1 relaxation time measurement. The phantom shown at the top of Figure 4.6 consisted of three 5mm NMR tubes filled with water. The phantom was placed next to the elliptical-shaped surface coil and imaging was done

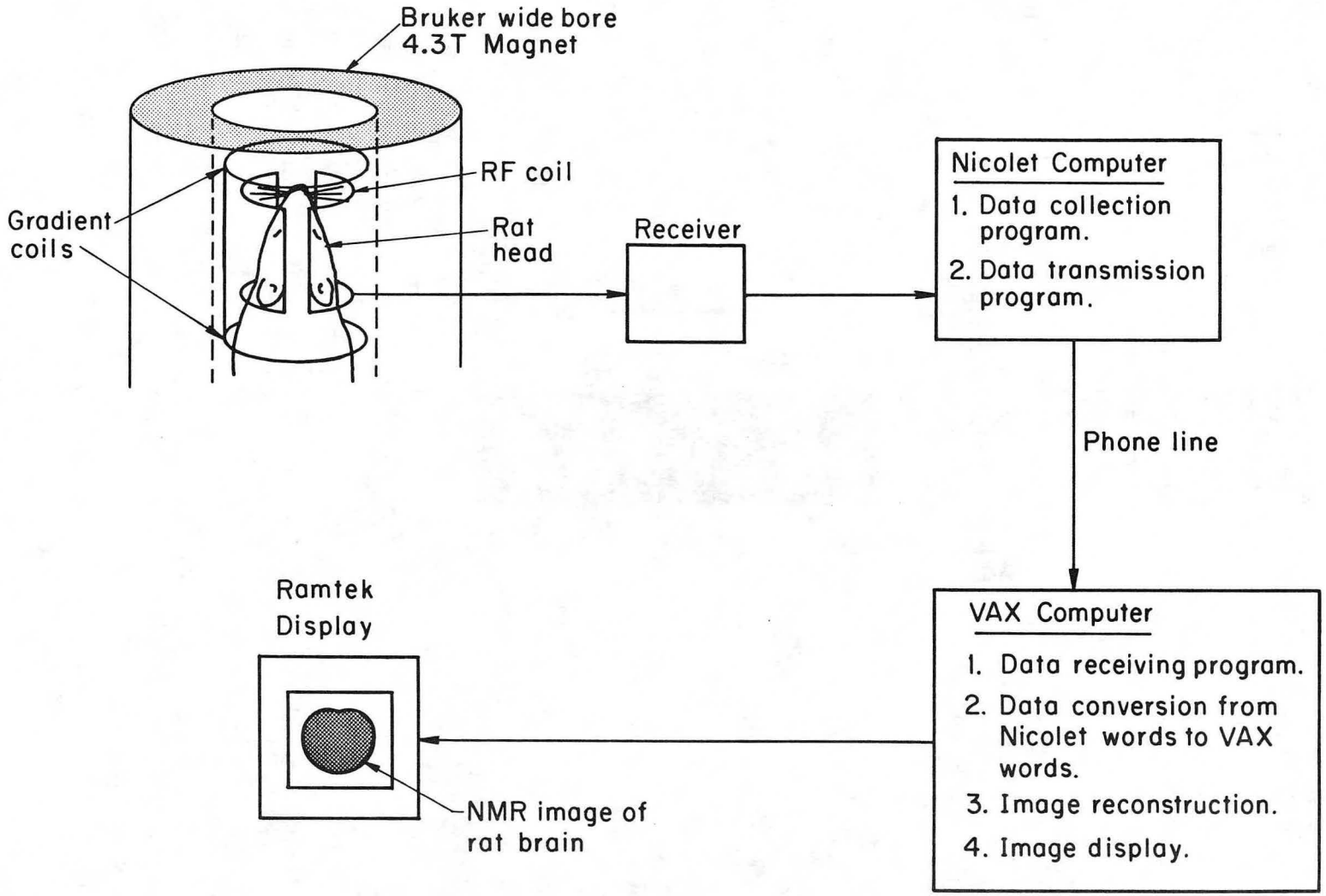

Figure 4.5 - Flow of NMR information from rat brain to image display. XBL842-7574

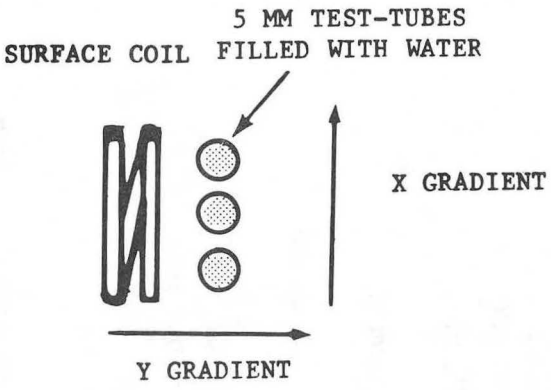

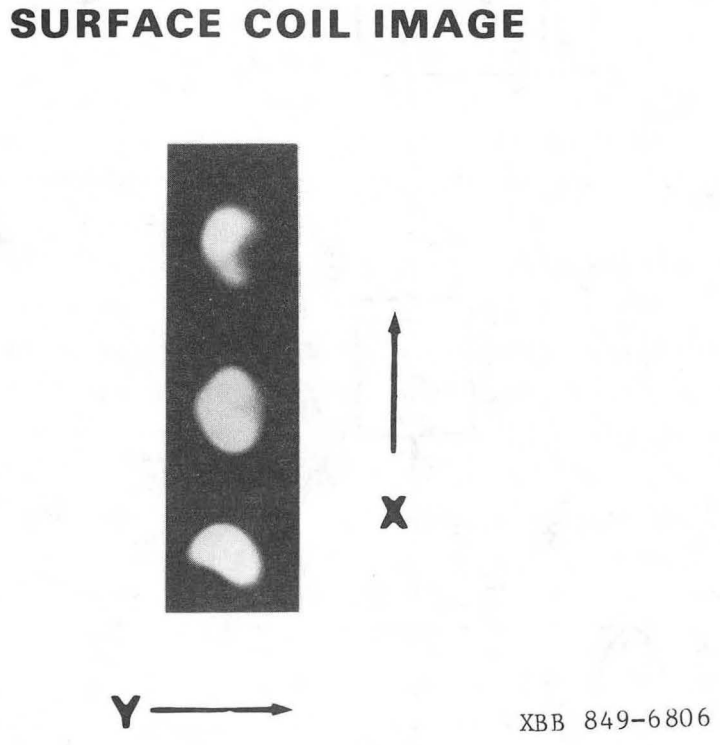

Figure 4.6 - Three test-tube phantom (top) and corresponding image (bottom).

at three different delay times (section 4.2.2). The bottom of Figure 4.6 shows the 3 second image of the phantom. There were some distortions in the image due to rf and main magnetic field inhomogeneities; however, the image still showed the three test-tubes very distinctly.

Another cylindrical water phantom was used to measure the image intensity uniformity and also the "slice thickness" defined by the two-turn elliptical shaped surface coil. Imaging was done in three orthogonal planes using projection gradients in the X-Y plane, Z-X plane, and the Z-Y plane. The approximate slice thickness in the most sensitive region of the coil was calculated from the ZX image and was found to be 1.0 +/- .2 cm.

4.3 Methods

4.3.1 Helium beam irradiation of the CNS

The right hemisphere of the brain of 10 Sprague-Dawley rats (age- 71 days, weight- 200 grams) was irradiated using the helium beam produced at the 184 inch cyclotron (see section 2.1). Groups of rats received 3000 and 5000 rads in the plateau region of the beam. Five rats served as controls. A second group of 5 rats (age - 84 days) was irradiated with 5000 rads so that imaging, histology, and brain extracts could be done at 4 days post-irradiation (time period of greatest decrease in T1 relaxation time of the irradiated side cortex.)

4.3.2 The NMR experiment.

The rats were imaged 4.5, 11, 25 and 81 days after irradiation. The rats were anesthetized with 5mg of pentobarbital and the elliptical shaped surface coil (section 4.1.4) was placed on the rat's head over the brain. The rats were placed in the probe and the magnetic field was shimmed to give a proton water line-width of 40-60 Hz. Imaging was then performed using the projection-reconstruction method with the saturation recovery procedure (see previous section for details). Saturation of the spins was achieved by giving several closely spaced "180" degree pulses at different phases. An image was produced at three different delay times; 1, 2, and 3 seconds (time between the saturation pulses and the "90" pulse). Figure 4.10 shows an example of the three different delay time images from one of the control rats.

4.3.3 T1 relaxation time calculation.

Four regions of the brain were contoured using computer software (program RAM, Sam Pitluck). First, the image was displayed on the Ramtek and the brain was identified by the dark band of surrounding skull (See figure 4.7). Then, regions of cortex and subcortical structures were contoured as shown in figure 4.8. The intensity values inside the regions were averaged and fit to the equation:

$$I(t) = A\,(\,1 - \exp(-t/T1) \qquad (4.1)$$

where I(t) - image intensity
A - amplitude at infinite delay time
t - delay time between the saturation pulse and the "90"
T1 - T1 relaxation time.

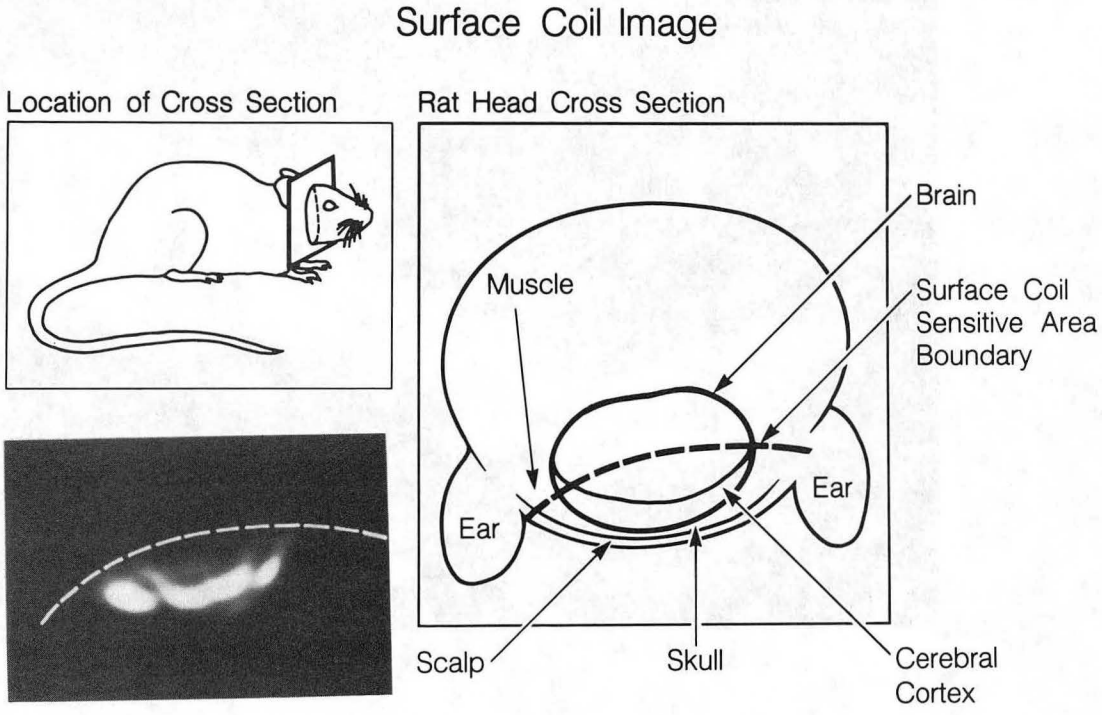

Figure 4.7 - Surface coil image and anatomical diagram with surface coil sensitive area boundary.

XBB 847-5629

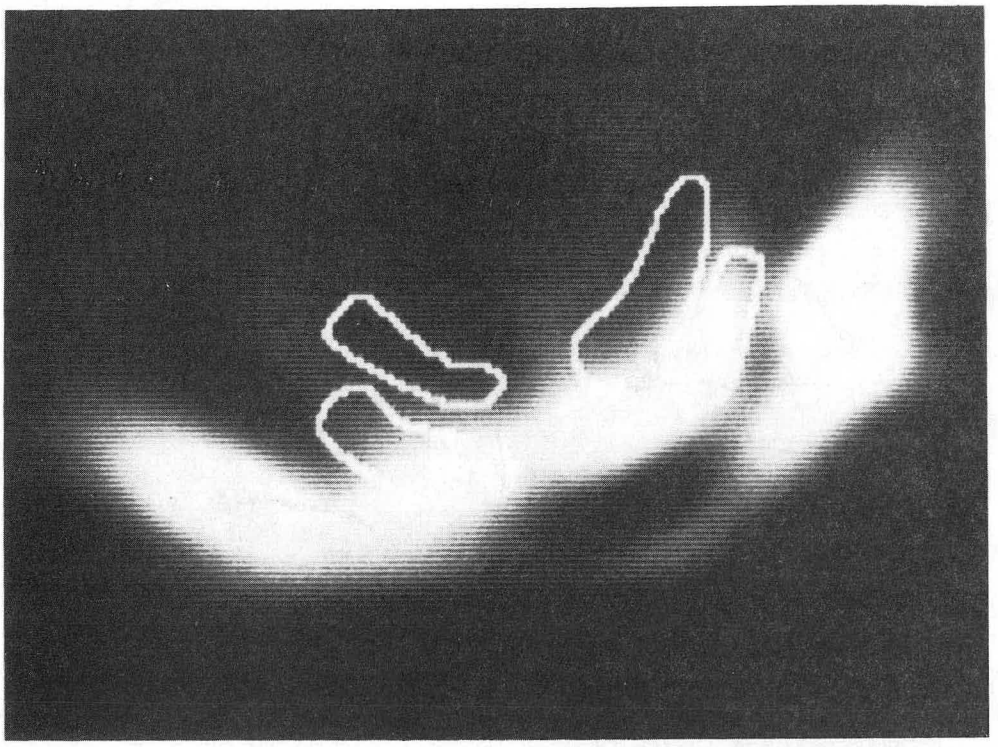

XBB 849-6807

Figure 4.8 - Surface coil image with regions of interest contours drawn on cortical and sub-cortical regions of the brain.

4.4 Results

At 4.5 days post-irradiation, 4 of the 5000 rad irradiated rats had a decreased T1 value on the irradiated side cortex and an elevated T1 on the control cortex relative to controls. The top of Figure 4.9 shows the three intensity images from an irradiated rat 4 days after irradiation. As seen in the relaxation curve from the bottom of Figure 4.9, the irradiated side cortex has a shorter T1 and A1 value than the opposite side of the brain. Figure 4.10 shows the result for one of the control animals where both sides of the brain had similar T1 and A1 values. In Figure 4.11, the calculated T1 images for the irradiated and control animals are displayed side by side, and a bright T1 region can be seen on the control side of the irradiated animal. The bottom of Figure 4.12 shows the time progression results for the irradiated side cortex. T1 decreased with dose on the irradiated side at 4.5 days, and then as time progressed, the T1 from the irradiated animals seemed to oscillate about the controls. At 81 days post-irradiation, the last time point measured, two of the rats had an increased T1 on the irradiated side cortex relative to controls. Each point on the plot is an average T1 value from 3 to 5 rats. The top of Figure 4.12 shows the results for the control side (left) cortex. The T1 values from the irradiated brains (bottom of Figure 4.12) were higher than controls at 4.5 days, dropped to the level of controls at 11 and 25 days post-irradiation, then climbed back up higher than controls at 81 days. For the irradiated side subcortex, there was a definite decrease in T1 as a function of dose at 81 days (Figure 4.13).

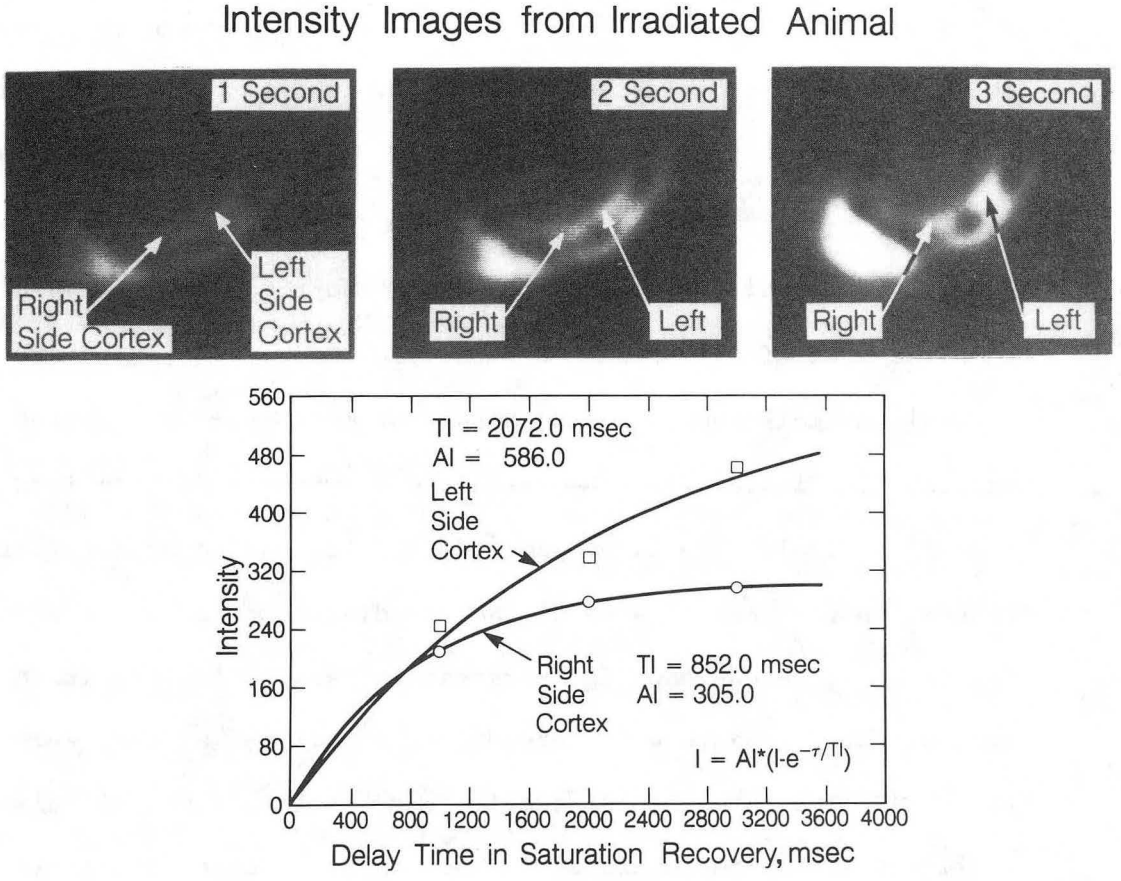

Figure 4.9 - Intensity images from irradiated animal (top) and relaxation curve (bottom). The solid line shows the computer fit to the data using equation 4.1.

XBB 847-5630

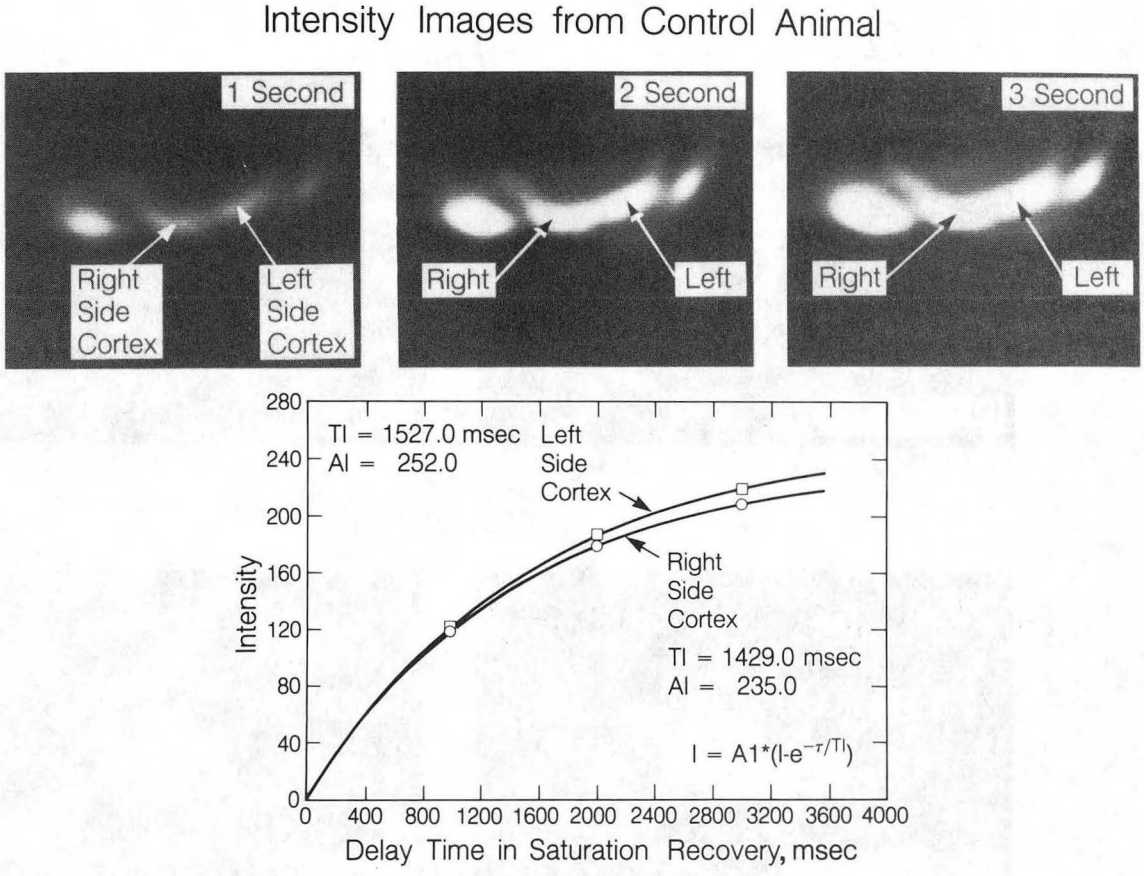

Figure 4.10 - Same as 4.9, for control animal.

XBB 847-5632

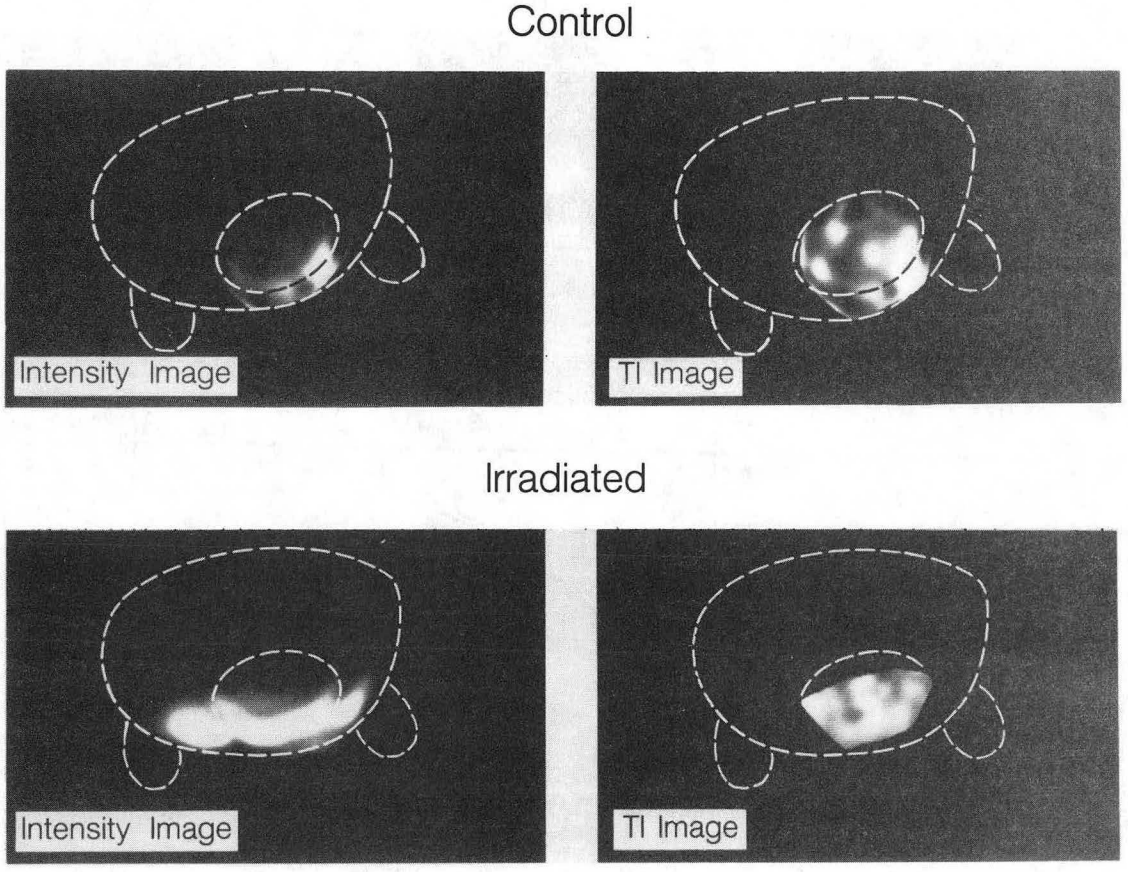

Figure 4.11 - Intensity image (left) and Tl images (right) for control and irradiated side cortex.

XBB 847-5631

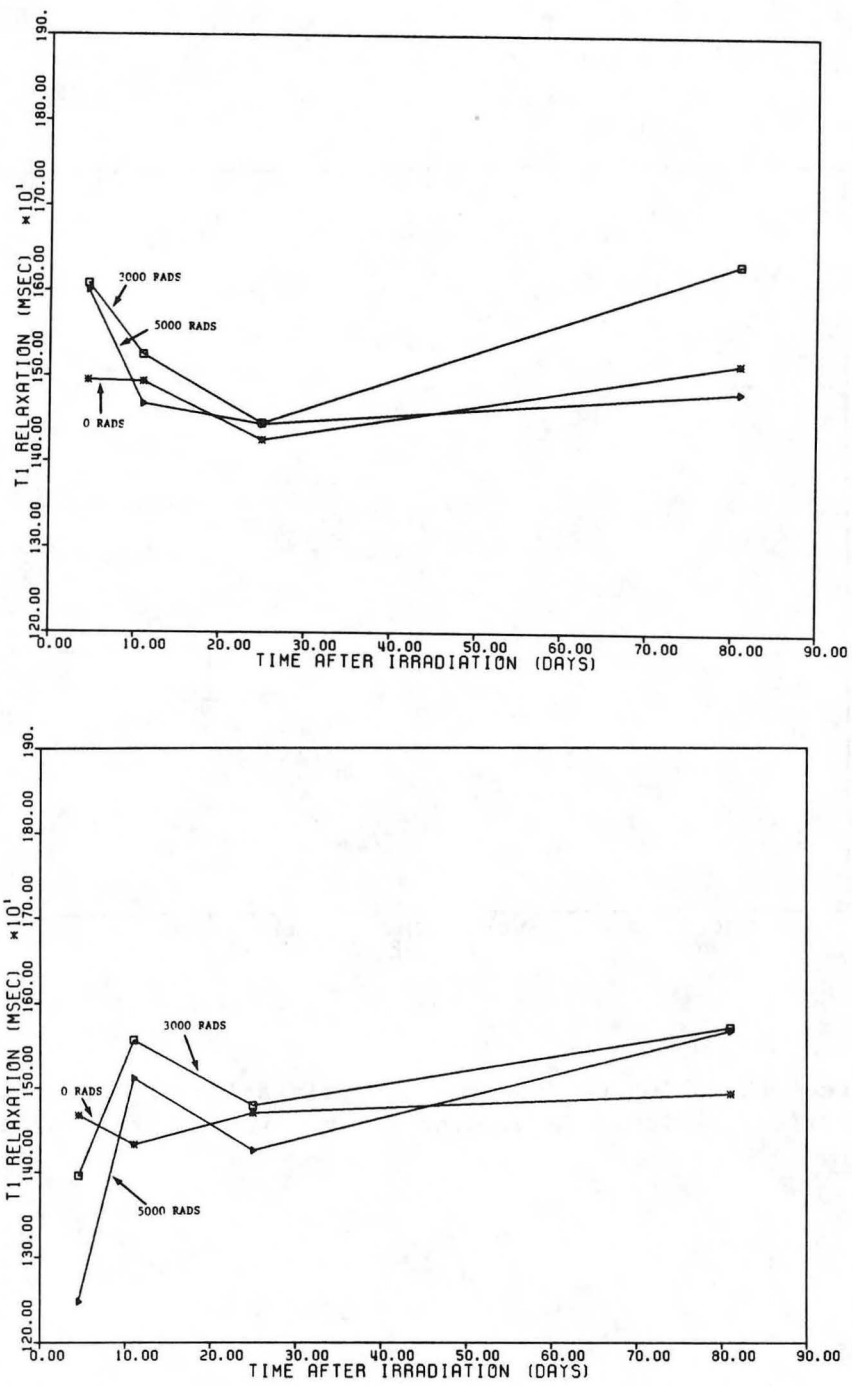

XBL 849-3684

Figure 4.12 - Plots of time after irradiation vs. T1 for the control side cortex (top plot) and irradiated side cortex (bottom plot).

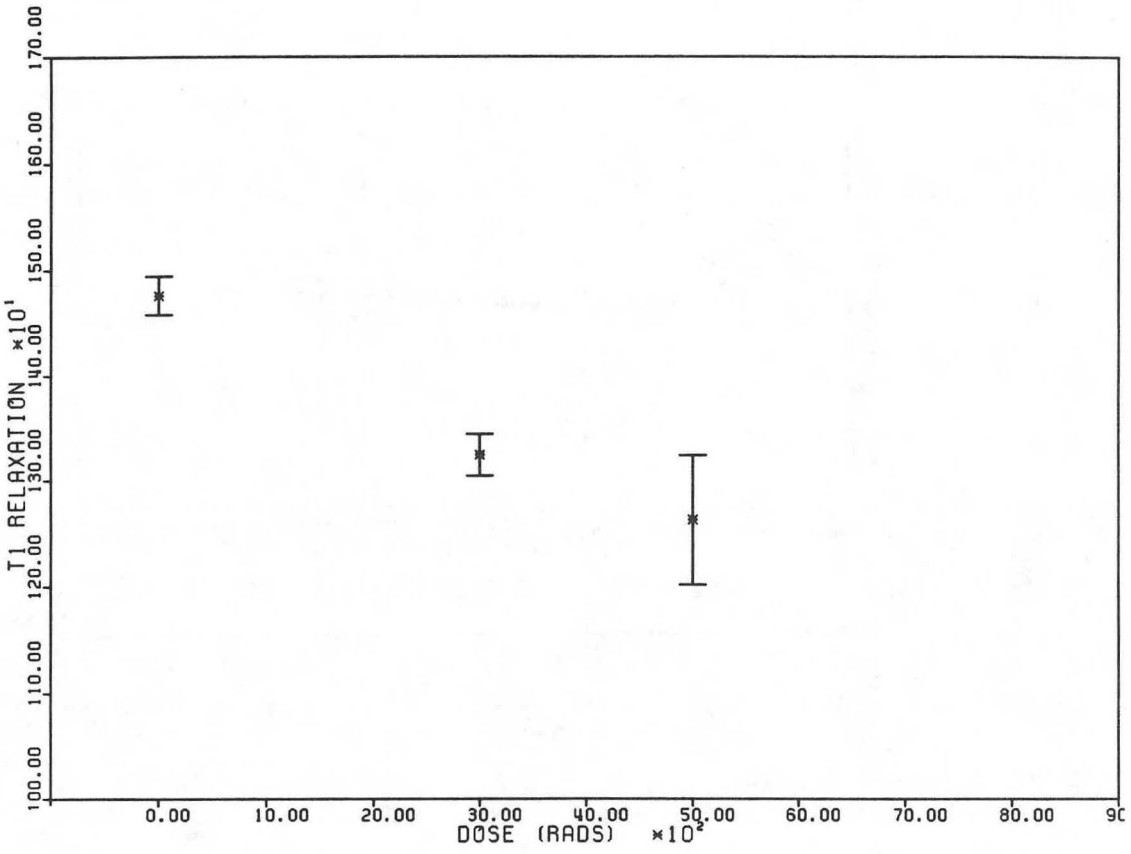

XBL 849-3683

Figure 4.13 - Plot of dose vs. T1 relaxation for the irradiated side subcortical region. Each point is the average of 3 - 5 points +/- SEM.

The most important facts from these experiments are: 1) T1 and A1 values decreased on the irradiated side cortex early after irradiation; 2) T1 increased on the control side; and 3) T1 values of irradiated animals changed with time after irradiation on both sides of the brain. These data are in conformity with the results of chapters 2 and 3 where different techniques were used to measure T1, T2, and spin density.

CHAPTER 5. SPIN-ECHO SPECTROSCOPY WITH RF ENERGY OPTIMIZATION

High resolution NMR spectroscopy has been used by chemists for years to study chemical structure, bonding, and molecular interactions. The nuclei (protons) within a molecule resonate at different frequencies because the electron cloud shields them by different amounts from the main magnetic field depending on the chemical structure (James, 1977). Proton spectroscopy has recently been applied to study the biochemistry of intact tissues. For example, lactate metabolism has been studied in the brain (Behar et al., 1983; Behar et al. 1984) and muscle (Arus et al., 1984; Ugurbil et al., 1984). Histidine, lipids, phosphocreatine, and creatine have been studied in muscle (Yoshizaki, 1981, Arus et al., 1984).

This chapter discusses techniques and results from the in vivo spectroscopic measurement of the rat brain. Proton spectroscopy was done in order to observe changes in proton resonances which may be associated with the changes seen in proton T1 relaxation time. Techniques were developed to make spectroscopic measurements of the rat brain in a non-invasive manner. Measurements were made on the same rats that were studied for proton relaxation by imaging methods.

5.1 Localization in surface coil spectroscopy

There are major problems in using the surface coil to measure NMR resonances of a structure that is a few layers deep within the sample. As shown in Figure 5.1, when the surface coil is placed next to the rat's head over the cerebrum, the brain lies 3-4 mm away from coil and the scalp and skull lie 1-3mm away from the coil. Since the B1 field drops off rapidly with distance away from the coil (Evelhock et al., 1984), the scalp tissue experiences a much greater radio-frequency field (B1) than does the brain. Therefore, in order to measure the spectrum of the brain with the surface coil non-invasively, a technique is needed which suppresses the strong signals from the scalp. Mapping the chemical shifts as a function of position can be achieved by performing the 2D- Fourier transform of the FIDs as a function of acquisition time and pulse duration (Garwood et al., 1984; Pekar et al., 1983; Hoult 1979; Cox and Styles, 1980; Haase et al., 1983). This would result in a set of spectra which represent chemicals from constant B1 field shells which surround the surface coil. In this chapter, we will show how it is possible to find the appropriate pulse duration for a given rf power and coil configuration to minimize the scalp tissue signal and augment the brain signal.

5.1.1 Computer simulation

The free induction decay signal from a pulsed Fourier transform spectrometer can be described by the following equation:

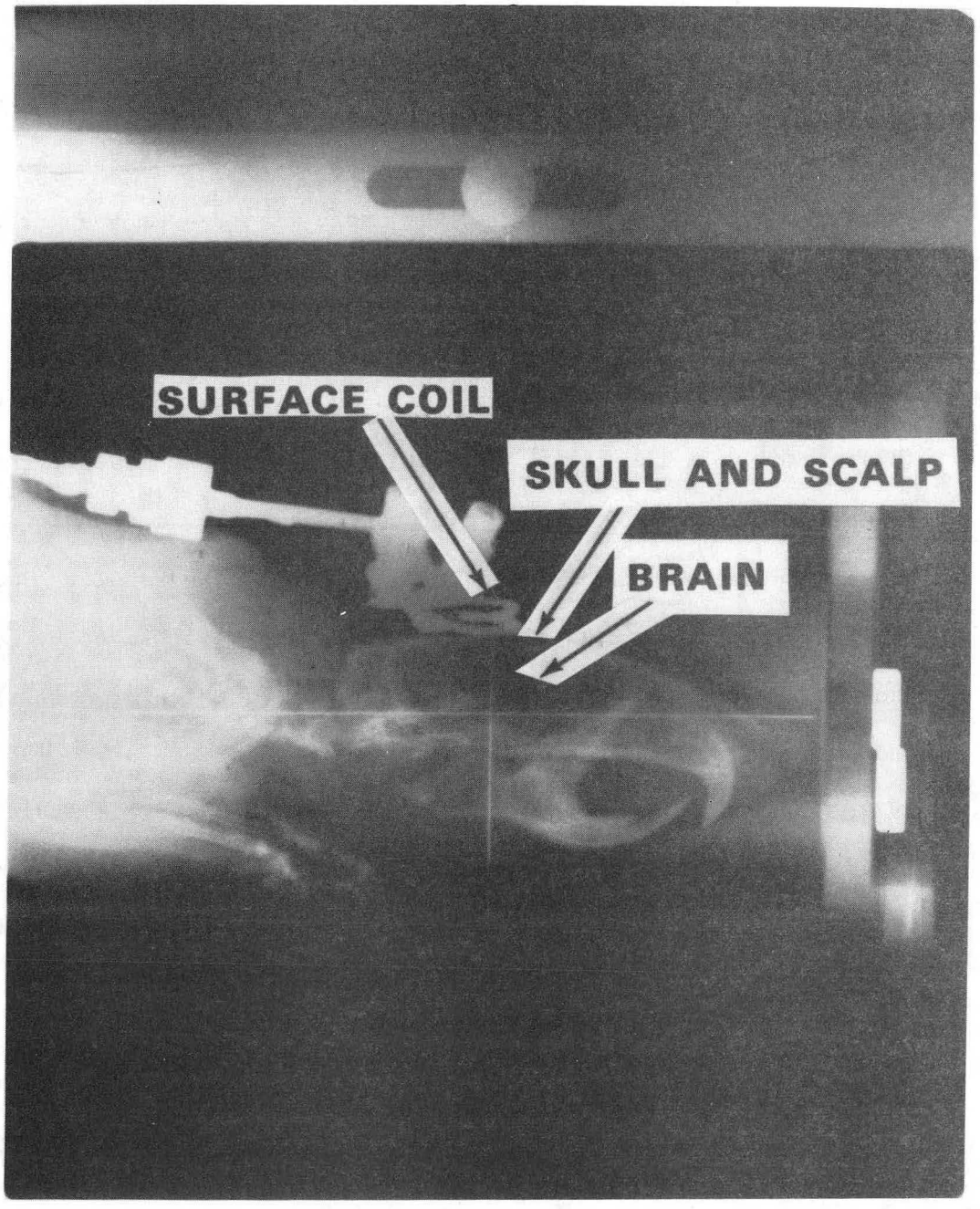

XBB 837-6633A

Figure 5.1 - X-ray of rat head in NMR probe (lateral view).

(Equation 5.1)

$$S1(t,tp) = \sum B1 * \sin(w1*tp) * \sin(wt + \phi) * \exp(-t/T2^* - tp/T2p) * T1f * V$$

$$S2(t,tp) = \sum B1 * \sin(w1*tp) * \cos(wt + \phi) * \exp(-t/T2^* - tp/T2p) * T1f * V$$

$$T1f = (1 - \exp(-\tau/T1) \; / \; (1 - \cos(w1*tp) \exp(-\tau/T1))$$

where:
S1, S2 = signal of the quadrature phase components
B1 = radio-frequency field component in the xy plane
w1 * tp = flip angle
w1 = B1 * factor
tp = pulse duration
w = resonant offset from carrier frequency
t = acquisition time
ϕ = phase
T2* = dephasing time constant during FID
T2p = dephasing time constant during the rf pulse
T1 = spin-lattice time constant
τ = time between pulses
V = volume element which has the same B1
(this equation was modified from Garwood et al., 1984)

The Fourier transform of the FIDs gives a set of frequency spectra with spectral intensity described by the following equation:

$$S(tp) = B1i * \sin(w1*tp) * T1f$$

(Chaillot et al, 1983)

Given a theoretical phantom of three different chemically shifted solutions placed at varying distances away from the surface coil, a pulse duration can be found which minimizes the signal from the first solution closest to the coil and maximizes the signal from the second solution. A computer simulation was done using equation 5.1 in order to see the relationship between the signal strength of the three different solutions and pulse duration. The NMR experiment was simulated in which

the FIDs were collected for several different pulse durations. The program (2DFT, see appendix) was written on the VAX (fortran) to perform the following: 1)calculate an FID matrix (64 X 64) for a phantom of three solutions described above where each solution has its own B1 field and frequency offset (w); 2)Fourier transform the matrix along the acquisition time axis; 3)transpose the matrix; 4)Fourier transform the matrix along the pulse duration axis; and 5)output all three matrices for 3D-display. Another program was written (ACMB1, see appendix) to display the matrices in 3D on the Versatek plotter which used a 3D plot package (Watkins, 1974). Figure 5.2 shows the FID matrix, the first FT matrix, and the second FT matrix. In the first FT matrix, it can been seen that the chemical shifted peaks from the different solutions oscillate at different rates as a function of pulse duration because they do not experience the same B1 field. A pulse duration can be found where the ratio of second solution signal to first solution signal is maximized.

An experiment was done with a real phantom (Figure 5.3) in order to verify the computer simulation. The phantom consisted of three capillary tubes filled with water, acetic acid, and tetramethylsilane (TMS) placed at 2, 4, and 6 mm away from the surface coil. The surface coil had two turns of copper wire with a diameter of 8 mm. Each of the chemicals resonates at different frequencies (4.8, 2.2, 0. ppm) so that the peak heights could be plotted separately as a function of pulse duration. The experiment was performed using 32 different pulse durations between 5 and 200 usec. Figure 5.4 shows the result after the FIDs are Fourier transformed. Notice that the water peak intensity

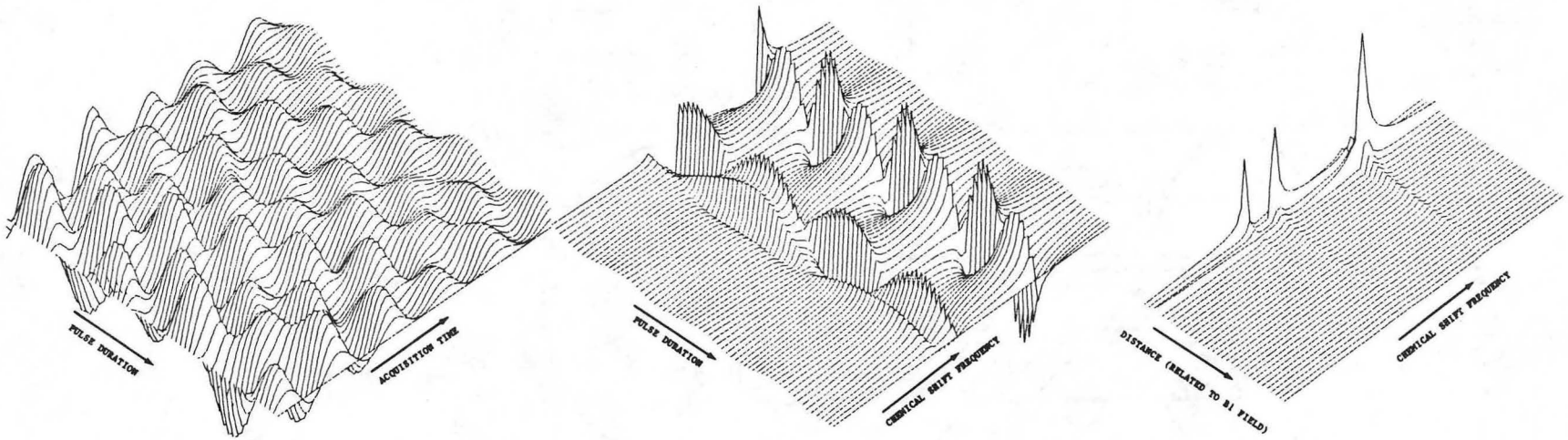

XBL 849-3682

Figure 5.2 - Computer simulation of pulse duration vs. acquisition time using the B1 field of a surface coil.

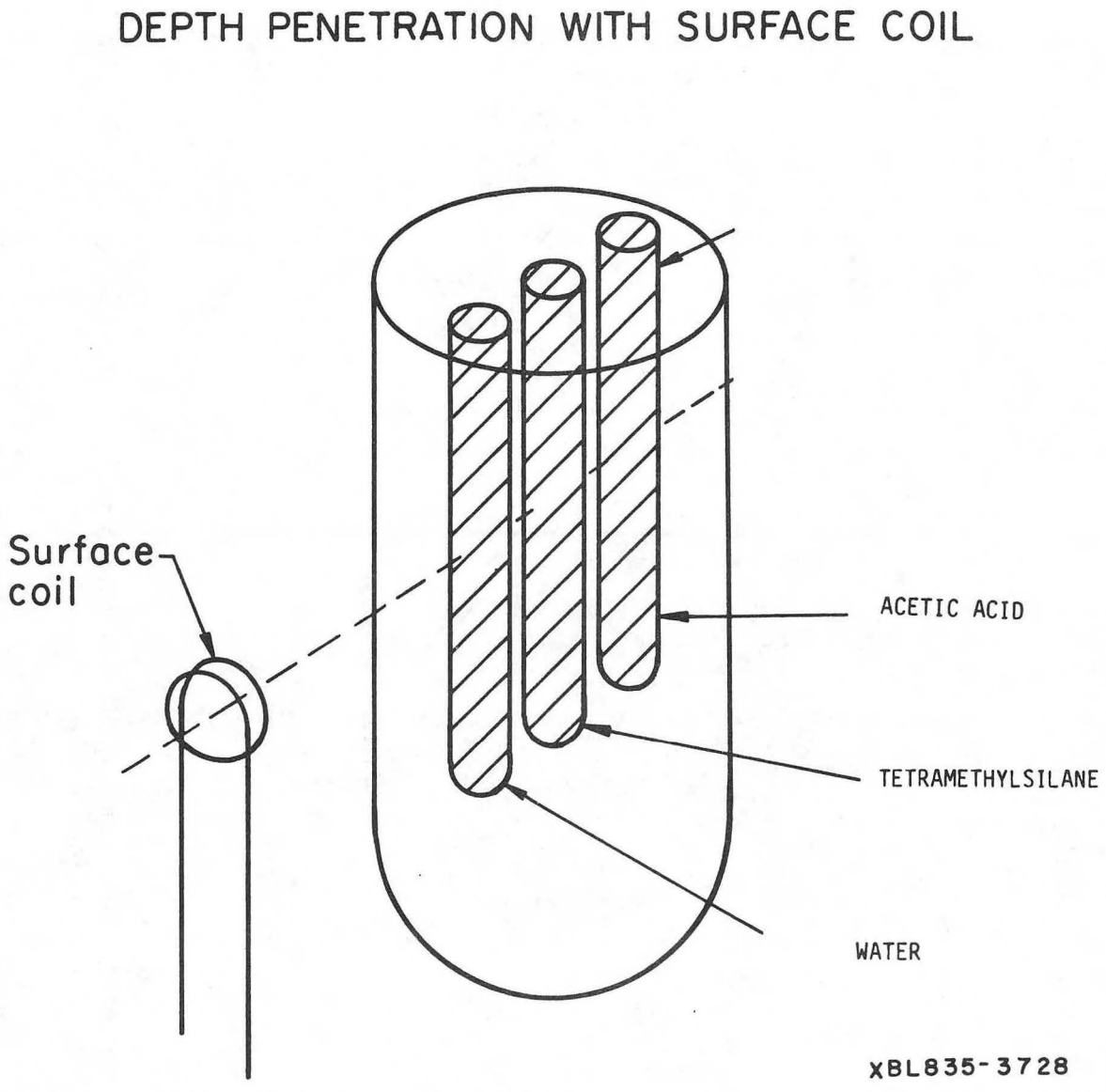

Figure 5.3 - Three test-tube phantom used to test depth penetration with the surface coil.

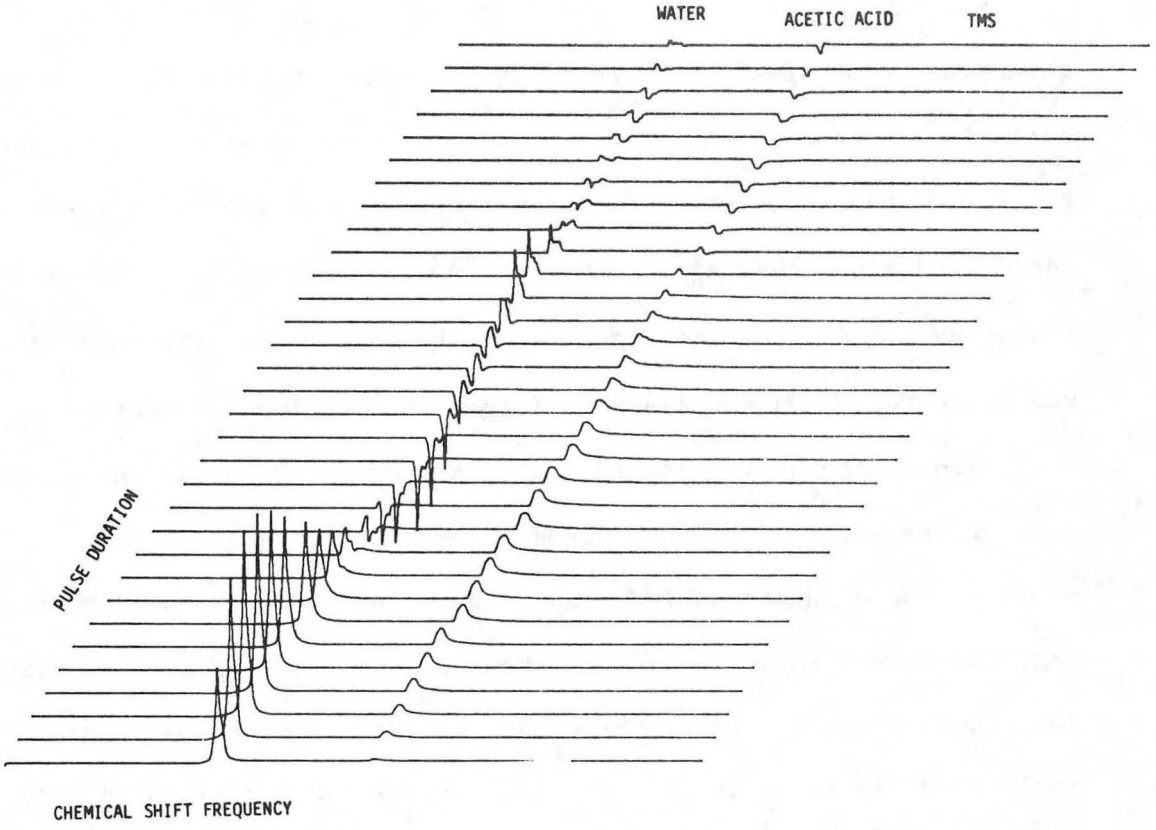

Figure 5.4 - Phantom proton spectrum as a function of pulse duration.

starts out with much higher peaks and goes through more cycles than the other peaks in the spectrum. As the water peak begins to go through a 180 degrees, the acetic acid peak approaches a maximum.

Another experiment was done with the help of Rudi Nunlist to determine the spatial selectivity of the surface coil using the following technique. A large homogeneous water phantom was placed in front of the surface coil and the static magnetic field gradient was positioned along the axis of the coil so that signal profile could be viewed as a function of distance away from the coil. The pulse duration was again varied 32 times and the FIDs were Fourier transformed to give the result shown in Figure 5.5. At very short pulse durations, the Fourier transform of the FID gives a profile close to the B1 field profile (as a function of distance away from the coil) because the flip angle is close to 0 degrees. However, as the pulse duration is increased, the water nearest the surface coil experiences a greater flip angle than the water further out and the maximum signal moves away from the coil. Along this same line of experiments, a 2D image of the rat brain was measured using the same 8 mm coil. The result shown in Figure 5.6 shows a dark band at the surface of the head which represents the region of tissue that received a 180 degree pulse. This dark bank covers most of the scalp.

From the experiments described in section 5.1, we see that the surface coil with the appropriate diameter and pulse duration can be used to minimize the NMR signal from the scalp.

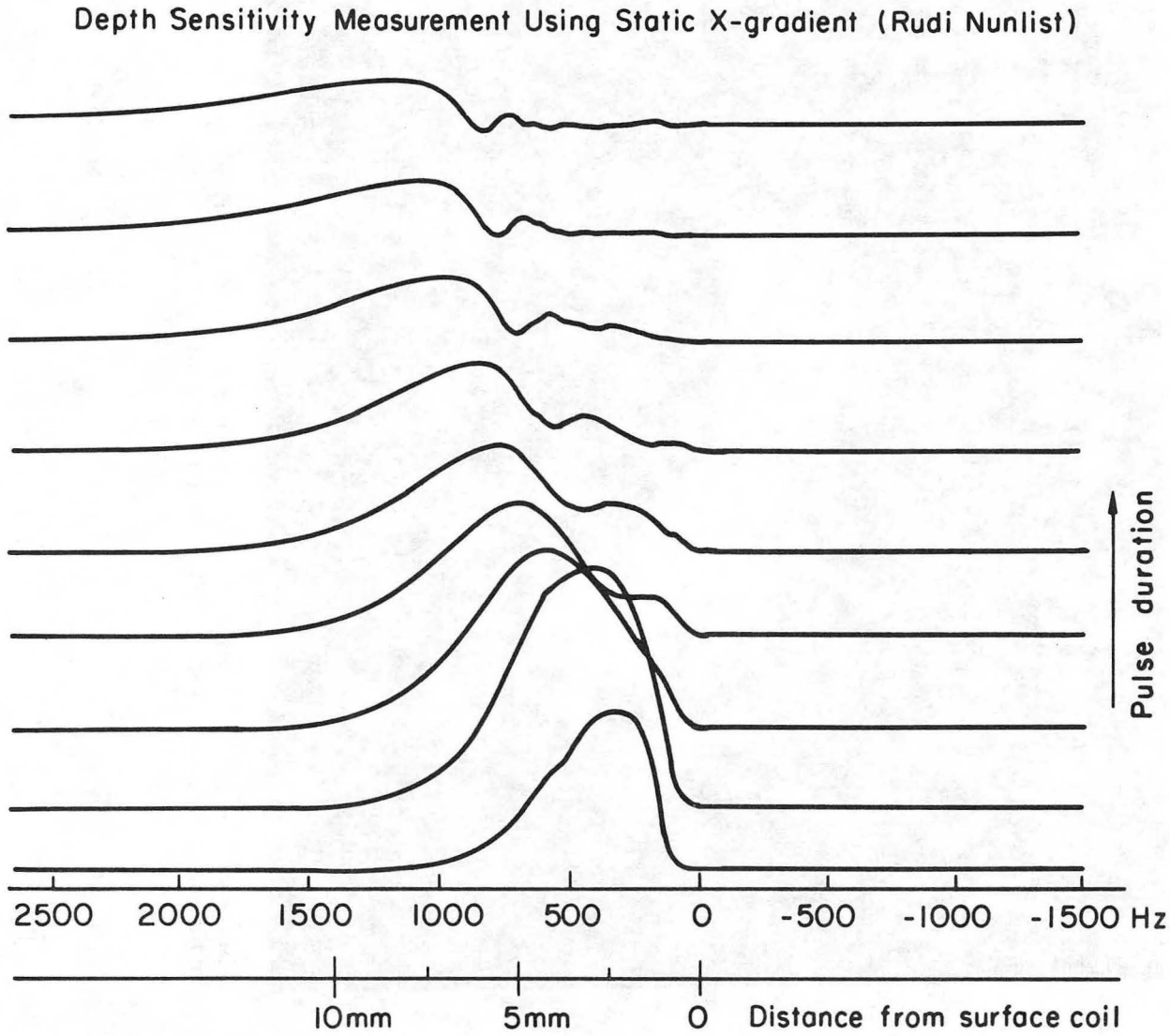

Figure 5.5 - One dimensional spatial localization of NMR signal along the axis of the coil as a function of pulse duration. XBL838-3937

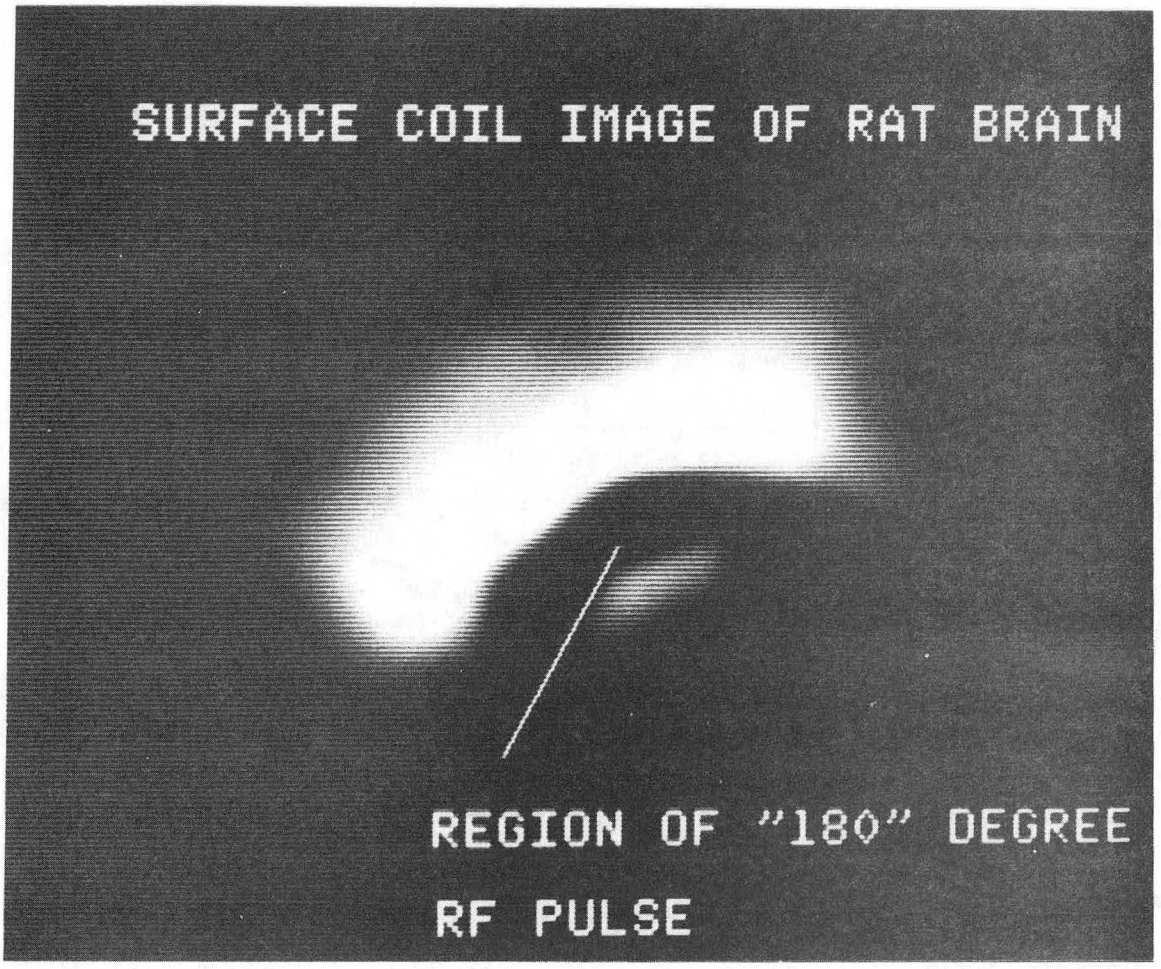

Figure 5.6 - Surface coil image of the rat brain with pulse duration adjusted to give a 180 degree at the scalp.

XBB 847-5314

5.2 Proton spectroscopy of irradiated rat brain

5.2.1 The NMR experiment

Proton spectroscopy was measured in vivo on 9 rats (5- 3000 rads, 4- controls, same group measured in chapter 3) at 7.3 months after irradiation using the 180 MHz spectrometer (described in section 4.1). The rats were anesthetized with nembutal and placed into the rat probe described in section 4.1. A two-turn surface coil (8 mm diameter) was placed on the head over the cerebrum. The field was shimmed using all off-axis and on-axis shims with the one-pulse sequence. The receiver gain was then reset for the spin-echo experiment to insure adequate ADC dynamic range to detect brain chemicals other than water. A spin-echo pulse sequence was used with a delay time of 100 mseconds between the "90" and the "180" degree pulses with a 2.2 second repetition time. The spin-echo was used to suppress the water and remove the broad-line components of the tissue (Brown et al., 1977, Behar et al. 1984). Quadrature phase detection, phase cycling and 4K data size collection were used while the signal was averaged 40-100 times. In a few instances, presaturation was used with the spin-echo experiment. The lipid and n-acetyl aspartate peaks were used to localize the signal to the brain because the proton spectrum of the brain has a small lipid peak (Pykett and Rosen, 1983) and a large n-acetyl aspartate peak (Behar et al., 1983). However, the opposite is true for the scalp and muscle proton spectrum. In fact, no n- acetyl aspartate peak is seen in muscle (Arus et al., 1984). The pulse duration was varied until the lipid peak

was at a minimum, which indicated that the signal was primarily coming from the brain.

5.2.2 Computer software

Software was written on the VAX to quantitate the areas under the peaks. Program NTCFT2 (appendix) performed the following functions: 1) apodization of the FID; 2) Fourier transformation of the FID; 3) zero and first order phase correction; 4) expansion of a selected region of the spectrum; 5) user-defined PPM offset using the bitpad; 6)peak area evaluation with automatic expansion of spectral regions near the peak of interest; and 7) integration over the curve defined in step 6 and disk output. The n-acetyl aspartate peak was set to 2.0 ppm and the following peak areas were analyzed: water (4.67 ppm); p-choline (3.2 ppm); total creatine (PCR+CR) (3.0 ppm) ; n-acetyl aspartate (2.0 ppm); and lipids (1.-1.7 ppm).

5.3 Results

5.3.1 Lipid and n-acetyl aspartate peak characteristics of the normal brain

The spin-echo spectrum from a short pulse duration has a large dominating lipid peak which originates from the scalp (bottom of Figure 5.7). As the pulse duration is increased, the lipid peak decreases while the n-acetyl aspartate peak increases. The top spectrum shows the result when a pulse duration is found which gives approximately a 180 degree pulse to the scalp and a 90 degree pulse to the brain. Figure

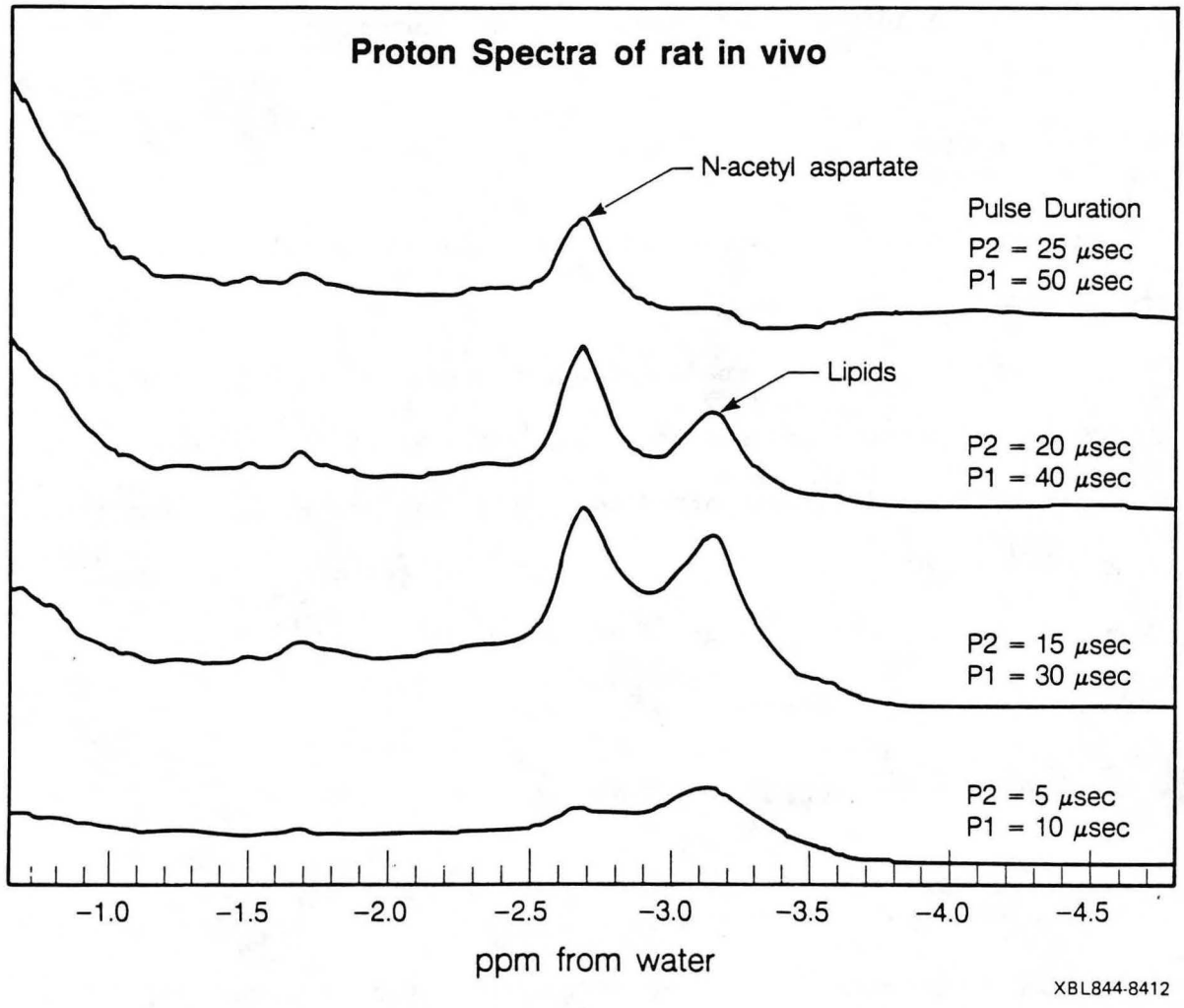

Figure 5.7 - Spin-echo proton spectrum of rat head as a function of pulse duration.

5.8 is the proton spectrum of the rat head when the pulse duration is optimized to give the smallest lipid peak with a relative peak height similar to the lipid peak in the excised brain spectrum.

5.3.2 Results with irradiated animals

Figure 5.9 shows an example of the in vivo proton spectra of control and irradiated animals. A decrease in p-choline (relative to PCR+CR) can be seen in the irradiated brain spectrum (middle spectrum) compared to the control (bottom spectrum). The spectrum was measured on one of the irradiated animals after the scalp was removed (top spectrum, Figure 5.9) to check the scalp signal-suppresion technique. The results of the computer analyzed peak areas are shown in Table 5.1.

Table 5.1 - PEAK AREA RATIOS RELATIVE TO WATER

	CONTROL	IRRADIATED	
N-ACETYL ASP	4.97 +/- 2.13	4.48 +/- 1.14	* 10E-3
TOTAL CREATINE	.808 +/- .138	.980 +/- .186	* 10E-3
P-CHOLINE	.868 +/- .069	.660 +/- .076	* 10E-3

NOTE: All ratios were calculated by dividing the peak area of interest by the water peak area. The values shown are the average of 4 animals for the controls and 5 animals for the irradiated (7.3 months post-irr.) +/- standard error of the mean.

For n-acetyl aspartate, quantitation of the area under the curve was difficult because the peak sat on top of the tail of the lipid and glutamate peaks. The standard error of the mean for the n-acetyl aspartate peak ratio and lipid peak ratio are very large. As seen in

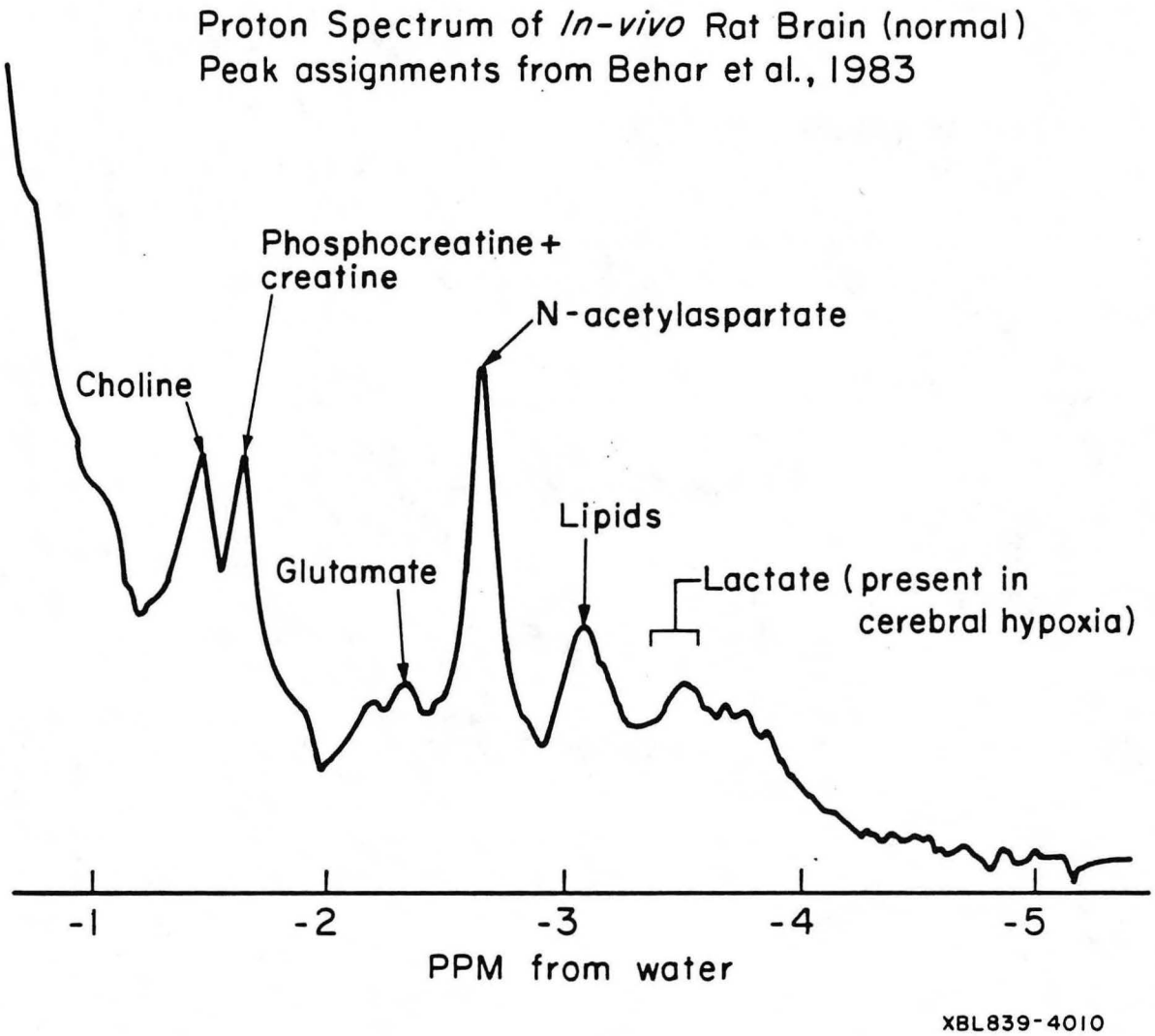

Figure 5.8 - Proton spectrum of rat head after rf pulse optimization to minimize the lipid peak from the scalp.

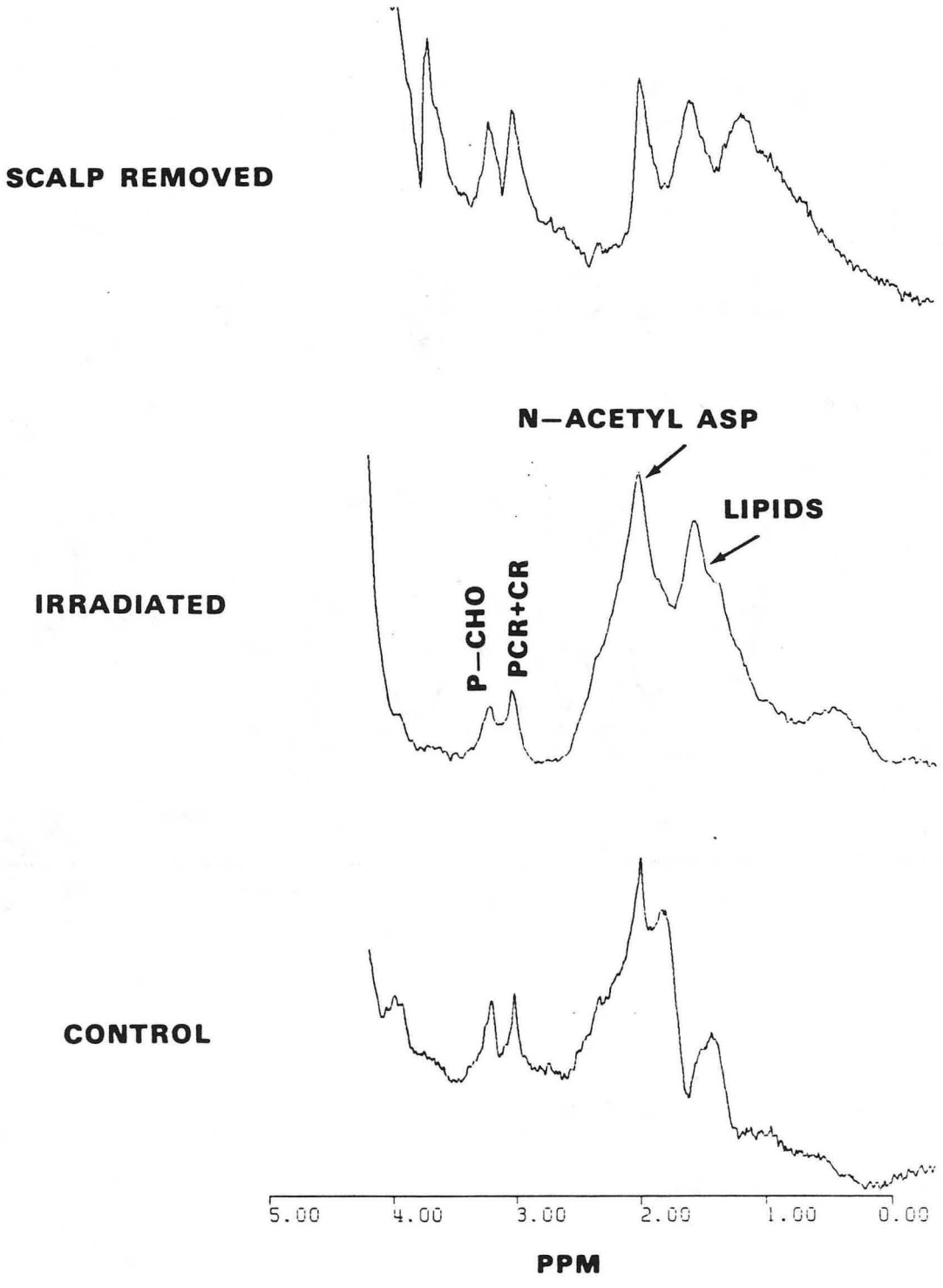

XBL 848-3316

Figure 5.9 - Proton spectra of irradiated rat brain (middle) compared to control (bottom) and to spectra of rat with scalp removed (top).

Table 5.1, a decrease was observed in the p-choline peak area ratio in the irradiated animals compared to controls. Since a decrease in spin density was noted in chapters 2 - 4 on irradiated brain, normalization of the peak areas to water may give misleading results. Therefore, p-choline peak area ratios were also calculated relative to total creatine and a decrease in the p-choline was still seen in irradiated animals as shown below.

	Control	Irradiated
P-choline peak area ratio relative to total creatine	1.23 +/- .15	.879 +/- .14

The main results of this chapter are: 1)the lipid peak and N-acetyl aspartate peak heights differ greatly between the brain and surrounding soft tissues of the head; 2)the surface coil with the appropriate diameter and pulse power and duration can be used to minimize the NMR signal arising from the scalp; and 3) a decrease in the p-choline resonance was found in 3000 rad animals 7.3 months post-irradiation relative to controls. In chapters 6 and 7, an increase was seen in the p-choline peak in 3000 and 5000 rad animals at earlier times after irradiation (4 days and 81 days). Therefore, the p-choline peak of the irradiated animals changed as a function of time after irradiation. A possible explanation of these results concerning brain lipids is given in chapter 9.

CHAPTER 6. 2D FOURIER TRANSFORM PROTON SPECTROSCOPY

6.1 Introduction

Chemical shift imaging is a new technique which allows the chemical shift information to be viewed as a function of position in the body (Brown et al, 1980; Maudsley et al., 1983; Pykett and Rosen, 1983). The 2D Fourier transform (phase-encoded) chemical shift technique gives the highest resolution in chemical shift information. However, data acquisition takes many times longer than the non-chemical shift phase-encoding experiment where a read-out gradient is on during signal acquisition. A compromise was made in our experiments so that the data could be acquired in a reasonable amount of time (20 minutes): the chemical shift information was acquired as a function of one spatial dimension only and localization was done in the other dimensions using surface coil techniques described in chapter 5.

6.2 Instrumentation and computer software

The instrumentation for phase encoded proton spectroscopy used the same probe body and electronics described in section 4.1. However, additional modifications were made in the power supply and the computer software. The response times of the X, Y, and Z gradients were measured to access the practicality of implementing the phase encoding experiment. The details of the experiment are listed in the appendix (gradient field response time).

6.2.1 Power supply

Gates were added to the X and Y channels of the power supply (Figure 6.1) in order to do the phase encoding chemical shift experiment (Haselgrove et al., 1983) shown in Figure 6.2. The gates were required to pulse the gradient during the spin-echo experiment because the current level of the power supply is controlled outside of the pulse programmer. In other words, the computer controls the gradient strength through the DACs and the pulse programmer controls the time and duration of gradient pulse through the gates of the power supply. During the experiment, the spectrometer computer sends an analog signal to the power supply which is used to control the level of current that goes out to the gradient coils. However, the power supply only responds to the analog signal unless a second TTL gate signal is received.

6.2.2 Computer software

6.2.2.1 Data acquisition

The experiment shown in Figure 6.2 was implemented on the spectrometer by 1) writing a subroutine on the Nicolet computer which increments the X DAC value outside of the pulse programmer (See Figure 6.1); 2)connecting a TTL gate line from the computer to the power supply; and 3)writing a pulse sequence which turns the TTL gate on between the 90 degree and the 180 degree pulse of the spin echo.

Phase encoding method

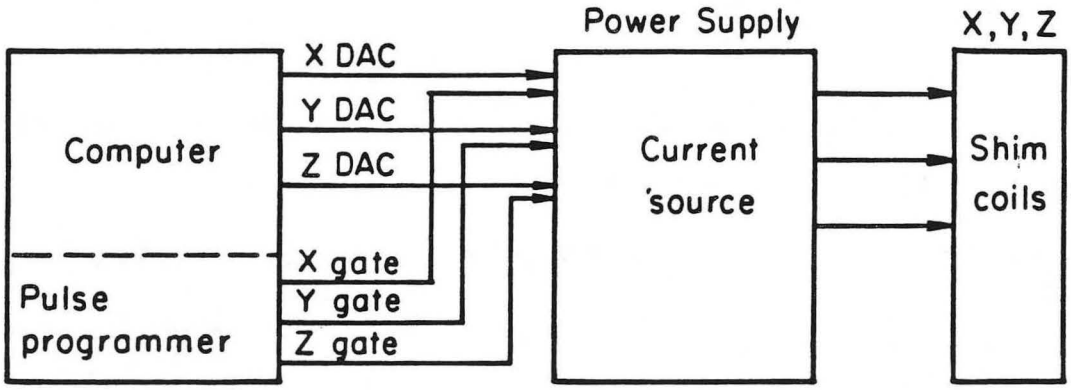

Figure 6.1 - Hardware for the phase encoding experiment.

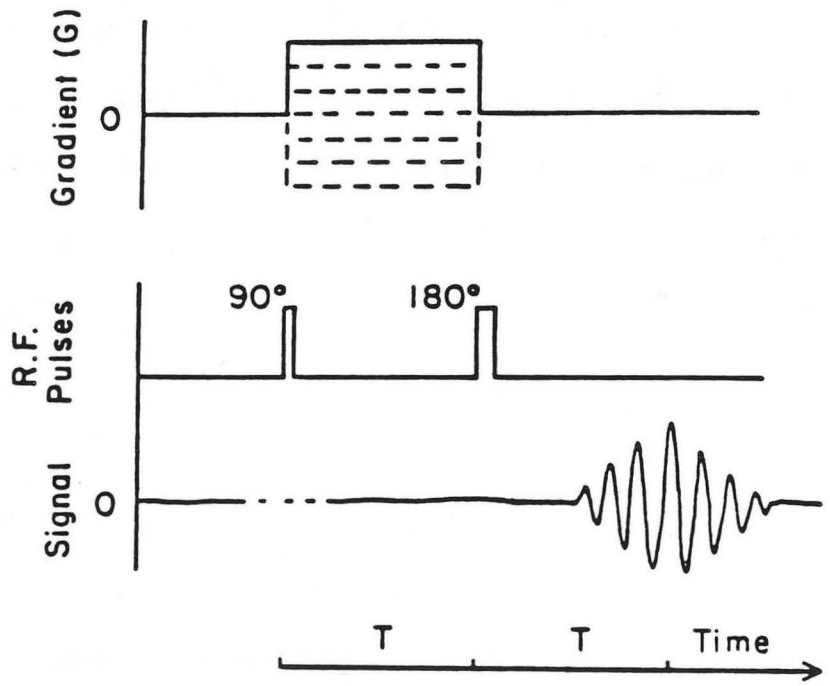

XBL 849-3674

Figure 6.2 - RF Pulse and gradient sequence for phase encoded spectroscopy. (From Haselgrove et al., 1983)

6.2.2.2 Data processing

The data are transmitted over the phone line to the VAX computer. The same software described in section 4.1.3.2 was used to convert the Nicolet words to VAX words and new software was written to perform the two-dimensional Fourier transformation (program NTCFTV). The program steps are: 1)apodization of the FID; 2)Fourier transformation of the FID; 3) phase correction of the spectra; 4)transposing of the matrix; 5)Fourier transformation in the second dimension; and 6)plotting of the spectra on the Versatek with the ppm scale.

6.3 Methods

6.3.1 Magnetic field gradient orientation

The direction of the X gradient was determined by placing two capillary tubes next the the surface coil. The probe was placed in the magnet and the field was shimmed. The X gradient was turned on and a one-pulse sequence was used to collect the FID. When the FID was Fourier transformed, two peaks were seen which represented the projection of the two capillary tubes relative to the X gradient. The probe assembly was rotated until the distance between the two capillary peaks was maximized. At this point, the plane of the surface coil was parallel to the X gradient direction.

6.3.2 The NMR experiment

Three to five rats from each radiation group (controls, 3000 rads, and 5000 rads) were measured with phase-encoded proton spectroscopy at 4, 25, and 81 days post-irradiation. The animals were anesthetized with pentobarbital and an elliptical-shaped surface coil (2.5 cm X 1.5 cm) was placed over the rats head in order to receive signals form both hemispheres of the brain. Since each spectrum comes from a plane of tissue orthogonal to the direction of the gradient, the rat was oriented in the probe so that the phase-encoding gradient traversed the head from left ear to right ear (see Figure 6.4). With the gradient in this orientation, spectra from right and left sides of the brain could be studied separately. Using the pulse sequence described in section 6.1, the phase-encoding (X) gradient was incremented 32 times and the spin-echos were processed by the two -dimensional Fourier transform method.

Imaging was then performed using the projection-reconstruction technique described in chapter 4. The intensity image was used to: (1) determine which spectral planes contained the brain; and (2) determine the signal contribution of the extra-neural tissues for the selected plane.

6.4 Results

6.4.1 Phantom studies

Phantom studies were performed in order to test the 2D Fourier transform procedure both in data acquisition and data processing. A phantom consisting of three test-tubes were placed next to the surface coil as shown at the top of Figure 6.3. Chloroform, water, and acetic acid were chosen to fill the test-tubes because each chemical has a proton line at a unique chemical shift frequency. The phase-encoding experiment was then performed as described in section 6.2.3, and the FIDs were processed by the 2D Fourier transform program NTCFTV. The bottom of Figure 6.3 shows the result of the 2D Fourier transform of the FIDs. The water and acetic acid peaks were well- resolved peaks both along the spatial axis and along the chemical shift axis. The chloroform peak was hard to see, possibly because of rf field and main field inhomogeneity. However, this broad peak was also seen after magnification of the 2D matrix shown in Figure 6.3.

6.4.2 Radiation results

Figure 6.4 shows the phase-encoded proton spectra and the corresponding proton image from a control rat. Each spectrum comes from a plane of tissue perpendicular to the direction of the phase encoding gradient. The proton spectra A and D show large lipid peaks which come from the soft tissues next to the brain. The spectra B and C show a prominent N-acetyl aspartate peak and no lipid peak characteristic of normal brain. In Figure 6.5, an increase in the lipid signal (1 - 1.5

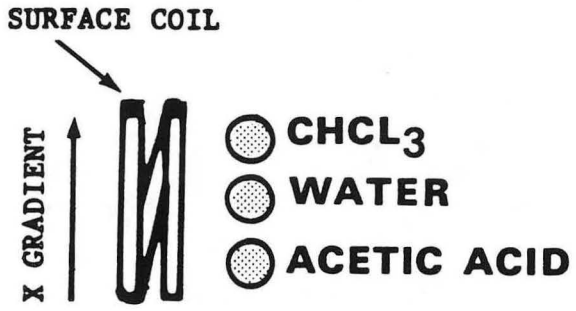

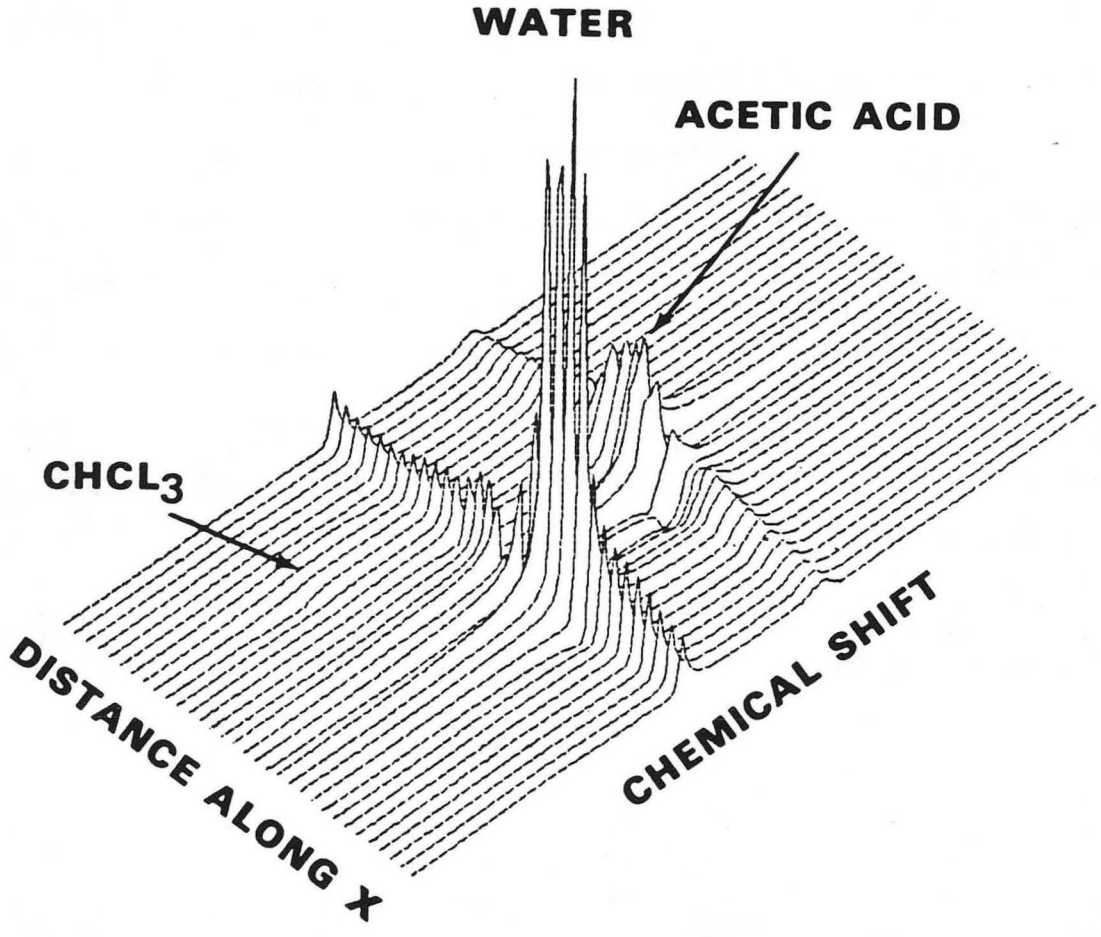

XBL 849-3675

Figure 6.3 - Three test-tube phantom (top) and 3-D plot (bottom) showing one-dimensional chemical shift imaging using the 2D Fourier transform technique.

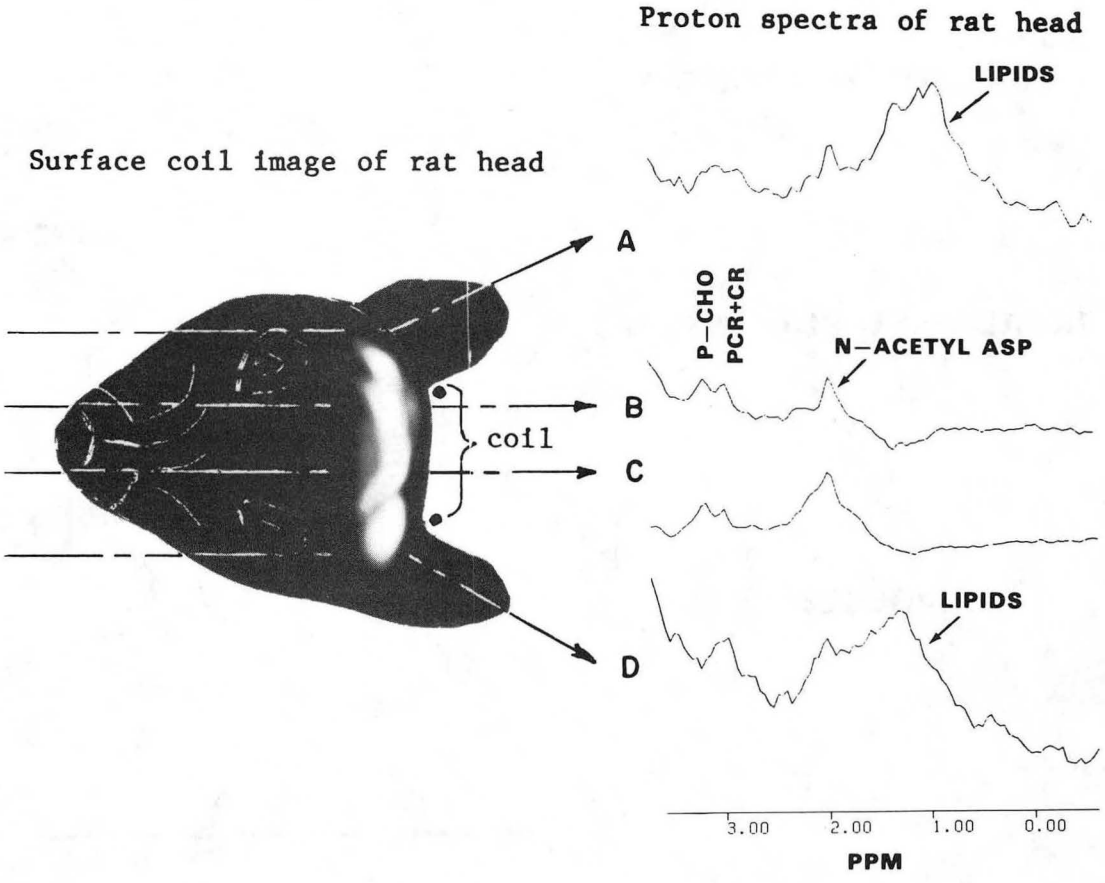

Figure 6.4 - Surface coil image and phase encoded spectra of the rat head.

XBB 847-5628

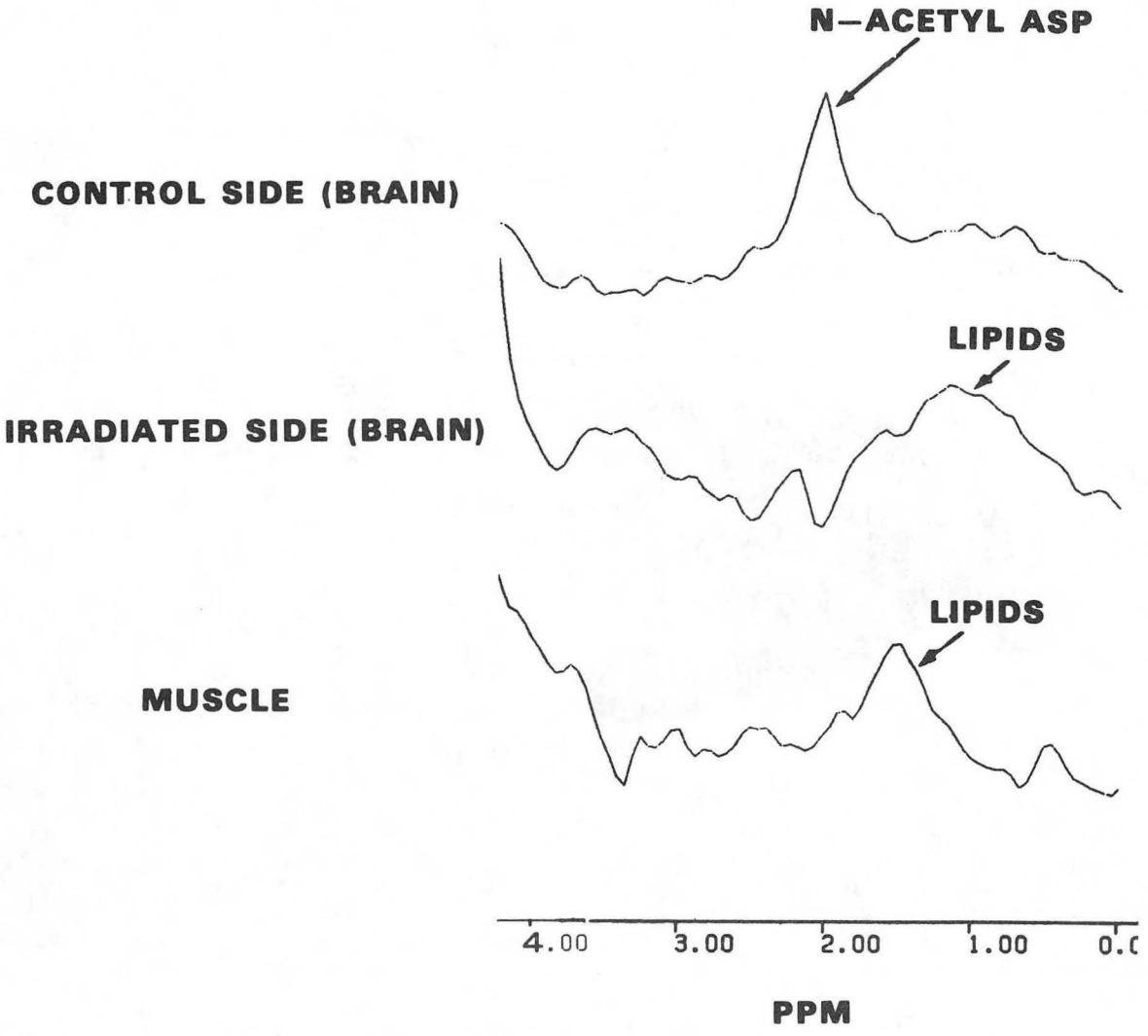

Figure 6.5 - Phase encoded proton spectrum of irradiated brain compared to scalp and control spectrum.

ppm) is seen in the spectra from the irradiated side of the 5000 rad rats 25 days post-irradiation. The phase-encoded spectra were also processed using the program NTCFT2 (section 5.2.2) to quantitate the areas under the following peaks: water, p-choline (81 days only), PCR+CR (81 days only), n-acetyl aspartate, and lipid peaks. Peak area ratios were calculated relative to water (Table 6.1). At 25 days, there was a large increase in the lipid peak area ratio on the right side of the 5000 rad brains. This radiation- induced change was also noticed qualitatively by viewing the spectra (Figure 6.5). At 81 days, a decrease in n-acetyl aspartate and total creatine peak area ratios was seen on the left side and a slight increase in p-choline was seen on the right side of irradiated brains (See table 6.1). These results assume that the area under the water peak remains constant. However, it has been shown in chapters 2-4, that the spin density is not constant in irradiated brains; therefore, peak area ratios were also calculated relative to N-acetyl aspartate (Table 6.2). At 25 days an increase in the lipid peak area ratio was still seen on the right side of the brain.

TABLE 6.1
PEAK AREA RATIOS RELATIVE TO WATER
FROM PHASE-ENCODED PROTON SPECTRA

DOSE	CHEMICAL	LEFT SIDE (CONTROL)	RIGHT SIDE (IRRAD.)
		4 DAYS POST-IRRADIATION	
0.	LIPIDS	2.00 +/- 1.82	1.7 +/- .37
5000.	LIPIDS	4.35 +/- 1.78	1.68 +/- .54
0.	N-ACETYL ASP	1.61 +/- .936	2.38 +/- .41
5000.	N-ACETYL ASP	2.61 +/- .69	3.00 +/- 2.41
		25 DAYS POST-IRRADIATION	
0.	LIPIDS	2.34 +/- .74	.427 +/- .048
3000.	LIPIDS	4.82 +/- 2.86	.253 +/- .261
5000.	LIPIDS	2.58 +/- 1.0	14.9 +/- .71
0.	N-ACETYL ASP	5.30 +/- 1.8	15.2 +/- 12.1
3000.	N-ACETYL ASP	4.63 +/- .98	7.26 +/- 4.66
5000.	N-ACETYL ASP	3.55 +/- 1.35	9.76 +/- 4.32
		81 DAYS POST-IRRADIATION	
0.	LIPIDS	.968 +/- .324	2.38 +/- .79
3000.	LIPIDS	3.00 +/- .531	.813 +/- .23
5000.	LIPIDS	2.33 +/- .49	2.83 +/- 1.8
0.	N-ACETYL ASP	5.93 +/- 2.11	9.92 +/- 1.15
3000.	N-ACETYL ASP	2.48 +/- .636	5.22 +/- 1.35
5000.	N-ACETYL ASP	3.15 +/- .79	5.46 +/- 3.0
0.	PCR + CR	.954 +/- .39	.785 +/- .22
3000.	PCR + CR	.779 +/- .24	.438 +/- .119
5000.	PCR + CR	.490 +/- .0098	.522 +/- .092
0.	P-CHO	.835 +/- .51	.933 +/- .087
3000.	P-CHO	.816 +/- .096	.948 +/- .078
5000.	P-CHO	.715 +/- .145	1.02 +/- .25

NOTE: All values were calculated by dividing the peak area of interest by the peak area of water and multiplying by 1000 +/- S.E.M.

TABLE 6.2
PEAK AREA RATIOS RELATIVE TO N-ACETYL ASPARTATE
FROM PHASE-ENCODED PROTON SPECTRA

DOSE	CHEMICAL	LEFT SIDE (CONTROL)	RIGHT SIDE (IRRAD.)
		4 DAYS POST-IRRADIATION	
0.	LIPIDS	.874 +/- .62	.71 +/- .031
5000.	LIPIDS	1.47 +/- .38	1.4 +/- .54
		25 DAYS POST-IRRADIATION	
0.	LIPIDS	.41 +/- .010	.069 +/- .051
3000.	LIPIDS	1.34 +/- .81	.059 +/- .079
5000.	LIPIDS	.99 +/- .63	3.77 +/- 3.611
		81 DAYS POST-IRRADIATION	
0.	LIPIDS	.165 +/- .0042	.252 +/- .104
3000.	LIPIDS	1.61 +/- .804	.154 +/- .017
5000.	LIPIDS	.76 +/- .07	2.49 +/- 2.2
0.	PCR+CR	.158 +/- .0088	.083 +/- .032
3000.	PCR+CR	.341 +/- .085	.11 +/- .053
5000.	PCR+CR	.177 +/- .045	.204 +/- .08
0.	P-CHO	.197 +/- .16	.096 +/- .011
3000.	P-CHO	.401 +/- .14	.21 +/- .054
5000.	P-CHO	.261 +/- .075	.33 +/- .10

NOTE: All values were calculated by dividing the peak area of interest by the peak area of N-acetyl aspartate +/- S.E.M.

CHAPTER 7. PROTON CHEMICAL SHIFTS OF AQUEOUS AND ORGANIC FRACTIONS OF BRAIN EXTRACTS

Proton spectroscopy was performed on brain extracts in order to measure radiation-induced changes in concentrations of several different brain chemicals that could not be seen in vivo. Using a new extraction method we developed (Jones et al., 1984), both aqueous and organic brains extracts were prepared for high resolution proton spectroscopy. Tissues were used from rats which were imaged and measured with phase-encoding spectroscopy in vivo (chapters 4 and 6).

7.1 Methods

Proton spectroscopy was performed on brain extracts from five rats of the 4 day group and from six rats of the 3 month post- irradiation group. The irradiation procedure was described in section 4.3.

7.1.1 Brain preparation

Brain tissue was frozen in situ by pouring liquid nitrogen through a funnel directly onto the exposed skull of the anesthetized rat (Poten et al., 1973). Pieces of frozen brain were chiseled from the right and left sides of the cerebrum and the two sides were processed separately. The frozen brain samples were weighed and then homogenized in cold 1:2 chloroform - methanol (3 ml/gm brain tissue). 100 micro-liters (.6 mg/ml) of 3 - (trimethylsilyl)- 1 - propane - sulfonic acid; sodium salt (DSS) was added to the homogenate to act as a chemical shift

reference as well as a peak area standard for the aqueous phase. The single phase homogenate was vortexed with 1:1 chloroform - water (2 ml/gm brain tissue). The added solvents forced the mixture to separate into 3 phases after centrifugation at 2900 rpm for 5 minutes. The organic and aqueous fractions were separated and frozen for storage. The fractions were lyophilized and reconstituted in 1 ml deuterium oxide for the aqueous phase and in 1 ml deuterated chloroform for the organic phase.

7.1.2 The NMR experiment

The reconstituted samples were placed in 5 mm NMR test-tubes and proton spectroscopy was performed on the 200 or 180 MHz spectrometer. Shimming was done automatically with the Z1, Z2, and Z3 shims and manually with the X and Y shims. A one-pulse sequence was used with the following parameters: 70 degree flip angle; 16k data points - aqueous, 8k data points - organic; quadrature phase cycling; quadrature phase detection; 2.05 second aquisition time; 5 second delay time; 60 transients - aqueous, 40 transients - organic; +/- 2000 hertz spectral width; sample spinning; and deuterium lock.

Data processing-

The FIDs were sent to the VAX computer by phone line (section 4.3) and program NTCFT2 (section 4.3) was used to quantitate the area under the peaks. For the aqueous fractions, the FIDs were apodized with 2 hertz line-broadening and the following peaks were analyzed: p-choline (3.22 ppm); total creatine (3.02 ppm); sarcosine (2.72 ppm);

glutamate (2.34 ppm); n-acetyl aspartate (2.00 ppm); GABA, acetate (1.90 ppm); alanine (1.48 ppm); and lactate (1.33 ppm). The chemical shifts were referenced to DSS (0.00 ppm). The peak area ratios in Table 7.4 were calculated relative to n-acetyl aspartate.

For the organic fraction, the FIDS were apodized with 4 hertz line-broadening and the following were analyzed: 5.37 ppm; 3.29 ppm; 2.84 ppm; 2.28 ppm; methylene 1.25 ppm; terminal methyls 1.01 ppm; .882 ppm; .848 ppm; and .679 ppm. The chemical shifts were referenced to chloroform at 7.27 ppm. Peak area ratios in Table 7.6 were calculated relative to the methylene peak area.

7.1.3 Calibration of NMR peak areas with chemical concentration

In order to test the linearity of NMR peak areas with concentration, a calibration curve was measured for sarcosine and methionine at 6 different concentrations. Bovine brain (1.2 grams) was homogenized and the extra amounts of sarcosine and methionine were added to the homogenate before the extraction procedure continued (section 7.1.1). The peak area ratios to DSS were calculated (section 7.1.2) and the following equation was to used to calculate the peak area responsible for the exogenous chemicals:

NMR conc. = [peak area (met.)/ peak area (DSS)] - Xo * brain weight

where Xo = [peak area (endogenous met.)/peak area (DSS)] / brain weight

The calibration curves, shown in Figure 7.1, are fairly linear with concentration except for the points near the origin. This curve could

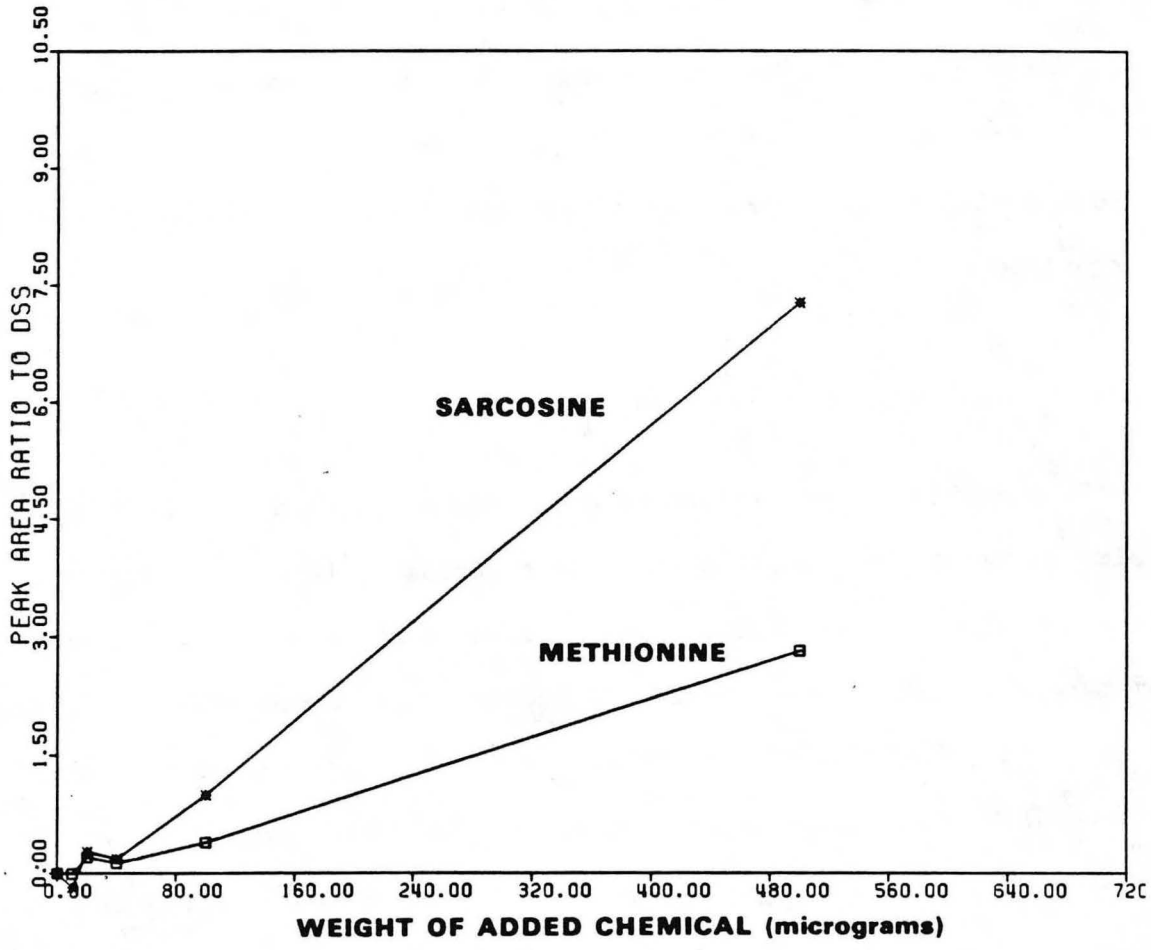

XBL 849-3676

Figure 7.1 - Plot of added chemical weight vs. peak area ratio to DSS for sarcosine (2.72 ppm) and methionine (2.13 ppm).

then be used to calculate the actual concentration of sarcosine and methionine in the sample. To check the reproducibility of the peak area ratio measurement, the N-acetyl aspartate and PCR+CR peaks were analyzed in all six spectra and the result is shown in Figure 7.2. These two curves should be flat because each test-tube contained similar pieces of homogenized brain.

7.1.4 Chemical shifts of isolated brain chemicals

Peak assignment of resonances observed in the proton spectrum of brain extracts was done using previous peak assignments found in the literature (Behar et al., 1983) and by measuring the proton spectrum on several chemicals known to be at relatively high concentrations in the brain (Biochemist's handbook, 1968). Table 7.1 shows the concentrations of several brain chemicals. Proton spectroscopy was measured separately for each of the following chemicals in aqueous solution: lactate, alanine, GABA, acetyl-l-glutamate, n-acetyl aspartate, glutamate, glutathione, glutamine, methionine, deanol, pyruvate, aspartate, sarcosine, creatine, phosphocreatine, creatinine, dimethyl glycine, choline, taurine, and betaine. Aqueous solutions were prepared for spectroscopy by placing the dry chemical in D2O (low solubility) or H2O (high solubility) and the pH was measured. Table 7.2 shows the chemical shifts (in ppm with reference to DSS = 0.) of all 22 chemicals. Proton spectroscopy was also done on phosphatidyl ethanolamine, phosphatidyl serine, lysolecithin, and sphingomyelin dissolved in deuterated chloroform. The results of the chemical shifts and peak heights are

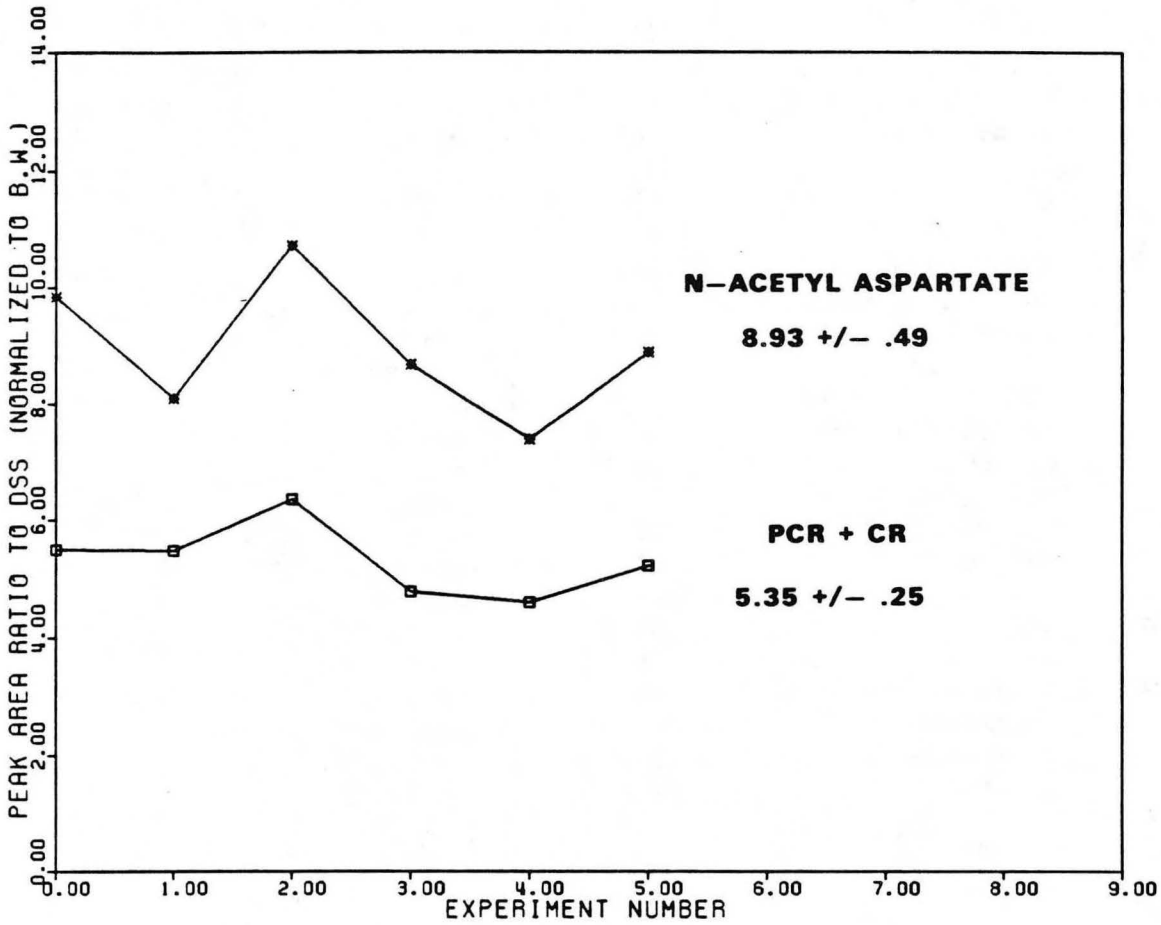

XBL 849-3677

Figure 7.2 - N-acetyl asp and PCR+CR peak area ratios for six different trials (normalized to brain weight). The values shown to the right of the curves are the average of six +/- SEM.

TABLE 7.1 - CONCENTRATIONS OF BRAIN CHEMICALS (LOW MOLECULAR WEIGHT)
(From Biochemist's handbook, 1968; and Reichelt et al., 1969)

lecithin	15.7 +/- .9	g/kg
glutamic acid	1300 - 1700	mg/kg
glutamine	480 - 780	mg/kg
aspartic acid	360 - 480	mg/kg
GABA	210 - 630	mg/kg
alanine	50 - 94	mg/kg
taurine	450 - 810	mg/kg
acetyl-choline	2.7	mg/kg
total creatine	1300	mg/kg
glutathione	705	mg/kg
methionine	10 - 14	mg/kg
ATP	1080 - 1325	mg/kg
phosphocreatine	560 - 760	mg/kg
phosphorylcholine	66 - 81	mg/kg
lactic acid	134 - 244	mg/kg
pyruvic acid	17.2	mg/kg
serine	87 - 115	mg/kg
histamine	4.3	mg/kg
n-acetyl aspartate	5.18	umoles/g
n-acetyl aspartyl-glu	.44	umoles/g
n-acetyl glutamate	.06	umoles/g
glutathione	1.10	umoles/g
aspartate	3.40	umoles/g
glutamate	9.85	umoles/g

TABLE 7.2 - CHEMICAL SHIFTS OF ISOLATED BRAIN CHEMICALS (AQUEOUS)

PPM	CHEMICAL	PPM	CHEMICAL
4.66	water	3.248	taurine
4.597	glutathione (pd 7.0)	3.214	taurine
4.566	glutathione	3.206	choline
4.536	glutathione	3.038	creatinine (pd 7.5)
4.414	n-acetyl asp (pd ~ 7.0)	3.032	GABA
4.395	n-acetyl asp	3.029	phosphocreatine (pd 7.3)
4.366	n-acetyl asp	3.023	creatine (pd 7.3)
4.346	n-acetyl asp	2.996	GABA
4.175	lactate (ph 7.0)	2.988	dimethyl glycine
4.137	lactate	2.958	GABA
4.128	acetyl-l-glu (pd 7.0)	2.957	glutathione (pd 7.0)
4.105	acetyl-l-glu	2.932	glutathione
4.099	lactate	2.921	glutathione
4.087	dimethyl glycine	2.777	aspartate
4.083	acetyl-l-glu	2.759	aspartate
4.064	choline	2.737	n-acetyl asp
4.062	acetyl-l-glu	2.723	sarcosine
4.060	lactate	2.718	n-acetyl asp
4.044	choline	2.717	aspartate
4.038	creatinine	2.677	aspartate
4.032	choline	2.659	n-acetyl asp
3.937	phosphocreatine	2.665	methionine
3.920	aspartate (ph 6.3)	2.640	n-acetyl asp
3.917	creatine	2.627	methionine
3.900	asp	2.591	methionine
3.880	asp	2.544	n-acetyl asp
3.878	methionine (pd 7.2)	2.522	deanol
3.862	asp	2.496	n-acetyl asp
3.846	methionine	2.490	deanol
3.816	methionine	2.481	glutamine
3.805	glutathione (pd 7.0)	2.467	n-acetyl asp
3.770	glutamate (ph 7.9)	2.460	deanol
3.769	glutathione	2.450	glutamine
3.745	glutamate	2.441	glutamine
3.742	glutathione	2.418	n-acetyl asp
3.737	glutamate	2.407	glutamine
3.712	glutamate	2.374	glutamate (ph 7.9)
3.693	deanol	2.372	pyruvate
3.661	deanol	2.319	GABA
3.630	deanol	2.339	glutamate
3.601	sarcosine (pd 7.5)	2.302	glutamate
3.550	choline	2.282	GABA
3.530	choline	2.264	acetyl-l-glutamate
3.510	choline	2.247	GABA
3.438	taurine (ph 7.2)	2.224	acetyl-l-glutamate
3.401	taurine	2.215	methionine
3.376	taurine	2.209	glutathione
3.338	betaine	2.208	deanol
3.279	taurine	2.187	acetyl-l-glutamate

TABLE 7.2 - CHEMICAL SHIFTS OF ISOLATED BRAIN CHEMICALS (AQUEOUS)
(continued)

PPM	CHEMICAL
2.185	methionine
2.180	glutamine
2.177	methionine
2.173	glutathione
2.15	methionine
2.149	glutamine
2.139	glutamate
2.138	glutathione
2.127	acetyl-l-glutamate
2.118	methionine
2.115	glutamate
2.108	glutamine
2.105	glutamate
2.103	glutathione
2.08	glutamate
2.071	glutamine
2.04	glutamate
2.02	acetyl-l-glutamate
2.007	n-acetyl asp
1.921	GABA
1.906	acetyl-l-glutamate
1.885	GABA
1.87	acetyl-l-glutamate
1.847	GABA
1.483	alanine
1.477	alanine
1.331	lactate
1.297	lactate
0.0	DSS (reference)

shown in Table 7.3. The spectrum of sphingomyelin had very broad peaks at 3.5 and 1.7 ppm with a sharp peak at 1.26 ppm.

7.2 Results

Aqueous fraction:

The aqueous fraction spectra had much sharper lines than the organic because the aqueous fraction molecules were smaller and therefore they could tumble more freely. The spectrum shown in Figure 7.3 demonstrates the .005 ppm resolution and the chemical information available from proton spectroscopy of brain extracts. In the region between 4.5 to 0. ppm, the chemicals identified were DSS, lactate, alanine, GABA, n-acetyl aspartate, glutamate, aspartate, creatine, phosphocreatine, and p-choline. In the region between 10. to 6. ppm, the peaks have not been clearly identified but they may be the ring protons of histidine and ATP.

As shown in Tables 7.4 and 7.5, at 4 days post-irradiation, on the controls side, an increase was seen in lactate, GABA+acetate, and PCR+CR. On the irradiated side, an increase was seen in GABA+acetate, PCR+CR, and P-choline relative to controls. At 3 months post-irradiation, on the controls side, an increase was seen in lactate, alanine (3000 rad), glutamate, and p- choline; and a decrease was seen in the GABA+acetate and alanine (5000 rad). On the irradiated side, an increase was seen in lactate, glutamate, PCR+CR, and p-choline; and a decrease was seen in alanine (3000 rad) and GABA+acetate.

Table 7.3 - CHEMICAL SHIFTS OF ISOLATED CHEMICALS (ORGANIC)

PHOSPHATIDYL ETHANOLAMINE		PHOSPHATIDYL SERINE		LYSOLECITHIN	
PPM	PEAK HEIGHT	PPM	PEAK HEIGHT	PPM	PEAK HEIGHT
5.370	263.82	5.360	149.46	4.074	59.73
4.164	57.03	2.841	84.13	3.807	62.16
4.137	73.79	2.324	68.19	3.343	463.10
4.105	86.25	2.288	71.06	2.310	74.56
3.987	66.71	2.006	113.52	2.241	457.67
3.959	92.97	1.814	943.09	1.348	57.83
3.929	59.38	1.648	71.38	1.263	1524.8
3.174	66.02	1.591	95.61	1.177	55.48
3.165	65.24	1.258	1851.8	.913	65.48
2.841	119.2	1.171	97.52	.888	127.71
2.814	133.07	.886	232.5	.856	57.62
2.784	68.74	.855	107.22	.008	266.38
2.388	53.68	.008	437.04		
2.323	123.27				
2.295	124.01				
2.257	171.23				
2.035	145.31				
1.848	1006.21				
1.592	121.49				
1.259	4241.42				
1.172	151.35				
.886	473.16				
.854	186.08				
.006	734.30				

NOTE: The chloroform peak was used as a chemical shift reference at 7.27 ppm.

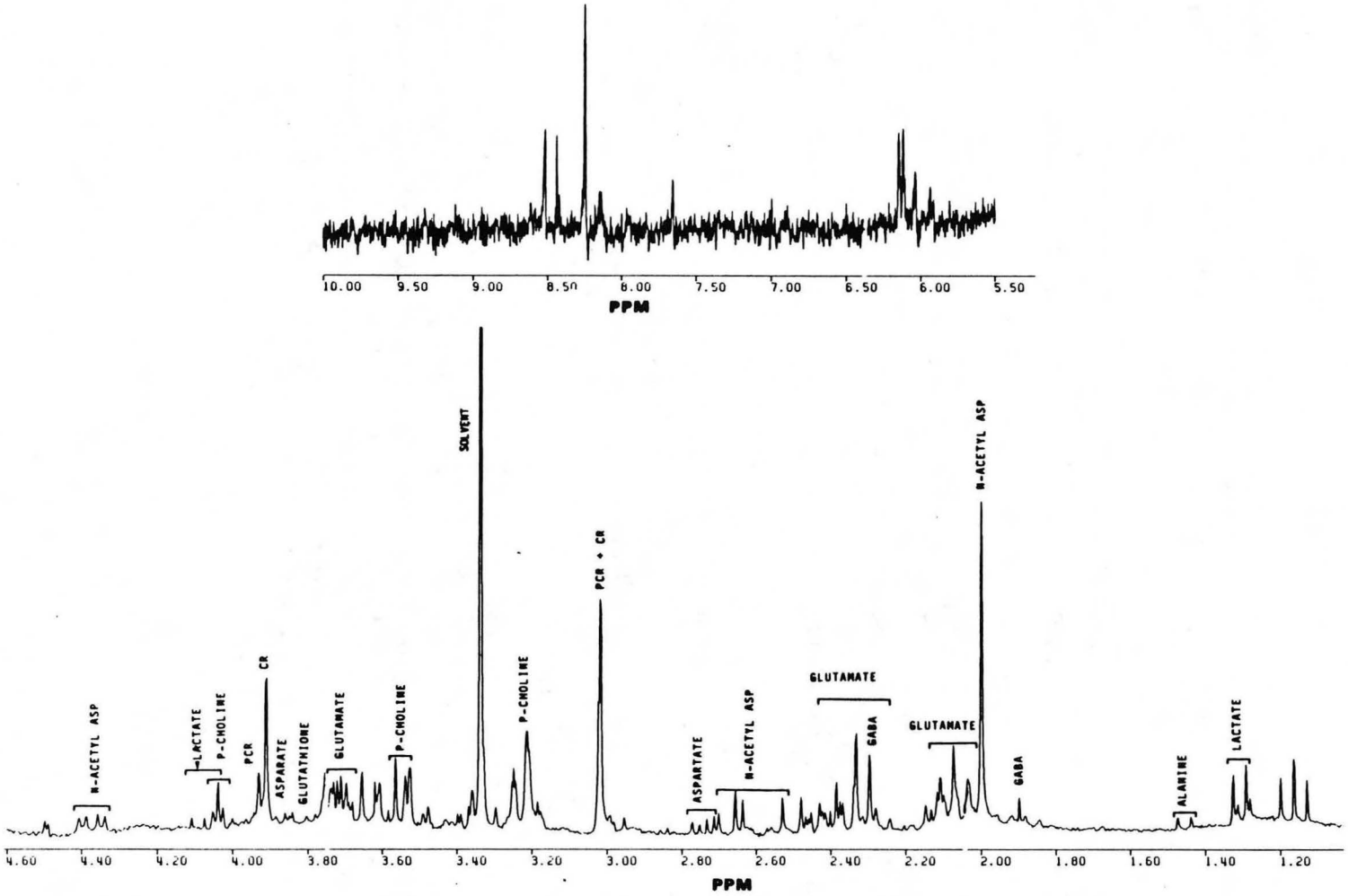

XBL 849-3678

Figure 7.3 - Proton spectrum of aqueous fraction of irradiated brain. Region 10. - 5.5 ppm is shown on the top and 4.5 - 1.2 ppm is shown on the bottom. (N-acetyl asp was set to 2.00 ppm for reference).

TABLE 7.4
AQUEOUS FRACTION PEAK AREA RATIOS TO N-ACETYL ASPARTATE

		4 DAYS POST		3 MONTHS POST			
CHEMICAL	CONTROL	5000C	5000I	3000C	3000I	5000C	5000I
LACTATE	.115 +/- .025	.37	.14	.28	.26	.082	.113
1.33 PPM		.071	.099	.125	.21	.117	
			.066				
ALANINE	.032 +/- .004	.023	.042	.045	.030	.030	.035
1.48 PPM		.032	.022	.036	.023	.027	
			.023				
GABA+ACET	.033 +/- .004	.042	.053	.017	.019	.018	.045
1.88 PPM		.035	.035	.019	.030	.026	
			.042				
GLUTAMATE	.384 +/- .055	.37	.44	.45	.52	.46	.39
2.34 PPM		.40	.38	.48	.41	.35	
			.42				
PCR+CR	1.25 +/- .101	1.57	1.28	1.21	1.57	1.6	1.19
3.02 PPM		1.28	1.58	1.35	1.30	1.1	
			1.38				
P-CHO	.51 +/- .038	.53	.92	.55	.65	1.05	.63
3.21 PPM		.59	.61	.67	.80	.62	

NOTE: 5000C refers to 5000 rads control side of the brain and 5000I refers to 5000 rads irradiated side of the brain. Control value is shown as the average of 8 +/- SEM. All values were calculated by dividing the peak area of interest by the peak area of n-acetyl aspartate. Values from each individual animal are shown in columns 3 - 8. For example, in the 5000I column, the peak area ratios for three different animals are shown for each chemical. These same data are displayed in Table 7.5 normalized to controls.

TABLE 7.5
AQUEOUS FRACTION PEAK AREA RATIOS TO N-ACETYL ASP
NORMALIZED TO CONTROLS

	4 DAYS POST		3 MONTHS POST			
CHEMICAL	5000C	5000I	3000C	3000I	5000C	5000I
LACTATE 1.30 PPM	1.93	.89	1.74	2.01	.86	.98
ALANINE 1.48 PPM	.87	.92	1.29	.83	.75	1.12
GABA+ACET 1.90 PPM	1.18	1.33	.55	.74	.68	1.37
GLUTAMATE 2.34 PPM	1.00	1.07	1.22	1.22	1.06	1.02
PCR+CR 3.03 PPM	1.14	1.13	1.02	1.15	1.08	.95
P-CHO 3.22 PPM	1.09	1.50	1.18	1.41	1.62	1.23

NOTE: Same as Table 7.4 except that the peak area ratios relative to n-acetyl aspartate are averaged and divided by the control peak area ratios in order to compare the irradiated values to controls.

Organic fraction:

The spectrum shown in Figure 7.4 is an example of the proton spectrum of the organic fraction of irradiated brain extract. The peaks in this spectrum represent the lipids of the brain. However, the heights of the peaks do not represent what would be seen in vivo because the lipid protons are more mobile in an organic solvent than as lipid bilayers in the myelin sheaths (Joffe et al, 1972). As shown in Tables 7.6 and 7.7, a decrease in the peaks at 2.84 and 3.29 ppm and an increase in the peak at 2.28 ppm were seen at 4 days post-irradiation. At 3 months post- irradiation decreases were seen in terminal methyl peaks (.68, .85, .88 1.01) and at peaks 2.28, 2.84, and choline methyls (3.29 ppm).

The main results from this investigation are: 1) increases were noted early after irradiation in lactate, GABA, PCR+CR, and p-choline peak area ratios relative to n-acetyl aspartate; 2) increases were noted late after irradiation in lactate, glutamate, and p-choline; 3) from the organic fraction spectra, decreases were noted on both sides of the brain at peaks 2.84 ppm (phosphatidyl ethanolamine, phosphatidyl serine), 3.29 ppm (lecithin) and the terminal methyls (5000 rads, 3 months post). These results show that radiation induces changes in brain energy metabolites and in lipid chemistry.

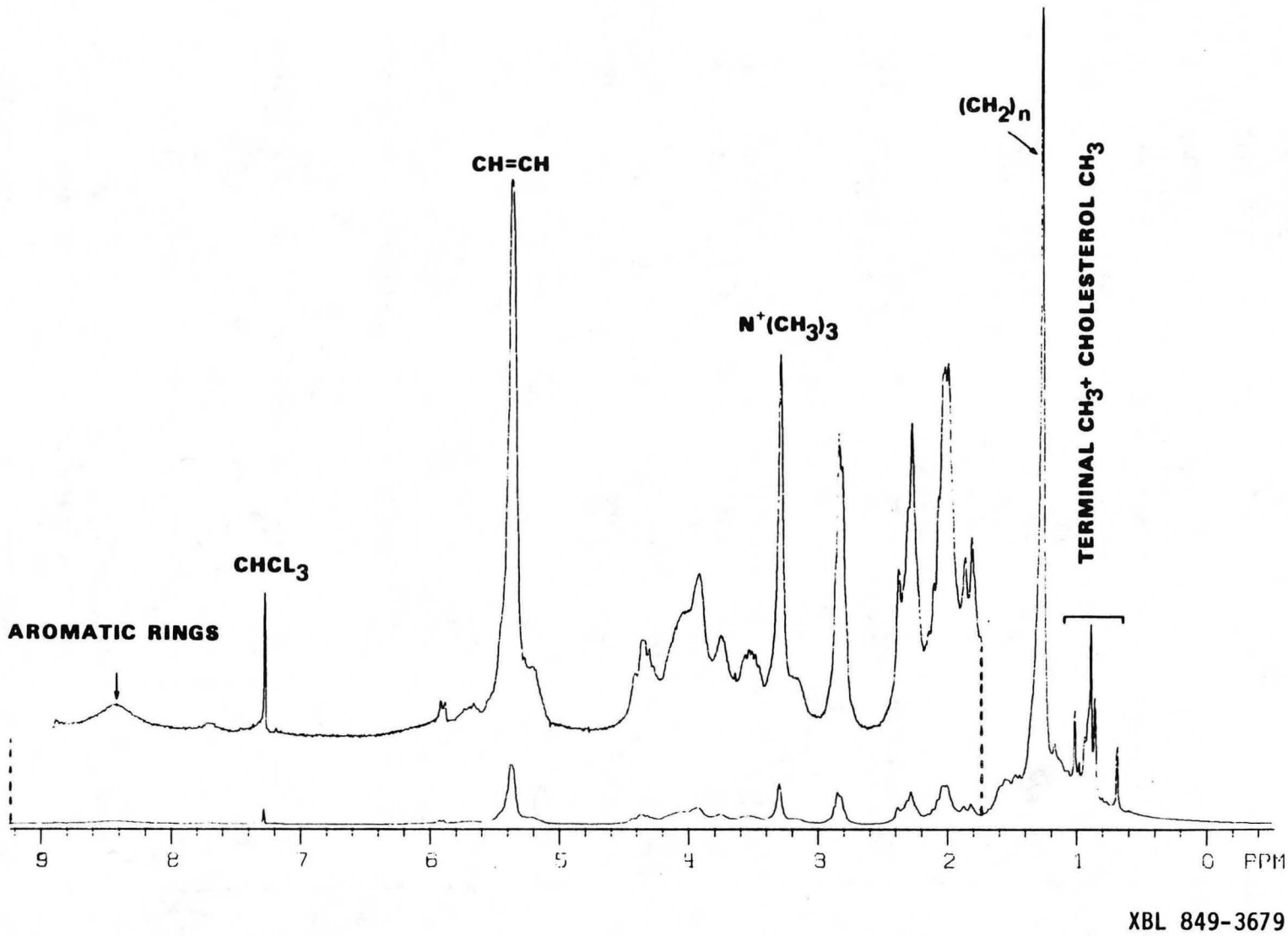

Figure 7.4 - Proton spectrum of organic fraction of irradiated brain. (Chloroform was set to 7.27 ppm for reference).

TABLE 7.6
ORGANIC FRACTION PEAK AREA RATIOS RELATIVE TO METHYLENE

		4 DAYS POST		3 MONTHS POST			
CHEMICAL	CONTROL	5000C	5000I	3000C	3000I	5000C	5000I
.68 PPM	.041 +/-.0015	.039	.042	.037	.038	.037	.038
(not		.041	.037	.045	.043	.041	.032
iden.)		.041	.037				
.85 PPM	.029 +/-.0022	.023	.028	.025	.0081	.030	.030
P-ETHAN		.034	.025	.024	.038	.033	.020
P-SERINE		.037	.032				
LECITHIN							
.88 PPM	.091 +/-.0030	.074	.095	.090	.076	.078	.067
P-ETHAN		.098	.088	.059	.105	.082	.091
P-SERINE		.11	.096				
LECITHIN							
1.01 PPM	.037 +/-.00093	.039	.038	.036	.036	.032	.030
(not		.038	.037	.042	.041	.036	.023
iden.)		.041	.036				
2.03 PPM	.092 +/-.0015	.086	.074	.092	.095	.088	.077
P-ETHAN		.093	.098	.088	.103	.095	.095
		.096	.091				
2.28 PPM	.095 +/-.0012	.131	.20	.092	.084	.079	.078
P-SERINE		.091	.088	.098	.105	.084	.086
		.069	.085				
2.84 PPM	.10 +/-.0045	.066	.078	.085	.071	.063	.071
P-ETHAN		.076	.073	.079	.152	.070	.083
P-SERINE		.074	.103				
3.29 PPM	.063 +/-.0012	.051	.067	.062	.057	.048	.052
LECITHIN		.060	.057	.063	.077	.053	.056
		.061	.062				
5.37 PPM	.14 +/-.0022	.113	.151	.146	.134	.118	.111
P-ETHAN		.140	.133	.160	.164	.126	.157
P-SERINE		.139	.145				

NOTE: 5000C refers to 5000 rads control side of the brain and 5000I refers to 5000 rads irradiated side of the brain. Control value is shown as the average of 8 +/- SEM. All values were calculated by dividing the peak area of interest by the peak area of the methylene peak (1.26 ppm). Values from each individual animal are shown in columns 3 - 8. For example, in the 5000I column, the peak area ratios for three different animals are shown for each chemical. These same data are displayed in Table 7.7 normalized to controls.

TABLE 7.7
ORGANIC FRACTION PEAK AREA RATIOS
NORMALIZED TO CONTROLS

PPM	4 DAYS POST		3 MONTHS POST			
	5000C	5000I	3000C	3000I	5000C	5000I
.68	0.98	0.94	1.01	0.99	0.95	0.86
.85	1.09	0.99	0.85	0.79	1.10	0.87
.88	1.02	1.02	0.82	0.99	0.88	0.87
1.01	1.07	1.01	1.06	1.04	0.92	0.72
2.03	0.99	0.95	0.97	1.07	0.99	0.93
2.28	1.02	1.32	1.00	1.00	0.86	0.87
2.84	0.72	0.84	0.82	1.11	0.66	0.77
3.29	0.91	0.98	0.98	1.06	0.80	0.86
5.37	0.95	1.04	1.11	1.09	0.89	0.98

NOTE: Same as Table 7.6 except that the peak area ratios relative to methylene are averaged and divided by the control peak area ratios in order to compare irradiated values to controls.

CHAPTER 8. HISTOLOGY OF IRRADIATED BRAINS

Histological techniques were used to evaluate the state of the irradiated brain tissue from rats which were previously imaged and measured with proton spectroscopy in vivo. Although pathology of radiation brain damage is well known using X-ray irradiation (Fajardo et al., 1982), there is very little literature concerning half brain helium beam irradiation. The histology was done in order to correlate cellular and structural changes with changes in the T1 relaxation time of the water signal in the brain.

8.1 Methods

Histology was performed on brains from rats sacrificed at the following intervals after irradiation; 4 days, 2.7 months, and 7.3 months. Evans blue was injected (.6cc of 2% solution in saline) into the tail vein of the rat 20 minutes before sacrificing to measure the integrity of the blood-brain barrier. The brains were removed immediately after death, (except in one case (r3e) in which the brain was removed one hour after death), and placed in Tellyesniczky acetic alcohol formalin (Telly's solution) for 3 days. Then, they were placed in 60% ethanol for one hour, 70% ethanol for one hour, and left in 80% for one week. The brains were embedded in paraffin and coronal sections were cut at 10 microns from the frontal cerebrum, mid- cerebrum, and hind-cerebrum areas. Selected sections were stained using the following techniques: hematoxylin and eosin; Mahon's myelin sheath stain, and

Vogt's method for nerve cell products (nissl). Figure 8.1 shows the hematoxylin and eosin sections from a control brain and Figure 8.2 shows the same sections using the Mahon's myelin sheath stain. Microscopic specimens were evaluated qualitatively for sites of tissue necrosis, demyelination, vessel wall thickening, gliosis, calcification, and hemorrhage. Alterations in the blood brain barrier were evaluated semi-quantitatively by counting the number of Evans blue stained spots on each side of the brain. The sections were also evaluated for gross anatomical changes such as ventricular enlargement and tissue swelling. Rat brain anatomy was identified using a rat brain atlas of coronal sections (Pellegrino et al., 1979).

8.2 Results

Early radiation damage-

The most consistent change in appearance between the irradiated and controls at 4 days and 3 months post-irradiation was an increase in Evans blue staining. The Evans blue spots were easily identified as purple regions on the hematoxylin and eosin sections viewed with dark field microscopy (See Figure 8.3). As shown in Table 8.1, there is an increase in the number of Evans blue spots both as a function of dose and time after irradiation. At 4 days after irradiation, the spots were mainly confined to the corpus callosum, however at 3 months, spots were also seen in the fimbria of the hippocampus, the internal capsule, and occasionally in the cerebral cortex. The myelin stained sections did not reveal any changes in myelin stain uptake for the 4 day and 3 month

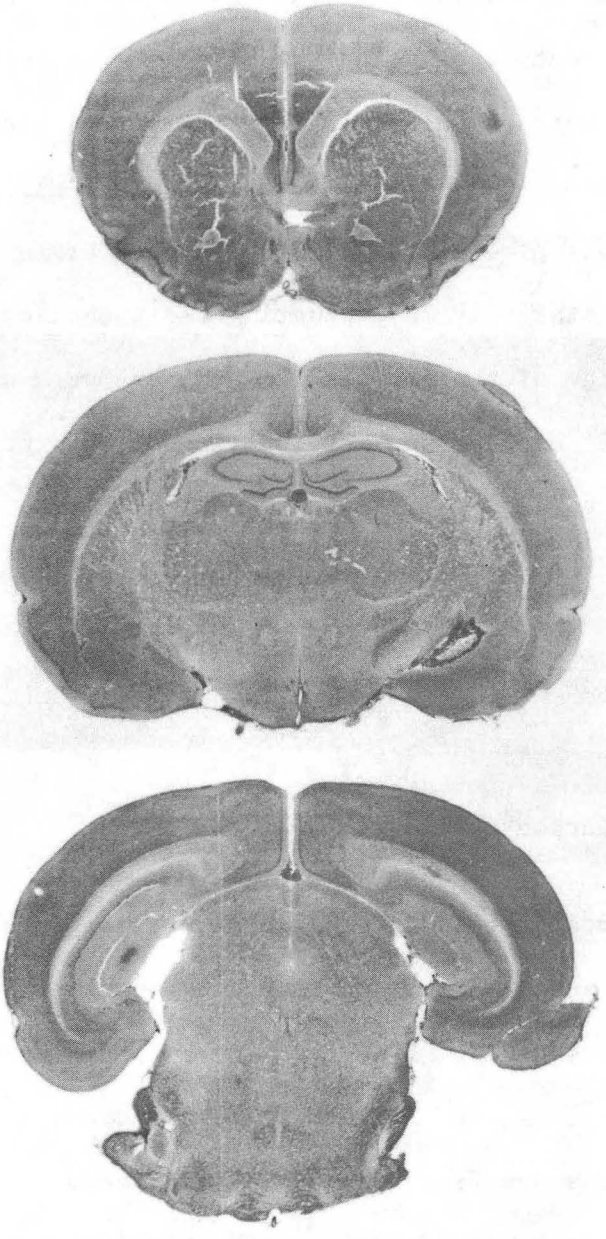

CBB 849-6708

Figure 8.1 - Three coronal paraffin sections of a control brain at three different levels: top section passes through the caudate nucleus; middle section passes through the hippocampus; and bottom section passes through the reticular formation (Hematoxylin and eosin stain, magnification X 6.3).

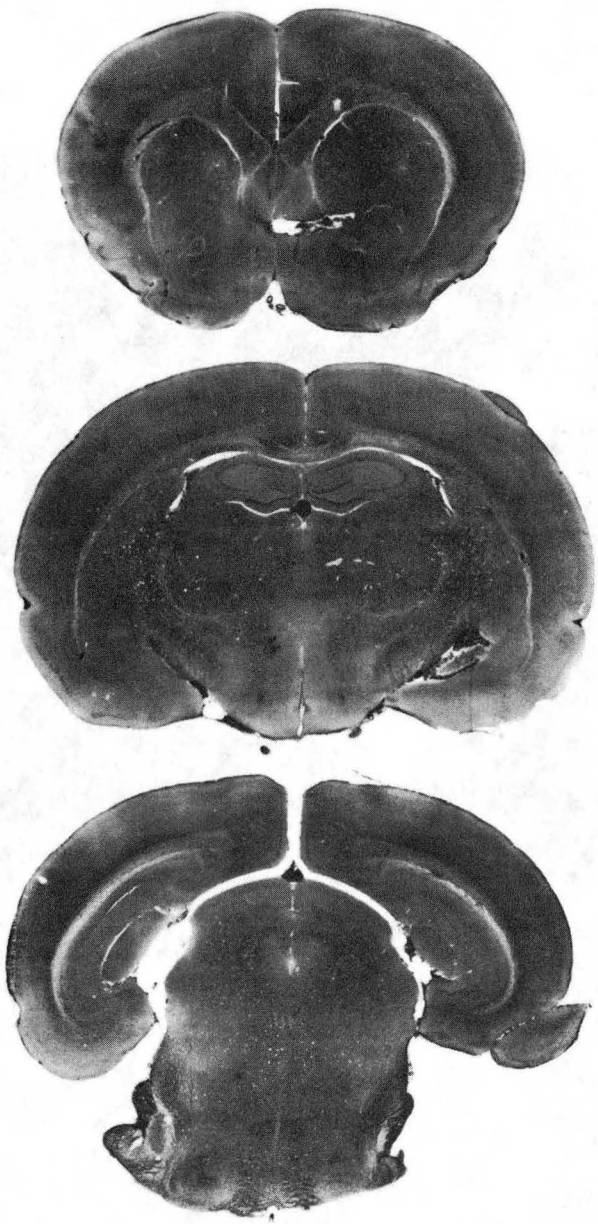

CBB 849-6710

Figure 8.2 - Same as in Figure 8.1 except with Mahon's myelin sheath stain.

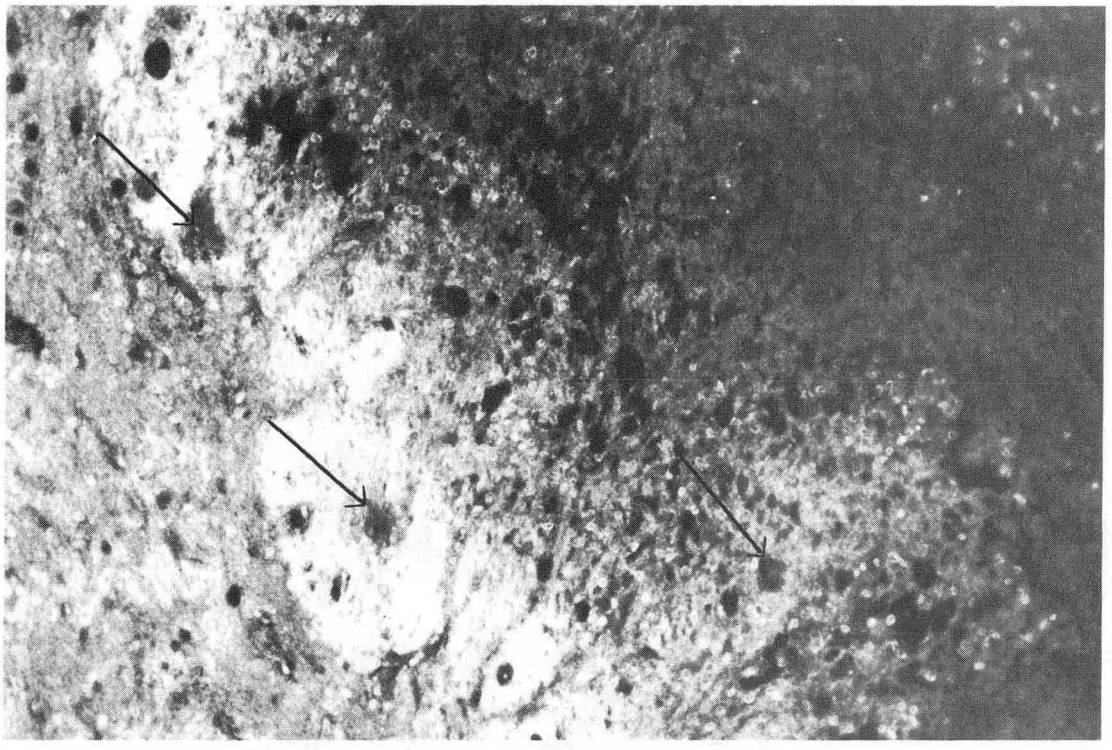

Figure 8.3 - Region from the internal capsule from the irradiated side of a rat that received 3000 rads (7 months post-irradiation). The purple areas (arrows) demonstrate Evans blue infiltration caused by blood-brain barrier alteration (HE stain, dark field micrograph, mag. X 130).

CBB 830-9839

TABLE 8.1 - NUMBER OF EVANS BLUE STAINED SPOTS

	FRONTAL		MID		HIND	
CONTROLS	2.0 +/- 1.4		.25 +/- .25		1.5 +/- .95	
	I	C	I	C	I	C
4 DAYS						
5000 RADS	0.	0.	0.	0.	7.	1.
3 MONTHS						
3000 RADS	23.	15.	6.	3.5	16.	6.5
5000 RADS	22.	14.5	32.	8.	16.	8.
7 MONTHS						
3000 RADS	-	-	87.	1.	-	-

NOTE: Control values are show as the average of 4 values +/- S.E.M.

Abbreviations: I - irradiated side; C - control side of the brain.

brains. The left ventrical on two irradiated brain sections (4 days post) and on one brain section (3 months post) was enlarged. Figure 8.4 shows an example of an irradiated rat that had an enlarged right ventrical which correlated with an increase in T1 relaxation time on the right side of the brain.

Late radiation damage-

Large lesions of radiation necrosis were seen in the brain sections at 7.3 months post-irradiation. The lesions were seen in the fimbria of the hippocampus, internal capsule and in the corpus callosum (See Figure 8.5). Figure 8.6 shows an example of a necrotic lesion in the internal capsule. The center of the lesion was devoid of blood vessels and no Evans blue staining was seen. However, at the edge of the lesion Evans blue staining was seen. Figure 8.3 shows the same region of brain as Figure 8.6 but with dark field lighting. Four spots of Evans blue can be seen around the periphery of the necrotic area. Demyelination was seen in the myelin stain sections (Figure 8.7) of irradiated animals but not in controls (Figure 8.8). Other radiation-induced changes included: calcification (Figure 8.9), vessel wall thickening, and gliosis.

In summary, no difference was seen between irradiated and control histological sections of the brain 4 days after irradiation, except for some Evans blue staining. As time after irradiation progressed, the Evans blue spots became more frequent and larger in the white matter. Demyelination was only seen in the myelin-sheath sections 7 months after irradiation. Ventricular enlargement was apparent in some animals at 3 months post-irradiation.

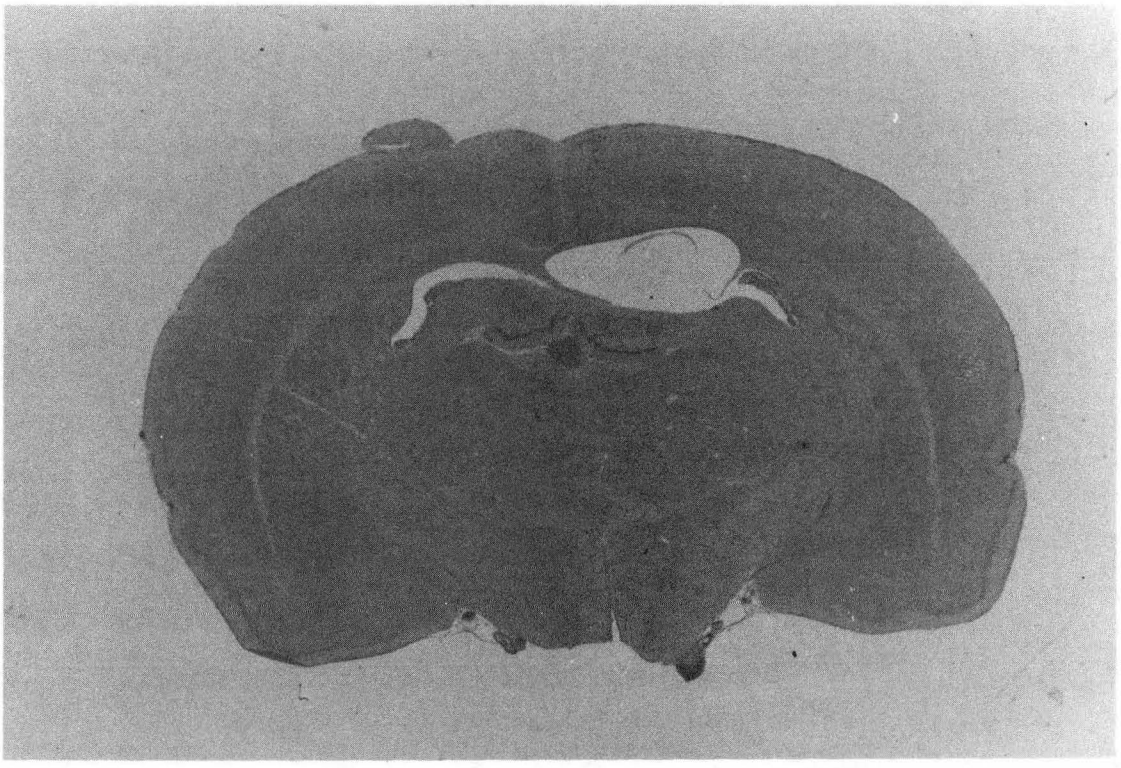

Figure 8.4 - Coronal section of brain from irradiated rat (5000 rads, 81 days post-irradiation). The irradiated side is on viewers right (HE stain, mag. X10).

XBC 847-5435

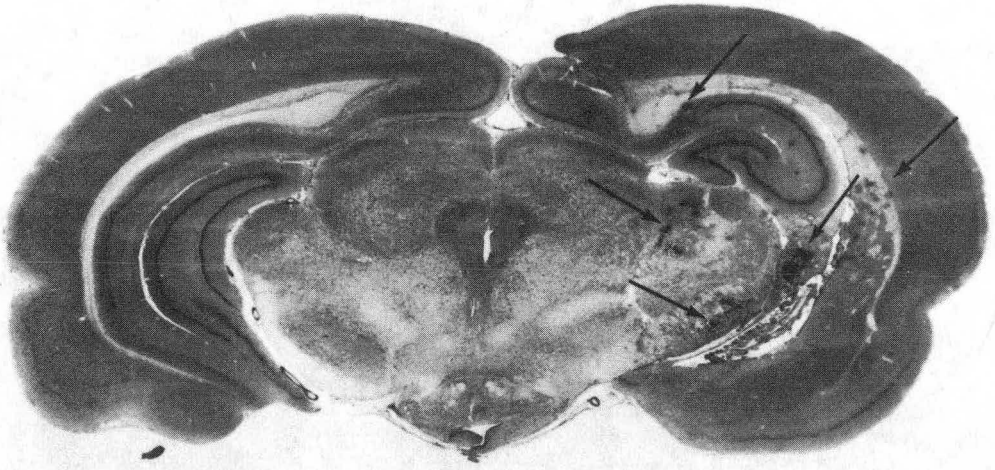

Figure 8.5 - Nissl stained section of rat that received 3000 rad (7 months post-irradiation. The arrows pointed out regions of abnormal staining (Mag. X10).

CBB 849-6927

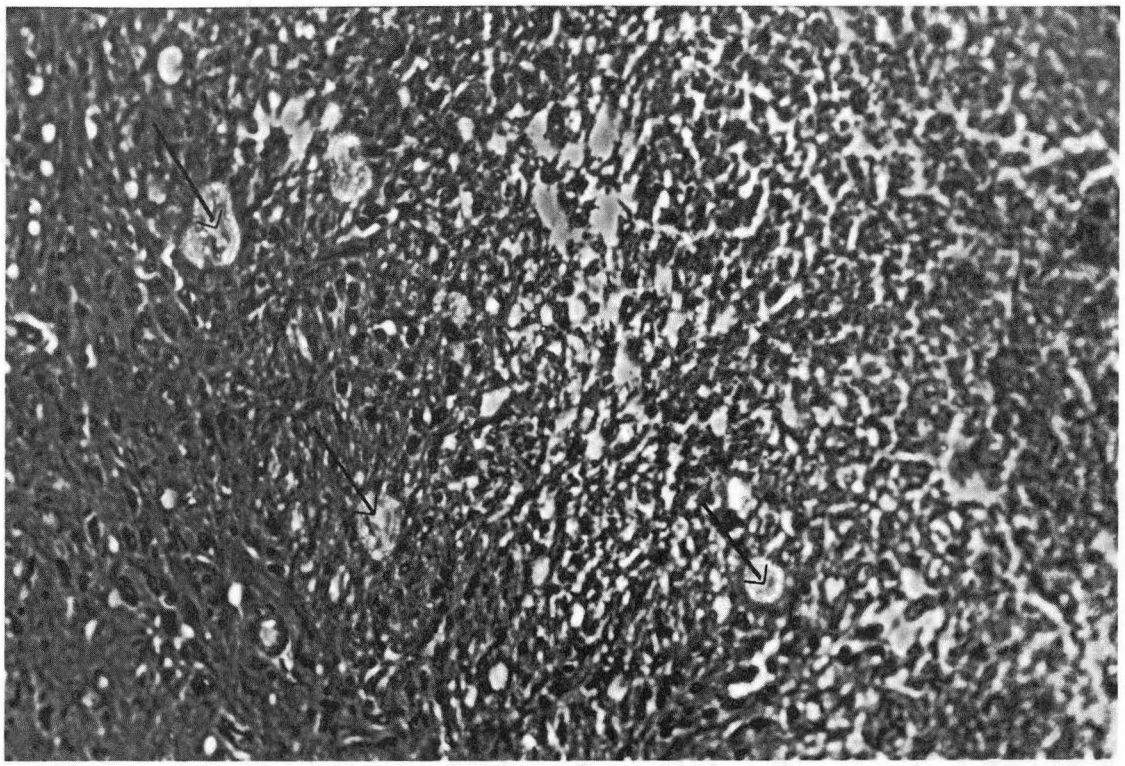

Figure 8.6 - Same as Figure 8.3 except with light field microscopy. The arrows point out the regions of Evans blue staining.

CBB 830-9841

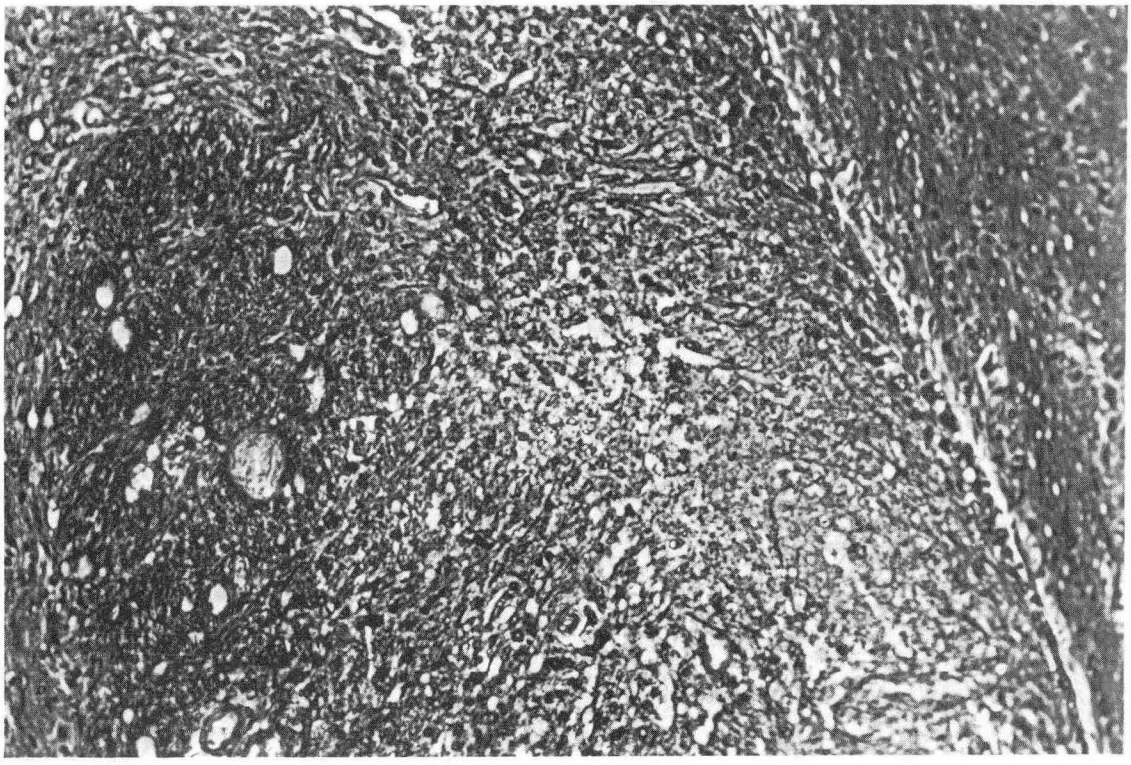

Figure 8.7 - Same region as in Figure 8.3 except with Mahon's myelin staining. Demonstration of demyelination (Mag. X130, phase contrast).

CBB 830-9837

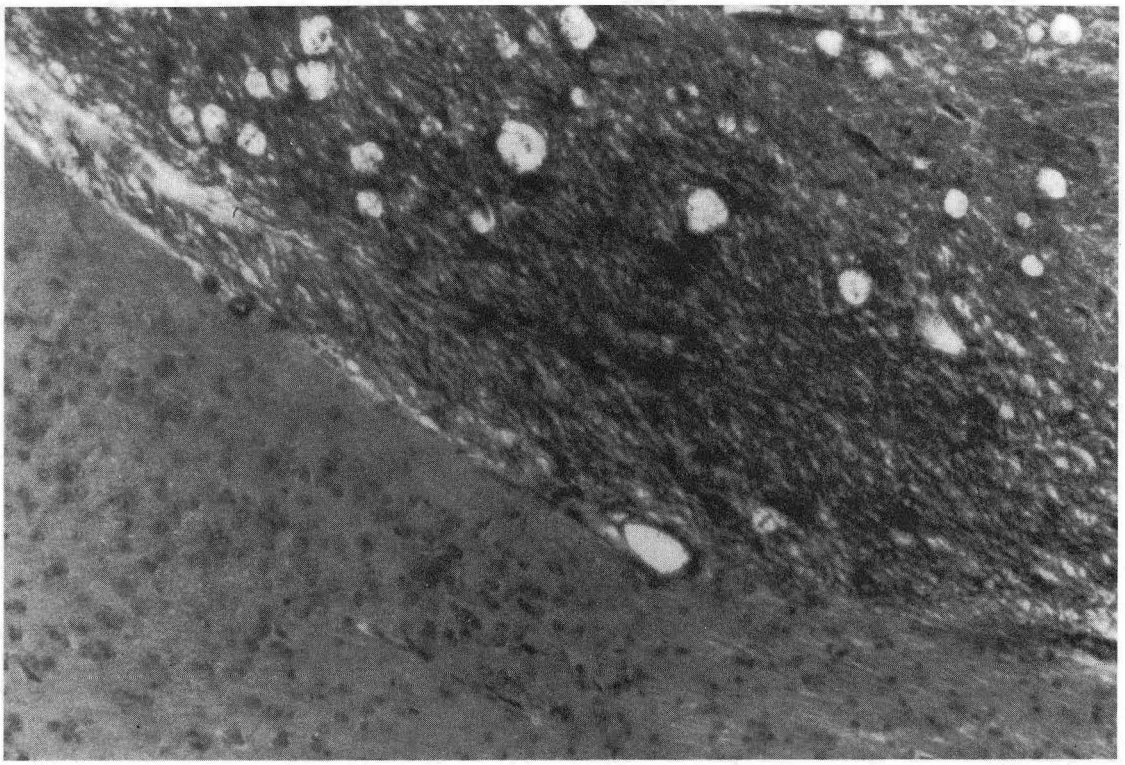

Figure 8.8 - Region from the internal capsule from control rat. Demonstration of normal myelin staining (Mahon's myelin stain, mag. X130).

XBC 847-5434

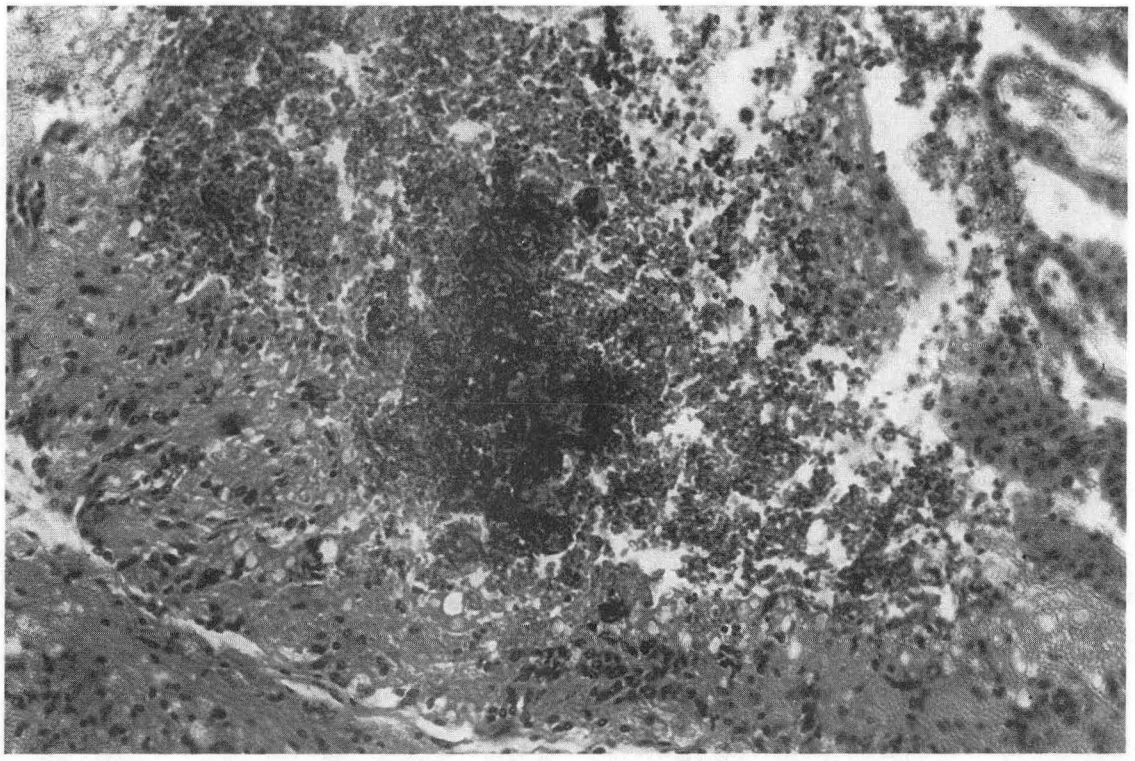

Figure 8.9 - Region from the fimbria of the hippocampus of a rat that received 3000 rads (7 months post-irradiation). Demonstration of calcification (HE stain, mag X130).

CBB 830-9829

CHAPTER 9. SUMMARY AND DISCUSSION

The observations reported in this dissertation were made possible by developement of methods for measuring the NMR parameters of the rodent brain in vivo and in vitro. These technological developements were a major part of this work. The methods include dual aqueous and organic tissue extraction technique for spectroscopy, depth selective spectroscopy using an optimization of rf pulse energy based on a priori knowledge of N-acetyl aspartate and lipid spectra of the normal brain, and phase-encoded proton spectroscopy of the living rodent using a surface coil.

From the experiments discussed in chapters 3 and 4, consistent results were found: early after irradiation (4 - 14 days) T1 and spin density decreased with dose in the cortex of the irradiated side; and T1 and spin density increased with dose in the cortex of the control side. At 4 days, accompanying the T1 decrease, there were small foci of breaks in the blood- brain barrier of the white matter (corpus callosum) and changes in proton spectra of the lipids in the organic fraction of the brain extracts. Table 9.1 summarizes all of the results. We propose two hypotheses to explain these results.

Protein theory:

Ionizing radiation causes chemical-bond breakage and disruption that would expose a greater amount of tissue water to protein surfaces. T1 relaxation time is dependent on structural and motional ordering of

Table 9.1
SUMMARY OF RESULTS FOR IRRADIATED SIDE RELATIVE TO CONTROLS

TIME DAYS	DOSE RADS	SPIN DENS.	T1	LACTATE	LIPIDS EXT	LIPIDS VIVO	P-CHO	EVANS BLUE # of spots
4	3000	NS	-10%					
	5000	-48%	-26%	NS	-16%a	NS	+50%	+366%
7	3000	-36%						
11	3000		+10%			NS		
	5000		+10%			NS		
14	1000	NS	NS					
	2000	NS	NS					
	3000	-25%	-13%					
25	3000	NS	NS			NS		
	5000	NS	NS			+100+		
81	3000	NS	+13%C -10%S	+101%	NS	NS	+41%	+1050%
	5000	NS	+10%C -14%S	NS	-23%a -14%b	NS	+23%	+1000%
220	3000						-40%	+3350%

NOTE: All values were calculated as a percent difference from controls. The spin density values were calculated relative to the control side of the irradiated brain, whereas the rest of the values were calculated relative to control animals. Abbreviations: NS - not significant; C - cortex; S - subcortex; a - peak at 2.84 ppm (phosphatidyl ethanolamine and phosphatidyl serine in organic solvent); b - peak at 3.29 ppm (lethicin in organic solvent). No entry means no measurement was made.

water in tissues (Mathur-De Vre, 1979) and therefore, an increase in the amount of water bound in the hydration layer of macromolecules would cause a decrease in T1 relaxation. Cross-relaxation between water protons and macromolecular protons provides an effective relaxation pathway for the water molecules that are held in the hydration layer in the immediate neighborhood of the macromolecular surface (Gaggelli et al., 1982). Radiation-induced protein damage has been reported (Egana, 1971) in aqueous solutions, and damage to metabolic machinery (enzymes) has been proposed (Haymaker, 1969) as an explanation for early glycogen accumulation in the glial cells. Bakker et al. (1983) have also suggested that protein denaturation might be the cause of a T1 decrease in irradiated tissue. The following questions then arise: how much protein damage is caused by radiation at the 1000-10,000 rad level, and is it enough to account for the changes seen in T1 relaxation after irradiation of the rat brain? In an attempt to answer these questions, aqueous solutions of albumin at several different concentrations were irradiated with X-rays (10,000 rads) and T1 relaxation time was measured in the 180 Mhz spectrometer with the inversion-recovery pulse sequence before and after irradiation. The results are shown below.

Albumin conc. (mg/cc)	T1 of irr. sol. (sec)	T1 of control sol. (sec)
60. (1 trial)	1.98	1.92
98. (2 trials)	1.57	1.82
	1.60	1.75
150. (2 trials)	1.44	1.29
	1.39	1.32

The results shown here tend to complicate the issue because at 98 mg/cc T1 was decreased after irradiation, but at 150 mg/cc T1 was increased after irradiation. Also, this experiment might not represent what would happen in vivo because of 1)the addition of other types of macromolecules in the tissue, and 2)cellular reactions to radiation. In any event, the T1 relaxation time of water in the CNS would change as a result of an increase in bound water due to either a conformational change in protein structure or a change in protein concentration.

Lipid theory -

NMR measurements were made on brain lipids in vivo (chapter 6) and in vitro (chapter 7) at different times after irradiation. In vitro measurements of lipids (organic fraction of brain extracts) were performed at 4 and 81 days after irradiation. In vivo measurements were made at 4, 11, 25, and 81 days after irradiation. The in vivo measurements did not correlate well with the T1 relaxation times measurements because at 25 days after irradiation, when a large abnormal lipid peak was observed, the T1 values of irradiated animals appeared to be normal. However, the in vitro observations did correlate with the T1 changes. At 4 days after irradiation, a decrease was seen in the peak area ratio (relative to methylene) at 2.84 ppm with no changes in peak area ratios at 3.29 ppm or at the terminal methyl groups. However, at 81 days when an increase in T1 was observed, a new set of changes were measured in the organic fraction spectra. These changes include a decrease in the peak are ratios at 2.84 ppm, 3.29 ppm, and the terminal methyl groups. Lipid membrane damage is evidenced by a decrease in the

the peak area ratio at 2.84 ppm of the organic fraction spectrum (resonance associated with phosphatidyl ethanolamine and phosphatidyl serine) and an increase in the p-choline resonance of the aqueous fraction (Table 9.1). Both phosphoryl choline and glycerol-3-phosphocholine (compounds which resonate at the p-choline frequency) are intermediates in the synthesis and possibly in the breakdown of phosphatidyl-choline. Therefore, an increase in the p-choline resonance might indicate membrane breakdown. Membrane damage was also indicated by Evans blue staining associated with damaged blood-brain barrier. These changes reflect structural alterations in the lipids and may be the result of the primary actions of radiation (e.g., lipid peroxidation) or of secondary reactions which act to disrupt membrane lipids (e.g., cellular digestion of damaged membranes). A hydration layer of water molecules also forms around the polar moiety of the lipid membrane and an increase in membrane surface area could cause a decrease in T1 relaxation time. Gaggelli et al (1982) have observed an inverse relationship between T1 relaxation time and both lecithin and rod outer segment (ROS) disk membrane concentration. They also observed a change in T1 as a consequence of the action of light on the ROS membranes and they suggested that this might be the result of a change in conformation of membrane proteins. Kennedy (1984) has observed a decrease in T1 and T2 relaxation times of the muscle methylene peak after neutron irradiation of mice with no change in percent water content. He suggests that these early changes after irradiation may be caused by lipid peroxidation. A loosening of the myelin sheath caused by lipid structural changes could result in a greater fraction of bound water near the membrane surface. An

experiment that might shed light on this issue is to measure T1 relaxation time of membrane preparations in aqueous solution before and after irradiation (C. Tobias, personal communication). If the radiation induces a decrease in T1 relaxation time of the water in vitro, then this would give evidence that the early T1 decrease in vivo may be caused by the "direct" result of radiation and not secondary radiation-induced cellular reactions.

The decrease in spin density on the irradiated side is probably due to a decrease in free water content or to a decrease in the fast T2 relaxation component because the apparent spin density (measured by imaging techniques) is influenced by T2.

On the control side of irradiated brains, an increase in T1 relaxation was accompanied by ventricular enlargement, a decrease in p-serine and p- ethanolamine peak area ratios relative to methylene, and an increase in lactic acid. Tanaka et al. (1979) also observed bilateral damage after irradiation of only the right occipital lobe in the monkey. According to Tanaka et al., brain swelling on the irradiated side of the brain caused compression of the contralateral hemisphere and enlargement of the contralateral ventricular system through embarrassment of the CSF system. A similar mechanism may be occuring in hemi-brain irradiation of the rat. An increase in CSF fluid volume on the contralateral side could account for an increase in T1 because CSF fluid has a much longer T1 than surrounding brain tissue (Crooks et al, 1982). The increased lactate on the control side may have been caused by a greater amount of tissue glucose which reacted to form lactate under the anaerobic conditions. The lactate probably

formed in the brain after sacrificing the animal because the lactate peak was not seen in vivo in the proton spectrum (chapters 5 and 6). Lactate has been shown to accumulate in the brain in hypoxic conditions (Behar et al, 1984).

Some other early effects of radiation that could cause a decrease in T1 are glycogen accumulation (Maxwell and Kruger, 1965) and the presence of free radicals (Singh and Singh, 1982). A test of the role of free radical mediated tissue damage on T1 relaxation could be made by injecting free radical scavengers.

At 81 days, an increase in T1 was seen on the irradiated side of two animals which had enlarged ventricles. Also, there was a decrease in T1 on the irradiated side subcortical region which was accompanied by breaks in the blood-brain barrier in the white matter (both in the internal capsule and corpus callosum). Both sides of the brain had decreases in p-serine and p-ethanolamine (2.84 ppm) peak area ratios (relative to methylene in organic solvent) and increased peak area ratios (relative to n-acetyl aspartate in aqueous solvent) in lactic acid and p-choline, and a decrease in GABA relative to controls. Egana observed a decrease in GABA after 500r whole-body irradiation (Egana, 1971). In the subcortical region of the irradiated side, the decrease in T1 is probably due to 1)breaks in the blood-brain barrier which permits an outpouring of protein-rich plasma constituents into the surrounding parenchyma (Tanaka et. al, 1979), and 2)astrocyte and oligodendrocyte reactions which act on the myelin sheaths (Kruger and Maxwell, 1966, Haymaker, 1969). At 7 months, although no imaging was done, an increase in T1 might be expected in the necrotic areas because

of edema. The change in p-choline may be related to a break down in membrane phosphatidyl choline.

The most likely explanation for the early decrease in T1 of irradiated brain is that radiation causes chemical-bond breakage and protein conformational changes that would expose a greater amount of water to relaxation centers of both proteins and lipids. The time related changes in T1 correlated with lipid changes measured in the organic fraction spectra at 4 and 81 days after irradiations. The increase in T1 on the control side of irradiated brains may be related to ventricular enlargement known to occur from examination of the histological sections. Future experiments could be done to correlate T1 measurements of irradiated brain with water content at several times after irradiation. This dissertation has presented new observations on the effects of radiation on the CNS measured by nuclear magnetic resonance.

APPENDIX

A.1 Magnetic field gradient calculation

The spatial resolution of the projection-reconstruction NMR imaging experiment is dependent on the gradient field strength. Therefore, in designing the current output for the gradient power supply, the maximum current was calculated in order to achieve a given spatial resolution. Other factors which determine the spatial resolution are: 1) the signal to noise ratio (which is dependent on field strength, the number of transients, etc.); 2) the receiving coil radius, and 3) the line width of the sample. At 180 MHz proton frequency, we assumed that the limiting factors were the gradient strength and the line width of the sample. The following equation was used to calculate the gradient field strength:

Gradient = (Sample line width (Hz)) / {Spatial resolution desired (cm)}

This equation applies only to the projection reconstruction technique and we assumed that the signal to noise ratio is not a limiting factor at 180 Mhz. To achieve a resolution of .01 cm, the gradient strength was calculated to be 3000 Hz/cm. This value was converted to current by calculating the frequency separation between two capillary tubes which were placed a known distance apart and the gradient was turned on at a known current. From this calibration, a value of 3 amps corresponded to a gradient field strength of 3000 Hz/cm.

In order to calculate the gradient strength necessary to achieve the same resolution for the phase encoding technique, the following equation was used:

(change in gradient) = 1 / [spatial resolution * gradient pulse time]

Therefore, assuming the gradient pulse time was 10 msec and that the gradient can go negative as well as positive, the maximum field gradient needed was 5000 Hz/cm.

A.2 Gradient field response time

The response times of the X, Y, and Z gradients were measure by performing the experiment shown in Figure A.1 The gradient was turned on for one second (under gate control of the pulse programmer) and then a 90 degree pulse was given after a variable delay time. The FID was Fourier transformed without any filtering and the full-width half maximum was measured as function of delay time. The data was fit a multiple exponential equation. Figure A.2 shows the results for the X gradient. The X and Y gradient response curve fit best to a double exponential with long time components of 19.9 and 16.3 msec, respectively. The Z gradient response fit best to a triple exponential with a long time component of 1.8 seconds. This means that the Z shim coil is strongly coupled to the main magnet and possibly to the other shim coils. This coupling causes a perturbation in the main field. The conclusion was reached that phase encoding schemes could only work with the X and Y shims if the Z gradient is not switched during the NMR experiment.

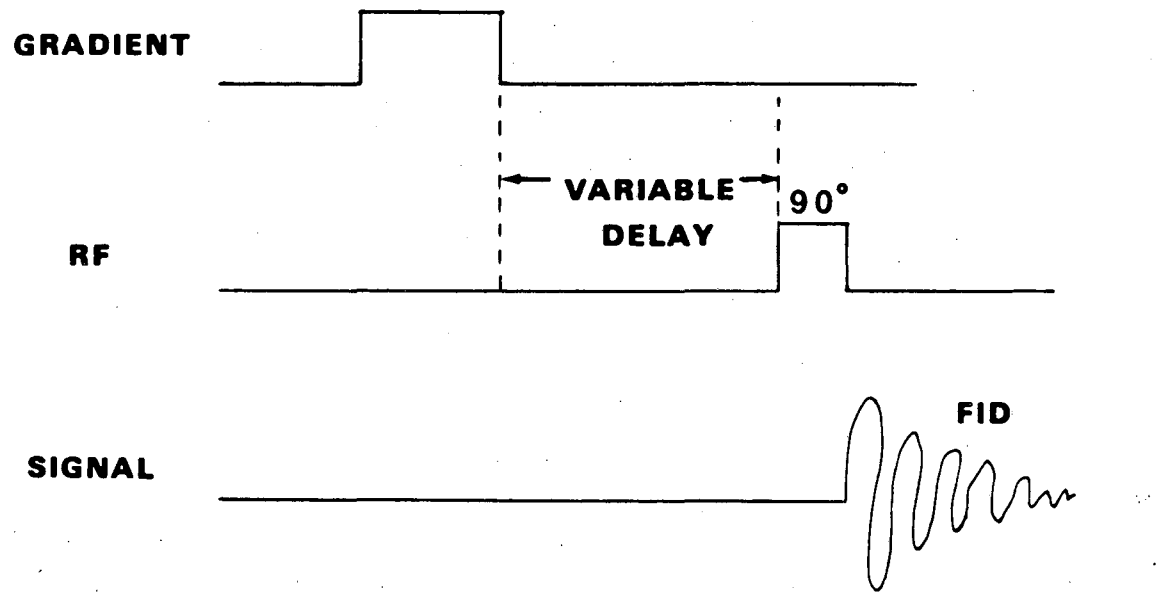

XBL 849-3680

Figure A.1 - Gradient and pulse sequence used to measure main magnetic field response time after gradient pulse.

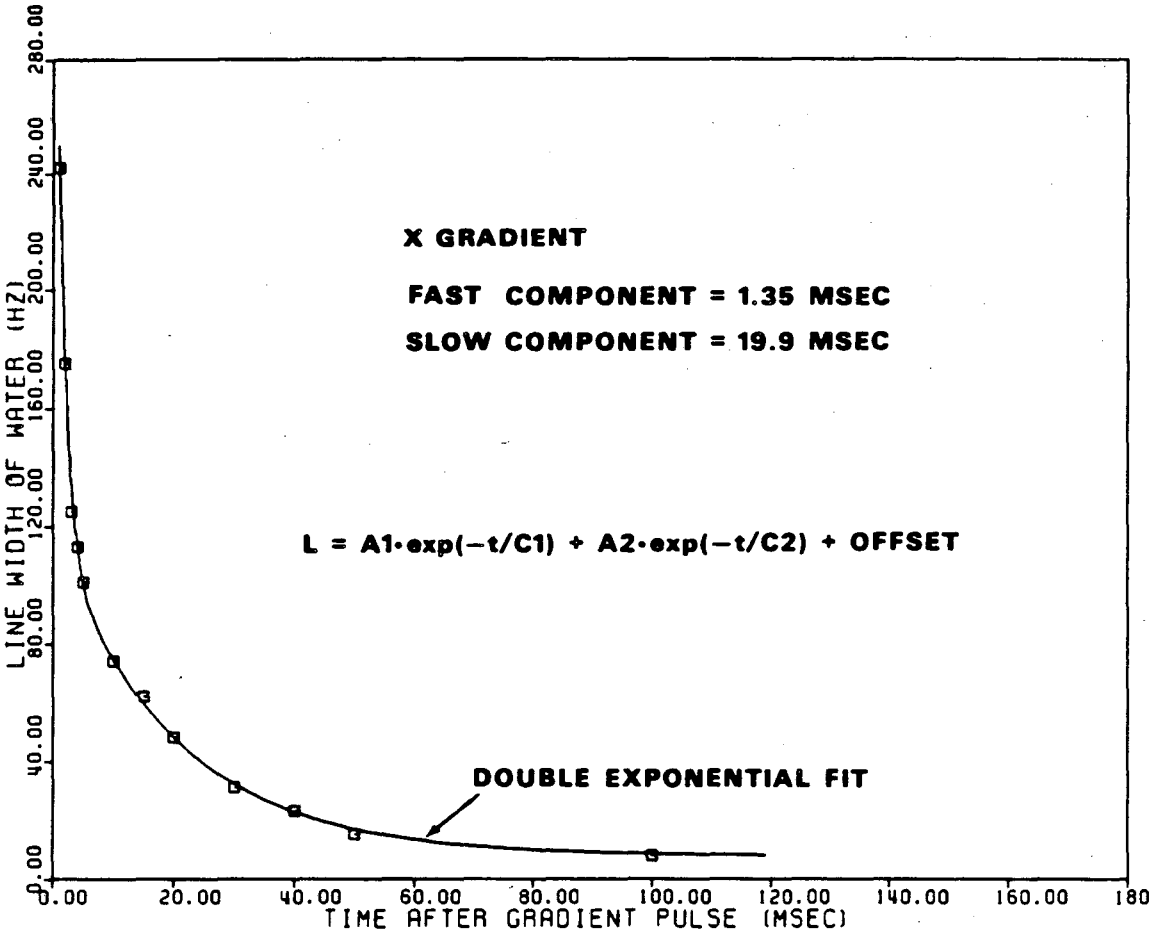

XBL 849-3681

Figure A.2 - Line width (related to gradient strength) time response after a magnetic field gradient pulse.

COMPUTER PROGRAM LISTINGS

```
! Read.com
! Command file used to set up receiving terminal port
! to receive all characters without interpretation
!
$ SET TERM/NOECHO/NOAUTOBAUD/PASSALL/EIGHTBIT TT
$ RUN DRC:[TODD]readntc
$ SET TERM/ECHO/AUTOBAUD/NOPASSALL/NOEIGHTBIT TT


c
c       READNTC.FOR
C
c       program to read data from nicolet computer
c       the following set of routines is used in the
c       data transmission package:
c       READNTC,INITTT,TTIO,CHHEAD,CHDATA,UNPACK
c
        BYTE HEAD(25)
        common /ttchan/tt_chan
        integer tt_chan
        BYTE TEST(4)
c
        byte re(1000),SE(2)
c
        call inittt
        CALL QIN2(RE,1,TT_CHAN,'WAIT')          !read cntrl Z
 300    CALL QIN2(RE,1,TT_CHAN,'WAIT')          !read SOH (001)
        if(re(1).ne.1)stop
c
        OPEN(UNIT=1,NAME='DRC:[TODD]NTC.OUT',TYPE='NEW',
     1          FORM='UNFORMATTED')
        WRITE (1) (RE(i),i=1,2)
 101    format(1x,203)
C
        se(1)="214              !ACK CHARACTER
c
 121    call qout(SE,1,tt_chan,'WAIT')
C       do jj=1,25
        CALL QIN2(RE,25,TT_CHAN,'WAIT')         !HEADER
        CALL CHHEAD(RE,IFSIZE,ISFLAG)
C       ISFLAG=1
        IF(ISFLAG.EQ.1)THEN
          SE(1)="214
          WRITE(1)(RE(I),I=1,25)
          GO TO 120
        ELSE
          SE(1)="377            !retransmit the data
          GO TO 121
        ENDIF
C
 120    CONTINUE
C       IFSIZE=607
        ILOOP=IFSIZE/352
```

```
C       iloop=91
        ILAST=MOD(IFSIZE,352)
C       ilast=0
        INC=1
C
 122    call qout(SE,1,tt_chan,'WAIT')
        IF(INC.LE.ILOOP)THEN
          NDATA=352
        ELSE
          NDATA=ILAST+1
        ENDIF
C       TYPE *,'NDATA',NDATA,ILAST,INC
C       INDATA=NDATA
C       NDATA=10
        IDLOOP=(NDATA/2)*5                      !2 WORDS PACKED IN 5 BYTES
C
C       THE BLOCK OF DATA IS FOLLOWED BY 3 BYTES CHECKSUM
C
C       DO JJ=1,IDLOOP+3
        CALL QIN2(RE,IDLOOP+3,TT_CHAN,'WAIT')           !DATA
        CALL CHDATA(RE,ISFLAG,NDATA+2)
        ISFLAG=1
C       NDATA=INDATA
        IF(ISFLAG.EQ.1)THEN
          SE(1)="214
          WRITE(1)(RE(I),I=1,IDLOOP+3)
          INC=INC+1
          IF(NDATA.EQ.(ILAST+1))GO TO 130                       !FINISHED
          GO TO 122
        ELSE
          SE(1)="377
          GO TO 122
        ENDIF


 130    CLOSE(UNIT=1)
        GO TO 300
c
        stop
        end



        subroutine inittt
C
C       Subroutine to initialize terminal port channel
c
        common /ttchan/tt_chan
        integer tt_chan
        character inname*12
        call get_name_chan('SYS$COMMAND',inname,inlength,tt_chan)
C       TYPE *,'TT_CHAN',TT_CHAN,INNAME,INLENGTH
        return
```

```
      end



C
C     SUBROUTINE TO UNPACK AND READ THE FILE SIZE AND CHECKSUM
C
      SUBROUTINE CHHEAD(HEAD,IFSIZE,ISFLAG)
C
C     ISFLAG = 1 IF CHECKSUM EQUALS ISUM
C     ISFLAG = 0 IF CHECKSUM DOES NOT EQUAL ISUM
C
      BYTE HEAD(1000),FBYTE(5)
      INTEGER IHD(25)
      ISUM=0
      IST=1
      DO I=1,5
        DO IJ=1,5
        FBYTE(IJ)=HEAD((I-1)*5 + IJ)
        ENDDO
      CALL UNPACK(FBYTE,IW1,IW2)
      IHD(IST)=IW1
      IST=IST+1
      IHD(IST)=IW2
      IST=IST+1
C
      IF(I.LT.5)THEN
      ISUM=ISUM+IW1+IW2
      ELSE
      ISUM=ISUM+IW1
      ENDIF
      IF(I.EQ.4)IFSIZE=IW1
      IF(I.EQ.5)ICH=IW2
C     TYPE *,'IW1,IW2',IW1,IW2
      ENDDO                    !MAIN LOOP
C
      IF(IFSIZE.GT.100000)IFSIZE=IHD(5)              !.DAT FILE
      I20BIT=2**20
      IRE=MOD(ISUM,I20BIT)
C     TYPE *,'ISUM,IRE',ISUM,IRE
      IF(IRE.EQ.ICH)THEN
      ISFLAG=1
      ELSE
      ISFLAG=0
      ENDIF
C
      RETURN
      END



C
C     PROGRAM TO READ OUTPUT FROM READNTC
```

```
C       AND TO CHECKSUM OF THE 352 BLOCK DATA
C
        SUBROUTINE CHDATA(DATA,ISFLAG,NDATA)
C
C       DATA- BYTE ARRAY CONTAINING THE DATA
C       ISFLAG=1 IF CHECKSUM IS OKAY
C       NDATA- NUMBER OF DATA POINTS
C
        BYTE DATA(1000),FBYTE(5)
        ISUM=0
C
        ILOOP=NDATA/2
        DO I=1,ILOOP
          DO IJ=1,5
          FBYTE(IJ)=DATA((I-1)*5 + IJ)
          ENDDO
        CALL UNPACK(FBYTE,IW1,IW2)
C       TYPE *,'IW1,IW2',IW1,IW2
        IF(I.LT.ILOOP)THEN
        ISUM=ISUM+IW1+IW2
        ELSE
        ISUM=ISUM+IW1
        ENDIF
        ENDDO
        I20BIT=2**20
        IRE=MOD(ISUM,I20BIT)
C       TYPE *,'ISUM,IRE',ISUM,IRE,I20BIT
C
        IF(IRE.EQ.IW2)THEN
        ISFLAG=1
        ELSE
        ISFLAG=0
        ENDIF
C
        RETURN
        END



C
C       PROGRAM TO UNPACK BITS FROM PROGRAM IOTRAN NICOLET
C
        SUBROUTINE UNPACK(FBYTE,IW1,IW2)
        BYTE FBYTE(5),TEST(5),IT
C
        IT=FBYTE(3)/16
C       WRITE(5,11)IT
 11     FORMAT(1X,'IT',O3)
        CALL LIB$INSV(FBYTE(1),12,8,IW1)
        CALL LIB$INSV(FBYTE(2),4,8,IW1)
        CALL LIB$INSV(IT,0,4,IW1)
        CALL LIB$INSV(FBYTE(3),16,4,IW2)
        CALL LIB$INSV(FBYTE(4),8,8,IW2)
```

```
CALL LIB$INSV(FBYTE(5),0,8,IW2)
RETURN
END
```

```
      PROGRAM UCBNMR
C
C     PROGRAM TO CALCULATE T1 AND A1 IMAGES FROM IMAGE INTENSITY
C     VALUES PIXEL BY PIXEL
C     THE FOLLOWING ROUTINES ARE USED IN THIS PACKAGE:
C
C    UCBNMR,T2FIT2,CXFIT,VA04A,CALC2,CHISQ,FUNCTION

C
      INTEGER*2 IBV(64,64,4),IVA(80),IVT2(80),IVT1(80),ibuf(256)
      INTEGER*2 IZ(80),IH(256),IBA(80),IBT(80),IBIGT(64,64),IBIGA(64,64)
      CHARACTER*40 CFN1,cfn2,cfn3
      COMMON /FUNC/IFUNC
      DIMENSION SVEC(4),X(4),Y(4),svec2(4),rbvec(128,128,3)
      dimension a1(128),t1(128)
      byte bb(48)
      IDIM=128
      NPTSS=3          !NUMBER OF DELAY POINTS IN THE RELAXATION
c
      ih(3)=3
C
      TYPE *,'ENTER THRESHOLD LIMIT'
      ACCEPT *,RLIM
      do i=1,
      TYPE *,'ENTER NAME OF IMAGE FILE 1'
      READ(5,10)CFN1
      TYPE *,'ENTER NAME OF IMAGE FILE 2'
      READ(5,10)CFN2
      TYPE *,'ENTER NAME OF IMAGE FILE 3'
      READ(5,10)CFN3
 10   FORMAT(A)
      OPEN(UNIT=1,NAME=CFN1,TYPE='OLD',FORM='UNFORMATTED',READONLY)
      read(1)          !HEADER
      OPEN(UNIT=2,NAME=CFN2,TYPE='OLD',FORM='UNFORMATTED',READONLY)
      read(2)          !HEADER
      OPEN(UNIT=3,NAME=CFN3,TYPE='OLD',FORM='UNFORMATTED',READONLY)
      read(3)          !HEADER
c
c     read in the nmr image data
c
      do k=1,NPTSS
        do j=1,idim
        read(k)(rbvec(i,j,k),i=1,idim)
        enddo
      enddo
      close(unit=1)
      close(unit=2)
      close(unit=3)
C
      OPEN(UNIT=4,NAME='A1IMAGE.R2',TYPE='NEW',FORM='UNFORMATTED')
      OPEN(UNIT=11,NAME='T1IMAGE.R2',TYPE='NEW',FORM='UNFORMATTED')
c
      WRITE(4)IH
```

```
      WRITE(11)IH
C
      X(1)=2000.              !TIME IN MSECONDS
      X(2)=3000.
      X(3)=3000.
C
      TYPE *,'X',X
C
      fact=1000.
C     TYPE *,'ENTER THE STARTING ROW'
      TYPE *,'ENTER THE ROW AND COLUMN OF THE POINT IN 320 SPACE'
      READ(5,*)IROW,ICOL
C
      IROW=IROW*(128./320.)   !CONVERT TO 128 SPACE
      ICOL=ICOL*(128./320.)
c
c
      do k=1,NPTSS
      SUM=0.
       DO J=IROW,IROW+1
       DO I=ICOL,ICOL+1
        SUM=rbvec(I,J,k)+SUM
       ENDDO
       ENDDO
      SVEC(K)=SUM/FACT
      enddo
      type *,'svec',svec
      CALL CHISQ(X,SVEC,NPTSS)
      if(svec(1).lt.0.)svec(1)=0.
c
      call t2fit2(x,svec,a1(i),t1(i))
      if(t1(i).gt.3000.)t1(i)=0.
      type *,'a1,t1',a1(i),t1(i),i,j
 99   continue

c
      close(unit=4)
      close(unit=11)
      stop
      end

c
C     ROUTINE TO FIND T1 AND A1 PARAMETERS BY FITTING THE DATA TO
C     THE EQUATION IN ROUTINE FUNCTION
c
      SUBROUTINE T2FIT2(X1,SVEC,a1,t1)
      parameter na=3
      dimension p(5),e(5),X1(4),Y1(4),SVEC(4)
      common /func/ifunc
c
      common/dat/npts,x(na),y(na),SVE(NA),sy(na)
      DO I=1,NA
      X(I)=X1(I)
```

```
        SVE(I)=SVEC(I)
        ENDDO
c
        N=2
        lip=1
c
40      continue
        npts=3
c
        do i=1,4
        sy(i)=sqrt(abs(svec(i)))
        IF(SY(I).LE..0001)SY(I)=1.
        enddo
c
c       do 10 i=1,npts
11      continue
c       type *,  ' input sheet #, intensity, sigma I for pt # ', i
c       accept *, x(i),y(i),sy(i)
c       if(sy(i).le.0.)go to 11
10      continue
c
        e(1)=10.
        ff=svec(1)/svec(2)
          p(2)=1000.
          p(1)=svec(2)*1.1
          e(2)=20.
        if(ff.gt..5)p(1)=100.
c
C       type 80, npts,((x(i),y(i),sy(i)),i=1,npts)
80      format(1x,16,' input data points'//'   X(I)',6X'Y(I)',6X'SY(I)'/
        1 (1X,3F10.4))
C
C       type 81, (p(i),i=1,n)
81      format( ' STARTING PARAMETER VALUES P(I)= ',5F10.4)
C
        call cxfit(p,e,n,chi)
        a1=p(1)
        t1=p(2)
        RETURN
        END
c  file name -- cxfit.for
c  author -- W R HOLLEY
c  date -- 7 nov 80
c
        subroutine cxfit(x,e,n,chi)
c
c  Program to call general least square fitting routine VA04A
c       x -- parameters of fit -- initialized with "best" guess values --
c            returned with fitted values
c       e -- "accuracy" required of fit
c       n -- Number of parameters to be fit
c       chi -- value of fitted chi-square
c       escale -- factor determining stepsize ( =escale*e(i)? )
```

```
c       iprint -- flag for print out (0,1,2) -- 0 for minimum P O
c       icon -- flag for convergence -- try =1
c       maxit -- maximum number of iterations allowed
c
c
        dimension e(n),x(n)
c
        escale=1.
        iprint=2
        icon=1
        maxit=50
c
C       type *,'Input fit control params -- ESCALE, IPRINT, ICON, MAXIT'
c       accept *, escale,iprint,icon,maxit
C       type *, 'Input fit accuracy required -- ',n,' E(I)s'
C       accept *, (e(i),i=1,n)
c  Set e's to default values (.01) if not already set
        do 10 i=1,n
        if(e(i).EQ. 0.)e(i)= 0.01
10      continue
c
C       TYPE *,'E INCXFIT',E
        call va04a(x,e,n,chi,escale,iprint,icon,maxit)
        return
        end
C  FILE NAME -- VA04A.FOR
C  SUBROUTINE TO DO NON-LINEAR LEAST SQUARES FITTING
C
        SUBROUTINE VA04A(x,e,n,f,escale,iprint,icon,maxit)
C
C       AUTHOR: M. J. D. POWELL
c
        dimension x(n),e(n)
        dimension w(500)        ! Workspace dim =n*n+3*n (n=20 ok)
        dimension delx(20)      ! OK for n up to 20
c
        lto=5           ! Lun for message OP -- set for terminal here
c
        ddmag=0.1*escale
        scer=0.05/escale
        jj=n*n+n
        jjj=jj+n
        k=n+1
        nfcc=1
        ind=1
        inn=1
c
        do 1 i=1,n
        do 2 j=1,n
        w(k)=0.
        if(i-j)4,3,4
3       w(k)=abs(e(i))
        w(i)=escale
```

```
4       k=k+1
2       continue
        iterc=1
1       continue
c
        isgrad=2
        call calcfid(n,x,f)     ! Initial calc of chi-sq
        fkeep=abs(f)+abs(f)
5       itone=1
        fp=f
        sum=0.
        ixp=jj
c
        do 6 i=1,n
        ixp=ixp+1
        w(ixp)=x(i)
6       continue
c
        idirn=n+1
        iline=1
7       dmax=w(iline)
        dacc=dmax*scer
        dmag=min(ddmag,0.1*dmax)
        dmag=max(dmag,20.*dacc)
        ddmax=10.*dmag
        go to (70,70,71), itone
70      dl=0.
        d=dmag
        fprev=f
        is=5
        fa=f
        da=dl
8       dd=d-dl
        dl=d
58      k=idirn
c
        do 9 i=1,n
        x(i)=x(i)+dd*w(k)
        k=k+1
9       continue
c
        fstore=f
        call calcfid(n,x,f)     ! Calculate chi-sq
        nfcc=nfcc+1
        go to (10,11,12,13,14,96), is
14      if(f-fa)15,16,24
16      if(abs(d)-dmax)17,17,18
17      d=d+d
        go to 8
18      write(1to,19)
19      format(5x,44hVA04A maximum change does not alter function)
        go to 20
15      fb=f
```

```
        db=d
        go to 21
24      fb=fa
        db=da
        fa=f
        da=d
21      go to (83,23), isgrad
23      d=db+db-da
        is=1
        go to 8
83      d=0.5*(da+db-(fa-fb)/(da-db))
        is=4
        if((da-d)*(d-db))25,8,8
25      is=1
        if(abs(d-db)-ddmax)8,8,26
26      d=db+sign(ddmax,db-da)
        is=1
        ddmax=ddmax+ddmax
        ddmag=ddmag+ddmag
        if(ddmax-dmax)8,8,27
27      ddmax=dmax
        go to 8
13      if(f-fa)28,23,23
28      fc=fb
        dc=db
29      fb=f
        db=d
        go to 30
12      if(f-fb)28,28,31
31      fa=f
        da=d
        go to 30
11      if(f-fb)32,10,10
32      fa=fb
        da=db
        go to 29
71      dl=1.
        ddmax=5.
        fa=fp
        da=-1.
        fb=fhold
        db=0.
        d=1.
10      fc=f
        dc=d
30      ak=(db-dc)*(fa-fc)
        b=(dc-da)*(fb-fc)
        if((ak+b)*(da-dc))33,33,34
33      fa=fb
        da=db
        fb=fc
        db=dc
        go to 26
```

```
34      d=0.5*(ak*(db+dc)+b*(da+dc))/(ak+b)
        di=db
        fi=fb
        if(fb-fc)44,44,43
43      di=dc
        fi=fc
44      go to (86,86,85), itone
85      itone=2
        go to 45
86      if(abs(d-di)-dacc)41,41,93
93      if(abs(d-di)-0.03*abs(d))41,41,999
999     if(abs(f-fstore)-0.01*abs(f))41,41,45
45      if((da-dc)*(dc-d)) 47,46,46
46      fa=fb
        da=db
        fb=fc
        db=dc
        go to 25
47      is=2
        if((db-d)*(d-dc)) 48,8,8
48      is=3
        go to 8
41      f=fi
        d=di-dl
        dd=sqrt((dc-db)*(dc-da)*(da-db)/(ak+b))
c
        do 49 i=1,n
        x(i)=x(i)+d*w(idirn)
        w(idirn)=dd*w(idirn)
c
c  ***************
c       delx(i)=w(idirn)
c  ***************
c
        idirn=idirn+1
49      continue
c
        w(iline)=w(iline)/dd
        iline=iline+1
        if(iprint-1)51,50,51
C50     write(1to,52) iterc,nfcc,f,(x(i),i=1,n)
 50     CONTINUE
52      format(/1x,9hiteration,i5,i15,16h function values,
        1 10x,'f=',e16.7/(1x,8e16.7))
        go to (51,53),iprint
51      go to (55,38), itone
55      if(fprev-f-sum) 94,95,95
95      sum=fprev-f
        jil=iline
94      if(idirn-jj) 7,7,84
84      go to (92,72), ind
92      fhold=f
        is=6
```

```
      ixp=jj
c
      do 59 i=1,n
      ixp=ixp+1
      w(ixp)=x(i)-w(ixp)
59    continue
c
      dd=1.
      go to 58
96    go to (112,87), ind
112   if(fp-f)37,37,91
91    d=2.*(fp+f-2.*fhold)/(fp-f)**2
      if(d*(fp-fhold-sum)**2-sum) 87,37,37
87    j=jil*n+1
      if(j-jj) 60,60,61
c
60    do 62 i=j,jj
      k=i-n
      w(k)=w(i)
62    continue
c
      do 97 i=jil,n
      w(i-1)=w(i)
97    continue
c
61    idirn=idirn-n
      itone=3
      k=idirn
      ixp=jj
      aaa=0.
c
      do 65 i=1,n
      ixp=ixp+1
      w(k)=w(ixp)
      if(aaa-abs(w(k)/e(i))) 66,67,67
66          aaa=abs(w(k)/e(i))
67    k=k+1
65    continue
c
      ddmag=1.
      w(n)=escale/aaa
      iline=n
      go to 7
37    ixp=jj
      aaa=0.
      f=fhold
c
      do 99 i=1,n
      ixp=ixp+1
      x(i)=x(i)-w(ixp)
      if(aaa*abs(e(i))-abs(w(ixp))) 98,99,99
98    aaa=abs(w(ixp)/e(i))
99    continue
```

```
c
        go to 72
38      aaa=aaa*(1.+di)
        go to (72,106), ind
72      if(iprint-2) 53,50,50
53      go to (109,88), ind
109     if(aaa-0.1) 89,89,76
89      go to (20,116), icon
116     ind=2
        go to (100,101),inn
100     inn=2
        k=jjj
c
        do 102 i=1,n
        k=k+1
        w(k)=x(i)
        x(1)=x(i)+10.*e(i)
102     continue
c
        fkeep=f
        call calcfid(n,x,f)     ! Calc chi-sq again
        nfcc=nfcc+1
        ddmag=0.
        go to 108
76      if(f-fp) 35,78,78
78      write(1to,80)
80      format(5x,37hVA04A ACCURACY LIMITED BY ERRORS IN F)
        go to 20
88      ind=1
35      ddmag=0.4*sqrt(fp-f)
        isgrad=1
108     iterc=iterc+1
        if(iterc-maxit) 5,5,81
c
c  ****************
81      continue
c  81   write(1to,82) maxit
82      format(i5,' iterations completed by VA04A')
c  ****************
c
        if(f-fkeep) 20,20,110
110     f=fkeep
c
        do 111 i=1,n
        jjj=jjj+1
        x(i)=w(jjj)
111     continue
c
        go to 20
101     jil=1
        fp=fkeep
        if(f-fkeep)105,78,104
104     jil=2
```

```
        fp=f
        f=fkeep
105     ixp=jj
c
        do 113 i=1,n
        ixp=ixp+1
        k=ixp+n
        go to (114,115), jil
114     w(ixp)=w(k)
        go to 113
115     w(ixp)=x(i)
        x(i)=w(k)
113     continue
c
        jil=2
        go to 92
106     if(aaa-0.1) 20,20,107
20      continue
c
c  ***************
c       write(lto,1000)  (delx(i),i=1,n)
1000    format('0 final set of directions.'/(1p10e12.4))
c  ***************
c
        return
107     inn=1
        go to 35
        end
c  file name -- calcfid.for
c
        subroutine calcfid(n,p,chi)
c
c  Routine to calculate chi-square fit using data
c  in vectors x,y and equation found in routine function
c
c       n -- number of parameters (4 for this case)
c       p -- parameter vector
c       p(1) -- center of intensity distribution
c
        parameter na=3
        dimension p(5)
c
        common/dat/npts,x(na),y(na),SVEC(NA),sy(na)
        COMMON /FUNC/IFUNC
c
c       npts -- # of data points
c       x -- independent variable -- time between 90 degree pulses
c       y -- measured (depentent) variable -- NMR intensity
c       sy -- standard deviation (error) on value y
c
        chi=0.
        do 10 i=1,npts
        CALL FUNCTION(X(I),FFUNC,P)
```

```
          CME=(FFUNC-SVEC(1))
c         TYPE *,'FUNC',fFUNC,svec(I),X(I)
c         TYPE *,'PARM',P(1),P(2),chi
          SUM=(CME**2)
          CHI=CHI+SUM
10        continue
          return
          end
          SUBROUTINE CHISQ(X,SVEC,NPTS)
          DIMENSION X(4),SVEC(4)
          COMMON /START/P(2)
C
C
          P(1)=SVEC(2)*1.5
          P(2)=1000.
          CHI=0.
          do 110 i=1,npts
          CALL FUNCTION(X(I),FUNC,P)
C         TYPE *,'FUNC',FUNC,SVEC(I),X(I)
          chi=(chi+(func - SVEC(i))**2)
110       continue
          CHI1=SQRT(CHI)/SVEC(3)
          TYPE *,'CHI1',CHI1
C
          RETURN
          END

C         ROUTINE CONTAINING THE EQUATION FOR FITTING
C
          SUBROUTINE FUNCTION(X,Y,P)
          DIMENSION P(2)
          YOFFSET=7.8
C
C
C         T1 FUNCTIONS
C
          Y = P(1)*(1 -  EXP(-X/P(2)) )
c         Y = P(4)*(1 - 2. * EXP(-X/P(3)) ) + Y
C         y = p(2) * (1-(1+p(3)*(1-exp(-8./p(1)) ))*exp(-x/p(1)) )
c         y = p(5) * (1-(1+p(6)*(1-exp(-8./p(4)) ))*exp(-x/p(4)) ) +y
C
C         T2 FUNCTIONS
C
c         Y = P(1)*EXP(-X/P(2))
c         Y = P(3)*EXP(-X/P(4)) +Y
c         Y = P(5)*EXP(-X/P(6)) +Y
c         Y = Y + YOFFSET
C         TYPE *,'X,Y',X,Y
C
C         SIN FIT FUNCTION
C
C         Y = P(1)*SIND(X*P(2) + P(3))
C         Y = Y * EXP(-X/P(4))
```

```
C       Y = Y+P(5)
C
        RETURN
        END
c
c       program tlanal.for-
c       to take contours written by program ram and find
c       the average intensity value inside the contours for each delay
c       time image. T1 relaxation time is found by fitting the data
c       to the equation in routine function
c
c       the following routines are used in this package
c  tlanal,-
c  drc:[sam.subs]odd,oncontour,link,cycle,-
c  drc:[histct.new]cull1,cull2,cull3,-
c  DRC3:[TODD.NMR]T2FIT2,CXFIT,VA04A,CALC2,CHISQ,FUNCTION
c
c
        character       cmaker*4,cdate*20,ans*3
        character       pname*20,date*23,dname*20 /' '/
        data            ncd /20/,nit/3/,not/2/
        real            vec(128,128),rvec2(500,3),RSUM(3)
        character*40    fn,cfn
        integer*2       nr,x(2000),y(2000),xmn,xmx,ymn,ymx,nchar
        integer*2       lpts,lx(20),ly(20)
        real            angl(20)
        byte            text(10,20)
        data            lmask/-21846/
        logical         print
        integer*2       ib(3000)
        logical         odd,oncontour
        integer         xx,count,sum,above,below
        CHARACTER*40 CFN1,cfn2,cfn3
        COMMON /FUNC/IFUNC
        DIMENSION SVEC(4),XFIT(4),svec2(4),rbvec(128,128,3)
        IDIM=128
        NPTSS=3
c
C
        TYPE *,'ENTER FILE NAME'
        READ(5,10)CFN1
        OPEN(UNIT=13,NAME=CFN1,TYPE='OLD',FORM='FORMATTED')
        do i=1,6
        read(13,*)
        enddo
c
        TYPE *,'ENTER NAME OF IMAGE FILE 1'
        READ(13,10)CFN1
c
        do i=1,4
        read(13,*)
        enddo
c
```

```
      TYPE *,'ENTER NAME OF IMAGE FILE 2'
      READ(13,10)CFN2
c
      do i=1,4
      read(13,*)
      enddo
      TYPE *,'ENTER NAME OF IMAGE FILE 3'
      READ(13,10)CFN3

 10   FORMAT(A)
      OPEN(UNIT=1,NAME=CFN1,TYPE='OLD',FORM='UNFORMATTED',READONLY)
      read(1)        !HEADER
      OPEN(UNIT=2,NAME=CFN2,TYPE='OLD',FORM='UNFORMATTED',READONLY)
      read(2)        !HEADER
      OPEN(UNIT=3,NAME=CFN3,TYPE='OLD',FORM='UNFORMATTED',READONLY)
      read(3)        !HEADER
c
c     read in the nmr image data
c
      do k=1,NPTSS
        do j=1,idim
        read(k)(rbvec(i,j,k),i=1,idim)
        enddo
      enddo
      close(unit=1)
      close(unit=2)
      close(unit=3)
C
C
      XFIT(1)=1000.          !TIME IN MSECONDS
      XFIT(2)=2000.
      XFIT(3)=3000.
      TYPE *,'XFIT',XFIT


      icode = lib$date_time(date)
      open(unit=3,name='fil.out',type='old',form='formatted')
      read(3,*)dose
c
c
c
c
      do 199 ifil=1,6        !number of contour files
c
      CFN(1:4)='RATP'
      CFN(6:9)='.PLT'

      ENCODE(1,1000,CFN(5:5))IFIL
 1000 FORMAT(I1)
      OPEN(UNIT=11,NAME=CFN,TYPE='OLD',FORM='FORMATTED',
     1         ERR=36)
C
 40   READ(11,*,END=37)D,T
```

```
        GO TO 40
C
C       COME HERE IF THE PLOT FILE HAS NOT BEEN CREATED
C
 36     OPEN(UNIT=11,NAME=CFN,TYPE='NEW',FORM='FORMATTED')
 37     CONTINUE


        read (nit,2000) fn
 2000   format(a)
        icode = str$upcase(fn,fn)
        open (unit=1,name=fn,status='old',form='unformatted')
        read (1) nr, (x(i),y(i),i=1,nr)
        close(unit=1)
c
c       convert points to 128X128 space
c
        do i=1,nr
        x(i)=nint(x(i)*128./320.)
        y(i)=nint(y(i)*128./320.)
        enddo
c
c
 300    continue
        if (x(1).eq.x(nr) .and. y(1).eq.y(nr)) then
         nr = nr - 1
         go to 300
        endif
        call cull1(nr,x,y)              ! clean up contour
        call cull2(nr,x,y)
        call cull3(nr,x,y)
c
 310    continue
        nrc = nr
        xmn = 500
        ymn = 500
        xmx = 0
        ymx = 0
        do i=1,nrc
          xmn = min(x(i),xmn)
          xmx = max(x(i),xmx)
          ymn = min(y(i),ymn)
          ymx = max(y(i),ymx)
        enddo
c
         ixl = xmn -1
         iyl = ymn - 1
         ixu = xmx + 1
         iyu = ymx + 1
        DO K=1,3
        rsum(K)=0.
        ENDDO
        ninp=1
```

```
          do 400 j=iyl,iyu
           count = 0
           xx = ixl
           do while (xx.le.ixu)
            if (.not.oncontour(xx,j,nrc,x,y)) then
             if (odd(count))  then                          ! pt inside contour
             DO K=1,3            !FOR THE THREE T1 DELAY TIMES
             rvec2(ninp,K)=RBVEC(xx,j,K)/1000.
             rsum(K)=rsum(K) + RBvec(xx,j,K)/1000.
C         type *,'sum',xx,j,RBvec(xx,j,K),ninp,rsum(K)
            ENDDO
            ninp=ninp+1
            endif
            xx = xx + 1
           else
            call link(xx,j,nrc,x,y,above,below)
            if ((above.eq.1) .and. (below.eq.1)) count=count + 1
            sum = above + below
            if ( (sum.ne.0) .and. (sum.ne.2)) then
             write (not,1070)
 1070        format(t5,'Error in filling algorithm; skipping to next row')
             go to 400
            endif
           endif
          enddo
 400      continue
c
         DO K=1,3
         SVEC(K)=rsum(K)/(ninp-1)
         type *,'average=',SVEC,ninp-1
c
c        find the st. dev.
c
         rsum2=0.
         do i=1,ninp-1
         a1=(rvec2(i,K)-SVEC(K))**2
         rsum2=rsum2+a1
         enddo
         f = rsum2/(ninp-2)
         f = sqrt(f)
c
         type *,'st.dev.',f
         ENDDO
C
C        FIT THE DATA TO EXP TO FIND T1
C
         CALL T2FIT2(XFIT,SVEC,A1,T1)
         TYPE *,'A1,T1',A1,T1
         write(11,*)dose,T1,(SVEC(II),II=1,3)
c
 199     continue
         close(unit=3)
         close(unit=11)
```

```
stop
end
```

```
      PROGRAM BKPRO
C
C     PROGRAM USED TO TAKE OUTPUT FROM PROGRAM NTCFTV
C     (OPTION AU) AND PERFORM A FILTERED BACKPROJECTION
C
C     THE FOLLOWING ROUTINES ARE USED IN THIS PACKAGE:
C
C  bkpro,bcd,[todd.centro]fft,-
C  [todd.nmr]filt,rdplot,shlo,ramp,buter,HAN,-
C  drc:[todd.centro]fname,talk,fill
C
C
C
      DIMENSION B(300000),PK(512),PKK(512)
      DIMENSION PKI(512),IB(300000),IVEC(320),ft(512)
      integer*2 ioutdat(256)
      dimension a(512,512)
      character*40 cfn
      COMMON /DIMEN/IND,IBPAD,IDIM,JBPAD,JDIM,IFINAL
      LOGICAL FIRST
C
c     open the parameter file
c
      open(unit=12,name='proj.par',type='old',form='formatted')
      read(14,55)cfn
 55   format(a)
c
C     TYPE *,'THIS PROGRAM IS SET UP TO DO A 128,128 RECON MATRIX'
c     type *,'Enter the number of bins per projection:'
      read(12,*)idim
C     TYPE *,'How many times smaller is this than the input array:'
C     read(5,*)ntime
      NTIME=1
c     type *,'enter the number of projections:'
      read(12,*)nang
c     TYPE *,'ENTER THE NUMBER OF CYCLES PER NANG'
      READ(12,*)NCYC
c     type *,'Enter the axis of rotation in pixels:'
      read(12,*)axis
      type *,'ax',axis
      n=128
C     PROJECTION DATA
C
      RN=IDIM
      NU=ALOG(RN)/ALOG(2.)
C
C
C     FOURIER TRANSFORM
C
c     type *,'Enter file of projection data:'
      read(12,111)cfn
 111  format(a)
      type 111,cfn
```

```
C       ZERO THE BACK-PROJECTION ARRAY
C
        NMAT=N**2
C
C       BACK-PROJECT THE PROJECTION DATA
C
        PI=4.*ATAN(1.)
        ANGINC=180./FLOAT(NANG)

        open(unit=2,name=cfn,type='old',form='unformatted',
     1          readonly)

        read(2)         !skip the header
c       type *,'how many files do you want to skip'
        read(12,*)iskip
c
        if(iskip.gt.0)then
        do i=1,iskip
        read(2)
        enddo
        endif
C
c       define the filter
c
        CALL BUTER(FT,IDIM)
C       call rdplot(ft,idim*2)
C
c
        DO ICYC=1,NCYC
        DO 21 I=1,NMAT
 21     B(I)=0.

        do np=1,nang
        do i=1,idim
        pk(i)=0.
        pki(i)=0.
        pkk(i)=0.
        enddo
c
        TYPE *,'PROJECTION NO.',NP
        read(2)(pkK(ii),ii=1,idim*NTIME)
        DO IJ=1,IDIM*NTIME,NTIME
        IJJ=(IJ/NTIME)+1
        PK(IJJ)=PKK(IJ)
        ENDDO
c       TYPE *,'PK',(PK(II),II=1,IDIM)
C
C       call rdplot(pk,idim*2)
        CALL FFT(PK,PKI,IDIM,NU,-1)
C       call rdplot(pk,idim*2)
        CALL FILT(PK,PKI,IDIM,ft)
C       call rdplot(pk,idim*2)
        CALL FFT(PK,PKI,IDIM,NU,1)
```

```
C       CALL RDPLOT(PK,IDIM*2)
c       WRITE(5,11) PK
c       WRITE(5,12)PKI
 11     FORMAT(' PK=',10F7.2)
 12     FORMAT(' PKI=',10F7.2)
        ANG=FLOAT(np)*ANGINC*PI/180.
c       type *,'ang',ang
 2      CALL BCd(B,PK,ANG,N,AXIS)
c
        enddo           !end of main proj loop
C
C       THE RESULTS OF THE BACKPROJECTION
C
c
        do j=1,n
          do i=1,n
          a(i,j)=b((j-1)*n + i)
c       type *,'a',a(i,j),i,j
          enddo
        enddo
c
        read(2,end=61)cfn       !file name for image
c
        go to 62
 61     cfn='test.out'
 62     continue
c
        open(unit=11,name=cfn,type='new',form='unformatted')
        ioutdat(3)=3
        write(11)ioutdat
C
        DO j=1,N
        WRITE(11)(A(II,J),II=1,N)
        ENDDO
C
        ENDDO   ! FOR EACH CYCLO

        close(unit=11)
        close(unit=2)
        STOP
        END
        SUBROUTINE BCD(B,P,TH,N,AXIS)
C
C       THE SUBROUTINE BCK BACK-PROJECTS A SINGLE PROJECTION
C       INTO THE ARRAY B.  THE PROJECTION HAS THE ANGLE TH. THE
C       PROJECTION BINS AND THE BACK-PROJECTION CELLS ARE ASSUMMED TO
C       BE THE SAME SIZE. THERE IS NO WEIGHTING FOR THE FRACTION
C       EACH RAY ENTERSECTS EACH CELL.
C
C       B       -THE BACK-PROJECTION ARRAY WHICH MUST BE SET TO
C               ZERO INITIALLY
C       P       -THE PROJECTION ARRAY
C       TH      -THE ANGLE IN RADIANS FOR THE PROJECTION
```

```
C       N       -THE LINEAR DIMENSION OF THE ARRAY B
C       AXIS    -THE PROJECTED LOCATION OF THE ROTATION AXIS IN THE
C               PROJECTION ARRY
C
        DIMENSION B(1),P(1)
C
        S=SIN(TH)
        C=COS(TH)
        ZN=.5*(N+1)
        ZZ=ZN*(S-C)+AXIS
        IJL=1
        DO 10 J=1,N
        ZZ=ZZ+C
        Z=ZZ
        IJU=IJL+N-1
        DO 11 IJ=IJL,IJU
        Z=Z-S
        K=Z
 11     B(IJ)=B(IJ)+(float(k+1)-z)*p(k)+(z-float(k))*p(k+1)
 10     IJL=IJL+N
C
        RETURN
        END
C       FILT.FTN        ROUTINE TO MULTIPLY THE FILTER WITH THE PROJECTION.
C
        SUBROUTINE FILT(PK,PKI,IDIM,ft)
        DIMENSION PK(512),PKI(512),FT(512),ra(2),fti(512)
        BYTE FN(40)
        DO 100 I=1,IDIM
        PK(I)=PK(I)*FT(I)
 100    PKI(I)=PKI(I)*FT(I)
        RETURN
        END
C       RDPLOT.FTN      ROUTINE TO GET A FILE READY FOR PLOTTING IN THE
C                       FAMOUS GPLOT PROGRAM. THE INPUT IS A VECTOR WHICH IS
C                       TO BE PLOTTED AGAINST ITS INDEX
        SUBROUTINE RDPLOT(RVEC,IDIM)
        DIMENSION RVEC(IDIM)
C       OPEN PLOT FILE
C
        OPEN(UNIT=3,NAME='RDPLOT.PLT',TYPE='NEW',FORM='FORMATTED')
        DO 100 I=1,IDIM
        RI=I
 100    WRITE(3,*) RI,RVEC(I)
        CLOSE(UNIT=3)
 120    FORMAT(2F10.3)
        RETURN
        END
        subroutine shlo(x,ra,m)
c
c       subroutine shlo generates the convolution funtion for
c       convolution reconstruction of paralell beam data. this
c       function is taken from the article by shepp and logan
```

```
c       ,IEEE TRANS. NUCL. SCI. VOL. NS-21, (3), (1974).
C
c       x - array in which convolution function is returned
c       ra - dummy arguement
c       m - if m is less than or equal to zero then flags are
c         return in the array p. otherwise the convolution
c         (length=2*m-1 is returned
c
        dimension x(256),ra(2)
        dimension flags(4)
        data flags/2.,-1.,0.,0./
c
        if(m.le.0)go to 12
c
        kk=2*m-1
        pi=4.* atan(1.)
        do 10 k=1,kk
 10     x(k)=-2./(pi*(4.*float(m-k)**2-1.))
c       type *,'x',x
        return
c
 12     do 14 i=1,4
 14     x(i)=flags(i)
        return
        end

c       ramp filter
c
        subroutine ramp(ft,idim)
c
        dimension ft(512)
c
        d=idim/4.
        dinc=d/16.
        do i=1,d
        ft(i)=(i-1)*dinc
        enddo
c
        ibeg=idim-d
        do i=idim,ibeg,-1
        ft(i)=abs(i-idim)*dinc
        enddo
        return
        end
c       buter filter
c
        subroutine buter(ft,idim)
c
        dimension ft(512)
c

C
        freq=.12 * idim
```

```
      order=12.
      do i=1,idim/2
      ft(i)=sqrt(1./(1.+(i/freq)**order))*(i-1)
      enddo
c
      ibeg=idim/2
      ii=2
      do i=idim,ibeg,-1
      ft(i)=ft(ii)
      ii=ii+1
      enddo
      return
      end
C

c     han filter
c
      subroutine han(ft,idim)
c
      dimension ft(512)
c

C
      freq=.5*idim
      pi=4. * atan(1.)
      ha=0.
c
      do i=1,idim/2
      ft(i)=.5 * (1. +cos(pi*i/freq))*i
      enddo
c
      ibeg=idim/2
      ii=1
      do i=idim,ibeg,-1
      ft(i)=ft(ii)
      ii=ii+1
      enddo
      return
      end
C
```

```
      PROGRAM 2DFT
C
C     Program to simulate the 2d Fourier transform experiment
c     with variable pulse duration and acquisition time.
c     The program calculates an FID matrix which is operated on
c     by the 2D Fourier transform.
c     The following routines are used in this package:
c
c    2DFT,fft,FUNCTION,FIMA,TRANSPOSE,RPLOT,-
c    power,OUTPUT

      dimension x(10000),y(10000),y2(10000),U(10000),V(10000),P(10)
      DIMENSION REAL(512,512,3),RIMA(512,512,3),pb(100),pw(100)
      CHARACTER*40 CFN
C
      TYPE *,'ENTER THE NAME OF FILE CONTAINING PARAMETERS'
      READ(5,11)CFN
 11   FORMAT(A)
      OPEN(UNIT=3,NAME=CFN,TYPE='OLD',FORM='FORMATTED')
C
      n=64
      type *,'n',n
      READ(3,*)NP,(P(I),I=1,NP)
      read(3,*)ncomp,((pb(i),pw(i)),i=1,ncomp)
C     TYPE *,'ENTER THE NUMBER OF PARAMETERS AND THE PARAMETERS'
      TYPE *,'PAR=',NP,(P(I),I=1,NP)
      type *,ncomp,((pb(i),pw(i)),i=1,ncomp)
      do i=1,ncomp
      pb(i)=pb(i)*14.
      enddo
C
      TYPE *,'ENTER FLIP FACTOR (10.)'
      READ(5,*)FFACT
      DO JJ=1,N
      INC=JJ-1
      PINC=INC*90./FFACT
      P(3)=pinc
      DO I=1,n
      X(i)=i-1
C     func =.1591549431 * width/ ((x(i)-averag)**2 + (width/2.)**2)
C     func = func*scale
        CALL FUNCTION(X(I),REAL(I,JJ,1),P,ncomp,pb,pw)
C       WRITE(9,100)X(i),Y(I)
        CALL FIMA(X(I),RIMA(I,JJ,1),P,ncomp,pb,pw)
C       WRITE(12,100)X(i),Y2(I)
 100  FORMAT(1F10.4,F10.3)
      ENDDO
      ENDDO
      CALL OUTPUT(REAL,1)
C
C
      TYPE *,'N=',N
```

```
C
c
c       fft
c
        ie=-1
C       N=N*2
        RN=N
        nu=alog(rn)/alog(2.)
        TYPE *,'BEFORE FFT N,NU',N,NU
C
        DO J=1,n
        call FFT(REAL(1,J,1),RIMA(1,J,1),N,NU,IE)
c       prepare fft output
c
C       IF(JJ.EQ.1)THEN
C         DO III=1,N
C         REAL(III,J,2)=REAL(III,J,1)
C         RIMA(III,J,2)=RIMA(III,J,1)
C         ENDDO
C       ELSE
        do i=1,n/2
        REAL(I+N,J,2)=REAL(1,J,1)
        REAL(I+N/2,J,2)=REAL(I+N/2,J,1)
        RIMA(I+N,J,2)=RIMA(1,J,1)
        RIMA(I+N/2,J,2)=RIMA(I+N/2,J,1)
C       TYPE *,'REAL 1',REAL(I,J,1),REAL(I+N,J,2),I,I+N
        y2(i+n)=y2(i)
        enddo
C
        do i=1,n
        y(i)=y(n/2+1)
        REAL(I,J,2)=REAL(N/2+I,J,2)
        RIMA(I,J,2)=RIMA(N/2+I,J,2)
C       TYPE *,'REAL 2',REAL(I,J,2),REAL(N/2+I,J,2),I,N/2+I
C       y2(i)=y2(n/2+1)
        XX=I
c       WRITE(7,13)XX,REAL(I,J,2)
C       WRITE(8,13)XX,RIMA(I,J,2)
        enddo
 13     FORMAT(2F10.3)
C
C       TYPE *,'REAL(I,J,2)',(REAL(I,J,2),I=1,128)
C       ENDIF
        ENDDO
C       CALL RPLOT(REAL,2)
        CALL OUTPUT(REAL,2)
C  A REAL ARRAY AND AN IMAGINARY ARRAY EACH OF DIMENSION N ARE INPUTS TO THIS
C  ROUTINE. NU IS THE POWER TO WHICH 2 IS RAISED TO GIVE N,I.E. N=2**NU
C  WHEN IE=+1, THE INVERSE TRANSFORM (E**+I) IS CALCULATED.
C  WHEN IE=-1, THE FORWARD TRANSFORM (E**-I) IS CALCULATED.
C  INITIALIZATION
c
c
```

```
C       do i=1,n
C       X(I)=I
C       WRITE(7,100)X(i),y(i)
C       enddo
        CALL TRANSPOSE(REAL,2)
        CALL TRANSPOSE(RIMA,2)
C       CALL OUTPUT(REAL,2)
C       CALL OUTPUT(RIMA,2)
        DO J=1,N
        call FFT(REAL(1,J,2),RIMA(1,J,2),N,NU,IE)
c       prepare fft output
c
        do i=1,n/2
        REAL(I+N,J,3)=REAL(i,J,2)
        REAL(I+N/2,J,3)=REAL(I+N/2,J,2)
C       y2(i+n)=y2(i)
        enddo
C
        do i=1,n
C       y(i)=y(n/2+i)
        REAL(I,J,3)=REAL(N/2+I,J,3)
C       y2(i)=y2(n/2+i)
        enddo
C
        ENDDO
        CALL TRANSPOSE(REAL,3)
C       CALL OUTPUT(REAL,3)
        call power(real,rima,3)
C
c
        stop
        end

C       ROUTINE CONTAINING THE REAL PART OF
C       THE EQUATION
C
        SUBROUTINE FUNCTION(X,Ysum,P,ncomp,pb,pw)
        DIMENSION P(10),pb(100),pw(100)
C
C
C       T1 FUNCTIONS
C
c       Y = P(2)*(1 - 2. * EXP(-X/P(1)) )
c       Y = P(4)*(1 - 2. * EXP(-X/P(3)) ) + Y
C       y = p(2) * (1-(1+p(3)*(1-exp(-8./p(1)) ))*exp(-x/p(1)) )
c       y = p(5) * (1-(1+p(6)*(1-exp(-8./p(4)) ))*exp(-x/p(4)) ) +y
C
C       T2 FUNCTIONS
C
C       Y = P(1)*EXP(-X/P(2))
C       Y = P(3)*EXP(-X/P(4)) +Y
C
C       SIN FIT FUNCTION
```

```
C
C
C       P(1)=MAXIMUM AMPLITUDE OF SPIN
C       Pw(1)=RESONANT FREQUENCY OF SPIN
C       P(3)=PHASE (RELATED TO FLIP ANGLE)
C       P(4)=T2 STAR (FARRER AND BECKER)
C       Pb(1)=B1 FIELD
C
        ysum=0.
        do i = 1,ncomp
        FLIP = Pb(1) *P(3)
        Y = P(1)*pb(1)
C       TYPE *,'Y 1',Y
        Y = Y * sind(flip) * SIND(X*Pw(1))
C       TYPE *,'Y 2',Y
        Y = Y * EXP(-X/P(4))
C       TYPE *,'Y 3',Y
        ysum =ysum +y
        enddo
C
        RETURN
        END
C       ROUTINE CONTAINING THE IMAGINARY PART
C       OF THE EQUATION
C
        SUBROUTINE FIMA(X,Ysum,P,ncomp,pb,pw)
        DIMENSION P(10),pb(100),pw(100)
C
C
C       T1 FUNCTIONS
C
c       Y = P(2)*(1 - 2. * EXP(-X/P(1)) )
c       Y = P(4)*(1 - 2. * EXP(-X/P(3)) ) + Y
C       y = p(2) * (1-(1+p(3)*(1-exp(-8./p(1)) ))*exp(-x/p(1)) )
c       y = p(5) * (1-(1+p(6)*(1-exp(-8./p(4)) ))*exp(-x/p(4)) ) +y
C
C       T2 FUNCTIONS
C
C       Y = P(1)*EXP(-X/P(2))
C       Y = P(3)*EXP(-X/P(4)) +Y
C
C       SIN FIT FUNCTION
C
C       FIRST COMPONENT
C
C       P(1)=MAXIMUM AMPLITUDE OF SPIN
C       P(2)=RESONANT FREQUENCY OF SPIN
C       P(3)=PHASE (RELATED TO FLIP ANGLE)
C       P(4)=T2 STAR (FARRER AND BECKER)
C       P(5)=B1 FIELD
C
        ysum=0.
        do i = 1,ncomp
```

```
        FLIP = Pb(i) *P(3)
        Y = P(1)*pb(i)
C       TYPE *,'Y 1',Y
        Y = Y * sind(flip) * SIND(X*Pw(i) -90.)
C       TYPE *,'Y 2',Y
        Y = Y * EXP(-X/P(4))
C       TYPE *,'Y 3',Y
        ysum =ysum +y
        enddo
c
C
        RETURN
        END
        SUBROUTINE TRANSPOSE(REAL,NDIM)
        DIMENSION REAL(512,512,3),TEMP(256,256)
C
C
C
        IDIM=64
        DO J=1,IDIM
                DO I=1,IDIM
                TEMP(I,J)=REAL(J,I,NDIM)
                ENDDO
        ENDDO
C
        DO J=1,IDIM
                DO I=1,IDIM
                REAL(I,J,NDIM)=TEMP(I,J)
                ENDDO
        ENDDO
        RETURN
        END
        SUBROUTINE RPLOT(REAL,NDIM)
        DIMENSION REAL(512,512,3)
C
        IDIM=64
        RMAX=-100000.
        DO J=1,IDIM
        DO I=1,IDIM
          RMAX=MAX(REAL(I,J,NDIM),RMAX)
          IF(RMAX.EQ.REAL(I,J,NDIM))RIMAX=I
        ENDDO
        ENDDO
        TYPE *,'RIMAX',RIMAX
C
        OPEN(UNIT=2,NAME='RPLOT.OUT',TYPE='NEW',FORM='FORMATTED')
C
        DO I=1,IDIM
          X=I
          WRITE(2,10)X,REAL(RIMAX,I,NDIM)
        ENDDO
 10     FORMAT(2F10.3)
C
```

```
      CLOSE(UNIT=2)
      RETURN
      END
      SUBROUTINE power(REAL,rima,NDIM)
C
C     ROUTINE TO CALCULATE THE MODULUS FROM THE REAL
C     AND IMAGINARY PARTS OF THE MATRIX
C
      DIMENSION REAL(512,512,3),rima(512,512,3),temp(512)
      CHARACTER*40 CFN
      INTEGER*2 IVEC(256),IH(256)
      IH(3)=1
C
      idim=64
C
C
 3    CFN(1:7)='power.RAM'
C
 4    CONTINUE
C
      OPEN(UNIT=2,NAME=CFN,TYPE='NEW',FORM='UNFORMATTED')
      WRITE(2)IH      !HEADER
      DO J=1,idim
            DO I=1,idim
            t1=real(i,j,ndim)**2 + rima(i,j,ndim)**2
            temp(i)=sqrt(t1)
            ENDDO
      write(2)(temp(i),i=1,idim)
      ENDDO
      CLOSE(UNIT=2)
C
      RETURN
      END
      SUBROUTINE output(REAL,NDIM)
C
C     ROUTINE TO OUTPUT MATRIX TO DISK FOR RAMTEK
C     OR VERSATEK DISPLAY
C
C
      DIMENSION REAL(512,512,3),rvec(256)
      CHARACTER*40 CFN
      INTEGER*2 IVEC(256),IH(256)
      IH(3)=1
      idim=64
C
C
C
      GO TO (1,2,3)NDIM
 1    CFN(1:7)='FID.RAM'
      GO TO 4
 2    CFN(1:7)='FF1.RAM'
      GO TO 4
 3    CFN(1:7)='FF2.RAM'
```

```
C
 4      CONTINUE
C
        OPEN(UNIT=2,NAME=CFN,TYPE='NEW',FORM='UNFORMATTED')
        WRITE(2)IH      !HEADER
        DO J=1,idim
                DO I=1,idim
                RVEC(I)=REAL(I,J,NDIM)
                ENDDO
        WRITE(2)(RVEC(I),I=1,IDIM)
        ENDDO
        CLOSE(UNIT=2)
C
        RETURN
        END


        Program acmb1
c
c       program to display two dimensional matrix on the versatek
c       using the 3d plot package from acm computer journal
c
c       The following routines are used in this package:
c       acmB1,plot3d,sys$library:phase1/lib

        dimension mask(4000),vertex(16),outbuf(256),z(256),A(512,256)
        dimension xdata(256),zdata(256)
        DIMENSION B(200,200),A1(200,200)
        CHARACTER*40 CFN
        sinc(x) = sin(x)/x
C
c  First figure
c  generate data running parellel to x-axis
        call plots(0.,0.,0.)
        call factor(.9)
        write(5,1000)
 1000   format('$Enter theta,phi: ')
        read (5,2000) theta,phi
 2000   format(2f10.0)
c
C
        TYPE *,'ENTER FILE NAME:'
        READ(5,152)CFN
        TYPE *,'ENTER X, Y DIMENSION OF INPUT'
        READ(5,*)IDIM,JDIM
        TYPE *,'ENTER INCREMENTS FOR X,Y'
        READ(5,*)IXINC,IYINC
        TYPE *,'ENTER DIVIDING SCALE FACTOR FOR INPUT VALUES'
        READ(5,*)FSCALE
        TYPE *,'ENTER THE XSCALE'
        READ(5,*)XSCALE
C
 152    FORMAT(A)
```

```
      open (unit=2,name=Cfn,type='old',
     .      form='UNformatted',readonly)
      READ(2)          !HEADER
      do 12 J=1,JDIM
      read (2) (A(I,J),I=1,IDIM)
C     TYPE *,'A',(A(I,J),I=1,100)
 12   continue
C
C     DO J=1,100,-1
C             DO I=1,100,-1
C             A1(I,J)=A(101-I,101-J)
C             ENDDO
C     ENDDO
C
      JJ=1
      II=1
      DO J=1,JDIM
             DO I=1,IDIM
             B(I,J)=A(I,J)
             ENDDO
      ENDDO
      DO J=5,8
      TYPE *,'J',J
      TYPE *,(B(I,J),I=50,150)
      ENDDO
      do 20 nline = 1,JDIM
             do 10 npoint=1,IDIM
             OUTBUF(NPOINT)=B(NPOINT,NLINE)/FSCALE
C     type*,xdata(npoint),outbuf(npoint),zdata(npoint)
 10          continue
c  Plot each line as it is computed
             z(1) = 0.
             xdata(1) = 0.
             call plot3d(10,xdata,outbuf,z,XSCALE,4.,-.1,
     .                nline,IDIM,phi,theta,4.6,3.,10.,mask,vertex)
 20   continue
      IANS=1
      IF(IANS.EQ.1)THEN
      GO TO 111
      ENDIF
c  Second figure
c  Generate array of z components
      do 30 nline=1,IDIM
      z(nline) = -.1*(nline-1)
 30   continue
c  Generate data running parallel to z-axis
      do 50 nline = 1,IDIM
      x = .1*(nline-1)
             do 40 npoinT=1,IDIM
             OUTBUF(NPOINT)=A(NLINE,NPOINT)/FSCALE
 40          continue
c  Plot each line as it is computed
             call plot3d(1011,x,outbuf,z,0.,4.,1.,
```

```
     .                    nline,IDIM,phi,theta,4.6,3.,10.,mask,vertex)
 50      continue
c  Draw a frame on the figure
c        call framer(3,vertex,mask)
 60      continue
 111     call plot(11.,0.,3)
         call plot(11.,0.,2)
         call plot(0.,0.,999)
         stop
         end
```

```
! NMR1.COM
! Command filed used to invoke programs
! to convert nicolet raw data files into
! vax readable files and reconstruct the image
!
$ P2=3
$ INQUIRE FILENAME
$ COPY 'FILENAME FOR013.DAT
$ run drc:[todd.nmr]ntcftv.128
$ LOOP:
$ RUN DRC3:[TODD.NMR]BKPRO
$ del rea.out;
$ P2=P2-1
$ IF P2.GT.0 THEN GOTO LOOP
$ del for000.dat;*
$ DEL REA.OUT;*
$ PUR FOR013.DAT


C       MAIN PROGRAM NTCFTV
C       PROGRAM TO TAKE THE NMR FID DATA AND PROCESS IN MANNER VERY SIMILAR
C       TO NICOLET NTCFT PROGRAM, IE, FOURIER TRANSFORM, APODIZATION,
C       PHASE CORRECTION, ETC. THE AU ROUTINE LINK IS SET UP FOR PROJECTION
C       DATA PROCESSING TO BE GIVEN TO PROGRAM BKPRO.
C       THE FOLLOWING ROUTINES ARE USED IN THIS PACKAGE:
C
C  NTCFTV,OUTRAM,NTCFTV.BD1/OPT,PHASEC,YSCALE,NTCDAT,FFT,-
C  ZOOM,APOD,AUTOPHASE,READ,CHDATA3,FOURIER,fourier2,POWER,buter,-
C  HAN,FILT,FINDP,CH16,BAS,MID,SMOOTH,TRANSPOSE,FOURIER3,PLOTNMR,-
C  PPM,headex,PRESPEC,PPM2,test2d,reverse,subsp,save,D3POI,-
C  [TODD.NMR]READOUT,UNPACK,CHHEAD,CHDATA2,CONVRT,INTCON,TEXTCON,-
C  DRC:[RAM]initrm,RMCROS,bell,upper,CLRPLN,TTIO,NEWP1,DASH,CIRC1,crvfit,-
C  DISPLAY/LIB,-
C  DRC:[SAM.SUBS]MARK,VTSUBS/LIB,-
C  'fip'
C
C
C       ROUTINES READ, APOD, FOURIER3, CH16, TRANSPOSE, AUTOPHASE, PRESPEC,
C       AND PPM2 ARE USED IN THE 2D FOURIER TRANSFORM ANALYSIS OF THE
C       PHASE-ENCODED SPECTROSCOPY DATA
C
C       ROUTINES READ, FOURIER3, CH16, BAS, MID, AND POWER ARE USED IN
C       PREPARING PROJECTION DATA FOR IMAGE RECONSTRUCTION
C
       PROGRAM NTCFTV
       INTEGER*2 IOUTDAT(256)
       COMMON /NMRDAT/DNMR(10000),ISIZE,YSC
       COMMON /NMRDAT2/DNMR2(1024,512)
       COMMON /PPMNMR/PNMR(10000)
       COMMON /APOD/LB
       COMMON /OPTION/OPT
       character*1 ans
```

```
      DIMENSION PK(20000),PKI(20000),FT(512)
      CHARACTER*2 OPT
      CHARACTER*40 CFN
      type *,'Do you want to use ramtek?'
      read(13,3)ans
 3    format(a)
      retcode=str$upcase(ans,ans)
      if(ans.eq.'Y')then
      CALL INITRM              !INITIALIZE RAMTEK
      CALL INITBP              !INITIALIZE BITPAD
      endif
C
C     DEFAULT VALUES
      LB=10
      Ipinc=3
C
 30   TYPE *,'OPTIONS;'
      TYPE *,'GA = GET NMR DATA FROM DISK     EM = EXPONENTIAL APOD'
      TYPE *,'GC = GET NMR DATA FROM .DAT FILE ON DISK'
      TYPE *,'GX = GET ASCII NMR DATA FROM DISK'
      TYPE *,'ZO = ZOOM IN ON PART OF THE DATA'
      TYPE *,'FT = FOURIER TRANSFORM          PH = PHASE CORRECTION'
      type *,'PC = AUTO PHASE                 AU = LINK COMMANDS'
      TYPE *,'SC = SCALE IN Y                 MO = EXIT'
c     FS = SYMMETRIC FID FILL BEFORE FT
C     MC= CALCULATE THE POWER SPECTRUM
C     bu=butterworth filter
c     ha= han filter
c     f3= fourier transform without zero
C     LV= LIST INTENSITY VALUES BETWEEN MARKS
C     LB = LINE BROADENING
C     CA = CHANGE ARTIFACT OF -16. ON FID
C     BC = BASE LINE CORRECTION
C     MA = MIDDLE POINT AVERAGE
C     SM = SMOOTHING 2 POINT
C     G1 = LOAD IN TOTAL DAT FILE
C     G2 = LOAD IN A GIVEN BLOCK OF DAT FILE FOR PROCESSING
C     TA = TRANSPOSE AND FT
C     11 = OUTPUT TO UNIT 11 FOR RAMTEK
C     PL = PREPARE FILE FOR PLOTTING
C     PM= RESCALE FOR PPM
C     PR= PREPARE 2D SPECTRA

c
      READ(13,10)OPT
 10   FORMAT(A)
      RETCODE = STR$UPCASE(OPT,OPT)
C
      IF(OPT.EQ.'GA'.OR.OPT.EQ.'GC')THEN
        CALL READOUT
        CALL OUTRAM
      ENDIF
C
```

```
        IF(OPT.EQ.'AU')THEN
 55     OPEN(UNIT=12,NAME='REA.OUT',TYPE='NEW',FORM='UNFORMATTED')
        IOUTDAT(3)=3     !RAMTEK HEADER
        WRITE(12)IOUTDAT
        TYPE *,'IPROJ,',IIPROJ
        DO II=1,IIPROJ-1
          DO I=1,ISIZE*2
          DNMR(I)=DNMR2(I,II)
          ENDDO
        CALL CH16
        CALL BAS
C       CALL APOD
        call fourier3
C       CALL AUTOPHASE
        call mid
c       CALL OUTRAM
        CALL POWER
C       CALL FOURIER
C       CALL MID
C       CALL SMOOTH
        WRITE(12)(DNMR(JJ),JJ=1,ISIZE)
C
C         DO I=1,ISIZE*2
C         DNMR2(I,II)=DNMR(I)
C         ENDDO
        ENDDO
          read(13,53)cfn
 53     format(a)
          write(12)cfn
        close(unit=12)
          IPINC=IPINC-1
        IF(IPINC.GT.0)THEN
          GO TO 56
        ELSE
          STOP
        ENDIF
        ENDIF
C
C
        IF(OPT.EQ.'G1')THEN
 56      CALL READ(IPROJ)
        IIPROJ=IPROJ-1
        GO TO 55
        ENDIF
C
        IF(OPT.EQ.'TA') CALL TRANSPOSE(IIPROJ)
C
        IF(OPT.EQ.'PR') CALL PRESPEC(IIPROJ)
C
        IF(OPT.EQ.'G2')THEN
        TYPE *,'ENTER THE BLOCK TO DISPLAY:'
        READ(5,*)II
c
```

```
          DO I=1,ISIZE*2
          DNMR(I)=DNMR2(I,II)
          if(ans.ne.'Y')then
          if(i.lt.isize)type *,i,pnmr(i),dnmr(i)
          endif
          ENDDO
        CALL OUTRAM
        ENDIF
C
        IF(OPT.EQ.'PL')CALL PLOTNMR
C
        IF(OPT.EQ.'11')WRITE(11)(DNMR(I),I=1,ISIZE)
C
        IF(OPT.EQ.'PM')CALL PPM
C
C       OPTION FOR ASCII DATA FILES
C
        IF(OPT.EQ.'GX')CALL NTCDAT
C       TYPE *,'DNMR',(DNMR(I),I=1,30)
C
        IF(OPT.EQ.'LB')THEN
        TYPE *,'LB=',LB
        READ(5,*)LB
        ENDIF
C
        IF(OPT.EQ.'CA')CALL CH16
C
        IF(OPT.EQ.'EM')CALL APOD
C
        IF(OPT.EQ.'LV')CALL FINDP
C
        IF(OPT.EQ.'MA')THEN
          CALL MID
          CALL OUTRAM
        ENDIF

C
        IF(OPT.EQ.'BC')CALL BAS
C
        IF(OPT.EQ.'SM')THEN
          CALL SMOOTH
          CALL OUTRAM
        ENDIF
c
c
        if(opt.eq.'BU')THEN
C
        IDIM=512
        ISIZE=512
        RN=IDIM
        NU=ALOG(RN)/ALOG(2.)
C
C
```

```
C
c       define the filter
c
        CALL BUTER(FT,IDIM)
        DO I=1,IDIM
        DNMR(I)=FT(I)
        ENDDO
C
        CALL OUTRAM
        READ(5,*)JUNK
C
c


        do i=1,idim
        pk(i)=0.
        pki(i)=0.
        enddo
c
        do i=240,270
        pk(i)=1.
        enddo
        DO I=1,IDIM
        DNMR(I)=PK(I)
        ENDDO
C
        CALL OUTRAM

c       TYPE *,'PK',(PK(II),II=1,IDIM)
C
        CALL FFT(PK,PKI,IDIM,NU,-1)
        DO I=1,IDIM
        DNMR(I)=PK(I)
        ENDDO
C
        CALL OUTRAM
        READ(5,*)JUNK

        CALL FILT(PK,PKI,IDIM,ft)
        DO I=1,IDIM
        DNMR(I)=PK(I)
        ENDDO
C
        CALL OUTRAM
        READ(5,*)JUNK

        CALL FFT(PK,PKI,IDIM,NU,1)
C
        DO I=1,IDIM
        DNMR(I)=PK(I)
        ENDDO
C
        CALL OUTRAM
C
```

```
      ENDIF
C
      IF(OPT.EQ.'MC')CALL POWER
C
      IF(OPT.EQ.'ZO')CALL ZOOM
C
      IF(OPT.EQ.'PC')CALL AUTOPHASE
C
C
      IF(OPT.EQ.'FT')CALL FOURIER
C
      IF(OPT.EQ.'FS')CALL FOURIER2
c
      if(opt.eq.'F3')call fourier3
C
C
      IF(OPT.EQ.'PH')CALL PHASEC
C
      IF(OPT.EQ.'SC')CALL YSCALE

C
      IF(OPT.EQ.'MO')STOP
C
C
      GO TO 30
      END

C
C     PROGRAM TO READ OUTPUT FROM READNTC
C
      SUBROUTINE READ(IIPROJ)
      CHARACTER*40 CFN
      COMMON /NMRDAT/DNMR(20000),ISIZE,YSC
      COMMON /OPTION/OPT
      CHARACTER*2 OPT
      BYTE HEAD(100),DATA(1000),FBYTE(5),AA(4),A2(4)
      EQUIVALENCE (AA,IW1),(A2,IW2)
      TYPE *,'ENTER FILE NAME'
      READ(13,10)CFN
 10   FORMAT(A)
      OPEN(UNIT=1,NAME=CFN,TYPE='OLD',FORM='UNFORMATTED')
      READ(1)(HEAD(I),I=1,2)
C     WRITE(5,11)(HEAD(I),I=1,2)
C     DO II=1,10
      READ(1)(DATA(I),I=1,25)
      CALL CHHEAD(DATA,IFSIZE,ISFLAG)
      TYPE *,'IFSIZE',IFSIZE,ISFLAG
      ISIZE=IFSIZE-351                    !TO PASS TO OUTRAM
        TYPE *,'ENTER THE SIZE OF THE ARRAY:'
        READ(13,*)ISIZE
        TYPE *,'ENTER THE TOTAL NUMBER OF PROJECTIONS'
        READ(13,*)NPROJ
        TYPE *,'ENTER THE STARTING BLOCK NOT COUNTING HEADER'
```

```
          READ(13,*)IBLOCK
C
c         ILOOP=IFSIZE/352
c         ILAST=MOD(IFSIZE,352)
          iloop=NPROJ+1
          ilast=0
          TYPE *,'ILOOP',ILOOP,ILAST
          INC=1
          iiproj=1
          ist=1              !index for dnmr data array
C
 122      CONTINUE
          IF(INC.LE.ILOOP)THEN
            NDATA=352
          ELSE
            NDATA=ILAST+1
          ENDIF
          IDLOOP=(NDATA/2)*5                          !2 WORDS PACKED IN 5 BYTES
c         TYPE *,'NDATA,IDLOOP',NDATA,IDLOOP,INC
          READ(1) (DATA(II),II=1,IDLOOP+3)
          if(inc.eq.1)call headex(data,rinfo)
          IF(INC.GE.IBLOCK+1)THEN
          CALL CHDATA3(DATA,ISFLAG,NDATA+2,INC,iiproj,ist)
          ENDIF
C         TYPE *,'ISFLAG',ISFLAG
            INC=INC+1
            IF(NDATA.EQ.(ILAST+1))GO TO 130                        !FINISHED
          GO TO 122

C
 130      CLOSE(UNIT=1)
          RETURN
          END

C
c         program to read header information from nmr data
c
C
          SUBROUTINE headex(DATA)
C
C         DATA- BYTE ARRAY CONTAINING THE DATA
C         ISFLAG=1 IF CHECKSUM IS OKAY
C         NDATA- NUMBER OF DATA POINTS
c
          BYTE DATA(1000),FBYTE(5),BB(60)
          INTEGER ITEXT(100),IB(352)
          COMMON /NMRDAT/DNMR(20000),ISIZE,YSC              !NMR DATA
          COMMON /OPTION/OPT
          common /passppm/rinfo(10)
          CHARACTER*2 OPT
          REAL*8 RR
          ISUM=0
          IBST=1
```

```
C
      ndata=352
      ILOOP=NDATA/2
      DO I=1,ILOOP-1
      IW1=0
      IW2=0
        DO IJ=1,5
        FBYTE(IJ)=DATA((I-1)*5 + IJ)
        ENDDO
      CALL UNPACK(FBYTE,IW1,IW2)
C
C     STORE THE UNPACKED BYTES FOR LATER PROCESSING
C
      IB(IBST)=IW1
      IBST=IBST+1
      IB(IBST)=IW2
      IBST=IBST+1
      enddo
C
      ir=1
      TYPE *,'NUMBER OF SCANS'
      DO I=1,10
      TYPE *,IB(I)
      ENDDO
      do i=323,331,2
      type *,i
      call convrt(ib(i),ib(i+1),rr)
      type *,'sweep width',rr
      rinfo(ir)=rr
      ir=ir+1
      enddo
      type *,rinfo
C     FOR .DAT FILES FROM THE 180 SPECTROMETER
C
      DO II=75,101,2
      CALL CONVRT(IB(II),IB(II+1),RR)
C     IF(II.EQ.75)WRITE(7,726)
 726  FORMAT(1X,'D2-D7 = IN USEC')
      IF(II.EQ.89.OR.II.EQ.91)THEN
      WRITE(7,728)
 728  FORMAT(1X,'P1-P2=')
      WRITE(7,727)RR/1.25
      ENDIF
C     IF(II.EQ.97)WRITE(7,729)
 729  FORMAT(1X,'D1 VALUES ARE')
 727  FORMAT(F20.9)
      TYPE *,'II,RR',II,RR/1.25
      ENDDO

c
      return
      end
C
```

```
C       PROGRAM TO READ OUTPUT FROM READNTC
C       AND TO CHECKSUM OF THE 352 BLOCK DATA
C
        SUBROUTINE CHDATA3(DATA,ISFLAG,NDATA,INC,IPROJ,istb)
C
C       DATA- BYTE ARRAY CONTAINING THE DATA
C       ISFLAG=1 IF CHECKSUM IS OKAY
C       NDATA- NUMBER OF DATA POINTS
C
        BYTE DATA(1000),FBYTE(5),BB(60)
        INTEGER ITEXT(100),IB(352)
        COMMON /NMRDAT/DNMR(20000),ISIZE,YSC            !NMR DATA
        COMMON /NMRDAT2/DNMR2(1024,512)
        COMMON /OPTION/OPT
        CHARACTER*2 OPT
        REAL*8 RR
        ISUM=0
C
        ILOOP=352/2
        DO I=1,ILOOP
        IW1=0
        IW2=0
          DO IJ=1,5
          FBYTE(IJ)=DATA((I-1)*5 + IJ)
          ENDDO
        CALL UNPACK(FBYTE,IW1,IW2)
C
C
C       FOR THE INTEGERS
C

        IF(INC.GT.1)THEN
        CALL INTCON(IW1,II2)
C
          DNMR2(ISTb,IPROJ)=II2
          istb=istb+1
c       type *,'istb,dnmr',istb,dnmr(istB)
C
        CALL INTCON(IW2,II2)
C
          DNMR2(ISTb,IPROJ)=II2
          istb=istb+1
          IF(ISTB.GE.ISIZE*2)THEN
          ISTB=1
          IPROJ=IPROJ+1
          GO TO 110
          ENDIF
        ENDIF
        ENDDO
C
 110    RETURN
        END
```

```
C       FILE NAME:              CONVRT.FTN
C
C       ORIGINAL AUTHOR:        R. P. SINGH
C                               RADIOTHERAPY SECTION
C                               DONNER LABORATORY
C                               LAWRENCE BERKELEY LABORATORY
C                               BERKELEY
C                               CALIFORNIA 94720
C
C                               415-843-2740  EXT. 6037 OR 6325
C
C       ORIGINAL DATE:          17 MAY 1977.
C
C       HISTORY OF MODIFICATIONS:
C       -------------------------
C
C       DATE            AUTHOR(S)
C       ----            ---------
C
C       18 MAY 77       R. P. SINGH
C       14 NOV 83       T. RICHARDS
C
C
C       SUBROUTINE TO CONVERT FROM NICOLET
C       TO FLOATING POINT FORMAT USED HERE.
C
C       NOTE:  ECLIPSE FLOATING POINT FORMAT IS IDENTICAL TO
C              IBM FLOATING POINT FORMAT.
C
C
C               FORTRAN CALL:
C
C               CALL CONVRT (I1,I2,R)
C
C       WHERE:
C
C       I1      --  IS THE WORD CONTAINING THE SIGN +
C                   HIGH ORDER MANTISSA.
C
C       I2      --  IS THE WORD CONTAINING
C                       SIGNED EXPONENT + THE LOW ORDER MANTISSA.
C
C       R       --  IS THE REAL VARIABLE IN WHICH TO PLACE THE
C                   RESULT.
C
C
      SUBROUTINE CONVRT (I1,I2,R)
      INTEGER IARR(40),MANT(50)
      REAL*8 R
C
C     TYPE *,'I1',I1,I2
      DO I=1,20
      IARR(I)=LIB$EXTZV(I-1,1,I1)
```

```
      IARR(I+20)=LIB$EXTZV(I-1,1,I2)
      ENDDO
C     TYPE *,'IARR',(IARR(I),I=1,40)
C
C     OBTAIN THE SIGN OF THE NUMBER.
C
      ISIGN=+1
      IF(IARR(20).NE.0) ISIGN=-1
C
C     NEXT, CALCULATE THE EXPONENT.
C
      J=30
      IEXP=0
      DO 10 I = 1,10
      J=J+1
C     TYPE *,'IARR(J)',IARR(J),I-1,IEXP
      IEXP=IEXP+IARR(J)*2**(I-1)
10    CONTINUE
C     TYPE *,'IEXP',IEXP
C
C     IEXP NOW CONTAINS THE EXPONENT.  THIS IS IN EXCESS 64, SO
C     SUBTRACT 64 FROM IT.
C
C     IEXP=IEXP-512
C
C     THIS EXPONENT IS NOW A TRUE POWER OF 16.  MULTIPLY IT BY 4 TO
C     CONVERT IT TO A POWER OF 2.
C
C
C     NOW COPY THE MANTISSA INTO THE ARRAY MANT, WITH THE MOST
C     SIGNIFICANT MANTISSA BIT IN MANT(1) AND THE LEAST SIGNIFICANT
C     MANTISSA BIT IN MANT(24).
C
      J=20
      DO 20 I = 1,19
      J=J-1
      MANT(I)=IARR(J)
20    CONTINUE
      J=31
      DO 30 I = 20,29
      J=J-1
      MANT(I)=IARR(J)
30    CONTINUE
C
C     FINALLY, CALCULATE THE VALUE OF THE NUMBER.
C
      R=0.0
      DO 40 I = 1,29
C     TYPE *,'R',MANT(I),IEXP-I
      R=R+MANT(I)*2.0**(IEXP-I)
40    CONTINUE
C
      IF(ISIGN.LT.0) R=-R
```

```
      RETURN
      END
C
C     PROGRAM TO CONVERT NICOLET INTEGERS TO VAX VMS INTEGERS
C
      SUBROUTINE INTCON(I1,I2)
C
C     I1- INPUT (NICOLET)
C     I2 - OUTPUT
C
      ITEMP=I1
      IBIT=0
      IBIT=LIB$EXTZV(19,1,I1)
C     TYPE *,'I1,IBIT',I1,IBIT
C
      IF(IBIT.EQ.0)THEN
        I2=I1
        RETURN
      ELSE
        DO I=20,31
        CALL LIB$INSV(IBIT,I,1,ITEMP)
        ENDDO
      I2=ITEMP
      ENDIF
C
      RETURN
      END
C
C     ROUTINE TO CONVERT 6 BIT ASCII NICOLET TO
C     VAX VMS ASCII
C
      SUBROUTINE TEXTCON(ITEXT,NEL,BB)
C
C     ITEXT - INPUT INTEGER ARRAY FROM UNPACK WHERE EACH
C     INTEGER CONTAINS 3 6BIT CHARACTERS
C
C     NEL - NUMBER OF INTEGER ELEMENTS IN THE ARRAY
C
C     TEXT - CHARACTER STRING CONTAINING ASCII OUTPUT
C
      INTEGER ITEXT(NEL)
      BYTE BB(60),B1(60)
C
C
      IBIT=1          !TO INSERT TO THE 7TH BIT
C
      DO INC=1,NEL
      DO I=1,3
      IPOS=(I-1)*6            !BIT POSITION OF INPUT INTEGER
      IBPOS=(INC-1)*3 + I     !BYTE POSITION OF OUTPUT CHARACTER
     B1(IBPOS)=LIB$EXTZV(IPOS,6,ITEXT(INC))
      IF(B1(IBPOS).LE.40)CALL LIB$INSV(IBIT,6,1,B1(IBPOS))
C
```

```
      ENDDO
      ENDDO
      DO II=1,NEL
      DO I=1,3
      IR1=(II-1)*3
      IRR=(II)*3 + 1
      BB(IR1+I)=B1(IRR-I)
      ENDDO
      ENDDO
C
      RETURN
      END

C
C     PROGRAM TO UNPACK BITS FROM PROGRAM IOTRAN NICOLET
C
      SUBROUTINE UNPACK(FBYTE,IW1,IW2)
      BYTE FBYTE(5),TEST(5),IT
C
      IT=FBYTE(3)/16
C     WRITE(5,11)IT
 11   FORMAT(1X,'IT',O3)
      CALL LIB$INSV(FBYTE(1),12,8,IW1)
      CALL LIB$INSV(FBYTE(2),4,8,IW1)
      CALL LIB$INSV(IT,0,4,IW1)
      CALL LIB$INSV(FBYTE(3),16,4,IW2)
      CALL LIB$INSV(FBYTE(4),8,8,IW2)
      CALL LIB$INSV(FBYTE(5),0,8,IW2)
      RETURN
      END
C
C     SUBROUTINE TO UNPACK AND READ THE FILE SIZE AND CHECKSUM
C
      SUBROUTINE CHHEAD(HEAD,IFSIZE,ISFLAG)
C
C     ISFLAG = 1 IF CHECKSUM EQUALS ISUM
C     ISFLAG = 0 IF CHECKSUM DOES NOT EQUAL ISUM
C
      BYTE HEAD(1000),FBYTE(5)
      INTEGER IHD(25)
      ISUM=0
      IST=1
      DO I=1,5
        DO IJ=1,5
        FBYTE(IJ)=HEAD((I-1)*5 + IJ)
        ENDDO
      CALL UNPACK(FBYTE,IW1,IW2)
      IHD(IST)=IW1
      IST=IST+1
      IHD(IST)=IW2
      IST=IST+1
C
      IF(I.LT.5)THEN
```

```
        ISUM=ISUM+IW1+IW2
        ELSE
        ISUM=ISUM+IW1
        ENDIF
        IF(I.EQ.4)IFSIZE=IW1
        IF(I.EQ.5)ICH=IW2
C       TYPE *,'IW1,IW2',IW1,IW2
        ENDDO                       !MAIN LOOP
C
        IF(IFSIZE.GT.100000)IFSIZE=IHD(5)                !.DAT FILE
        I20BIT=2**20
        IRE=MOD(ISUM,I20BIT)
C       TYPE *,'ISUM,IRE',ISUM,IRE
        IF(IRE.EQ.ICH)THEN
        ISFLAG=1
        ELSE
        ISFLAG=0
        ENDIF
C
        RETURN
        END

C
C       SUB TO TAKE NMR DATA IN MEMORY , SCALE IT AND PUT IT UP ON THE
C       RAMTEK
C
        SUBROUTINE OUTRAM
C
        COMMON /NMRDAT/DNMR(20000),ISIZE,YSC
        COMMON /XFACTOR/IFACT
        COMMON /SPARAM/RMIN,SCALE,IOFFSET
        DIMENSION DD(20000)
        INTEGER*2 IV(4096),IOUT
C
c       TYPE *,'ISIZE',ISIZE
        RMIN=1000000.
        RMAX=-1000000.
        DO I=1,ISIZE
        RMIN=MIN(RMIN,DNMR(I))
        RMAX=MAX(RMAX,DNMR(I))
        ENDDO
C
C       TYPE *,'RMIN,RMAX',RMIN,RMAX
C
C       SCALE THE DATA
C
        SCALE = (RMAX-RMIN)/400.
        IF(YSC.NE.0.)SCALE=SCALE/YSC
        IOFFSET=(512-400)/2
        DO I=1,ISIZE
        DD(I)=(DNMR(I) - RMIN)/SCALE
        DD(I)=DD(I)+IOFFSET
        DD(I)=512.-DD(I)
```

```
        ENDDO
C
C       FIT THE DATA ONTO 512X512 GRID
C
        RFACT=ISIZE/512.
        IF(RFACT.GT.1.)THEN
        IFACT=INT(RFACT)
        R2=IFACT
          IF(RFACT.GT.R2)THEN
          IFACT=R2 + 1
          ELSE
          IFACT=R2
          ENDIF
        ENDIF
C
        IF(RFACT.LE.1.)IFACT=1
c       TYPE *,'IFACT',IFACT,ISIZE
        IST=0
        DO I=1,ISIZE,IFACT
        IST=IST+1
        IV(IST)=(IST/2) + 1
        IST=IST+1
C       TYPE *,'DD',DD(I),IST
c       rmin=1.e10
c       do jj=1,ifact
c       rmin=min(rmin,dd(i+jj-1))
c       IV(IST)=NINT(rmin)
c       enddo
        iv(ist)=dd(i)
        IF(IV(IST).LE.0)IV(IST)=0
        IF(IV(IST).GT.511)IV(IST)=511
        ENDDO
C
C       OUTPUT TO THE RAMTEK
C
        IF(ISIZE.LT.511)THEN
          IOUT=ISIZE-1
        ELSE
          IOUT=510
        ENDIF
C       TYPE *,'IOUT',IOUT
        CALL RSET(IERR)
        CALL COP(IV(1),IV(2),IERR)
        CALL WV(IV(3),IOUT,IERR)
C
        RETURN
        END

C
C       SUB TO PHASE CORRECT THE SPECTRUM
C
        SUBROUTINE PHASEC
C
```

```
      COMMON /NMRDAT/DNMR(20000),ISIZE,YSC
      DIMENSION PK(20000),PKI(20000)
      common /phase/angsum,angbsum
      INTEGER*2 IPLANE,OUT(2,2000)
      CHARACTER*2 OP
C
      ANG=0.
      ANGB=0.
      ANGBINC=0.
      TYPE *,'TYPE PA OR PB FOR ZERO OR SECOND ORDER CORRECTION:'
      READ(5,10)OP
 10   FORMAT(A)
      RETCODE=STR$UPCASE(OP,OP)
C
      TYPE *,'USE THE BIT PAD TO CHANGE THE PHASE'
      TYPE *,'-100 DEGREES - FAR LEFT;          +100 DEG. - FAR RIGHT'
      TYPE *,'HIT BOX LABELED THREE TO EXIT'

 100  CONTINUE
C
      DO I=1,ISIZE
      PK(I)=DNMR(I)
      PKI(I)=DNMR(I+ISIZE)
      ENDDO
      NOUT=1
      IPLANE="2000
      CALL BPOINTR(IPLANE,OUT,NOUT,ICODE)      !READ FROM BITPAD
      TYPE *,'OUT(1,1)',OUT(1,1),OUT(2,1)
      IF(ICODE.EQ.3)RETURN

C
      IF(OP.EQ.'PA')THEN
      ANG=(OUT(1,1)-256)/5.
      ELSE
      ANGB=(OUT(1,1)-256)/5.
      ANGBINC=ANGB/ISIZE
      ENDIF
C
      DO I=1,ISIZE
      ADDANG=ANGBINC*I
      ANG1=ANG+ADDANG
      DNMR(I)=PK(I)*COSD(ANG1) - PKI(I)*SIND(ANG1)
      DNMR(I+ISIZE)=PKI(I)*COSD(ANG1) + PK(I)*SIND(ANG1)
      ENDDO
C
      ANGSUM=ANGSUM+ANG
      ANGBSUM=ANGBSUM+ANGB
C
      TYPE *,'TP,PA=',ANGSUM
      TYPE *,'TP,Pb=',ANGBSUM
      CALL OUTRAM
      GO TO 100
C
```

```
      END

C
C     SUB TO SCALE THE DATA IN THE YDIRECTION
C
      SUBROUTINE YSCALE
      COMMON /NMRDAT/DNMR(20000),ISIZE,YSC
      INTEGER*2 IPLANE,OUT(2,2000)
      DIMENSION DD(20000)
      INTEGER*2 IV(1024),IOUT
      DIMENSION PK(20000),PKI(20000)
C
      RMIN=1000000.
      RMAX=-1000000.
      DO I=1,ISIZE
      RMIN=MIN(RMIN,DNMR(I))
      RMAX=MAX(RMAX,DNMR(I))
      ENDDO
C
      TYPE *,'USE THE BITPAD TO SCALE THE Y AXIS'
      TYPE *,'SCALE = 1, FAR LEFT     SCALE = 50, FAR RIGHT'
      TYPE *,'HIT BOX LABELED 3 TO EXIT'
 100  CONTINUE
C
      NOUT=1
      IPLANE="2000
      CALL BPOINTR(IPLANE,OUT,NOUT,ICODE)      !READ FROM BITPAD
      TYPE *,'OUT(1,1)',OUT(1,1),OUT(2,1)
      IF(ICODE.EQ.3)RETURN
C
C
      YSC=OUT(1,1)/10.
C
      CALL OUTRAM
C
      GO TO 100
C
      END



      SUBROUTINE FOURIER3
C     ROUTINE USED IN 2DFT ... THIS ROUTINE DOES NOT ZERO EXTENT
C
C
      COMMON /NMRDAT/DNMR(20000),ISIZE,YSC
      DIMENSION PK(40000),PKI(40000)
C     TYPE *,'DNMR',(DNMR(I),I=1,30)
C
C     ZERO FILL
C
      DO I=1,ISIZE
      PK(I)=0.
```

```
        PKI(I)=0.
        ENDDO
C
C       LOAD FID
C
        DO I=1,ISIZE
        PK(I)=DNMR(I)
        PKI(I)=DNMR(I+(ISIZE))
C       TYPE *,'PK,PKI',PK(I),PKI(I)
        ENDDO
C       CALL OUTRAM
C       READ(5,*)III
C       DO I=1,ISIZE
C       DNMR(I)=PKI(I)
C       ENDDO
C       CALL OUTRAM
C       READ(5,*)III
C       ISIZE=ISIZE*2
C
        ie=-1
C       TYPE *,'ISIZE INFFT',ISIZE
        N=ISIZE
        RN=N+1
        nu=alog(rn)/alog(2.)
C       TYPE *,'N',N,NU,IE
        call FFT(PK,PKI,N,NU,IE)
C
c       prepare fft output
c
        do i=1,N/2
        PK(i+n)=PK(i)
        PKI(i+n)=PKI(i)
        enddo
C
        do i=1,n
        PK(i)=PK(n/2+i)
        PKI(i)=PKI(n/2+i)
        enddo

        DO I=1,N
        DNMR(I)=PK(N-I+1)
        DNMR(I+ISIZE)=PKI(N-I+1)
        ENDDO
C
        ISIZE=ISIZE*2
        CALL OUTRAM
        ISIZE=ISIZE/2
        RETURN
        END

        SUBROUTINE FFT(PK,PKI,N,NU,IE)
        DIMENSION PK(40000),PKI(40000)
C  A REAL ARRAY AND AN IMAGINARY ARRAY EACH OF DIMENSION N ARE INPUTS TO THIS
```

```
C  ROUTINE. NU IS THE POWER TO WHICH 2 IS RAISED TO GIVE N,I.E. N=2**NU
C  WHEN IE=+1, THE INVERSE TRANSFORM (E**+I) IS CALCULATED.
C  WHEN IE=-1, THE FORWARD TRANSFORM (E**-I) IS CALCULATED.
C  INITIALIZATION
       N2=N/2
       NU1=NU-1
       K=0
       DO 100 L=1,NU
 102   DO 101 I=1,N2
       P=IBITR(K/2**NU1,NU)
C  THE FUNCTION IBITR EFFECTS A BIT REVERSAL, E.G.,1011 REVERSED IS 1101
       ARG=6.283185*P/FLOAT(N)
C  THIS IS THE MAIN TWIDDLE PHASE SHIFT
       C=COS(ARG)
       S=SIN(ARG)
       IF (IE.GT.0) S=-S
       K1=K+1
       K1N2=K1+N2
       TPK=PK(K1N2)*C+PKI(K1N2)*S
       TPKI=PKI(K1N2)*C-PK(K1N2)*S
       PK(K1N2)=PK(K1)-TPK
       PKI(K1N2)=PKI(K1)-TPKI
       PK(K1)=PK(K1)+TPK
       PKI(K1)=PKI(K1)+TPKI
 101   K=K+1
       K=K+N2
       IF (K.LT.N) GO TO 102
       K=0
       NU1=NU1-1
 100   N2=N2/2
       DO 103 K=1,N
       I=IBITR(K-1,NU)+1
       IF (I.LE.K) GO TO 103
       TPK=PK(K)
       TPKI=PKI(K)
       PK(K)=PK(I)
       PKI(K)=PKI(I)
       PK(I)=TPK
       PKI(I)=TPKI
 103   CONTINUE
       IF (IE.LT.0) GO TO 104
       DO 105 K=1,N
       PK(K)=PK(K)/N
       PKI(K)=PKI(K)/N
 105   CONTINUE
 104   CONTINUE
       RETURN
       END
       FUNCTION IBITR(J,NU)
       J1=J
       IBITR=0
       DO 200 I=1,NU
       J2=J1/2
```

```
        IBITR=IBITR*2+(J1-2*J2)
 200    J1=J2
        RETURN
        END
C
C       SUB TO ZOOM IN ON PART OF THE DISPLAYED DATA
C
        SUBROUTINE ZOOM
C
        COMMON /NMRDAT/DNMR(20000),ISIZE,YSC
        COMMON /PPMNMR/PNMR(20000)
        COMMON /XFACTOR/IFACT
        COMMON /OFFSET/LEDGE,DSAV(20000),PSAV(20000),ISIZE2
        DIMENSION PK(20000),PKI(20000)
        INTEGER*2 IPLANE,OUT(2,2000)
        CHARACTER*2 OP
C
C
C       SAVE THE DATA
C
        TYPE *,'TYPE 1 IF YOU WANT TO SAVE SPECTRA BEFORE ZOOM'
        TYPE *,'TYPE 2 TO UNSAVE'
        READ(5,*)ISAV
        IF(ISAV.EQ.1)THEN
        DO I=1,ISIZE*2
        DSAV(I)=DNMR(I)
        PSAV(I)=PNMR(I)
        ENDDO
        ISIZE2=ISIZE
        ENDIF
C
        IF(ISAV.EQ.2)THEN
        DO I=1,ISIZE2
        DNMR(I)=DSAV(I)
        PNMR(I)=PSAV(I)
        ENDDO
        ISIZE=ISIZE2
        CALL OUTRAM
        ENDIF
C
        type *,'type 1 for ppm selection, type 2 for bitpad selection'
        read(5,*)icho
        if(icho.eq.1)then
          type *,'Enter the ppm boundaries'
          read(5,*)ppml,ppmr
          do i=1,isize
c         type *,'pnmr',pnmr(i)
          if(pnmr(i).ge.ppml)ledge=i
          if(pnmr(I).ge.ppmr)iredge=i
          enddo
        type *,'ledge, iredge',ledge,iredge
        else
```

```
        TYPE *,'USE THE BIT PAD TO SELECT REGION OF INTEREST'
        TYPE *,'ALONG THE X AXIS'
        NOUT=1
        IPLANE="2000
C
 100    CONTINUE
C
        TYPE *,'CHOOSE THE LEFT EDGE'
        CALL BPOINTR(IPLANE,OUT,NOUT,ICODE)     !READ FROM BITPAD
C       TYPE *,'OUT(1,1)',OUT(1,1),OUT(2,1)
        CALL DELAY(80,IERR)
C
        RSCA=IFACT
        LEDGE=OUT(1,1)*RSCA
        TYPE *,'CHOOSE THE RIGHT EDGE'
        CALL BPOINTR(IPLANE,OUT,NOUT,ICODE)     !READ FROM BITPAD
        CALL DELAY(60,IERR)
C       TYPE *,'OUT(1,1)',OUT(1,1),OUT(2,1)
C
        IREDGE=OUT(1,1)*RSCA
        TYPE *,'L R',LEDGE,IREDGE,RSCA
        endif
C
C       SAVE THE DATA
C
        DO I=1,ISIZE*2
        PK(I)=DNMR(I)
        PKI(I)=PNMR(I)
        ENDDO
        IDIM=ISIZE
        ISIZE=IREDGE-LEDGE+1
        TYPE *,'ISIZE',ISIZE
        IST=1
        DO I=LEDGE,IREDGE
        DNMR(IST)=PK(I)                 !REAL
        PNMR(IST)=PNMR(I)
        DNMR(IST+ISIZE)= PK(I+IDIM)     !IMAGINARY
C       TYPE *,'DNMR',DNMR(IST),IST
        IST=IST+1
        ENDDO
C
        TYPE *,'ISIZE IN ZOOM',ISIZE,YSC
        CALL OUTRAM
C
C       ISIZE=IDIM
C       DO I=1,ISIZE*2
C       DNMR(I)=PK(I)
C       ENDDO
C
        END

C
C       SUB FOR APODIZATION OF FID
```

```
C
      SUBROUTINE APOD
C
      COMMON /NMRDAT/DNMR(20000),ISIZE,YSC
      COMMON /APOD/LB
C
      TC=-LB
C
      IDIM=ISIZE
      DO I=1,IDIM
      RIN=(I-1)*TC/(IDIM)
      DNMR(I)=DNMR(I) * EXP(RIN)                !REAL PART
      DNMR(I+IDIM)=DNMR(I+IDIM) * EXP(RIN)      !IMAG PART
      ENDDO
C
      CALL OUTRAM
C
      RETURN
      END
C
C     SUB TO PHASE CORRECT THE SPECTRUM
C
      SUBROUTINE autophase
C
      COMMON /NMRDAT/DNMR(20000),ISIZE,YSC
      DIMENSION PK(20000),PKI(20000)
      INTEGER*2 IPLANE,OUT(2,2000)
      common /phase/angsum,angbsum
      CHARACTER*2 OP
C

C
      DO I=1,ISIZE
      PK(I)=DNMR(I)
      PKI(I)=DNMR(I+ISIZE)
      ENDDO

C
      ANG=angsum
      ANGBINC=ANGBsum/ISIZE
C
      DO I=1,ISIZE
      ADDANG=ANGBINC*I
      ANG1=ANG+ADDANG
      DNMR(I)=PK(I)*COSD(ANG1) - PKI(I)*SIND(ANG1)
      DNMR(I+ISIZE)=PKI(I)*COSD(ANG1) + PK(I)*SIND(ANG1)
      ENDDO
C
C
C     TYPE *,'TP,PA=',ANGSUM
C     TYPE *,'TP,Pb=',ANGBSUM
      CALL OUTRAM
C
```

```
      return
      END
C
C     SUB FOR APODIZATION OF FID
C
      SUBROUTINE POWER
C
      COMMON /NMRDAT/DNMR(20000),ISIZE,YSC
      COMMON /APOD/LB
C
      TC=-LB
C
      DO I=1,ISIZE
      DNMR(I)=(DNMR(I)**2  + DNMR(I+ISIZE)**2)**.5
      ENDDO
C
c     CALL OUTRAM
C
      RETURN
      END
C
C     SUBROUTINE TO CHANGE ARTIFACT IN RAW DATA
C
C
      SUBROUTINE CH16
C
      COMMON /NMRDAT/DNMR(20000),ISIZE,YSC
      COMMON /APOD/LB
C
      DO I=1,ISIZE*2
      IF(DNMR(I).EQ.-16.)DNMR(I)=0.
      ENDDO
C
c     CALL OUTRAM
C
      RETURN
      END
C
C     SUB FOR BASE LINE CORRECTION
C
      SUBROUTINE BAS
C
      COMMON /NMRDAT/DNMR(20000),ISIZE,YSC
C
C     DEFINE THE AREA TO AVERAGE
C
      I1=ISIZE- (ISIZE/4)
      I2=ISIZE*2- (ISIZE/4)
C
C     FIND THE BASE LINE OFFSET FOR THE REAL PART
C
      ISUM=0
      DO I=I1,ISIZE
```

```
      ISUM=ISUM+DNMR(I)
      ENDDO
C
      ADIV=(ISIZE)-I1 +1
      AVER=ISUM/ADIV
      TYPE *,'ADIV',ADIV,AVER,I1,I2
C
C     MAKE THE CORRECTION
C
      DO I=1,ISIZE
      DNMR(I)=DNMR(I)-AVER
      ENDDO
C
C     FIND THE OFFSET OF THE IMAGINARY PART OF THE FID
C
      IST=ISIZE  +1
C
      ISUM=0
      DO I=I2,ISIZE
      ISUM=ISUM+DNMR(I)
      ENDDO
C
      ADIV=(ISIZE*2)-I2 +1
      AVER=ISUM/ADIV
C
      DO I=IST,ISIZE*2
      DNMR(I)=DNMR(I)+AVER
      ENDDO
C
C
C
C
      CALL OUTRAM
C
      RETURN
      END
C
      SUBROUTINE MID
C
      COMMON /NMRDAT/DNMR(20000),ISIZE,YSC
C
      IS1=ISIZE/2
      ISS=2
C     AVER=(DNMR(IS1+ISS)+DNMR(IS1-ISS))/2.
      RA=(DNMR(IS1+ISS) - DNMR(IS1-ISS))/4.
      DO I=1,3
      II=I+IS1-ISS
      DNMR(II)=DNMR(IS1-ISS) + (RA*I)
      ENDDO
C
      IS1=ISIZE * 1.5
      RA=(DNMR(IS1+ISS) - DNMR(IS1-ISS))/4.
      DO I=1,3
```

```
        II=I+IS1-ISS
        DNMR(II)=DNMR(IS1-ISS) + (RA*I)
        ENDDO
C       AVER=(DNMR(IS1+ISS)+DNMR(IS1-ISS))/2.
C       DNMR(IS1)=AVER
C
        RETURN
        END
C
C       TRANSPOSE.FOR
C       ROUTINE TO TAKE THE 2D MATRIX AND TRANSPOSE IT
C       AND FT IN THE SECOND DIMENSION
C
        SUBROUTINE TRANSPOSE(IIPROJ)
        INTEGER*2 IH(256)
C
C       IIPROJ- IS THE SECOND DIMENSION
C
        COMMON /NMRDAT/DNMR(20000),ISIZE,YSC
        COMMON /NMRDAT2/DNMR2(1024,512)
        DIMENSION DINS(512,512)
        CHARACTER*1 ANS
C
C
C
        TYPE *,'ENTER THE STARTING AND ENDING POINTS TO TRANSPOSE:'
        READ(5,*)NSTR,NEND
C
C       REALS
C
        DO J=1,IIPROJ
          DO I=NSTR,NEND
          II=I-NSTR+1
          DINS(J,II)=DNMR2(I,J)
          ENDDO
        TYPE *,'DINS',DINS(J,50),J
        ENDDO
C
C       IMAGINARY
C
        DO J=1,IIPROJ
          DO I=NSTR,NEND
          II=I-NSTR+1
          DINS(J+IIPROJ,II)=DNMR2(I+ISIZE,J)
          ENDDO
        TYPE *,'DINS',DINS(J+IIPROJ,50),J+IIPROJ
        ENDDO
C
        NTOT=NEND-NSTR+1
C
C       PUT BACK INTO DNMR2 FOR MAIN PROGRAM
C
        DO J=1,NTOT
```

```
          DO I=1,IIPROJ*2
          DNMR2(I,J)=DINS(I,J)
          ENDDO
        ENDDO
C
        ISIZE=IIPROJ
C
        TYPE *,'DO YOU WANT TO STOP AFTER TRANSPOSE'
        READ(5,60)ANS
 60     FORMAT(A)
        RETCODE=STR$UPCASE(ANS,ANS)
        IF(ANS.EQ.'Y')THEN
        RETURN
        ENDIF
C
C       FOURIER TRANSFORM
C
C
        DO J=1,NTOT
        DO JJ=1,ISIZE*2
        DNMR(JJ)=0.
        ENDDO
          DO I=1,ISIZE
          DNMR(I)=DINS(I,J)                !REAL
          DNMR(I+ISIZE)=DINS(I+IIPROJ,J)         !IMAGINARY
          ENDDO
C

        if(j.eq.20)CALL OUTRAM
C       READ(5,*)IW
        CALL FOURIER3
C       READ(5,*)IW
C       CALL POWER
C
C       TRANSPOSE AGAIN
C
        DO I=1,ISIZE
        DNMR2(J,I)=DNMR(I)
        DNMR2(J+NTOT,I)=DNMR(I+ISIZE)
C       DNMR2(J,I)=(DNMR2(J,I)**2 +DNMR2(J+NTOT,I)**2)**.5
        ENDDO
C
        ENDDO
        ISIZE=NTOT
        WRITE(11)IH
        DO I=1,128
        WRITE(11)(DNMR2(II,I),II=1,ISIZE)
        ENDDO
C
        RETURN
        END
C
C       SUB TO OUTPUT A PLOT FILE
```

```
C         FOR THE VERSATEK
C
          SUBROUTINE PLOTNMR
C
          COMMON /NMRDAT/DNMR(20000),ISIZE,YSC
          COMMON /PPMNMR/PNMR(20000)
C

          OPEN(UNIT=1,NAME='PLOTNMR.DAT',TYPE='NEW',FORM='FORMATTED')
C
          DO I=1,ISIZE
          WRITE(1,*)PNMR(I),DNMR(I)
          ENDDO
C
          CLOSE(UNIT=1)
          RETURN
          END
C
C         ROUTINE TO CALCULATE PPM SCALE FOR X AXIS
C
          SUBROUTINE PPM
C
          COMMON /NMRDAT/DNMR(20000),ISIZE,YSC
          COMMON /PPMNMR/PNMR(20000)
          COMMON /PASSPM/ISZBEG
          COMMON /OFFSET/LEDGE,DSAV(20000),PSAV(20000),ISIZE2
          common /passppm/rinfo(10)
C
 5        TYPE *,'ENTER X1 AND CHEM. SHIFT'
          READ(5,*,ERR=5)X1,CY1
C         x1=32
C         cy1=0.
c         TYPE *,'ENTER X2 AND CHEM. SHIFT'
c         READ(5,*)X2,CY2
C
C         CALCULATE PPM PARAMETERS
C
C         B=(CY2-CY1)/(X2-X1)
          ppmfac=1./rinfo(5)      !to convert from hertz to ppm
          fac1=rinfo(2)/(ISZBEG)  !to convert from pixel to hertz
          B=PPMFAC*FAC1
          type *,'fac1,ppm',fac1,ppmfac
          A=CY1+(B*X1)
C
C         USE THE PARAMETERS TO GET TO PPM
C
          DO I=1,ISIZE2
          PSAV(I)=A-(B*I)
          ENDDO
C
          RETURN
          END
```

```
C
C       PRESPEC.FOR
C       ROUTINE TO TAKE THE 2D MATRIX AND PREPARE THE SPECTRA
C       FOR PLOTTING
C
        SUBROUTINE PRESPEC(IIPROJ)
        INTEGER*2 IH(256)
C
C       IIPROJ- IS THE SECOND DIMENSION
C
        COMMON /NMRDAT/DNMR(20000),ISIZE,YSC
        COMMON /NMRDAT2/DNMR2(1024,512)
        COMMON /PPMNMR/PNMR(20000)
        common /phase/angsum,angbsum
        DIMENSION DINS(512,512),IPHASVEC(9),PH2(9,2)
        CHARACTER*1 ANS
        CHARACTER*40 CFN
        DATA IPHASVEC/1,10,12,14,16,18,20,28,32/
C
C
C
        TYPE *,'PHASE CORRECT THE FOLLOWING SPECTRA'
C
C
C       FIND THE PHASE CORRECTED PARAMETERS FOR THE 5 SPECTRA
C
        ANGBSUM=0.
        DO JJ=1,9
        TYPE *,'ROW',IPHASVEC(JJ)
          DO I=1,ISIZE*2
          DNMR(I)=DNMR2(I,IPHASVEC(JJ))
          ENDDO
        CALL OUTRAM
        CALL AUTOPHASE
        CALL PHASEC
        PH2(JJ,1)=ANGSUM
        PH2(JJ,2)=ANGBSUM
        TYPE *,'ANGSUM,',ANGSUM,ANGBSUM
        ENDDO
C
C       PHASE CORRECT ALL THE SPECTRA BY LINEAR INTERPOLATION
C
C
        DO I=1,ISIZE*2
        DNMR(I)=DNMR2(I,1)
        ENDDO
        ANGSUM=PH2(1,1)
        ANGBSUM=PH2(1,2)
C
        CALL AUTOPHASE
C
        CALL PPM2                !FIND THE PPM SCALE
        DO I=1,ISIZE
```

```
        DINS(I,1)=PNMR(I)
        ENDDO
        DO I=1,ISIZE*2
        DNMR2(I,1)=DNMR(I)
        ENDDO
C
        II=2
        DO JJ=1,8
        IDIV= (IPHASVEC(JJ+1)-IPHASVEC(JJ))
        AIN1=(PH2(JJ+1,1)-PH2(JJ,1)) / IDIV
        AIN2=(PH2(JJ+1,2)-PH2(JJ,2)) / IDIV
C
          DO I=1,IDIV
          ANGSUM=(AIN1*(I)) + PH2(JJ,1)
          ANGBSUM=(AIN2*(I)) +PH2(JJ,2)
        TYPE *,'ANGSUM 2,',ANGSUM,ANGBSUM
          DO IJ=1,ISIZE*2
          DNMR(IJ)=DNMR2(IJ,II)
          ENDDO
C
          CALL AUTOPHASE
C
        CALL PPM2                !FIND THE PPM SCALE
        DO IJ=1,ISIZE
        DINS(IJ,II)=PNMR(IJ)
        ENDDO
          DO IJ=1,ISIZE*2
          DNMR2(IJ,II)=DNMR(IJ)
          ENDDO
          II=II+1
          ENDDO
        ENDDO
C
C       OUTPUT TO DISK
C
        TYPE *,'OUTPUT FILE NAME'
        READ(5,111)CFN
 111    FORMAT(A)
        OPEN(UNIT=11,NAME=CFN,TYPE='NEW',FORM='UNFORMATTED')
        WRITE(11)IH
        DO I=1,32
c
c       to output file for ramtek or 3-d plotting comment out the next two
c       write statements
c
c       WRITE(11)ISIZE
c       WRITE(11)(DINS(II,I),II=1,ISIZE)
        WRITE(11)(DNMR2(II,I),II=1,ISIZE)
        ENDDO
        CLOSE(UNIT=11)
C
C
        RETURN
```

```
      END
C
C     SUB FOR APODIZATION OF FID
C
      SUBROUTINE PPM2
C
      COMMON /NMRDAT/DNMR(20000),ISIZE,YSC
      COMMON /PPMNMR/PNMR(20000)
      COMMON /PASSPM/ISZBEG

      common /passppm/rinfo(10)
C
C     TYPE *,'ENTER X1 AND CHEM. SHIFT'
C     READ(5,*)X1,CY1
      RMAX =0.
      DO I=1,ISIZE
      RMAX=MAX(RMAX,DNMR(I))
      IF(RMAX.EQ.DNMR(I))IMAR=I
      ENDDO
      X1=IMAR
      CY1=4.68
C
C     x1=32
C     cy1=0.
c     TYPE *,'ENTER X2 AND CHEM. SHIFT'
c     READ(5,*)X2,CY2
C
C     CALCULATE PPM PARAMETERS
C
C     B=(CY2-CY1)/(X2-X1)
      ppmfac=1./rinfo(5)      !to convert from hertz to ppm
      fac1=rinfo(2)/(ISZBEG)  !to convert from pixel to hertz
      B=PPMFAC*FAC1
      type *,'fac1,ppm',fac1,ppmfac
      A=CY1+(B*X1)
C
C     USE THE PARAMETERS TO GET TO PPM
C
      DO I=1,ISIZE
      PNMR(I)=A-(B*I)
      ENDDO
C
      RETURN
      END
```

```
C
C       PROGRAM TO TAKE THE NMR FID AND PROCESS IN A MANNER VERY SIMILAR
C       TO NICOLET NTCFT PROGRAM, IE, FOURIER TRANSFORM, APODIZATION,
C       PHASE CORRECTION,
C       ADDITIONAL ROUTINES WERE ADDED TO FIND THE AREA UNDER THE PEAKS
C       WHOSE PPMS WERE LISTED IN FILE PPM.IN.
C
C       THE FOLLOWING ROUTINES ARE USED IN THIS PACKAGE:
C  NTCFT2,OUTRAM,NTCFTV.BD1/OPT,PHASEC,YSCALE,FFT,-
C  ZOOM,APOD,AUTOPHASE,POWER,OUTPK,VIVSP2,-
C  FINDP,CH16,BAS,SMOOTH,FOURIER3,PLOTNMR,READSP,GETAREA,-
C  PPM,headex,reverse,subsp,save,ZOOM2,VIVSP,GETAREA2,-
C  [TODD.NMR]READOUT,UNPACK,CHHEAD,CHDATA2,CONVRT,INTCON,TEXTCON,-
C  DRC:[RAM]initrm,RMCROS,bell,upper,CLRPLN,TTIO,NEWPl,DASH,CIRCl,crvfit,-
C  DISPLAY/LIB,-
C  DRC:[SAM.SUBS]MARK,VTSUBS/LIB,-
C  'fip'

C
        PROGRAM NTCFTV
        INTEGER*2 IOUTDAT(256)
        COMMON /NMRDAT/DNMR(20000),ISIZE,YSC
        COMMON /PPMNMR/PNMR(20000)
        COMMON /APOD/LB
        COMMON /OPTION/OPT
        character*1 ans
        DIMENSION PK(20000),PKI(20000),FT(512)
        CHARACTER*2 OPT
        CHARACTER*40 CFN
        type *,'Do you want to use ramtek?'
        read(5,3)ans
 3      format(a)
        retcode=str$upcase(ans,ans)
        if(ans.eq.'Y')then
        CALL INITRM             !INITIALIZE RAMTEK
        CALL INITBP             !INITIALIZE BITPAD
        endif
C
C       DEFAULT VALUES
        LB=10
        pinc=3
C
 30     TYPE *,'OPTIONS;'
        TYPE *,'GA = GET NMR DATA FROM DISK     EM = EXPONENTIAL APOD'
        TYPE *,'GC = GET NMR DATA FROM .DAT FILE ON DISK'
        TYPE *,'GX = GET ASCII NMR DATA FROM DISK'
        TYPE *,'ZO = ZOOM IN ON PART OF THE DATA'
        TYPE *,'FT = FOURIER TRANSFORM          PH = PHASE CORRECTION'
        type *,'PC = AUTO PHASE                 AU = LINK COMMANDS'
        TYPE *,'SC = SCALE IN Y                 MO = EXIT'
c       FS = SYMMETRIC FID FILL BEFORE FT
C       MC= CALCULATE THE POWER SPECTRUM
C       bu=butterworth filter
```

```
c       ha= han filter
c       f3= fourier transform without zero
C       LV= LIST INTENSITY VALUES BETWEEN MARKS
C       LB = LINE BROADENING
C       CA = CHANGE ARTIFACT OF -16. ON FID
C       BC = BASE LINE CORRECTION
C       MA = MIDDLE POINT AVERAGE
C       SM = SMOOTHING 2 POINT
C       G1 = LOAD IN TOTAL DAT FILE
C       DS = DISPLAY NEW SIZE
C       EX = EXTRACT POINT FOR 3D FT
C       G2 = LOAD IN A GIVEN BLOCK OF DAT FILE FOR PROCESSING
C       TA = TRANSPOSE AND FT
C       11 = OUTPUT TO UNIT 11 FOR RAMTEK
C       PL = PREPARE FILE FOR PLOTTING
c       TS = test 2dft  with 3 sines
C       PM= RESCALE FOR PPM
c       sr = spectral reverse
c       sa= save spectra
c       as = subtract two spectra
C       GR = READ FORMATTED FILE
C       AG = GET AREA
C       OP = OUTPUT PEAK AREAS
C       A2 = EXECUTE LINK 2
c


c
        READ(5,10)OPT
 10     FORMAT(A)
        RETCODE = STR$UPCASE(OPT,OPT)
C
        IF(OPT.EQ.'DS')THEN
        TYPE *,'ENTER SIZE:'
        READ(5,*)ISIZE
        CALL OUTRAM
        ENDIF
C
        IF(OPT.EQ.'GA'.OR.OPT.EQ.'GC')THEN
          CALL READOUT
        type *,'isize in ntc',isize
          CALL OUTRAM
          ISIZE=ISIZE/2
        ENDIF
C
        IF(OPT.EQ.'AU')THEN
 5      TYPE *,'ENTER PPM FILE NAME'
        READ(5,199)CFN
 199    FORMAT(A)
        OPEN(UNIT=13,NAME=CFN,TYPE='OLD',FORM='FORMATTED',ERR=5)
        READ(13,*)NPEAKS
        DO I=1,NPEAKS
        CALL ZOOM2
        CALL GETAREA
```

```
        ENDDO
C
        CALL OUTPK
        ENDIF
C
C
        IF(OPT.EQ.'A2')CALL VIVSP
C
        IF(OPT.EQ.'A3')CALL VIVSP2
C
        IF(OPT.EQ.'GR')CALL READSP
C
        IF(OPT.EQ.'PL')CALL PLOTNMR
C
        IF(OPT.EQ.'11')WRITE(11)(DNMR(I),I=1,ISIZE)
C
        IF(OPT.EQ.'PM')CALL PPM
C
C       OPTION FOR ASCII DATA FILES
C
        IF(OPT.EQ.'LB')THEN
        TYPE *,'LB='',LB
        READ(5,*)LB
        ENDIF
C
        IF(OPT.EQ.'EM')CALL APOD
C
        IF(OPT.EQ.'LV')CALL FINDP
C

C
        IF(OPT.EQ.'BC')CALL BAS
C
        IF(OPT.EQ.'SM')THEN
          CALL SMOOTH
          CALL OUTRAM
        ENDIF
c
c
C
        IF(OPT.EQ.'MC')CALL POWER
C
        IF(OPT.EQ.'ZO')CALL ZOOM
C
        IF(OPT.EQ.'PC')CALL AUTOPHASE
C
C
c
        if(opt.eq.'F3')call fourier3
C
C
        IF(OPT.EQ.'PH')CALL PHASEC
C
```

```
      IF(OPT.EQ.'SC')CALL YSCALE
C
      if(opt.eq.'SR')call reverse
C
      if(opt.eq.'SA')call save
C
      if(opt.eq.'AS')call subsp
C
      IF(OPT.EQ.'AG')CALL GETAREA
C
      IF(OPT.EQ.'OP')CALL OUTPK

C
      IF(OPT.EQ.'MO')STOP
C
C
      GO TO 30
      END

C
C     ROUTINE TO OUTPUT PEAK AREAS TO DISK
C
      SUBROUTINE OUTPK
      CHARACTER*40 CFN
C
      COMMON /PEAKS/PEAK(500,2),IPE

 5    TYPE *,'ENTER FILE NAME'
      READ(5,10)CFN
 10   FORMAT(A)
      OPEN(UNIT=12,NAME=CFN,TYPE='NEW',FORM='FORMATTED',ERR=5)
      TYPE *,'IPE',IPE
      TYPE *,'PEAK',PEAK(1,1),PEAK(1,2)
      DO I=1,IPE
      TYPE *,'PEAK',PEAK(I,1),PEAK(I,2)
      WRITE(12,*)PEAK(I,1),PEAK(I,2)
      ENDDO
C
      CLOSE(UNIT=12)
      RETURN
      END

C
C     SUB TO ZOOM IN ON PART OF THE DISPLAYED DATA
C     AND LIST THE INTENSITY VALUES AND FIND THE PEAKS
C
      SUBROUTINE FINDP
C
      COMMON /NMRDAT/DNMR(20000),ISIZE,YSC
      COMMON /PPMNMR/PNMR(20000)
      COMMON /XFACTOR/IFACT
      COMMON /OFFSET/LLEDGE,DSAV(20000),PSAV(20000),ISIZE2
      COMMON /SPARAM/RMIN,SCALE,IOFFSET
```

```
      DIMENSION PK(20000),PKI(20000),PEAKS(100,2)
      INTEGER*2 IPLANE,OUT(2,2000),IM,JM
      CHARACTER*2 OP
      CHARACTER*1 ANS
      CHARACTER*40 CFN
C
C
      RSCA=IFACT
      TYPE *,'USE THE BIT PAD TO SELECT REGION OF INTEREST'
      TYPE *,'ALONG THE X AXIS'
      NOUT=1
      IPLANE="2000
C
  100 CONTINUE
C
      TYPE *,'CHOOSE THE LEFT EDGE'
      CALL BPOINTR(IPLANE,OUT,NOUT,ICODE)     !READ FROM BITPAD
C     TYPE *,'OUT(1,1)',OUT(1,1),OUT(2,1)
      CALL DELAY(80,IERR)
C
      LEDGE=OUT(1,1)*RSCA
      TYPE *,'CHOOSE THE RIGHT EDGE'
      CALL BPOINTR(IPLANE,OUT,NOUT,ICODE)     !READ FROM BITPAD
      CALL DELAY(60,IERR)
C     TYPE *,'OUT(1,1)',OUT(1,1),OUT(2,1)
C
      IREDGE=OUT(1,1)*RSCA
C     TYPE *,'L R',LEDGE,IREDGE,RSCA
C
C     SAVE THE DATA
C
      TYPE *,'TYPE 1 TO PRINT OUT VALUES'
      READ(5,*)IPR
      TYPE *,'ENTER THE THRESHOLD'
      READ(5,*)ITH
      TYPE *,'PARAM',RMIN,SCALE,IOFFSET
      IDIFF=IREDGE-LEDGE
      IPX=1
      DO I=LEDGE,IREDGE
      IF(IPR.EQ.1)TYPE *,'X, Y=',I+LLEDGE-1,PNMR(I),DNMR(I)
      IF(DNMR(I).LT.DNMR(I+1).AND.DNMR(I+1).lt.DNMR(I+2))THEN
      if(dnmr(i+2).gt.dnmr(i+3).and.dnmr(I+3).gt.dnmr(i+4))then
      it=i+2
      IDD=(DNMR(it)-DNMR(It-1)) + (DNMR(it)-DNMR(it+1))
      IF(IDD.GT.ITH)THEN
        TYPE *,'PEAKS=',it+LLEDGE-1,PNMR(it),DNMR(it)
        PEAKS(IPX,1)=PNMR(it)
        PEAKS(IPX,2)=DNMR(it)
        IPX=IPX+1
        IM=I/IFACT
        S1=(DNMR(it)-RMIN)/SCALE
        S2=S1+IOFFSET
        JM=512 - NINT(S2)
```

```
          CALL WCS(0,IM,JM,.TRUE.,.FALSE.,IERR)
          CALL DELAY(60,IERR)
        ENDIF
        endif
        ENDIF
        ENDDO
C
        TYPE *,'DO YOU WANT TO OUTPUT PEAKS TO DISK'
        READ(5,101)ANS
 101    FORMAT(A)
        RETCODE=STR$UPCASE(ANS,ANS)
        IF(ANS.EQ.'Y')THEN
        TYPE *,'ENTER FILE NAME'
        READ(5,101)CFN
        OPEN(UNIT=1,NAME=CFN,TYPE='NEW',FORM='FORMATTED')
        WRITE(1,*)IPX-1
        DO I=1,IPX-1
        WRITE(1,*)PEAKS(I,1),PEAKS(I,2)
        ENDDO
        ENDIF
C
        RETURN
        END

C
C       ROUTINE TO READ IN TO MEMORY A FILE PREVIOUSLY
C       CREATED BY ROUTINE PLOTNMR
C
        SUBROUTINE READSP
C
        COMMON /NMRDAT/DNMR(20000),ISIZE,YSC
        COMMON /PPMNMR/PNMR(20000)
        COMMON /APOD/LB
        CHARACTER*40 CFN
C
        TYPE *,'ENTER FILE NAME'
        READ(5,10)CFN
 10     FORMAT(A)
        OPEN(UNIT=11,NAME=CFN,TYPE='OLD',FORM='FORMATTED')
        DO I=1,8192
        READ(11,*,END=31)PNMR(I),DNMR(I)
        ENDDO
 31     ISIZE=I-1
C
        CALL OUTRAM
C
        RETURN
        END
C       ROUTINE WHICH OPERATES ON FILES CREATED BY ROUTINE PRESPEC
C       OF PROGRAM NTCFTV. THESE FILES CONTAIN THE PHASE ENCODED SPECTRA.
C       A SELECTED ROW FROM THIS FILE IS DISPLAY AND AREAS UNDER THE
C       PEAKS ARE DEFINED WITH THE BIT PAD
```

```
C
      SUBROUTINE VIVSP
C
      COMMON /NMRDAT/DNMR(20000),ISIZE,YSC
      COMMON /PPMNMR/PNMR(20000)
      CHARACTER*40 CFN
C
      OPEN(UNIT=13,NAME='VIV.IN',TYPE='OLD',FORM='FORMATTED')
      READ(13,*)NSPEC          !NUMBER OF SPECTRA
C
      DO I=1,NSPEC
      READ(13,111)CFN
      write(2,113)cfn
 113  format(1x,a)
 111  FORMAT(A)
      READ(13,*)IROW
      retcode=str$upcase(cfn,cfn)
      OPEN(UNIT=11,NAME=CFN,TYPE='OLD',FORM='UNFORMATTED')
      READ(11)IH
      TYPE *,'IROW=',IROW
        DO J=1,IROW-1
        READ(11)ISIZE
      TYPE *,'ISIZE',ISIZE
      IF(ISIZE.GT.150.AND.ISIZE.LT.250)READ(11)
        READ(11)
        ENDDO
      READ(11)ISIZE
      READ(11)(PNMR(II),II=1,ISIZE)
      READ(11)(DNMR(II),II=1,ISIZE)
      CLOSE(UNIT=11)
      CALL OUTRAM
C     CALL ZOOM
C
      CALL YSCALE
      READ(13,*)NPEAKS
      DO JI=1,NPEAKS           !EVALUATE FOUR PEAKS
C     CALL ZOOM2
      CALL GETAREA2
      ENDDO
C
      ENDDO
      CALL OUTPK
C
      RETURN
      END

C
C
C     ROUTINE TO FIND THE AREA UNDER THE PEAKS
C
      SUBROUTINE VIVSP2
C
      COMMON /NMRDAT/DNMR(20000),ISIZE,YSC
```

```
      COMMON /PPMNMR/PNMR(20000)
      CHARACTER*40 CFN
C
      OPEN(UNIT=13,NAME='VIV.IN',TYPE='OLD',FORM='FORMATTED')
C
C
      CALL YSCALE
      READ(13,*)NPEAKS
      DO JI=1,NPEAKS          !EVALUATE FOUR PEAKS
C     CALL ZOOM2
      CALL GETAREA2
      ENDDO
C
      CALL OUTPK
C
      RETURN
      END

C
C
      SUBROUTINE GETAREA
C
C     ROUTINE TO FIND THE AREA UNDER THE PEAK BY ALLOWING
C     THE USER TO DEFINE THE BASELINE WITH CURSOR CONTROL
C
      COMMON /NMRDAT/DNMR(20000),ISIZE,YSC
      COMMON /PPMNMR/PNMR(20000)
      COMMON /XFACTOR/IFACT
      COMMON /SPARAM/RMIN,SCALE,IOFFSET
      COMMON /PEAKS/PEAK(500,2),IPE
      DIMENSION PK(20000),PKI(20000),PEAKS(100,2)
      INTEGER*2 IPLANE,IM,JM,IV(4),IOUT
      CHARACTER*2 OP
      CHARACTER*1 ANS
      CHARACTER*40 CFN
C
C
      TYPE *,'ENTER THE X INCREMENT'
C
      READ(5,*)IXS
      I=ISIZE/2
C
 99     IM=I/IFACT
        S1=(DNMR(I)-RMIN)/SCALE
        S2=S1+IOFFSET
        JM=512 - NINT(S2)
        CALL WCS(0,IM,JM,.TRUE.,.FALSE.,IERR)          !MOVE THE CURSOR
      TYPE *,'TYPE 1 TO MOVE X AMOUNT TO THE LEFT'
      TYPE *,'TYPE 2 TO MOVE X AMOUNT TO THE RIGHT'
      TYPE *,'TYPE 3 TO ENTER FIRST POINT'
      TYPE *,'TYPE 4 TO ENTER SECOND POINT'
      READ(5,*)II
      IF(II.EQ.3)GO TO 100
```

```
        IF(II.EQ.4)GO TO 200
        IF(II.EQ.1)I=I-IXS
        IF(II.EQ.2)I=I+IXS
        GO TO 99
C
 100    TYPE *,'POINT=',I,DNMR(I)
        IP1=I
        B1=DNMR(I)
        GO TO 99
C
 200    TYPE *,'POINT2 = ',I,DNMR(I)
        IP2=I
        B2=DNMR(I)
C
C       DRAW THE LINE FOR BASELINE SUBTRACTION
C
        IV(1)=IP1/IFACT
        IV(3)=IP2/IFACT
C
        D1=(B1-RMIN)/SCALE
        D1=D1+IOFFSET
        D1=512. - D1
        IV(2)=D1
C
        D2=(B2-RMIN)/SCALE
        D2=D2+IOFFSET
        D2=512. - D2
        IV(4)=D2
C
        CALL COP(IV(1),IV(2),IERR)
        IOUT=1
        CALL WV(IV(3),IOUT,IERR)
        im=256
        jm=256
          CALL WCS(0,IM,JM,.TRUE.,.FALSE.,IERR)

C
C       CALCULATE THE AREA
C
        IDIFF=IP2-IP1
        DINC=(B2-B1)/IDIFF
        RSUM=0.
        DO I=1,IDIFF-1
C       TYPE *,'DNMR',IP1+I,DNMR(IP1+I)
        RSUM=(DNMR(IP1+I)-(B1+DINC*I)) + RSUM
        ENDDO
C
        TYPE *,'RSUM=',RSUM
C
C       SAVE THE AREA AND PPM FOR PEAK
C
        RMAX=0.
        DO I=IP1,IP2
```

```
      RMAX=MAX(DNMR(I),RMAX)
      IF(DNMR(I).EQ.RMAX)IMAX=I
      ENDDO
C
      IPE=IPE+1
      PEAK(IPE,1)=PNMR(IMAX)
      PEAK(IPE,2)=RSUM
      TYPE *,'IPE',IPE
C
      RETURN
      END

C
C
C     SAME AS GETAREA EXCEPT THAT IT READS INPUT FROM
C     DISK FILE INSTEAD OF TERMINAL
C
      SUBROUTINE GETAREA2
C
      COMMON /NMRDAT/DNMR(20000),ISIZE,YSC
      COMMON /PPMNMR/PNMR(20000)
      COMMON /XFACTOR/IFACT
      COMMON /SPARAM/RMIN,SCALE,IOFFSET
      COMMON /PEAKS/PEAK(500,2),IPE
      DIMENSION PK(20000),PKI(20000),PEAKS(100,2)
      INTEGER*2 IPLANE,IM,JM,IV(4),IOUT
      CHARACTER*2 OP
      CHARACTER*1 ANS
      CHARACTER*40 CFN
C
C
      TYPE *,'ENTER THE X INCREMENT'
C
c     READ(5,*)IXS
      ixs=1
      READ(13,*)PP
      DO II=1,ISIZE
      IF(PNMR(II).GE.PP)I=II
C     TYPE *,PNMR(II),PP,II,I
      ENDDO
C     I=ISIZE/2
C
 99     IM=I/IFACT
      TYPE *,'IM',IM,I,IFACT
        S1=(DNMR(I)-RMIN)/SCALE
        S2=S1+IOFFSET
        JM=512 - NINT(S2)
        CALL WCS(0,IM,JM,.TRUE.,.FALSE.,IERR)
C       CALL DELAY(60,IERR)
      TYPE *,'TYPE 1 TO MOVE X AMOUNT TO THE LEFT'
      TYPE *,'TYPE 2 TO MOVE X AMOUNT TO THE RIGHT'
      TYPE *,'TYPE 3 TO ENTER FIRST POINT'
      TYPE *,'TYPE 4 TO ENTER SECOND POINT'
```

```
      READ(5,*)II
      IF(II.EQ.3)GO TO 100
      IF(II.EQ.4)GO TO 200
      IF(II.EQ.1)I=I-IXS
      IF(II.EQ.2)I=I+IXS
      IF(II.EQ.5)I=I-3
      IF(II.EQ.6)I=I+3
      IF(II.EQ.7)I=I-10
      IF(II.EQ.8)I=I+10
      GO TO 99
C
 100  TYPE *,'POINT=',I,DNMR(I)
      IP1=I
      B1=DNMR(I)
      GO TO 99
C
 200  TYPE *,'POINT2 = ',I,DNMR(I)
      IP2=I
      B2=DNMR(I)
C
C     DRAW THE LINE FOR BASELINE SUBTRACTION
C
      IV(1)=IP1/IFACT
      IV(3)=IP2/IFACT
C
      D1=(B1-RMIN)/SCALE
      D1=D1+IOFFSET
      D1=512. - D1
      IV(2)=D1
C
      D2=(B2-RMIN)/SCALE
      D2=D2+IOFFSET
      D2=512. - D2
      IV(4)=D2
C
      TYPE *,'IV,',IV
      CALL FGD("2000,IERR)
      CALL MSK("2000,IERR)
      CALL COP(IV(1),IV(2),IERR)
      IOUT=1
      CALL WV(IV(3),IOUT,IERR)
      im=256
      jm=256
        CALL WCS(0,IM,JM,.TRUE.,.FALSE.,IERR)

C
C     CALCULATE THE AREA
C
      IDIFF=IP2-IP1
      DINC=(B2-B1)/IDIFF
      RSUM=0.
      DO I=1,IDIFF-1
c     TYPE *,'DNMR',IP1+I,DNMR(IP1+I)
```

```
      RSUM=(DNMR(IP1+I)-(B1+DINC*I)) + RSUM
      ENDDO
C
      TYPE *,'RSUM=',RSUM
C
C     SAVE THE AREA AND PPM FOR PEAK
C
      RMAX=0.
      DO I=IP1,IP2
      RMAX=MAX(DNMR(I),RMAX)
      IF(DNMR(I).EQ.RMAX)IMAX=I
      ENDDO
C
      IPE=IPE+1
      PEAK(IPE,1)=PNMR(IMAX)
      PEAK(IPE,2)=RSUM
      write(2,*)peak(ipe,1),peak(ipe,2)
      TYPE *,'IPE',IPE
C
      RETURN
      END

C
C     SUB TO ZOOM IN ON PART OF THE DISPLAYED DATA
C     READ ANSWERS FROM DISK FILE
C

      SUBROUTINE ZOOM2
C
      COMMON /NMRDAT/DNMR(20000),ISIZE,YSC
      COMMON /PPMNMR/PNMR(20000)
      COMMON /XFACTOR/IFACT
      COMMON /OFFSET/LEDGE,DSAV(20000),PSAV(20000),ISIZE2
      DIMENSION PK(20000),PKI(20000)
      INTEGER*2 IPLANE,OUT(2,2000)
      CHARACTER*2 OP
C
C
C     SAVE THE DATA
C
      TYPE *,'TYPE 1 IF YOU WANT TO SAVE SPECTRA BEFORE ZOOM'
      TYPE *,'TYPE 2 TO UNSAVE'
C     READ(5,*)ISAV
      ISAV=2
      IF(ISAV.EQ.1)THEN
      DO I=1,ISIZE*2
      DSAV(I)=DNMR(I)
      PSAV(I)=PNMR(I)
      ENDDO
      ISIZE2=ISIZE
      ENDIF
C
      IF(ISAV.EQ.2)THEN
```

```
        DO I=1,ISIZE2
        DNMR(I)=DSAV(I)
        PNMR(I)=PSAV(I)
        ENDDO
        ISIZE=ISIZE2
        CALL OUTRAM
        ENDIF
C
        type *,'type 1 for ppm selection, type 2 for bitpad selection'
C       read(5,*)icho
        ICHO=1
        if(icho.eq.1)then
          type *,'Enter the ppm boundaries'
          READ(13,*)PPMC
          PPML=PPMC+.3
          PPMR=PPMC-.3
          do i=1,isize
c         type *,'pnmr',pnmr(i)
          if(pnmr(i).ge.ppml)ledge=i
          if(pnmr(I).ge.ppmr)iredge=i
          enddo
        type *,'ledge, iredge',ledge,iredge
        else

        TYPE *,'USE THE BIT PAD TO SELECT REGION OF INTEREST'
        TYPE *,'ALONG THE X AXIS'
        NOUT=1
        IPLANE="2000
C
 100    CONTINUE
C
        TYPE *,'CHOOSE THE LEFT EDGE'
        CALL BPOINTR(IPLANE,OUT,NOUT,ICODE)     !READ FROM BITPAD
C       TYPE *,'OUT(1,1)',OUT(1,1),OUT(2,1)
        CALL DELAY(80,IERR)
C
        RSCA=IFACT
        LEDGE=OUT(1,1)*RSCA
        TYPE *,'CHOOSE THE RIGHT EDGE'
        CALL BPOINTR(IPLANE,OUT,NOUT,ICODE)     !READ FROM BITPAD
        CALL DELAY(60,IERR)
C       TYPE *,'OUT(1,1)',OUT(1,1),OUT(2,1)
C
        IREDGE=OUT(1,1)*RSCA
        TYPE *,'L R',LEDGE,IREDGE,RSCA
        endif
C
C       SAVE THE DATA
C
        DO I=1,ISIZE*2
        PK(I)=DNMR(I)
        PKI(I)=PNMR(I)
        ENDDO
```

```
      IDIM=ISIZE
      ISIZE=IREDGE-LEDGE+1
      TYPE *,'ISIZE',ISIZE
      IST=1
      DO I=LEDGE,IREDGE
      DNMR(IST)=PK(I)                    !REAL
      PNMR(IST)=PNMR(I)
      DNMR(IST+ISIZE)= PK(I+IDIM)        !IMAGINARY
C     TYPE *,'DNMR',DNMR(IST),IST
      IST=IST+1
      ENDDO
C
      TYPE *,'ISIZE IN ZOOM',ISIZE,YSC
      CALL OUTRAM
C
C     ISIZE=IDIM
C     DO I=1,ISIZE*2
C     DNMR(I)=PK(I)
C     ENDDO
C
      END

C
C     ROUTINE TO REVERSE THE SPECTRUM IN MEMORY
C
      SUBROUTINE reverse
C
      COMMON /NMRDAT/DNMR(20000),ISIZE,YSC
      COMMON /APOD/LB
      dimension dtem(20000)
C
      TC=-LB
C
C
      do i=1,isize*2
      dtem(i)=dnmr(i)
      enddo
c
      j=1
      jj=isize+1
      do i=isize,1,-1
      dnmr(j)=dtem(i)
      dnmr(jj)=dtem(i+isize)
      j=j+1
      jj=jj+1
      enddo
c
      CALL OUTRAM     !DISPLAY THE SPECTRUM
C
      RETURN
      END
```

BIBLIOGRAPHY

Ackerman, J. J. H., T. H. Grove, G. G. Wong, D. G. Gadian, and G. K. Radda, Mapping of metabolites in whole animals by P-31 NMR using surface coils, Nature 283, 167-170, 1980.

Altman, K. I., G. B. Gerber, and S. Okada, In Radiation Biochemistry, Vol. I and II, Academic Press, New York, 1970.

Andrews, H. L., Radiation Biophysics, Prentice Hall, Englewood Cliffs, New Jersey, 1974.

Arus, C., M. Barany, W. M. Westler, J. L. Markley, H1 NMR of intact tissues at 11.1 T, J. Magn. Res. 57, 519-525, 1984.

Asato, R., H. Hajime, T. Hashi, J. Hatta, M. Komoike, and T. Yazaki, Chronological sequence and blood-brain barrier permeability changes in local injury as assessed by nuclear magnetic resonance (NMR) from sliced rat brain. Stroke 14, 191-197, 1983.

Ashley, D. L., and F. H. Goldstein, The application of dextranmagnetite as a relaxation agent in the measurement of erythrocyte water exchange using pulsed nuclear magnetic resonance spectroscopy, Biochem. Biophys. Res. Commun. 97, 114-120, 1980.

Bakay, L., R. J. Kurlank, R. G. Parrish, J. C. Lee, R. J. Peng, and H. M. Bartkowski, Nuclear magnetic resonance studies in normal and

edematous brain tissue, Exp. Brain Res. 23, 241-248, 1975.

Bakker, C. J. G. and J. Vriend, Proton spin-lattice relaxation studies of tissue response to radiotherapy in mice. Phys. Med. Biol. 28, 331-340, 1983.

Bartkowski, H. M., J. Bederson, M. Nishimura, K. Moon, L. H. Pitts, Nuclear Magnetic Resonance imaging and spectroscopy in experimental brain edema, Magnetic Resonance in Medicine 1, 98-99, 1983.

Beall P. T., Application of cell biology to an understanding of biological water. In Cell Associated Water, eds. W. Drost-Hansen, J. Clegg, pp. 271- 362, Academic Press, New York, 1979.

Behar, K. L., J. A. den Hollander, M. E. Stromski, T. Ogino, R. G. Shulman, O. A. C. Petroff, and J. W. Prichard, High-resolution Hl nuclear magnetic resonance study of cerebral hypoxia in vivo, Proc. Natl. Acad. Sci. 80, 4945-4948, 1983.

Behar, K. L., D. L. Rothman, R. G. Shulman, O. A. C. Petroff, J. W. Prichard, Detection of cerebral lactate in vivo during hypoxemia by Hl NMR at relatively low field strengths (1.9 T), Proc. Natl. Acad. Sci. 81, 2517-2519, 1984.

Berendsen, H. J. C., Specific interactions of water with biopolymers, In Water a comprehensive treatise, Vol. 5, Water in disperse systems, ed. F. Franks, pp. 293-330, Plenum Press, New York, 1975.

Biochemical handbook, ed. Cyril Long, pp. 640, D. Van Nostrand Company Inc, New York, 1968

Blicharska, B., Z. Florkowski, J. W. Hennel, G. Held, and F. Noack, Investigation of protein hydration by proton spin lattice relaxation time measurements, Biochimica et Biophysica Acta 207, 381-389, 1970.

Bradley, W. G., R. A. Yadley, R. R. Wycoff, The appearance of different forms of brain edema on NMR, Magnetic Resonance in Medicine 1, 114-115,1983.

Brasch, R. C., Work in progress, methods of contrast enhancement for NMR imaging and potential applications, Radiology 147, 781-788, 1983.

Brown, F. F., I. D. Campbell, P. W. Kuchel, D. C. Rabenstein, Human erythrocyte metabolism studies by H1 spin echo NMR, FEBS Letters 82, 12-16, 1977.

Caveness, W. F., Experimental observation; delayed necrosis in normal monkey brain, In Radiation Damage to the Nervous System, ed. H. A. Gilbert and A. R. Kagan, pp. 1-38, Raven Press, New York, 1980.

Coniglio, J. G., J. T. Davis, F. Windler, V. Tsiung, Lipid metabolism in acute radiation injury - effects of radiation on brain biochemistry, In Response of the Nervous System to Ionizing Radiation, eds. T. J. Haley and R. S. Snider, pp. 377-387, Little, Brown, and Company, Boston, 1964.

Cope, F. W., Nuclear magnetic resonance evidence using D20 for structured water in muscle and brain. Biophys. J. 9, 303-319, 1969.

Cox S. J. and P. Styles, Towards biochemical imaging, J. Magn. Res. 40, 209-212, 1980.

Crooks, L. E., Overview of NMR imaging techniques, In Nuclear Magnetic Resonance in Medicine, eds. L. Kaufman, L. E. Crooks, A. R. Margulis, pp. 30-52, Igaku-Shoin, New York, 1981.

Crooks, L. E., C. M. Mills, P. L. Davis, M. Brant-Zawadzki, J. Hoenninger, M. Arakawa, J. Watts, L. Kaufman, Visualization of cerebral and vascular abnormalities by NMR imaging. The effects of imaging parameters on contrast, Radiology 144, 843-852, 1982.

Crowell, C. D. et al., J. Dent. Res. 14, 25, 1934.

Dodson, C. M., P. A. Evans, K. L. Williamson, Proton NMR studies of denatured lysozyme, FEBS 168, 331-334, 1984.

Egana, E., Effects of ionizing radiation, In Handbook of Neurochemistry Vol. VI, Alterations of chemical equilibrium in the nervous system, ed. A. Lajtha, pp. 525-573, Plenum Press, New York, 1971.

Elkind and Painter, Proc. Fourth International conference on Peaceful Uses of Atomic Energy, Vol. 13, p.361, International Atomic Energy Agency, Vienna, 1971.

Evelhoch, J. L., M. G. Crowley, and J. J. H. Ackerman, Signal-to-noise optimization and observed volume localization with circular surface coils, J. Magn. Res. 56, 110-124, 1984.

Fajardo L-G, L. F., Pathology of Radiation Injury, Masson Publishing U. S. A., Inc., New York, pp. 216-230, 1982.

Ferrar, T. C., and E. D. Becker, Pulse and Fourier transform NMR, Academic Press, New York, 1971.

Fike, J. R., C. E. Cann, R. L. Davis, F. K. Borcich, T. L Phillips, L. B. Russell, CT analysis of canine brain: Effects of hemibrain X irradiation, Radiation Research (in the press), 1984.

Fullerton, G. D., J. L. Potter, N. C. Dornbluth, NMR relaxation of protons in tissues and other macromolecular water solutions, Magnetic Resonance Imaging, 1, 209-288, 1982.

Gaggelli, I. N. Niccolai, G. Valensin, H1-NMR relaxation investigation of water bound to bovine rod outer segment disk membranes, Biophys. J. 37, 559-561, 1982.

Garwood, M., T. Schleich, G. B. Matson, G. Acosta, Spatial localization of tissue metabolites by phosphorus-31 NMR rotating frame zeugmatography, J. Magn. Res. (in the press), 1984.

Gerber, G. B., and K. I. Altman, Tissues and body fluids, In Radiation

Biochemistry, Vol. II, eds. K. I. Altman, G. B. Gerber, S. Okakda, pp.219-234, Academic Press, New York, 1970.

Go, K. G., and H. T. Edzes, Water in brain edema, Arch. Neurol. 32, 462-465, 1975.

Haase A., C. Malloy, G. K. Radda, Spatial localization of high resolution P-31 spectra with a surface coil, J. Magn. Res. 55, 164-169, 1983.

Haselgrove, J. C., V. Harihara Subramanian, J. S. Leigh, Jr., L. Gyulai, B. Chance, In vivo one-dimensional imaging of phosphorus metabolites by phosphorus -31 nuclear magnetic resonance, Science 220, 1170-1173, 1983.

Hazlewood, C. F., A view of the significance and understanding of the physical properties of cell-associated water, In Cell Associated Water, eds. W. Drost-Hansen, J. Clegg, pp. 165-259, Academic Press, New York, 1979.

Haymaker, W., Effects of ionizing radiation on Nervous Tissue, In The Structure and Function of Nervous Tissue, ed. G. H. Bourne, Vol. III, Biochemistry and Disease, pp. 441-536, Academic Press, New York, 1969.

Hoult, D. I., Rotating frame zeugmatography, J. Magn. Res. 33, 183-197, 1979.

James, T. L., Nuclear Magnetic Resonance in Biochemistry; Principles and

Application, Academic Press, New York, 1975.

Joffe, S.,R. E. Block, Nuclear magnetic resonance studies suggestive of a lipid population tightly bound to myelin structural proteins, Brain Research 46, 381-390, 1972.

Jones, R. M., T. Richards, T. F. Budinger, Proton and carbon spectroscopy of lipids and aqueous metabolites extracted from brain, Scientific Meeting, In Scientific Program, Society of Magnetic Resonance in Medicine, Third Annual Meeting, August 13-17, 1984, New York, New York, pp. 395-396, 1984.

Kennedy, W. L., Work in progress, radiation-induced changes in NMR relaxation times of tissue protons, In the press, 1984.

Klots, C. E., In Fundamental Processes in Radiation Chemistry, ed. P. Ausloos, pp. 1, Interscience, New York, 1968.

Kuntz, I. D. and W. Kauzmann, Hydration of proteins and polypeptides, Adv. Protein Chem. 28, 239-345, 1974.

Lampert, P. W., and R. L. Davis, Delayed effects of radiation on the human central nervous system, Neurology 14, 912-917, 1964.

Lierse, W. and D. Franke, Effects of X-irradiation on guinea pig brain, In Brain Edema, ed. I. Klatzo, pp. 639-644, Springer-Verlac, New York, 1967.

Logan, J. E., In Blood and Other Body Fluids, eds. P. L. Altman and D. S. Dittmer, Federation of American Society for Experimental Biology, Washington, D. C., pp. 329-328, 1961.

Mathur-De Vre, R., The NMR studies of water in biological systems, Prog. Biophs. Molec. Biol. 35, 103-134, 1979.

Maudsley, A. A., S. K. Hilal, H. E. Simon, and S. Wittekoek, Multi-nuclear application of chemical-shift imaging, Magnetic Resonance in Medicine 1, 202-203, 1984.

Maxwell, D. S. and L. Kruger, Electron microscopy of radiation induced laminar lesions in the cerebral cortex of the rat, In Response of the Nervous System to Ionizing Radiation, eds. T. J. Haley and R. S. Snider, pp. 54-83, Little, Brown, and Company, Boston, 1964.

Maxwell, D. S. and L. Kruger, The fine structure of astrocytes in the cerebral cortex and their response to focal injury produced by heavy ionizing paritcles , J. Cell Biol. 25, 141-157,

Maxwell, D. S. and L. Kruger, The reactive oligodendrocyte, Am. J. Anat. 118, 437-459, 1966.

Mills, C., S. Lukes, D. Norman, T. H. Newton, M. Brant-Zawadzki, L. Crooks, P. Sheldon, L. Kaufman, Normal and abnormal anatomy of the head, dependence on imaging technique and parameters, In Scientific Program, Society of Magnetic Resonance in Medicine, First Annual Meeting, August

16-18, 1982, Boston Massachusetts, pp. 107-108, 1982.

Miquel, J., W. Haymaker, Brain edema induced by particle and ultraviolet radiation, In Brain Edema, ed. I. Klatzo, pp. 615-631, Springer- Verlac, New York, 1967.

Moustafa, H. F. and J. W. Hopewell, Later functional changes in the vasculature of the rat brain after local X-irradiation, British Journal of Radiology 53, 21-25, 1980.

Naruse, S., Y. Horikawa, C. Tanaka, K. Hirakawa, H. Nishikawa, K. Yoshisaki, Proton nuclear magnetic resonance studies on brain edema, J. Neurosurg. 56, 747-752, 1982.

Okada, S., M. Imamura, T. Terashima, H. Yamaguchi, Radiation Research, Proceedings, Sixth International Congress of radiation research. Japan Association for Radiation Research, Tokyo, 1979.

Pekar, J., J. S. Leigh, B. Chance, Depth-resolved biochemical imaging with surface coils, Magnetic Resonance in Medicine 1, 224, 1984.

Pellegrino, L. J., A. S. Pellegrino, A. J. Cushman, A Stereotaxic Atlas of the rat brain, Plenum Press, New York and London, 1979.

Ponten, U., R. A. Ratcheson, L. G. Salford, B. K. Siesjo, Optimal freezing conditions for cerebral metabolites in rats, Journal of Neurochemistry, 21, 1127-1138, 1973.

Pritchard, E. T. and H. Singh, Can. J. Biochem. Physiol. 39, 1231, 1961.

Pykett, I. L., and B. R. Rosen, Nuclear Magnetic Resonance: In vivo proton chemical shift imaging, Radiology 149, 197-201, 1983.

Reichelt, K. L. and F. Fonnum, Subcellular localization of n-acetyl aspartyl-glutamate, n-acetyl-glutamate, and glutathione in brain, Journal of Neurochemistry 16, 1409-1416, 1969.

Remler, M. P. and W. H. Marcussen, Time course of early delayed blood-brain barrier changes in individual cats after ionizing radiation, Experimental Neurology 73, 310-314, 1981.

Richards, T., T. F. Budinger, R. Nunlist, Proton NMR relaxation times of gray and white matter before and after tissue preservation, Scientific Meeting, In Scientific Program, Society of Magnetic Resonance in Medicine, First Annual Meeting, August 16-18, 1982, Boston Massachusetts, pp. 131-132, 1982.

Richards, T., T. F. Budinger, G. Wesbey, and B. Engelstad, Evaluation of heavy ion radiation damage to the rat brain using proton NMR imaging, Magnetic Resonance in Medicine, 1, 234-235, 1983.

Roberts, J. J., In Advances in Radiation Biology, eds. J T. Lett and H. Adler, Vol. 7, p.211, Academic Press, New York, 1975.

Schneiders, N. J., H. Post, P. Brunner, J. Ford, R. N. Bryan, M. R.

Willcott, Accurate T2 NMR images, Med. Phys. 10, 642-645, 1983.

Sheline, G. E., Irradiation injury of the human brain: A review of clinical experience, In Radiation Damage to the Nervous System, eds. H. A. Gilbert and A. R. Kagan, Raven Press, New York, 1980.

Sherwood, N. M., G. P. Welch, P. S. Timiras, Changes in electroconvulsive thresholds and patterns in rats after x-rays and high-energy proton irradiation, Radiation Research 30, 374-390, 1967.

Singh, A. and H. Singh, Time scale and nature of radiation-biological damage: Approaches to radiation protection and post-irradiation therapy, Prog. Biophys. Molec. Biol. 39, 69-107, 1982.

Tanaka, A., H. Ueno, Y. Yamashita, and W. Caveness, Regional cerebral blood flow in delayed brain swelling following X-irradiation of the right occipital lobe in the monkey, Brain Research 96,233-246, 1975.

Timiras, P. S., J. A. Moguilevsky, S. Geel, Respiratory gas exchange of cerebral cortex, hypothalamus, and aorta of adult rats after early postnatal whole-body x-radiation, In Response of the Nervous System to Ionizing Radiation, eds. T. J. Haley and R. S. Snider, pp. 365-376, Little, Brown, and Company, Boston, 1964.

Tobias, C. A., The use of accelerated heavy particles for production and stimulation in the central nervous system, In Response of the Nervous System to Ionizing Radiation, eds. T. J. Haley and R. S. Snider, pp.

325-343, Academic Press, New York, 1962.

Todo T., S. Yonei, and M. Kato, Radiation-induced structural changes in Human Erythrocyte membrane proteins revealed by sodium dodecyl sulfate/ polyacrylamide gel electrophoresis, Radiation Research 89, 408-419, 1982.

Ugurbil, K., M. Petein, R. Maidan, S. Michurski, J. N. Cohn, A. H. From, High resolution proton NMR studies of perfused rat hearts, FEBS Letters 167, 73-78, 1984.

Van Dyke, D. C., P. Janssen, C. A. Tobias, Fluoroscein as a sensitive, semi-quantitative indicator of injury following alpha particle irradiation of the brain, In Response of the Nervous System to Ionizing Radiation, eds. T. J. Haley and R. S. Snider, pp. 369-383, Academic Press, New York, 1962.

Watkins, S. L., Masked three-dimensional plot program with rotations, Communications of the ACM 17, 520-523, 1974.

Wesbey, G., M. Moseley, M. Hrovat, R. Ehman, Measurements of translational molecular self-diffusion in proton magnetic resonance imaging (MRI), Scientific Meeting, In Scientific Program, Society of Magnetic Resonance in Medicine, Third Annual Meeting, August 13-17, 1984, New York, New York, pp. 751-752, 1984.

Yoshizaki, K., Y. Seo, H. Nishikawa, High resolution proton magnetic

resonance spectra of muscle, Biochimica et Biophysica Acta, 678, 283-291, 1981.

Zeman, W. and T. Samorajski, Effects of irradiation on the nervous system, In Pathology of Irradiation, ed. C. C. Berdjis, pp. 213-276, William and Wilkins, Baltimore, 1971.

This report was done with support from the Department of Energy. Any conclusions or opinions expressed in this report represent solely those of the author(s) and not necessarily those of The Regents of the University of California, the Lawrence Berkeley Laboratory or the Department of Energy.

Reference to a company or product name does not imply approval or recommendation of the product by the University of California or the U.S. Department of Energy to the exclusion of others that may be suitable.

TECHNICAL INFORMATION DEPARTMENT
LAWRENCE BERKELEY LABORATORY
UNIVERSITY OF CALIFORNIA
BERKELEY, CALIFORNIA 94720